

TURKISH JOURNAL OF PHARMACEUTICAL SCIENCES



TURKISH JOURNAL OF PHARMACEUTICAL SCIENCES



Editor-in-Chief

Feyyaz ONUR, Prof. Dr.
Ankara University, Ankara, Turkey,
E-mail: onur@pharmacy.ankara.edu.tr
ORCID ID: orcid.org/0000-0001-9172-1126

Vice Editor

Gülgün KILCIGİL, Prof. Dr.
Ankara University, Ankara, Turkey
E-mail: Gulgun.A.Kilcigil@pharmacy.ankara.edu.tr
ORCID ID: orcid.org/0000-0001-5626-6922

Associate Editors

Rob VERPOORTE, Prof. Dr.
Leiden University, Leiden, Netherlands

Bezhan CHANKVETADZE, Prof. Dr.
Ivane Javakishvili Tbilisi State University,
Tbilisi, Georgia

Ülkü ÜNDEĞER-BUCURGAT, Prof. Dr.
Hacettepe University, Ankara, Turkey
ORCID ID: orcid.org/0000-0002-6692-0366

Luciano SASO, Prof. Dr.
Sapienze University of Rome, Rome, Italy

Müge KILIÇARSLAN, Assoc. Prof. Dr.
Ankara University, Ankara, Turkey
ORCID ID: orcid.org/0000-0003-3710-7445

Fernanda BORGES, Prof. Dr.
Porto University, Porto, Portugal

Tayfun UZBAY, Prof. Dr.
Üsküdar University, İstanbul, Turkey

İpek SUNTAR, Assoc. Prof. Dr.
Gazi University, Ankara, Turkey
ORCID ID: orcid.org/0000-0001-5626-6922

Advisory Board

- Ali H. MERİÇLİ, Prof. Dr., Near East University, Nicosia, Turkish Republic of Northern Cyprus
Ahmet BAŞARAN, Prof. Dr., Hacettepe University Faculty of Pharmacy, Department of Pharmacognosy, Ankara, Turkey
Berrin ÖZÇELİK, Prof. Dr., Gazi University, Ankara, Turkey
Betül DORTUNÇ, Prof. Dr., Marmara University, İstanbul, Turkey
Christine LAFFORGUE, Prof. Dr., Paris-Sud University, Paris, France
Cihat ŞAFAK, Prof. Dr., Hacettepe University, Ankara, Turkey
Filiz ÖNER, Prof. Dr., Hacettepe University, Ankara, Turkey
Gülten ÖTÜK, Prof. Dr., İstanbul University, İstanbul, Turkey
Hermann BOLT, Prof. Dr., Dortmund University Leibniz Research Centre, Dortmund, Germany
Hildebert WAGNER, Prof. Dr., Ludwig-Maximilians University, Munich, Germany
Jean-Alain FEHRENTZ, Prof. Dr., Montpellier University, Montpellier, France
Joerg KREUTER, Prof. Dr., Johann Wolfgang Goethe University, Frankfurt, Germany
Makbule AŞIKOĞLU, Prof. Dr., Ege University, İzmir, Turkey
Meral KEYER UYSAL, Prof. Dr., Marmara University, İstanbul, Turkey
Meral TORUN, Prof. Dr., Gazi University, Ankara, Turkey
Mümtaz İŞCAN, Prof. Dr., Ankara University, Ankara, Turkey
Robert RAPOPORT, Prof. Dr., Cincinnati University, Cincinnati, USA
Sema BURGAZ, Prof. Dr., Gazi University, Ankara, Turkey
Wolfgang SADEE, Prof. Dr., Ohio State University, Ohio, USA
Yasemin YAZAN, Prof. Dr., Anadolu University, Eskişehir, Turkey
Yusuf ÖZTÜRK, Prof. Dr., Anadolu University, Eskişehir, Turkey
Yücel KADIOĞLU, Prof. Dr., Atatürk University, Erzurum, Turkey
Zühre ŞENTÜRK, Prof. Dr., Yüzüncü Yıl University, Van, Turkey

TURKISH JOURNAL OF PHARMACEUTICAL SCIENCES

AIMS AND SCOPE

The Turkish Journal of Pharmaceutical Sciences is the only scientific periodical publication of the Turkish Pharmacists' Association and has been published since April 2004.

Turkish Journal of Pharmaceutical Sciences is an independent international open access periodical journal based on double-blind peer-review principles. The journal is regularly published 3 times a year and the publication language is English. The issuing body of the journal is Galenos Yayınevi/Publishing House.

The aim of Turkish Journal of Pharmaceutical Sciences is to publish original research papers of the highest scientific and clinical value at an international level.

The target audience includes specialists and physicians in all fields of pharmaceutical sciences.

The editorial policies are based on the "Recommendations for the Conduct, Reporting, Editing, and Publication of Scholarly Work in Medical Journals (ICMJE Recommendations)" by the International Committee of Medical Journal Editors (2016, archived at <http://www.icmje.org/>) rules.

Editorial Independence

Turkish Journal of Pharmaceutical Sciences is an independent journal with independent editors and principles and has no commercial relationship with the commercial product, drug or pharmaceutical company regarding decisions and review processes upon articles.

ABSTRACTED/INDEXED IN

Web of Science-Emerging Sources Citation Index (ESCI)

SCOPUS SJR

ProQuest

Chemical Abstracts Service (CAS)

EBSCO

EMBASE

Analytical Abstracts

International Pharmaceutical Abstracts (IPA)

Medicinal & Aromatic Plants Abstracts (MAPA)

TÜBİTAK/ULAKBİM TR Dizin

Türkiye Atıf Dizini

OPEN ACCESS POLICY

This journal provides immediate open access to its content on the principle that making research freely available to the public supports

a greater global exchange of knowledge.

Open Access Policy is based on the rules of the Budapest Open Access Initiative (BOAI) <http://www.budapestopenaccessinitiative.org/>. By "open access" to peer-reviewed research literature, we mean its free availability on the public internet, permitting any users to read, download, copy, distribute, print, search, or link to the full texts of these articles, crawl them for indexing, pass them as data to software, or use them for any other lawful purpose, without financial, legal, or technical barriers other than those inseparable from gaining access to the internet itself. The only constraint on reproduction and distribution, and the only role for copyright in this domain, should be to give authors control over the integrity of their work and the right to be properly acknowledged and cited.

CORRESPONDENCE ADDRESS

Editor-in-Chief, Feyyaz ONUR, Prof.Dr.

Address: Ankara University, Faculty of Pharmacy, Department of Analytical Chemistry, 06100 Tandoğan-Ankara, TURKEY

E-mail: onur@pharmacy.ankara.edu.tr

PERMISSION

Requests for permission to reproduce published material should be sent to the editorial office. Editor-in-Chief, Prof. Dr. Feyyaz ONUR

ISSUING BODY CORRESPONDING ADDRESS

Issuing Body : Galenos Yayınevi

Address: Molla Gürani Mah. Kaçamak Sk. No: 21/1, 34093 İstanbul, TURKEY

Phone: +90 212 621 99 25 Fax: +90 212 621 99 27

E-mail: info@galenos.com.tr

INSTRUCTIONS FOR AUTHORS

Instructions for authors are published in the journal and on the website <http://turkjps.org>

MATERIAL DISCLAIMER

The author(s) is (are) responsible for the articles published in the JOURNAL.

The editor, editorial board and publisher do not accept any responsibility for the articles.

This work is licensed under a Creative Commons Attribution-NonCommercial-NoDerivatives 4.0 International License.



Publisher
Erkan Mor

Publication Director
Nesrin Çolak

Web Coordinators
Soner Yıldırım
Turgay Akpınar

Graphics Department
Ayda Alaca
Çiğdem Birinci

Web Assistant
Başak Yılmaz

Project Coordinators
Eda Kolukısa
Hatice Balta
Lütfiye Ayhan İrtem
Zeynep Altındağ

Project Assistants
Esra Semerci
Günay Selimoğlu
Sedanur Sert

Research&Development
Deniz Sleptsov

Finance Coordinator
Sevinç Çakmak

Publisher Contact

Address: Molla Gürani Mah. Kaçamak Sk. No: 21/1 34093 İstanbul, Turkey

Phone: +90 (212) 621 99 25

Fax: +90 (212) 621 99 27

E-mail: info@galenos.com.tr/yayin@galenos.com.tr

Web: www.galenos.com.tr

Printing at: Özgün Ofset Ticaret Ltd. Şti.

Yeşilce Mah. Aytekin Sok. No: 21, 34418 4. Levent, İstanbul-Turkey

Phone: +90 280 00 09

Printing date: March 2018

ISSN: 1304-530X

E-ISSN: 2148-6247

TURKISH JOURNAL OF PHARMACEUTICAL SCIENCES

INSTRUCTIONS TO AUTHORS

Turkish Journal of Pharmaceutical Sciences is the official double peer-reviewed publication of The Turkish Pharmacists' Association. This journal is published every 4 months (3 issues per year; April, August, December) and publishes the following articles:

- Research articles
- Reviews (only upon the request or consent of the Editorial Board)
- Preliminary results/Short communications/Technical notes/Letters to the Editor in every field or pharmaceutical sciences.

The publication language of the journal is English.

The Turkish Journal of Pharmaceutical Sciences does not charge any article submission or processing charges.

A manuscript will be considered only with the understanding that it is an original contribution that has not been published elsewhere.

The Journal should be abbreviated as "Turk J Pharm Sci" when referenced.

The scientific and ethical liability of the manuscripts belongs to the authors and the copyright of the manuscripts belongs to the Journal. Authors are responsible for the contents of the manuscript and accuracy of the references. All manuscripts submitted for publication must be accompanied by the Copyright Transfer Form [copyright transfer]. Once this form, signed by all the authors, has been submitted, it is understood that neither the manuscript nor the data it contains have been submitted elsewhere or previously published and authors declare the statement of scientific contributions and responsibilities of all authors.

Experimental, clinical and drug studies requiring approval by an ethics committee must be submitted to the JOURNAL with an ethics committee approval report including approval number confirming that the study was conducted in accordance with international agreements and the Declaration of Helsinki (revised 2013) (<http://www.wma.net/en/30publications/10policies/b3/>). The approval of the ethics committee and the fact that informed consent was given by the patients should be indicated in the Materials and Methods section. In experimental animal studies, the authors should indicate that the procedures followed were in accordance with animal rights as per the Guide for the Care and Use of Laboratory Animals (<http://oacu.od.nih.gov/regs/guide/guide.pdf>) and they should obtain animal ethics committee approval.

Authors must provide disclosure/acknowledgment of financial or material support, if any was received, for the current study.

If the article includes any direct or indirect commercial links or if any institution provided material support to the study, authors must state in the cover letter that they have no relationship with the commercial product, drug, pharmaceutical company, etc. concerned; or specify the type of relationship (consultant, other agreements), if any.

Authors must provide a statement on the absence of conflicts of interest among the authors and provide authorship contributions.

All manuscripts submitted to the journal are screened for plagiarism using the 'iThenticate' software. Results indicating plagiarism may result in manuscripts being returned or rejected.

The Review Process

This is an independent international journal based on double-blind peer-review principles. The manuscript is assigned to the Editor-in-Chief, who reviews the manuscript and makes an initial decision based on manuscript quality and editorial priorities. Manuscripts that pass

initial evaluation are sent for external peer review, and the Editor-in-Chief assigns an Associate Editor. The Associate Editor sends the manuscript to at least two reviewers (internal and/or external reviewers). The reviewers must review the manuscript within 21 days. The Associate Editor recommends a decision based on the reviewers' recommendations and returns the manuscript to the Editor-in-Chief. The Editor-in-Chief makes a final decision based on editorial priorities, manuscript quality, and reviewer recommendations. If there are any conflicting recommendations from reviewers, the Editor-in-Chief can assign a new reviewer.

The scientific board guiding the selection of the papers to be published in the Journal consists of elected experts of the Journal and if necessary, selected from national and international authorities. The Editor-in-Chief, Associate Editors may make minor corrections to accepted manuscripts that do not change the main text of the paper.

In case of any suspicion or claim regarding scientific shortcomings or ethical infringement, the Journal reserves the right to submit the manuscript to the supporting institutions or other authorities for investigation. The Journal accepts the responsibility of initiating action but does not undertake any responsibility for an actual investigation or any power of decision.

The Editorial Policies and General Guidelines for manuscript preparation specified below are based on "Recommendations for the Conduct, Reporting, Editing, and Publication of Scholarly Work in Medical Journals (ICMJE Recommendations)" by the International Committee of Medical Journal Editors (2016, archived at <http://www.icmje.org/>).

Preparation of research articles, systematic reviews and meta-analyses must comply with study design guidelines:

CONSORT statement for randomized controlled trials (Moher D, Schulz KF, Altman D, for the CONSORT Group. The CONSORT statement revised recommendations for improving the quality of reports of parallel group randomized trials. JAMA 2001; 285: 1987-91) (<http://www.consort-statement.org/>);

PRISMA statement of preferred reporting items for systematic reviews and meta-analyses (Moher D, Liberati A, Tetzlaff J, Altman DG, The PRISMA Group. Preferred Reporting Items for Systematic Reviews and Meta-Analyses: The PRISMA Statement. PLoS Med 2009; 6(7): e1000097.) (<http://www.prisma-statement.org/>);

STARD checklist for the reporting of studies of diagnostic accuracy (Bossuyt PM, Reitsma JB, Bruns DE, Gatsonis CA, Glasziou PP, Irwig LM, et al., for the STARD Group. Towards complete and accurate reporting of studies of diagnostic accuracy: the STARD initiative. Ann Intern Med 2003;138:40-4.) (<http://www.stard-statement.org/>);

STROBE statement, a checklist of items that should be included in reports of observational studies (<http://www.strobe-statement.org/>);

MOOSE guidelines for meta-analysis and systemic reviews of observational studies (Stroup DF, Berlin JA, Morton SC, et al. Meta-analysis of observational studies in epidemiology: a proposal for reporting Meta-analysis of observational Studies in Epidemiology (MOOSE) group. JAMA 2000; 283: 2008-12).

Authorship

Each author should have participated sufficiently in the work to assume public responsibility for the content. Any portion of a manuscript that is critical to its main conclusions must be the responsibility of at least 1 author.

TURKISH JOURNAL OF PHARMACEUTICAL SCIENCES

INSTRUCTIONS TO AUTHORS

GENERAL GUIDELINES

Manuscripts can only be submitted electronically through the Journal Agent website (<http://journalagent.com/tjps/>) after creating an account. This system allows online submission and review.

The manuscripts are archived according to ICMJE, Web of Science-Emerging Sources Citation Index (ESCI), SCOPUS, Chemical Abstracts, EBSCO, EMBASE, Analytical Abstracts, International Pharmaceutical Abstracts, MAPA (Medicinal & Aromatic Plants Abstracts), Tübitak/Ulakbim Turkish Medical Database, Türkiye Citation Index Rules.

Format: Manuscripts should be prepared using Microsoft Word, size A4 with 2.5 cm margins on all sides, 12 pt Arial font and 1.5 line spacing.

Abbreviations: Abbreviations should be defined at first mention and used consistently thereafter. Internationally accepted abbreviations should be used; refer to scientific writing guides as necessary.

Cover letter: The cover letter should include statements about manuscript type, single-Journal submission affirmation, conflict of interest statement, sources of outside funding, equipment (if applicable), for original research articles.

The ORCID (Open Researcher and Contributor ID) number of the all authors should be provided while sending the manuscript. A free registration can be done at <http://orcid.org>.

REFERENCES

Authors are solely responsible for the accuracy of all references.

In-text citations: References should be indicated as a superscript immediately after the period/full stop of the relevant sentence. If the author(s) of a reference is/are indicated at the beginning of the sentence, this reference should be written as a superscript immediately after the author's name. If relevant research has been conducted in Turkey or by Turkish investigators, these studies should be given priority while citing the literature.

Presentations presented in congresses, unpublished manuscripts, theses, Internet addresses, and personal interviews or experiences should not be indicated as references. If such references are used, they should be indicated in parentheses at the end of the relevant sentence in the text, without reference number and written in full, in order to clarify their nature.

References section: References should be numbered consecutively in the order in which they are first mentioned in the text. All authors should be listed regardless of number. The titles of Journals should be abbreviated according to the style used in the Index Medicus.

Reference Format

Journal: Last name(s) of the author(s) and initials, article title, publication title and its original abbreviation, publication date, volume, the inclusive page numbers. Example: Collin JR, Rathbun JE. Involitional entropion: a review with evaluation of a procedure. Arch Ophthalmol. 1978;96:1058-1064.

Book: Last name(s) of the author(s) and initials, book title, edition, place of publication, date of publication and inclusive page numbers of the extract cited.

Example: Herbert L. The Infectious Diseases (1st ed). Philadelphia; Mosby Harcourt; 1999:11;1-8.

Book Chapter: Last name(s) of the author(s) and initials, chapter title,

book editors, book title, edition, place of publication, date of publication and inclusive page numbers of the cited piece.

Example: O'Brien TP, Green WR. Periocular Infections. In: Feigin RD, Cherry JD, eds. Textbook of Pediatric Infectious Diseases (4th ed). Philadelphia; W.B. Saunders Company; 1998:1273-1278.

Books in which the editor and author are the same person: Last name(s) of the author(s) and initials, chapter title, book editors, book title, edition, place of publication, date of publication and inclusive page numbers of the cited piece. Example: Solcia E, Capella C, Kloppel G. Tumors of the exocrine pancreas. In: Solcia E, Capella C, Kloppel G, eds. Tumors of the Pancreas. 2nd ed. Washington: Armed Forces Institute of Pathology; 1997:145-210.

TABLES, GRAPHICS, FIGURES, AND IMAGES

All visual materials together with their legends should be located on separate pages that follow the main text.

Images: Images (pictures) should be numbered and include a brief title. Permission to reproduce pictures that were published elsewhere must be included. All pictures should be of the highest quality possible, in JPEG format, and at a minimum resolution of 300 dpi.

Tables, Graphics, Figures: All tables, graphics or figures should be enumerated according to their sequence within the text and a brief descriptive caption should be written. Any abbreviations used should be defined in the accompanying legend. Tables in particular should be explanatory and facilitate readers' understanding of the manuscript, and should not repeat data presented in the main text.

MANUSCRIPT TYPES

Original Articles

Clinical research should comprise clinical observation, new techniques or laboratories studies. Original research articles should include title, structured abstract, key words relevant to the content of the article, introduction, materials and methods, results, discussion, study limitations, conclusion references, tables/figures/images and acknowledgement sections. Title, abstract and key words should be written in both Turkish and English. The manuscript should be formatted in accordance with the above-mentioned guidelines and should not exceed 16 A4 pages.

Title Page: This page should include the title of the manuscript, short title, name(s) of the authors and author information. The following descriptions should be stated in the given order:

1. Title of the manuscript (Turkish and English), as concise and explanatory as possible, including no abbreviations, up to 135 characters
2. Short title (Turkish and English), up to 60 characters
3. Name(s) and surname(s) of the author(s) (without abbreviations and academic titles) and affiliations
4. Name, address, e-mail, phone and fax number of the corresponding author
5. The place and date of scientific meeting in which the manuscript was presented and its abstract published in the abstract book, if applicable

Abstract: A summary of the manuscript should be written in both Turkish and English. References should not be cited in the abstract. Use of abbreviations should be avoided as much as possible; if any abbreviations are used, they must be taken into consideration

TURKISH

JOURNAL OF PHARMACEUTICAL SCIENCES

INSTRUCTIONS TO AUTHORS

independently of the abbreviations used in the text. For original articles, the structured abstract should include the following sub-headings:

Objectives: The aim of the study should be clearly stated.

Materials and Methods: The study and standard criteria used should be defined; it should also be indicated whether the study is randomized or not, whether it is retrospective or prospective, and the statistical methods applied should be indicated, if applicable.

Results: The detailed results of the study should be given and the statistical significance level should be indicated.

Conclusion: Should summarize the results of the study, the clinical applicability of the results should be defined, and the favorable and unfavorable aspects should be declared.

Keywords: A list of minimum 3, but no more than 5 key words must follow the abstract. Key words in English should be consistent with "Medical Subject Headings (MESH)" (www.nlm.nih.gov/mesh/MBrowser.html). Turkish key words should be direct translations of the terms in MESH.

Original research articles should have the following sections:

Introduction: Should consist of a brief explanation of the topic and indicate the objective of the study, supported by information from the literature.

Materials and Methods: The study plan should be clearly described, indicating whether the study is randomized or not, whether it is retrospective or prospective, the number of trials, the characteristics, and the statistical methods used.

Results: The results of the study should be stated, with tables/figures given in numerical order; the results should be evaluated according to the statistical analysis methods applied. See General Guidelines for details about the preparation of visual material.

Discussion: The study results should be discussed in terms of their favorable and unfavorable aspects and they should be compared with the literature. The conclusion of the study should be highlighted.

Study Limitations: Limitations of the study should be discussed. In

addition, an evaluation of the implications of the obtained findings/results for future research should be outlined.

Conclusion: The conclusion of the study should be highlighted.

Acknowledgements: Any technical or financial support or editorial contributions (statistical analysis, English/Turkish evaluation) towards the study should appear at the end of the article.

References: Authors are responsible for the accuracy of the references. See General Guidelines for details about the usage and formatting required.

Review Articles

Review articles can address any aspect of clinical or laboratory pharmaceuticals. Review articles must provide critical analyses of contemporary evidence and provide directions of or future research. Most review articles are commissioned, but other review submissions are also welcome. Before sending a review, discussion with the editor is recommended.

Reviews articles analyze topics in depth, independently and objectively. The first chapter should include the title in Turkish and English, an unstructured summary and key words. Source of all citations should be indicated. The entire text should not exceed 25 pages (A4, formatted as specified above).

CORRESPONDENCE

All correspondence should be directed to the Turkish Journal of Pharmaceutical Sciences editorial board;

Post: Turkish Pharmacists' Association

Address: Willy Brandt Sok. No: 9 06690 Ankara, TURKEY

Phone: +90 312 409 8136

Fax: +90 312 409 8132

Web Page: <http://turkjps.org/home/>

E-mail: onur@pharmacy.ankara.edu.tr

TURKISH JOURNAL OF PHARMACEUTICAL SCIENCES

CONTENTS

Original articles

- 1 Real-time Analysis of Impedance Alterations by the Effects of Vanadium Pentoxide on Several Carcinoma Cell Lines
Vanadyum Pentoksidin Çeşitli Kanser Hücre Hatlarındaki Etkilerinin Empedans Değişiklikleri ile Gerçek Zamanlı Analizi
Ebru ÖZTÜRK, Ayşe Kübra KARABOĞA ARSLAN, Alim Hüseyin DOKUMACI, Mükerrerem Betül YERER
- 7 Preparation and *In Vitro* Evaluation of Ibuprofen Spherical Agglomerates
Ibuprofen Küresel Aglomeralarının Hazırlanması ve İn Vitro Değerlendirmesi
Nagaraju RAVOURU, Subhash Chandra Bose PENJURI, Saritha DAMINENI, Raja Lakshmi MUNI, Srikanth Reddy POREDDY
- 16 Development of Nanocochleates Containing Erlotinib HCl and Dexketoprofen Trometamol and Evaluation of *In Vitro* Characteristic Properties
Erlotinib HCl ve Deksketoprofen Trometamol İçeren Nanokohleatların Geliştirilmesi ve İn vitro Karakteristik Özelliklerinin Değerlendirilmesi
Özlem ÇOBAN, Zelihagül DEĞİM
- 22 Development and Validation of a High-performance Liquid Chromatography–Diode-array Detection Method for the Determination of Eight Phenolic Constituents in Extracts of Different Wine Species
Çeşitli Şarap Örneklerinde Sekiz Fenolik İçeriğın Tayini için Bir HPLC-DAD Yönteminin Geliştirilmesi ve Geçerli Kılınması
Ebru TÜRKÖZ ACAR, Mehmet Engin CELEP, Mohammad CHAREHSAZ, Gülşah Selin AKYÜZ, Erdem YEŞİLADA
- 29 Orally-disintegrating Tablets in Fixed-dose Combination Containing Ambroxol Hydrochloride and Salbutamol Sulphate Prepared by Direct Compression: Formulation Design, Development and *In Vitro* Evaluation
Doğrudan Basım ile Hazırlanan Ambroksol Hidroklorür ve Salbutamol Sülfat İçeren Sabit Doz Kombinasyonu Oral-dağılan Tabletler: Formülasyon Tasarımı, Geliştirilmesi ve İn Vitro Değerlendirilmesi
Deepak SHARMA, Rajindra SINGH, Gurmeet SINGH
- 38 A Simple Isocratic High-performance Liquid Chromatography Method for the Simultaneous Determination of Shikonin Derivatives in Some *Echium* Species Growing Wild in Turkey
Türkiye’de Yabani Yetişen Bazı Echium Türlerindeki Şikonin Türevlerinin Basit İzokratik HPLC Yöntemiyle Eşzamanlı Olarak Belirlenmesi
Nuraniye ERUYGUR
- 44 Use of Water Soluble and Phosphorescent MPA-capped CdTe Quantum Dots for the Detection of Urea
Üre Tayini için Suda Çözünebilen ve Fosforesan MPA Kaplı CdTe Kuantum Noktacıklarının Kullanımı
Tülay OYMAK, Nusret ERTAŞ, Uğur TAMER
- 50 Calcium Mobilization and Inhibition of Akt Reduced the Binding of PEO-1 Cells to Fibronectin
Ca²⁺ Mobilizasyonu ve Akt İnhibisyonu ile PEO-1 Hücrelerinin Fibronektine Bağlanmasında Azalma
Seda Mehtap SARI KILIÇASLAN, Aysun AYRIM, Elif APAYDIN, Zerrin İNCESU
- 57 Synthesis and Evaluation of Vanillin Derivatives as Antimicrobial Agents
Vanilin Türevlerinin Antimikrobiyal Ajanlar Olarak Sentezi ve Değerlendirilmesi
Rakesh YADAV, Dharamvir SAINI, Divya YADAV

TURKISH JOURNAL OF PHARMACEUTICAL SCIENCES

CONTENTS

- 63** The Structural, Crystallinity, and Thermal Properties of pH-responsive Interpenetrating Gelatin/Sodium Alginate-based Polymeric Composites for the Controlled Delivery of Cetirizine HCl
Setirizin HCl'nin Kontrollü Salımı için pH Duyarlı İnterpenetrasyon Jelatin/Sodyum Aljinat- esaslı Polimerik Kompozitlerin Yapı, Kristalinite ve Termal Özellikleri
Samrin AFZAL, Samiullah KHAN, Nazar Mohammad RANJHA, Aamir JALIL, Amina RIAZ, Malik Salman HAIDER, Shoaib SARWAR, Fareha SAHER, Fahad NAEEM
- 77** *In Vitro* Protection by *Crataegus microphylla* Extracts Against Oxidative Damage and Enzyme Inhibition Effects
Crataegus microphylla Ekstrelerinin Oksidatif Hasara Karşı İntro Koruma ve Enzim İnhibisyonu Etkileri
Arzu ÖZEL
- 85** Composition of Volatile Oil of *Iris pallida* Lam. from Ukraine
Iris pallida Lam'ın Uçucu Yağı Bileşimi Ukrayna
Olga MYKHAILENKO
- 91** Development and Characterization of Insulin-loaded Liposome-chitosan-Nanoparticle (LCS-NP) Complex and Investigation of Transport Properties Through a Pancreatic Beta Tc Cell Line
İnsülin Yüklü Lipozom-Kitosan-Nanopartikül (LCS-NP) Kompleksinin Geliştirilmesi ve Karakterizasyonu ve Pankreatik Beta Tc Hücre Hattından Geçiş Özelliklerinin Araştırılması
Merve ÇELİK TEKELİ, Çiğdem YÜCEL, Sedat ÜNAL, Yeşim AKTAŞ
- 97** Screening Effects of Methanol Extracts of *Diplotaxis tenuifolia* and *Reseda lutea* on Enzymatic Antioxidant Defense Systems and Aldose Reductase Activity
Diplotaxis tenuifolia ve *Reseda lutea* Metanol Özüünün Antioksidan Savunma Sistemi Enzimleri ve Aldoz Redüktaz Aktivitesi Üzerinde Olan Etkisinin İncelenmesi
Khalid Sharro ABDALRAHMAN, Merve Gülşah GÜNEŞ, Naznoosh SHOMALI, Belgin Sultan İŞGÖR, Özlem YILDIRIM
- 103** Chemical Constituents of *Cymbocarpum erythraeum* (DC.) Boiss., and Evaluation of Its Anti-*Helicobacter pylori* Activity
Cymbocarpum erythraeum (DC.) Boiss.'in Kimyasal Bileşikleri ve *Helicobacter pylori*'ye Karşı Etkisi
Samaneh HEIDARI, Azadeh MANAYI, Soodabeh SAEIDNIA, Hossein MIGHANI, Hamid Reza MONSEF ESFAHANI, Ahmad Reza GOHARI, William N SETZER
- 107** Anti-inflammatory Effects of *Pelargonium endlicherianum* Fenzl. Extracts in Lipopolysaccharide-stimulated Macrophages
Pelargonium endlicherianum Fenzl. Ekstrelerinin Lipopolisakkarit ile Uyarılan Makrofajlarda Anti-enflamatuvar Etkileri
Ahmet CUMAĞLU, Gökçe Şeker KARATOPRAK, Mükerrrem Betül YERER, Müberra KOŞAR

TURKISH JOURNAL OF PHARMACEUTICAL SCIENCES

Volume: 15, No: 1, Year: 2018

CONTENTS

Original articles

- Real-time Analysis of Impedance Alterations by the Effects of Vanadium Pentoxide on Several Carcinoma Cell Lines
Ebru ÖZTÜRK, Ayşe Kübra KARABOĞA ARSLAN, Alim Hüseyin DOKUMACI, Mükerrerem Betül YERER..... 1
- Preparation and *In Vitro* Evaluation of Ibuprofen Spherical Agglomerates
Nagaraju RAVOURU, Subhash Chandra Bose PENJURI, Saritha DAMINENI, Raja Lakshmi MUNI,
Srikanth Reddy POREDDY 7
- Development of Nanocochleates Containing Erlotinib HCl and Dexketoprofen Trometamol and Evaluation of
In Vitro Characteristic Properties
Özlem ÇOBAN, Zelihağül DEĞİM..... 16
- Development and Validation of a High-performance Liquid Chromatography-Diode-array Detection Method
for the Determination of Eight Phenolic Constituents in Extracts of Different Wine Species
Ebru TÜRKÖZ ACAR, Mehmet Engin CELEP, Mohammad CHAREHSAZ, Gülşah Selin AKYÜZ, Erdem YEŞİLADA..... 22
- Orally-disintegrating Tablets in Fixed-dose Combination Containing Ambroxol Hydrochloride and Salbutamol
Sulphate Prepared by Direct Compression: Formulation Design, Development and *In Vitro* Evaluation
Deepak SHARMA, Rajindra SINGH, Gurmeet SINGH 29
- A Simple Isocratic High-performance Liquid Chromatography Method for the Simultaneous Determination of
Shikonin Derivatives in Some *Echium* Species Growing Wild in Turkey
Nuraniye ERUYGUR..... 38
- Use of Water Soluble and Phosphorescent MPA-capped CdTe Quantum Dots for the Detection of Urea
Tülay OYMAK, Nusret ERTAŞ, Uğur TAMER..... 44
- Calcium Mobilization and Inhibition of Akt Reduced the Binding of PEO-1 Cells to Fibronectin
Seda Mehtap SARI KILIÇASLAN, Aysun AYRIM, Elif APAYDIN, Zerrin INCESU 50
- Synthesis and Evaluation of Vanillin Derivatives as Antimicrobial Agents
Rakesh YADAV, Dharamvir SAINI, Divya YADAV 57
- The Structural, Crystallinity, and Thermal Properties of pH-responsive Interpenetrating Gelatin/Sodium
Alginate-based Polymeric Composites for the Controlled Delivery of Cetirizine HCl
Samrin AFZAL, Samiullah KHAN, Nazar Mohammad RANJHA, Aamir JALIL, Amina RIAZ, Malik Salman HAIDER,
Shoaib SARWAR, Fareha SAHER, Fahad NAEEM..... 63
- In Vitro* Protection by *Crataegus microphylla* Extracts Against Oxidative Damage and Enzyme Inhibition Effects
Arzu ÖZEL..... 77
- Composition of Volatile Oil of *Iris pallida* Lam. from Ukraine
Olga MYKHAILENKO 85
- Development and Characterization of Insulin-loaded Liposome-chitosan-Nanoparticle (LCS-NP) Complex and
Investigation of Transport Properties Through a Pancreatic Beta Tc Cell Line
Merve ÇELİK TEKELİ, Çiğdem YÜCEL, Sedat ÜNAL, Yeşim AKTAŞ 91
- Screening Effects of Methanol Extracts of *Diplotaxis tenuifolia* and *Reseda lutea* on Enzymatic Antioxidant Defense
Systems and Aldose Reductase Activity
Khalid Sharro ABDALRAHMAN, Merve Gülşah GÜNEŞ, Naznoosh SHOMALI, Belgin Sultan IŞGÖR, Özlem YILDIRIM.. 97
- Chemical Constituents of *Cymbocarpum erythraeum* (DC.) Boiss., and Evaluation of Its Anti-*Helicobacter pylori* Activity
Samaneh HEIDARI, Azadeh MANAYI, Soodabeh SAEIDNIA, Hossein MIGHANI, Hamid Reza MONSEF ESFAHANI,
Ahmad Reza GOHARI, William N SETZER 103
- Anti-inflammatory Effects of *Pelargonium endlicherianum* Fenzl. Extracts in Lipopolysaccharide-stimulated
Macrophages
Ahmet CUMAĞLU, Gökçe Şeker KARATOPRAK, Mükerrerem Betül YERER, Müberra KOŞAR..... 107



Real-time Analysis of Impedance Alterations by the Effects of Vanadium Pentoxide on Several Carcinoma Cell Lines

Vanadyum Pentoksidin Çeşitli Kanser Hücre Hatlarındaki Etkilerinin Empedans Değişiklikleri ile Gerçek Zamanlı Analizi

© Ebru ÖZTÜRK^{1*}, © Ayşe Kübra KARABOĞA ARSLAN¹, © Alim Hüseyin DOKUMACI², © Mükerrerem Betül YERER¹

¹Erciyes University, Faculty of Pharmacy, Department of Pharmacology, Kayseri, Turkey

²Erciyes University, Graduate School of Health Sciences, Department of Pharmacology, Kayseri, Turkey

ABSTRACT

Objectives: Vanadium compounds have various pharmacologic effects and all available evidence reveals that the effects of vanadium compounds depend on many factors, mainly on the type of cells and dose. The proapoptotic or antiapoptotic effect of vanadium compounds depends strongly on the cell type.

Materials and Methods: In this study, the effects of vanadium pentoxide (V_2O_5) were investigated using several tumor cell lines: a colorectal cancer cell line (Colo-205), a human breast adenocarcinoma cell line (MCF-7), and a normal human fibroblast cell line. Five different concentrations of V_2O_5 between 25-200 μM were applied on the cells and xCELLigence real-time cell analysis was conducted to evaluate the impedance alterations. This study is the first to show V_2O_5 's effects on Colo-205 and MCF-7 and human fibroblast cell lines in a real-time manner.

Results: In the Colo-205 cell line, cell index (CI) alterations decreased slightly at 25 μM and 50 μM , and increased at 100 μM , 150 μM and 200 μM concentrations. In the MCF-7 cell line, CI alterations increased at all concentrations compared with the untreated control. However, in the healthy fibroblast cell line, the CI alterations decreased at all concentrations compared with the untreated control, which limits the use of V_2O_5 for its cytotoxic effect *in vivo*.

Conclusion: The combination of conventional anticancer drugs can be used to increase the effectiveness and reduce the adverse effects of these drugs considering stages of cancer and cancer type. Our results suggest that V_2O_5 has disparate effects on several cancer cells at different concentrations.

Key words: xCELLigence, Colo-205, MCF-7, human fibroblast cell line, vanadium pentoxide

ÖZ

Amaç: Vanadyum bileşiklerinin çeşitli farmakolojik etkileri vardır ve tüm kanıtlar, vanadyum bileşiklerinin etkilerinin, başta doz ve hücre tipi olmak üzere birçok faktöre bağlı olduğunu ortaya koymaktadır. Vanadyum bileşiklerinin proapoptotik veya antiapoptotik etkisi esas olarak hücre türüne bağlıdır.

Gereç ve Yöntemler: Bu çalışmada, çeşitli kanser hücre hatlarında; kolorektal kanser hücre hattı (Colo-205), insan meme adenokarsinoma hücre hattı (MCF-7) ve normal insan fibroblast hücre hattı kullanılarak vanadyum pentoksidin (V_2O_5) sitotoksik aktivitesi araştırıldı. Sitotoksik etkilerini incelemek için V_2O_5 25-200 μM arasında 5 farklı konsantrasyonda hücrelere uygulandı ve empedans değişikliklerini değerlendirmek için xCELLigence gerçek zamanlı hücre analizi yapıldı. Bu çalışma, V_2O_5 'in Colo-205, MCF-7 ve insan fibroblast hücre hatlarındaki etkilerini gerçek zamanlı olarak gösteren ilk çalışmadır.

Bulgular: V_2O_5 , normal insan fibroblastında 12 saat sonuçlarına göre tüm konsantrasyonlarda Colo-205 ve MCF-7'den daha düşük sitotoksik etki gösterdi. Sağlıklı fibroblast hücre hattında, cell indeks (CI) kontrol ile karşılaştırıldığında tüm konsantrasyonlarda azaldı. Colo-205 hücre hattında CI, 25 μM ve 50 μM 'de azaldı; 100 μM , 150 μM ve 200 μM konsantrasyonlarında arttı. MCF-7 hücre hattında, CI kontrole kıyasla tüm konsantrasyonlarda arttı.

Sonuç: Konvansiyonel anti-kanser ilaçlar ile kombinasyonu, kanser türü ve evreleri dikkate alınarak bu ilaçların yan etkilerini azaltmak ve etkinliği arttırmak için kullanılabilir. Bulgularımız; V_2O_5 'in farklı konsantrasyonlarda çeşitli kanser hücreleri üzerinde farklı etkilere sahip olduğunu düşündürmektedir.

Anahtar kelimeler: xCELLigence, Colo-205, MCF-7, insan fibroblast hücre hattı, vanadyum pentoksit

*Correspondence: E-mail: ecz_ebru_ozturk@hotmail.com, Phone: +90 352 207 66 66/28276 ORCID-ID: orcid.org/0000-0002-7088-7490

Received: 13.01.2017, Accepted: 09.03.2017

©Turk J Pharm Sci, Published by Galenos Publishing House.

INTRODUCTION

Cancer is a disease in which the control of growth is lost in one or more cells, leading either to a solid mass of cells known as a tumor or to a liquid cancer. It is one of the leading causes of death throughout the world.¹ Colorectal carcinoma is the most common gastrointestinal neoplasm and the second highest cause of death from cancer in the western world. In spite of recent advances in neoadjuvant therapeutic modalities, treatment success is limited in advanced stages of colorectal carcinoma.² Breast cancer has become the most prevalent cancer and the leading cause of death among women worldwide despite the fact that available therapeutics have successfully controlled breast cancer mortality, particularly in advanced countries.³

Vanadium (V) is a trace element that is present in the mammalian body. Recent studies have shown that both inorganic compounds of vanadium (IV) or V and their complexes with organic ligands, in which V valency may vary from III to V, exhibit cytostatic activity and suppress tumor cell growth *in vitro* and *in vivo*.⁴ Studies on various cell lines revealed that V exerts its antitumor effects by means of inhibition of cellular tyrosine phosphatases and/or activation of tyrosine phosphorylases. Both effects activate signal transduction pathways leading either to apoptosis and/or to activation of tumor suppressor genes. Moreover, V compounds (VCs) may induce cell-cycle arrest and/or cytotoxic effects through DNA cleavage and fragmentation, and plasma membrane lipoperoxidation. V may also exert inhibitory effects on cancer cell metastatic potential via modulation of cellular adhesive molecules and reverse antineoplastic drug resistance.⁵

In different cancer cell lines, some VCs acted as inhibitors of cell proliferation in the whole range of tested concentrations. These VCs were then evaluated as potentially antitumor agents.⁶ V pentoxide (V_2O_5) was appointed to be studied by the National Cancer Institute as a representative of the metals class.⁷ It is obvious that tumor cells could be treated with various metal oxide nanoparticles, and specifically, V_2O_5 nanoparticles have an admirable potential due to the high cytotoxicity and antitumor effects of V. Vanadium oxides could be more toxic than V salts. Additionally, it has been shown that the same VCs could possess selective cytotoxicity to various cell lines.⁸

The Roche xCELLigence real-time cell analysis (RTCA) system provides incessant, quantitative, and real-time monitoring of cells based on impedance measurements for analyzing the status of adherent cells *in vitro*. The measurement of electrical impedance gives an idea about the adherence, proliferation, and migration of cells. The changes observed in impedance due to cell attachment and spreading are expressed as the cell index (CI). The CI reflects cell viability; cell number, attachment quality, and cell morphology.^{9,10} Monitoring of cell viability is critical and the xCELLigence system enables continuous measurement and quantification of cells.¹¹ Also, time-dependent physiologic inhibitory concentration (IC_{50}) values can be calculated. It is a

more reliable test because classic toxicity tests measure single IC_{50} end-points at one time point.¹⁰

The present study was designed to detect impedance alterations reflecting the cytotoxicity of V_2O_5 on different cell lines. The xCELLigence technology was chosen because it has been used previously for monitoring cell viability in real time.⁹ In this study we investigated the effect of the compound on the growth of a colorectal cancer cell line (Colo-205), a human breast adenocarcinoma cell line (MCF-7), and also a normal human fibroblast cell line at different doses *in vitro*. This study is the first to show V_2O_5 's effects on Colo-205, MCF-7, and human fibroblast cell lines in a real-time manner.

EXPERIMENTAL

Chemicals

Trypsin-ethylenediaminetetraacetic acid (EDTA) (T3924), fetal bovine serum (FBS, F2442), penicillin-streptomycin (P4333), V_2O_5 (CAS Number: 1314-62-1), Dulbecco's Modified Eagle's Medium (DMEM, D5546) were purchased from Sigma Aldrich.

Cell culture

MCF-7 [American Type Culture Collection (ATCC), HTB-22] human breast cancer cell line, Colo-205 (CCL-222) human Colo-205 purchased from ATCC. Human fibroblast cell line gifted to us from GENKOK (Kayseri/Turkey). MCF-7 (12.500 cells/well) and Colo-205 (12.500 cells/well) cells cultured with DMEM containing FBS 10%, L-glutamin 1%, 100 U/mL penicillin and 100 μ g/mL streptomycin. Human fibroblast cells (3000 cells/well) cultured with DMEM containing FBS 20%, L-glutamin 1%, 100 U/mL penicillin and 100 μ g/mL streptomycin. The cells were grown to 80% confluence at 37°C and humidified in an atmosphere with 5% CO_2 . When cells reached approximately 80% confluence, we detached cells with 0.25% trypsin-EDTA. The cells were centrifuged using a Universal 320R (Hettich, Zentrifugen, 1406 Germany) at 1000 rpm for 5 min at 25°C and seeded on a 96-well E-plate for xCELLigence analysis. When the cells reached the log growth phase approximately 24 h later from seeding to E-plate, we treated the cells with V_2O_5 for 25, 50, 100, 150, 200 μ M concentrations.

Xcelligence real-time cell analysis

The cytotoxic effect of V_2O_5 was monitored using an xCELLigence RTCA as described by manufacturer's instructions (Roche Applied Science and ACEA Biosciences) with slight modifications. First, optimal seeding concentrations of MCF-7, Colo-205, and fibroblast cells were determined and then the cells were seeded in 96-well E-plates. Cell proliferation, attachment, and spreading were monitored every 15 min via the impedance of the E-plate wells. Approximately 24 h post-seeding, when the cells were in the log growth phase, we treated cells with V_2O_5 and controls received only medium and replicated 4-times; the experiments were run for about 72 h.

Cell growth and proliferation assay using the xcelligence system

At the end of the experiment, all calculations were made using

the integrated software of the xCELLigence RTCA system (Figure 1). A unitless parameter termed CI is derived to represent cell status based on the measured relative change in electrical impedance that occurs in the presence and absence of cells in the wells, which is calculated based on the following formula: $CI = (Z_i - Z_0) / 15$, where Z_i is the impedance at an individual point of time during the experiment, and Z_0 is the impedance at the start of the experiment (Figure 2). The RTCA software performs the curve-fitting of the selected “sigmoidal dose-response equation” and calculated logarithmic half maximum effect of concentration [$\log(IC_{50})$] values at a given time points based on log concentrations producing a 50% reduction of CI value relative to the control CI value (100%).

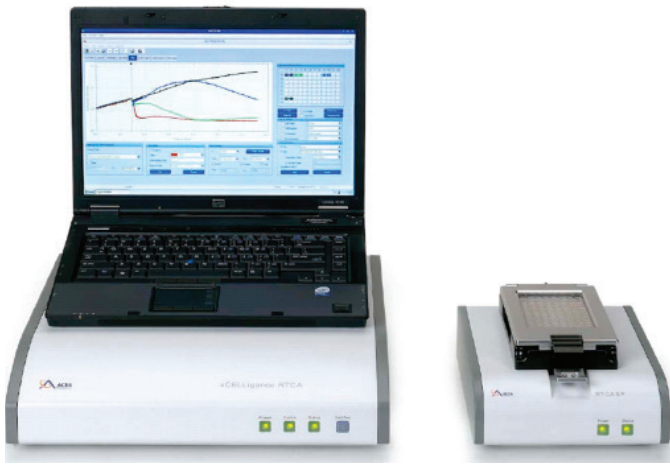


Figure 1. xCELLigence real time cell analyser single plate¹⁰

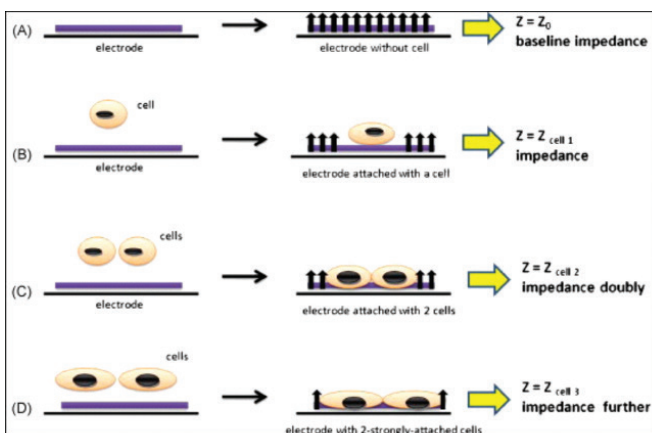


Figure 2. Scheme of xCELLigence impedance alteration¹⁰

Baseline impedance: No cells on an electrode surface (A). **Impedance:** A cell attaches to the electrode surface and partially blocks the electrical current in the circuit, inducing an increase in the electrode impedance (B). **Impedance doubly:** Two cells attach to the electrode surface and even further reduce the electrical current, as compared with B, inducing doubly-increased impedance (C). **Impedance further:** Two cells attach to the electrode surface with more extension, which induces much more impedance in comparison with C (D)

Statistical analysis

For each study group, data were derived from at least three independent experiments. Statistical analysis was performed using the GraphPad Prism Software Version 5.03 using Sidak's multiple comparisons test to compare differences in values between the control and experimental group. Data are expressed as mean \pm standard deviation. Values of all significant correlations ($p < 0.05$) are given with degrees of significance indicated (* $p < 0.01$, ** $p < 0.001$, *** $p < 0.0001$, **** $p < 0.00001$).

RESULTS

The xCELLigence system was used to analyse impedance alterations by the cytotoxic effect of V_2O_5 on normal human fibroblast, Colo-205 and MCF-7 cell lines. Normal human fibroblasts, Colo-205, and MCF-7 cell lines were exposed to V_2O_5 25 μM , 50 μM , 100 μM , 150 μM and 200 μM for 72 h. V_2O_5 exhibited a cytotoxic effect on normal human fibroblasts at 25 μM , 50 μM , 100 μM , 150 μM , and 200 μM concentrations (Figure 3). In the healthy fibroblast cell line, the CI alterations decreased at all concentrations compared with the untreated control (Figure 4). In the Colo-205 cell line, the CI alterations decreased slightly at 25 μM and 50 μM , and increased at 100 μM , 150 μM , and 200 μM concentrations (Figure 5 and Figure 6). In the MCF-7 cell line, the CI alterations increased at all concentrations compared with the untreated control (Figure 7 and Figure 8). The IC_{50} values obtained in the studied concentrations for 12 h and 24 h incubations in these cell lines are shown in Table 1.

Table 1. IC_{50} values for V_2O_5

Cell line	IC_{50} 12 h	IC_{50} 24 h
Human fibroblast cells	136.741 μM	101.18 μM
Colo-205	118.58 μM	145.29 μM
MCF-7	64.14 μM	219.82 μM

V_2O_5 : Vanadium pentoxide, Colo-205: Colorectal cancer cell line, IC_{50} : Inhibitory concentration

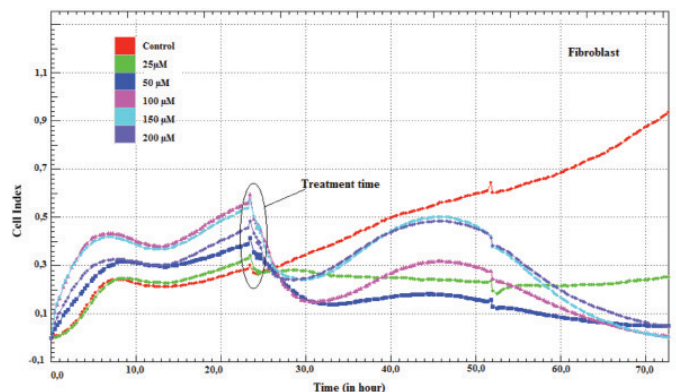


Figure 3. Dynamic monitoring of fibroblast cell adhesion and proliferation using the xCELLigence system. Fibroblast at a density of 3000 cells/well in E-plates were observed over 72 h

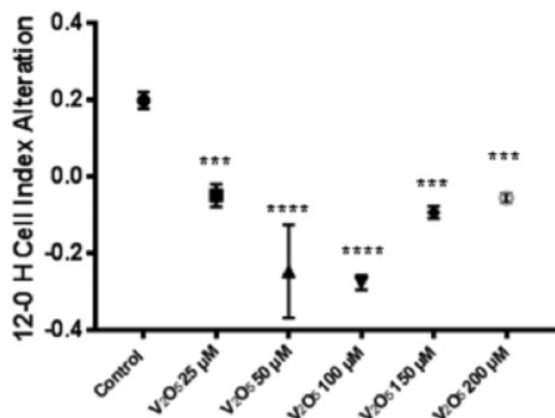


Figure 4. CI alterations after 12 h incubation of the healthy fibroblast cell line by V₂O₅ treatment. Data were calculated from three independent experiments. Data are presented as mean ± standard deviation, ***p<0.0001 and ****p<0.00001 compared with the untreated control

V₂O₅: Vanadium pentoxide, CI: Cell index

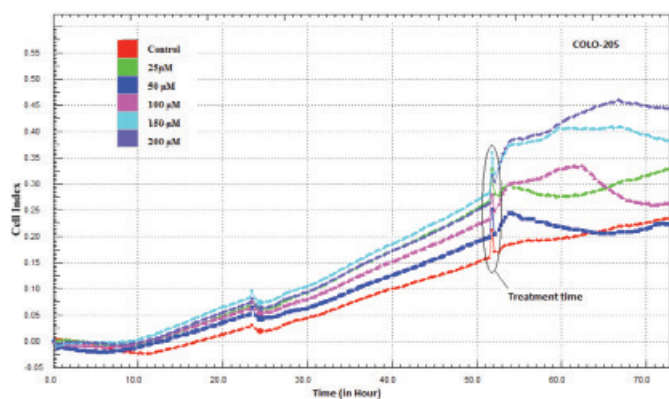


Figure 5. Dynamic monitoring of Colo-205 cell adhesion and proliferation using the xCELLigence system. Colo-205 at a density of 12.500 cells/well in E-Plates were observed over 72 h

Colo-205: Colorectal cancer cell line

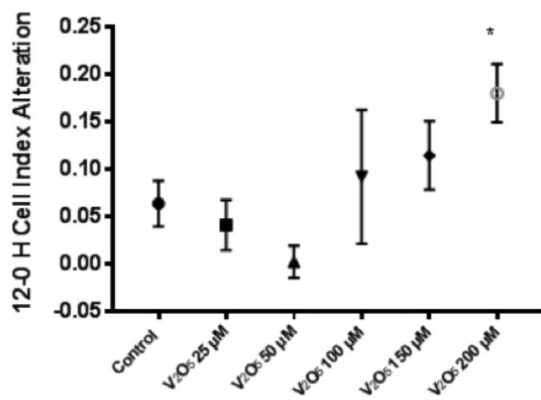


Figure 6. CI alterations after 12 h incubation of the Colo-205 cell line by V₂O₅ treatment. Data are presented as mean ± standard deviation, *p<0.01 compared with the untreated control

Colo-205: Colorectal cancer cell line, V₂O₅: Vanadium pentoxide

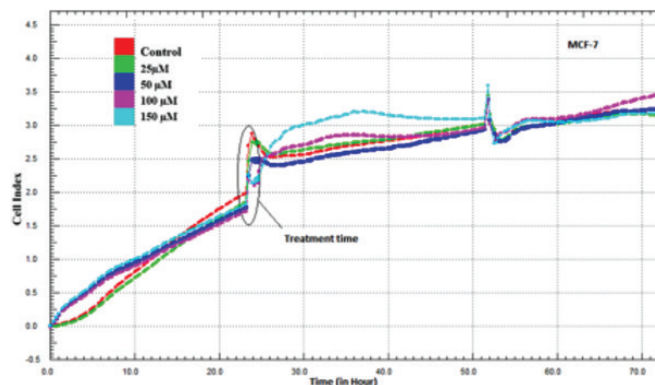


Figure 7. Dynamic monitoring of MCF-7 cell adhesion and proliferation using the xCELLigence system. MCF-7 at a density of 12.500 cells/well in E-Plates were observed over 72 h

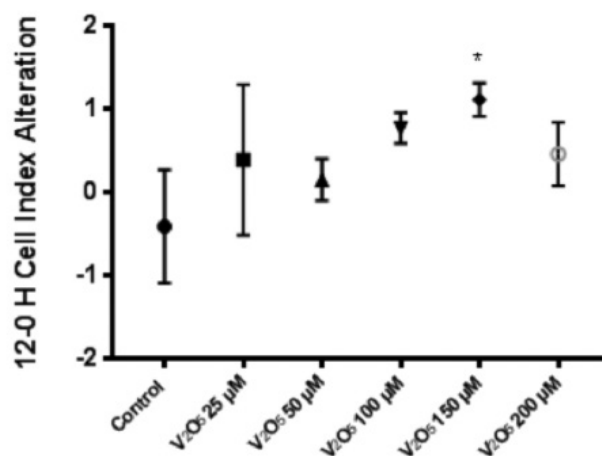


Figure 8. CI alterations after 12 h incubation of the MCF-7 cell line by V₂O₅ treatment. Data are presented as mean ± standard deviation, *p<0.01, compared with the untreated control

V₂O₅: Vanadium pentoxide

DISCUSSION

Metallodrugs in particular represent new and powerful tools for diverse therapeutic applications. To date, various metallodrugs have shown interesting biologic activities for chemotherapy. In this field, cisplatin was the first inorganic compound with high relevance in cancer treatment. This compound was a leader agent in clinical use. Toxicity and resistance problems triggered the development of other platinum drugs with better clinical perspective and also raised scientific interest in the putative antitumor properties of VCs. Various scientific articles reviewed by León et al.¹² showed that complexes of these metals were the new metal-based drugs used in the treatment of several cancers, such as lung, colon, breast, and bladder cancer. Vanadate is a transition element that is present in nature and was shown to be a nonspecific inhibitor of protein tyrosine phosphatases. VCs exhibit antitumor actions in several cancer cell lines.^{12,13}

The xCELLigence RTCA equipment uses specific microtiter E-plates coated with gold-microelectrodes that detect the attachment of adherent cells, thus modifying the impedance signal. The xCELLigence RTCA is a non-invasive, impedance-based biosensor system that can measure cell viability, migration, growth, spreading, and proliferation. Alterations in cell morphology and behavior are continuously monitored in real-time using microelectronics located in the wells of RTCA E-plates. As shown previously, the xCELLigence system is well-suited to analyze drug effects on cell proliferation, cytostasis, and cytotoxicity in real-time. In comparison with single endpoint assays, the availability of drug effect profiles over the whole experimental period allows building of dynamic growth curves. To evaluate the utility of this system for analysis of targeted therapies, Ruiz et al.¹⁴ subjected two established non-small cell lung cancer cell lines, H522 and H3122, to crizotinib treatment. The real-time monitoring system allowed them to determine the latency time of the drug effect on cell growth.

Tumor cell lines with various proliferative rates were equally sensitive to orthovanadate cytotoxicity. Sodium orthovanadate (Na_3VO_4) at concentrations greater than 5 μM has antineoplastic properties *in vitro* and *in vivo*.¹⁵ Within the concentration range of 1–20 μM , Na_3VO_4 demonstrated a time- and dose-dependent inhibition of autocrine growth of the human carcinoma cell lines A549 (lung), HTB44 (kidney) and DU145 (prostate), as compared with appropriate controls (without Na_3VO_4). Klein et al.¹⁶ also revealed that HTB44, A549, and DU15 cell lines had different sensitivity to Na_3VO_4 . Kordowiak et al.¹⁷ showed progressive growth inhibition of rat hepatoma H35-19 cells within the range 0.5–20.0 μM concentrations of three V salts. The most effective (and/or toxic) was sodium metavanadate (NaVO_3), whereas vanadyl sulfate showed a relatively mild action. As compared with metavanadate or vanadyl sulphate, and especially organic V derivatives, previously studied by the same authors under similar experimental conditions, Na_3VO_4 showed an intermediate effect.¹⁷ Yang et al.¹³ demonstrated that sodium vanadate had cytotoxic effects on esophageal squamous carcinoma cell line EC109 at 50 μM . The antiproliferative effect of bis(acetylacetonato)-oxidovanadium(IV) and NaVO_3 and the underlying mechanisms were investigated in the human pancreatic cancer cell line AsPC-1. VCs can be regarded as a novel type of anticancer drug through the prolonged activation of the mitogen-activated protein kinase/extracellular signal-regulated kinase pathway but retained AKT activity.¹⁸ V has no carcinogenic effect but its presence in cancer cells and its interactions with many key enzymatic processes results in modified expression of p53 and Bax and in down-regulation of Bcl-2 proteins and in antiproliferative activity. The anticancer effects of V in various forms have been demonstrated using *in vitro* and *in vivo* experiments.¹⁹ VCs were introduced into therapy due to their low IC_{50} , and antiproliferative and proapoptotic effects. Additionally, VCs stimulate the cell cycle, thereby inhibiting apoptosis, because both processes are mutually related. The above processes promote tumor cell growth at early stages of the disease and have an antitumor effect in the

advanced stages of cancer. VCs used at low concentrations had selective effects on tumor cells in *in vivo* and *in vitro* studies. The effects of VCs depend on many factors, mainly on the type of cells, the type of VC, and its dose. It appears that the proapoptotic or antiapoptotic effect of VCs depends strongly on the cell type.²⁰

In our study, we investigated the effects of V_2O_5 on three different cell lines, including human fibroblast cells, MCF7, and Colo-205. In the Colo-205 cell line, CI alterations decreased slightly at 25 μM and 50 μM , and increased at 100 μM , 150 μM and 200 μM concentrations. In the MCF-7 cell line, CI alterations increased at all concentrations compared with the untreated control. In the human fibroblast cell line, CI alterations decreased at all concentrations. Our results suggest that although V_2O_5 causes toxicity on human fibroblast cells, it also shows an antiproliferative effect at 25 and 50 μM concentrations and a proliferative effect at high concentrations on Colo-205, and a proliferative effect on MCF-7 cell lines at all concentrations used.

CONCLUSION

VCs have various pharmacologic effects and affect various biochemical processes, and all evidence suggests that the effects of VCs depend on many factors, mainly on the type of cells and their doses. It appears that the proapoptotic or antiapoptotic effect of VCs depends largely on the cell type. Our results are important for further mechanism of action studies because we have shown that trace amounts of V_2O_5 with conventional therapies might strengthen or weaken the impact of the treatment. Additional mechanism-of-action studies should be performed to confirm the beneficial and toxic effects of V_2O_5 in different experiments and cancer cell types at high or low doses. Combinations of conventional anticancer drugs can be used to increase the effectiveness and reduce the adverse effects of these drugs with consideration to the stages of cancer and cancer type. Our results suggest that V_2O_5 has disparate effects on several cancer cells at different concentrations. This study is the first to show V_2O_5 's effects on Colo-205, MCF-7, and human fibroblast cell lines in a real-time manner.

ACKNOWLEDGEMENT

The project received no financial support.

Conflict of interest: The authors declare that there are no conflicts of interest.

REFERENCES

1. Nussbaumer S, Bonnabry P, Veuthey JL, Fleury-Souverain S. Analysis of anticancer drugs: a review. *Talanta*. 2011;85:2265–2289.
2. Reuveni D, Halperin D, Shalit I, Priel E, Fabian I. Moxifloxacin enhances etoposide-induced cytotoxic, apoptotic and anti-topoisomerase II effects in a human colon carcinoma cell line. *Int J Oncol*. 2010;37:463–471.
3. Wei H, Fu P, Yao M, Chen Y, Du L. Breast cancer stem cells phenotype and plasma cell-predominant breast cancer independently indicate poor survival. *Pathol Res Pract*. 2016;212:294–301.

4. Abakumova Oyu, Podobed OV, Belayeva NF, Tochilkin AI. Anticancer activity of oxovanadium compounds. *Biochem (Mosc) Biomed Chem Suppl Ser.* 2012;6:164-170.
5. Evangelou AM. Vanadium in cancer treatment. *Crit Rev Oncol Hematol.* 2002;42:249-265.
6. Pessoa JC, Etcheverry S, Gambino D. Vanadium compounds in medicine. *Coordin Chem Rev.* 2015;301:24-48.
7. National Toxicology Program. NTP toxicology and carcinogenesis studies of vanadium pentoxide (CAS No. 1314-62-1) in F344/N rats and B6C3F1 mice (inhalation). *Natl Toxicol Program Tech Rep Ser.* 2002:1-343.
8. Ivankovic S, Music S, Gotic M, Ljubešić N. Cytotoxicity of nanosize V2O5 particles to selected fibroblast and tumor cells. *Toxicol in vitro.* 2006;20:286-294.
9. Keogh RJ. New technology for investigating trophoblast function. *Placenta* 2010;31:347-350.
10. Urcan E, Haertel U, Styllou M, Hickel R, Scherthan H, Reichl FX. Real-time xCELLigence impedance analysis of the cytotoxicity of dental composite components on human gingival fibroblasts. *Dent Mater.* 2010;26:51-58.
11. Golke A, Cymerys J, Słonska A, Dzieciatkowski T, Chmielewska A, Tucholska A, Banbura MW. The xCELLigence system for real-time and label-free analysis of neuronal and dermal cell response to Equine Herpesvirus type 1 infection. *Pol J Vet Sci.* 2012;15:151-153.
12. León IE, Cadavid-Vargas JF, Di Virgilio AL, Etcheverry SB. Vanadium, Ruthenium and Copper Compounds: A New Class of Nonplatinum Metallodrugs with Anticancer Activity. *Curr Med Chem.* 2017;24:112-148.
13. Yang J, Zhang Z, Jiang S, Zhang M, Lu J, Huang L, Zhang T, Gong K, Yan S, Yang Z, Shao G. Vanadate-induced antiproliferative and apoptotic response in esophageal squamous carcinoma cell line EC109. *J Toxicol Environ Health A.* 2016;79:864-868.
14. Ruiz C, Kustermann S, Pietilae E, Vlainic T, Baschiera B, Arabi L, Lorber T, Oeggerli M, Savic S, Obermann E, Singer T, Rothschild SI, Zippelius A, Roth AB, Bubendorf L. Culture and Drug Profiling of Patient Derived Malignant Pleural Effusions for Personalized Cancer Medicine. *PLoS One.* 2016;11:e0160807.
15. Cruz TF, Morgan A, Min W. *In vitro* and *in vivo* antineoplastic effects of orthovanadate. *Mol Cell Biochem.* 1995;153:161-166.
16. Klein A, Holko P, Ligeza J, Kordowiak AM. Sodium orthovanadate affects growth of some human epithelial cancer cells (A549, HTB44, DU145). *Folia Biol (Krakow).* 2008;56:115-121.
17. Kordowiak AM, Klein A, Goc A, Dabros W. Comparison of the effect of VOSO₄, Na₃VO₄ and NaVO₃ on proliferation, viability and morphology of H35-19 rat hepatoma cell line. *Pol J Pathol.* 2007;58:51-57.
18. Wu JX, Hong YH, Yang XG. Bis (acetylacetonato)-oxidovanadium (IV) and sodium metavanadate inhibit cell proliferation via ROS-induced sustained MAPK/ERK activation but with elevated AKT activity in human pancreatic cancer AsPC-1 cells. *J Biol Inorg Chem.* 2016;21:919-929.
19. Novotny L, Kombian SB. Vanadium: possible use in cancer chemoprevention and therapy. *J Can Res Updates.* 2014;3:97-102.
20. Korbecki J, Baranowska-Bosiacka I, Gutowska I, Chlubek D. Biochemical and medical importance of vanadium compounds. *Acta Biochim Pol.* 2012;59:195-200.



Preparation and *In Vitro* Evaluation of Ibuprofen Spherical Agglomerates

İbuprofen Küresel Aglomeralarının Hazırlanması ve *In Vitro* Değerlendirmesi

¹ Nagaraju RAVOURU¹, ² Subhash Chandra Bose PENJURI^{2*}, ³ Saritha DAMINENI³, ⁴ Raja Lakshmi MUNI¹, ⁵ Srikanth Reddy POREDDY²

¹Sri Padmavati Mahila Visvavidyalayam, (Women's University), Institute of Pharmaceutical Technology, Tirupati, Andhra Pradesh, India

²MNR College of Pharmacy, Department of Pharmaceutics, Sangareddy, Telangana, India

³Sultan-ul-Uloom College of Pharmacy, Department of Pharmaceutics, Hyderabad, Telangana, India

ABSTRACT

Objectives: Ibuprofen, an anti-inflammatory drug, is characterized by poor water solubility, which limits its pharmacologic effects. The present work aimed to the study the effect of agglomeration on the micromeritic properties and dissolution of ibuprofen.

Materials and Methods: Ibuprofen agglomerates were prepared by solvent change method using water, dichloromethane and DMSO as poor solvent, bridging liquid and good solvent respectively in the ratio of 57.5:12.5:30. Process variables such as amount of bridging liquid, mode of addition, temperature and stirring rate were optimized.

Results: SEM studies indicate that agglomerates produced were spherical and exhibit irregular shape. X-Ray Powder Diffraction spectra revealed the absence of polymorphism. DSC spectra showed no change in melting point indicating absence of crystal modification. The agglomerates exhibited improved solubility, dissolution rate and micromeritic properties compared to pure drug.

Conclusion: Anti-inflammatory studies were conducted in Wistar strain male albino rats and ibuprofen agglomerates showed more significant activity than the pure drug which may be due to better absorption. Ulcerogenic potential study was carried out for pure ibuprofen and agglomerates. Better ulcerogenic potential was observed in ibuprofen agglomerates treated rats.

Key words: Ibuprofen, spherical agglomeration, anti-inflammatory activity, ulcerogenic potential

ÖZ

Amaç: Bir anti-inflamatuvar ilaç olan ibuprofen, zayıf suda çözünürlüğü ile karakterize olup, farmakolojik etkileri sınırlar. Bu çalışmada aglomerasyonun mikromeritik özellikler ve çözünme üzerindeki etkilerinin incelenmesi amaçlanmıştır.

Gereç ve Yöntemler: İbuprofen aglomeraları, su, diklorometan ve zayıf solvent olarak sırasıyla 57.5:12.5:30 oranında sıvı ve iyi çözücü köprü halindeki dimetil sülfoksit kullanılarak çözücü değiştirme yöntemi ile hazırlandı. Köprü sıvısı miktarı, ilave modu, sıcaklık ve karıştırma oranı gibi proses değişkenleri optimize edildi.

Bulgular: Taramalı elektron mikroskopu çalışmaları, üretilen aglomeraların küresel olduğunu ve düzensiz şekli olduğunu göstermektedir. X-Işın Pudrası Difraksiyon spektrumu polimorfizm yokluğunu ortaya koydu. Diferansiyel tarama kalorimetrisi spektrumu, erime noktasında kristal modifikasyonun yokluğunu gösteren herhangi bir değişiklik göstermedi. Aglomeralar, saf ilaca kıyasla gelişmiş çözünürlük, çözünme hızı ve mikromeritik özellikler sergiledi.

Sonuç: Anti-inflamatuvar çalışmalar Wistar suşu erkek albino sıçanlarında yürütülmüş ve ibuprofen aglomeraları saf ilaca göre daha iyi bir absorpsiyona bağlı olarak daha belirgin bir aktivite gösterdi. Saf ibuprofen ve aglomera için ülserojenik potansiyel çalışması gerçekleştirildi. İbuprofen aglomeraları ile tedavi edilen sıçanlarda daha iyi ülserojenik potansiyel gözlenmiştir.

Anahtar kelimeler: İbuprofen, küresel toplanma, anti-inflamatuvar aktivite, ülserojenik potansiyel

*Correspondence: E-mail: penjurisubhash@gmail.com, Phone: +919848033974 ORCID-ID: orcid.org/0000-0002-9365-0701

Received: 29.01.2017, Accepted: 13.04.2017

©Turk J Pharm Sci, Published by Galenos Publishing House.

INTRODUCTION

Tablets are known to be the most popular dosing form of all pharmaceutical preparations for oral route administration because of easy administration by the patient, least content variability, and great precision. Apart from these advantages, the formulation and manufacturing of tablets is the most convenient and easy process. One of important factors that influence the success of tablet formation is the flowability and compressibility of materials. Direct compressibility is one of the best and most economical techniques for manufacturing tablets. This facilitates processing without the need for moisture or heat, and involves a small number of processing steps. However, the technique depends on the flowability, particle size and particle size distribution, bulk density, and the compressibility of the crystalline drug substances.¹⁻³ Most drugs such as non-steroidal anti-inflammatory drugs exhibit poor compressibility and flowability and are not suitable for direct compression. To enhance the flow properties and compressibility of drugs, several methods have been introduced by researchers. In addition to increasing the efficiency of the manufacturing process, it is also important to increase the bioavailability of the drug by improving the solubility of the bulk drug powder.⁴⁻⁶

Spherical crystallization/agglomeration is a novel method to increase the bioavailability of drugs that inherently have poor aqueous solubility. It is a multiple unit process in which crystallization, agglomeration, and spheronization can be performed simultaneously in one step. The resultant crystals have a characteristic shape, therefore, the micromeritic properties such as flowability, packability, and compressibility of the resultant crystals are dramatically improved, thereby direct tableting or coating is possible without further processing steps like mixing, agglomeration, and sieving.⁷⁻⁹

Spherical crystallization/agglomeration is a process of formation of crystal aggregates held together by liquid bridges. The agglomerates are formed by agitating the crystals in a liquid suspension in the presence of a bridging liquid. The bridging liquid should be immiscible in the suspending medium, but capable of cementing the particles to be agglomerated.¹⁰ This technique can also be exploited to increase solubility, dissolution, and hence bioavailability of poorly soluble drugs.¹¹ These modifications allow for the practice of more efficient manufacturing methods that could save time and reduce economic risk.

MATERIALS AND METHODS

Materials

Ibuprofen was obtained as a gift sample from Granules India, Hyderabad, India. Dimethyl sulfoxide (DMSO) and dichloromethane were procured from Qualigens fine chemicals, Chennai, India and SRL chemicals, Mumbai, India, respectively. All chemicals and buffers used were of analytical grade.

Methods

Selection of liquid proportions for spherical agglomeration

A typical spherical agglomeration process requires a good

solvent, a poor solvent for a drug, and a bridging liquid.³ The selection of these solvents depends on the miscibility of the solvents and solubility of the ibuprofen in individual solvents. A ternary phase diagram of DMSO, dichloromethane, and water was constructed to select a suitable zone with an appropriate ratio of the three solvents for the preparation of spherical agglomerates.

Effect of amount of bridging liquid on agglomeration

A bridging liquid is used to cause spherical agglomeration. It should be capable of wetting the particle surface so as to form liquid bridges and dissolving the sample particles.¹² Hence, the bridging liquid exerts marked influence on the yield and rate of agglomeration as well as on the strength of the resulting agglomerates. The rate determining step in spherical agglomeration is when the bridging liquid is squeezed out of the pores of the initial flocs, and later transformed into small aggregates or spherical crystals. Accordingly, the amount of bridging liquid used is one of the critical operating variables.¹² The amounts of solvents selected from the ternary diagram were further modified and studied for influence of the bridging liquid on the process and product. The effect of the type of bridging liquid on agglomeration was seen using dichloromethane, chloroform, and cyclohexane as bridging liquids.

Effect of mode of addition of bridging liquid on the agglomeration

To investigate the effect of the mode of addition of bridging liquid, the bridging liquid was added dropwise and the as the whole amount, separately.¹²

Effect of agitation speed of the system on agglomeration

The impact of agitation speeds of 300±25, 500±25, and 700±25 rpm was observed on the preparation of spherical agglomeration of ibuprofen.¹²

Effect of agitation time of the system on agglomeration

The impact of agitation times of 20 min, 30 min, and 60 min was observed on the preparation of spherical agglomeration of ibuprofen.¹²

Effect of temperature on agglomeration

The effect of different temperatures on the formation of spherical agglomerates of ibuprofen was observed at 20±5°C, 40±5°C, and 60±5°C.¹²

Preparation of ibuprofen agglomerates

Ibuprofen (4 g) was dissolved in 30 mL of DMSO at 40°C and the solution was added to 57.5 mL of water, which was maintained at 20°C under continuous stirring at 500 rpm with a propeller on a mechanical stirrer. When fine crystals of ibuprofen began to precipitate, 12.5 mL of dichloromethane (bridging liquid) was slowly added dropwise. After 30 min of stirring, agglomerates thus obtained were separated by filtration and dried. The dried agglomerates were then stored in a screw-capped jar in a desiccator.^{13,14}

Determination of drug content

Spherical agglomerates (50 mg) were triturated and dissolved in 250 mL of phosphate buffer pH 7.2. The solution was then

filtered. After suitable dilution with phosphate buffer pH 7.2, the solution was analyzed spectrophotometrically (1601 A, Shimadzu corporation, Kyoto, Japan) at 221 nm.¹⁵

Determination of melting point

The melting point of ibuprofen agglomerates were determined by placing the drug-filled capillary tubes in digital melting point apparatus (CDMP-300, Contech Instruments Ltd., Mumbai, India) and the melting point was noted (triplicates) and compared with the pure drug.¹⁶

Scanning electron microscopy (SEM) studie

The morphology of agglomerates was examined using a SEM (LEO 440I, Cambridge, England) operating at 15 KV.¹⁶

Fourier transform infrared spectroscopy (FTIR)

FTIR spectral measurements were taken at ambient temperature using a Perkin Elmer Model 1600 (Minneapolis, Minnesota, USA). Samples were dispersed in KBr powder and the pellets were made by applying 5-ton pressure. FTIR spectra were obtained through powder diffuse reflectance on the FTIR spectrophotometer.^{17,18}

Differential scanning calorimetric (DSC) studies

DSC (DSC-60, Shimadzu Corporation, Kyoto, Japan) studies were performed to authenticate the formation of the spherical crystals or agglomerates. DSC was used after calibration with indium and lead standards, and samples of the crystals (3-5 mg) were heated (range 30-200°C) at 10°C/min in crimped aluminium pans under a nitrogen atmosphere. The enthalpy of fusion and melting point were automatically calculated.^{17,18}

X-ray powder diffraction studies

X-ray powder diffraction patterns were obtained at room temperature using a Philips X'pert MPD diffractometer, with Cu as the anode material and graphite monochromator, operated at a voltage of 40 Ma, 45 Kv. The process parameters used were set as scan step size of 0.0170 (2θ).^{17,18}

Micromeritic properties

Determination of angle of repose

The flow properties of the powder were evaluated by determining the static angle of repose. This was measured according to the fixed funnel and free-standing cone method.¹⁹ A funnel with the end of the stem cut perpendicular to the axis of symmetry was secured with its tip 2.5 cm above graph paper placed on a flat horizontal surface. The powder was carefully poured through the funnel until the apex of the conical pile that formed just reached the tip of the funnel (h). The mean diameter (D=2r) of the powder cone was determined and the tangent of the angle of repose was given by:

$$\theta = \tan^{-1} (h/r)$$

Where, θ is the repose angle; h is the height; r is the radius.¹⁹

Measurement of compressibility index

Flowability of pure and agglomerated samples prepared was also assessed using Carr's index (CI). The CI was calculated from the bulk density and tapped densities. Tapped density was

determined by tapping the samples using digital bulk density apparatus (Veego, Mumbai, India). The CI was calculated according to the following equation²⁰:

$$CI (\%) = [(\rho_b - \rho_t) / \rho_b] \times 100$$

Where, ρ_t is tapped density and ρ_b is bulk density.

In vitro dissolution studies

The dissolution of ibuprofen pure drug and agglomerates were determined using the USP dissolution apparatus type II (Electrolab, Mumbai, India). The dissolution medium used was 900 mL of gastric simulating fluid without enzymes (pH 1.2). Five milliliters of sample solution were withdrawn at predetermined time intervals (10, 20, 30, 40, 50, and 60 min) and then filtered through Whatman filter paper No: 40 and the same amount was replaced in the dissolution flask to maintain sink conditions. The amount of dissolved ibuprofen was analyzed spectrophotometrically at 221 nm.¹⁵ *In vitro* dissolution data were statistically analyzed using One-Way ANOVA followed by the Tukey post hoc test for multiple comparisons using Graph Pad Prism. Differences were considered to be significant at a level of $p < 0.05$.

In vivo evaluation of agglomerates

Evaluation of anti-inflammatory activity

Healthy male albino rats weighing between 150-200 g were used for the study and individually maintained under standard conditions (12-hr light-dark cycles, 25±2°C, and 35-60% humidity). Food and water were available; the animals were fasted overnight before the experiment but they continued to have free water. The experimental protocol was designed and approved by the Institutional Animal Ethics Committee (Reg. No. 557/02/c/ CPCSEA). The animals were divided into three groups, each containing 6 animals.²¹

Group I: Inflammation-induced and vehicle-treated control.

Group II: Inflammation-induced and ibuprofen suspension [20 mg pure ibuprofen in 1% carboxymethylcellulose (CMC)]-administered animals.

Group III: Inflammation-induced and ibuprofen suspension (20 mg ibuprofen agglomerate in 1% CMC)- administered animals.

The pure ibuprofen suspension (in 1% CMC) and ibuprofen agglomerate suspension (in 1% CMC) were given orally. All the animals were treated as per the treatment schedule. After one hour, paw edema was induced by injecting 50 μ L of 1% w/v carrageenan into the sub planar region of the left hind paw. Paw volume was determined after one hour in all groups. Using a digital plethysmometer (PLM-01 plus, Orchid Scientifics, India), percentage inhibition of edema was calculated using the following equation.^{22,23}

$$\% \text{ inhibition} = (\text{paw volume of control} - \text{paw volume of treated}) \times 100 / \text{paw volume of control.}$$

The anti-inflammatory activity of ibuprofen and ibuprofen spherical agglomerates was statistically analyzed using One-Way ANOVA followed by the Tukey post-hoc test for multiple comparisons using Graph Pad Prism. Differences were considered to be significant at a level of $p < 0.05$.

Assessment of ulcerogenic potential of ibuprofen agglomerates

Healthy male albino rats weighing between 150-200 g were used for the study and individually maintained under standard conditions (12-hr light-dark cycles, $25\pm 2^\circ\text{C}$, and 35-60% humidity). The rats were fed with animal feed pellets and given water²⁴⁻²⁶. The rats were divided into three groups, each containing 6 animals as the control (group I), standard (group II), and test group (group III).

Group I: Vehicle treated control.

Group II: Inflammation-induced and ibuprofen suspension (20 mg pure ibuprofen in 1% CMC)-administered animals.

Group III: Inflammation-induced and ibuprofen suspension (20 mg ibuprofen agglomerate in 1% CMC)- administered animals.

The animals were kept fasting for 48 hr before test, but water was permitted. The pure ibuprofen suspension (in 1% CMC) and ibuprofen agglomerate suspension (in 1% CMC) were given orally. All the animals were treated as per the treatment schedule. The animals were then sacrificed after 6 hr.^{25,26} The stomachs were isolated and opened along the greater curvature, the mucosa was washed under slow running tap water and the number and size of ulcers was scored as per the method of Rao et al.²⁴ The pH of the stomach contents was determined using broad range pH paper.²⁷

Severity score:

0 = Normal-colored stomach

0.5 = Red coloration of stomach

1 = Spot ulcer

1.5 = Hemorrhagic streaks

2 = Ulcers ≥ 3 but ≤ 5

3 = Ulcers > 5

RESULTS AND DISCUSSION

Selection of solvent proportions of spherical agglomeration

Spherical agglomerates of ibuprofen were prepared using the simple agglomeration technique using a three-solvent system.^{16,18} A typical spherical agglomeration system involves a good solvent, a poor solvent for the drug, and a bridging liquid. The selection of these solvents depends on the miscibility of the solvents and solubility of the drug in individual solvents. Accordingly, acetone, DMSO, and octanol were chosen as good solvents for ibuprofen. Water acts as a non-solvent. Dichloromethane, cyclohexane, and chloroform were chosen as bridging liquids. Different combinations were tried using the ternary phase diagram to produce the optimum solvent system. Similar trials were conducted by Saritha et al.¹⁶ and Maghsoodi and Yari.¹⁸ The drug solubility and mutual miscibility of solvent systems were examined and DMSO, dichloromethane, and water were selected as a good solvent, bridging liquid, and poor solvent, respectively, for the preparation of ibuprofen agglomerates.

Preparation of spherical agglomerates

To select the best solvent composition, a ternary diagram was envisaged and DMSO: Dichloromethane: Water (30:12.5:57.5) were chosen for the study (Table 1) and (Figure 1).

To optimize ibuprofen spherical agglomeration by DMSO: Dichloromethane: Water system, several parameters were considered: among these, temperature difference between drug solution in DMSO and water, stirring time, stirring speed, and amount of dichloromethane (bridging liquid). A bridging liquid is used to cause spherical agglomeration, the same was stated by Saritha et al.¹⁶ and Maghsoodi and Yari¹⁸ and Maghsoodi and Hajipour.²⁸ It should be capable of wetting the particle surface so as to form liquid bridges and dissolving the sample particles; the same phenomenon was explained by Xia et al.²⁹ Hence, the bridging liquid exerts influence on the yield and rate of agglomeration, as well as the strength of the formed agglomerates. The same mechanism was described by Maghsoodi.³⁰

Agglomerates were formed by agitating the crystals in a liquid suspension and adding a bridging liquid, which preferentially wets the crystal surface to cause binding. The addition of a bridging liquid (dichloromethane) promotes the formation of liquid bridges between the drug crystals to form agglomerates. To optimize ibuprofen spherical agglomeration by DMSO/dichloromethane/water system, other process parameters were considered such as the amount and mode of addition of the bridging liquid, stirring speed and time, and temperature; similar conditions were followed by Saritha et al.¹⁶ The diameter of agglomerates was found to increase with increasing amounts of bridging liquid in the medium due to excessive bridging liquid on the surface for coalescence. Size of agglomerates

Table 1. Amount of solvents selected from the phase diagram used to prepare agglomerates of ibuprofen

DMSO (mL)	Dichloromethane (mL)	Water (mL)	% of bridging liquid
30	12.5	57.5	12.5
30	30	40	30
30	15	55	15
40	10	50	10

DMSO: Dimethyl sulfoxide

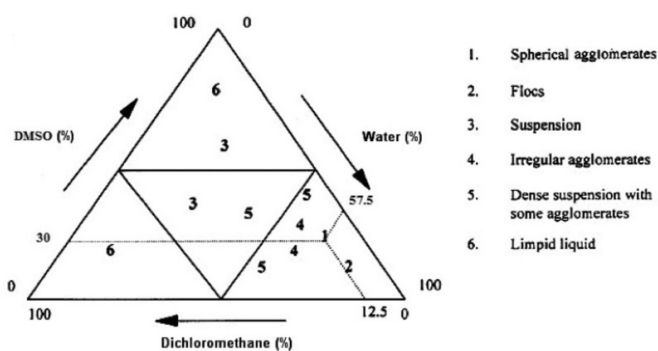


Figure 1. Ternary phase diagram of ibuprofen-DMSO/water/DCM

DMSO: Dimethyl sulfoxide

is very much dependent on the degree of agitation because agitation droplets form in the agglomeration medium, which induce movement of the droplets from in to out; the same was reported by Saritha et al.¹⁶ The intensity of this internal circulation depends on the speed. A lower stirring rate (300 rpm) reduces the possibility of obtaining agglomerates due to the slow circulation of droplets in the medium and slight collision between the droplets; similar procedures were followed by Kulkarni and Subhash Chandra Bose³¹ and Subhash Chandra Bose et al.³² At optimum speed (500 rpm), more compact and dense agglomerates were obtained (Table 2). Higher speed (700 rpm) induces agglomerate destruction due to more impact energy for collision because of the increased turbulence resulting in formation of agglomerates with irregular shape; the same results were observed by Bose et al.³² Therefore, 500 rpm was selected for the preparation of ibuprofen agglomerates, similarly by Saritha et al.¹⁶ and Kulkarni and Subhash Chandra Bose.³¹ The temperature of the solvent system was found to have a pronounced effect on the process of agglomeration. Agglomeration was not observed when the process was performed at $20\pm 5^\circ\text{C}$. This could be due to the reduced solubility of the drug in the solvent system. When the temperature was increased to $60\pm 5^\circ\text{C}$, very large agglomerates were produced due to enhanced solubility (saturation of the drug in the medium). Optimum agglomeration was achieved at $40\pm 5^\circ\text{C}$ due to the optimum solubility of the drug. Accordingly, $40\pm 5^\circ\text{C}$ was selected for the preparation of ibuprofen agglomerates; a similar procedure was followed by Kulkarni and Subhash Chandra Bose³¹ and Bose et al.³² The addition of a bridging liquid plays a vital role in the formation of agglomerates. When all the bridging liquid was added at one time the agglomerates were of irregular geometry, which may be due to its localization and hence its unavailability for efficient agglomeration; the same theory was reported by Bose et al.³² Dropwise addition with continuous agitation resulted in agglomerates of regular geometry, which can be attributed to the uniform distribution of the bridging liquid; the same theory was reported by Bose et al.³² Therefore, dropwise addition was selected for the preparation of ibuprofen agglomerates.

From the above study, ibuprofen agglomerates were prepared by using the following conditions:

DMSO: Dichloromethane: Water : 30:12.5:57.5

Table 2. Optimization of process variables for ibuprofen spherical agglomeration

S. No	Parameter	Variables	Observations
1	Concentration of bridging liquid (dichloromethane)	10%*	No agglomeration
		12.5%*	Agglomeration
		15%*	No agglomeration
		20 min*	No agglomeration
2	Agitation time	30 min*	Agglomeration
		1 hr min*	Fine particles are formed

*At $40^\circ\text{C}\pm 5^\circ\text{C}$, 500 ± 25 rpm and dropwise addition of bridging liquid

Mode of addition of DCM	: Dropwise
Agitation speed	: 500 ± 25 rpm
Agitation time	: 30 min
Temperature	: $40^\circ\text{C}\pm 5^\circ\text{C}$

Drug content

The drug content was determined in triplicate and was found to be in the range of 98.94 ± 1.73 - $99\pm 0.93\%$.

Melting point

The melting point of the ibuprofen and spherical agglomerates of ibuprofen were 72°C and 71°C , respectively. No change in the melting points of the pure and prepared agglomerates were observed. Thus, formation of polymorphs was overruled because crystal habit will not change the melting point. Similar findings were reported by Kumar et al.³³

SEM studies

The crystal habits and surface features were examined using SEM studies. The pure ibuprofen was in the form of rod-like particles and the agglomerates had round-shaped particles of irregular shape (Figure 2a and 2b). Under high magnification, it was further observed that the surfaces were not smooth and no liquid bridges were found in between two particles. Thus,

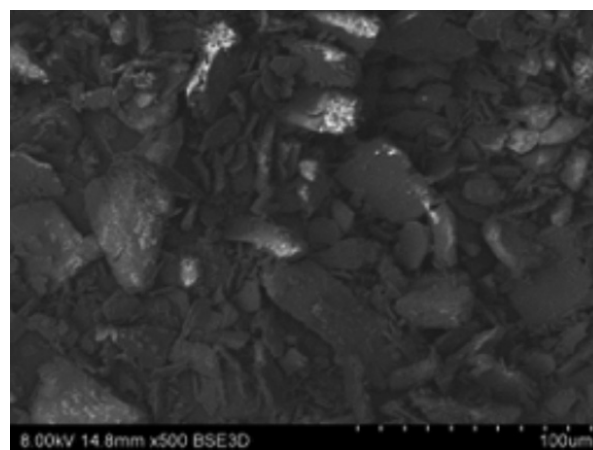


Figure 2a. SEM of pure ibuprofen

SEM: Scanning electron microscopy

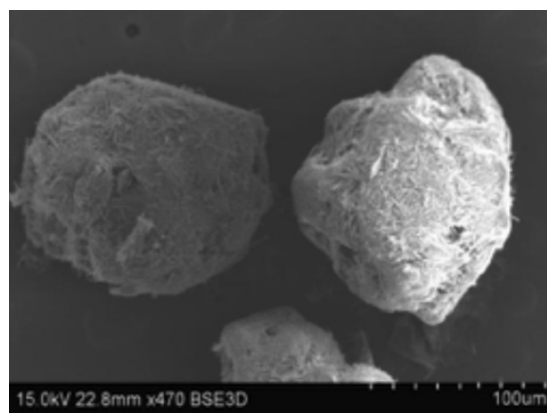


Figure 2b. SEM of agglomerates

SEM: Scanning electron microscopy

the produced clusters may be spherical agglomerates. Similar observations were reported by Viswanathan et al.³⁴ and Kulkarni and Dixit³⁵ who prepared spherical agglomerates of ibuprofen using the neutralization method.

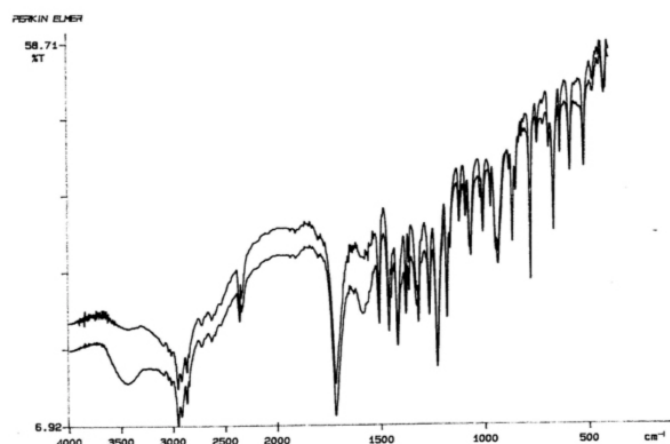


Figure 3. Fourier transform infrared spectroscopy spectra of ibuprofen and its agglomerates

FTIR studies

FTIR spectra (Figure 3) showed the characteristic absorption peaks of ibuprofen (according to Klaus Florey³⁶) at 1260 (CH₃ stretching vibration), 3000 (CO=OH stretch), 1710-1665 (C=O stretch) and 1600-1585 (C-C stretch) wave numbers, which indicates the presence of alkane, carboxylic, ketone group, and ring structure, respectively, in both pure and agglomerates of ibuprofen; similar findings were observed by Kachrimanis et al.³⁷ From the spectral data, it can be concluded that there was not much difference in spectra and absence of polymorphs. Similar observations were reported by Kulkarni et al.³⁸

DSC studies

DSC thermograms of pure and ibuprofen crystals are illustrated in Figure 4. The DSC pattern of pure ibuprofen and agglomerates showed a sharp endothermic peak at 77.51°C and 77.80°C, respectively, corresponding to its melting point. There was a sharp melting point with flat base line, which indicated that the material was not affected by hydration, solvation, and polymorphic transition. In addition, there was no interaction of drug with solvents. Similar observations were reported by Kulkarni and Dixit³⁵ and Kulkarni et al.³⁸, Kachrimanis et al.³⁷, and Pawar et al.³⁹

X-ray powder diffraction studies

XRD spectra of the prepared agglomerates showed no significant change in crystal structure and crystal habit when compared with pure ibuprofen. The small differences in the relative intensities of their peaks (Figure 5a and 5b) at the respective 2θ values (Table 3) may be attributed to differences in the particle size or crystallinity of the sample. Similar observation were reported by Kulkarni and Dixit³⁵ and Kulkarni et al.³⁸, Pawar et al.³⁹, and Rasenack and Muller.⁴⁰ This indicates that ibuprofen

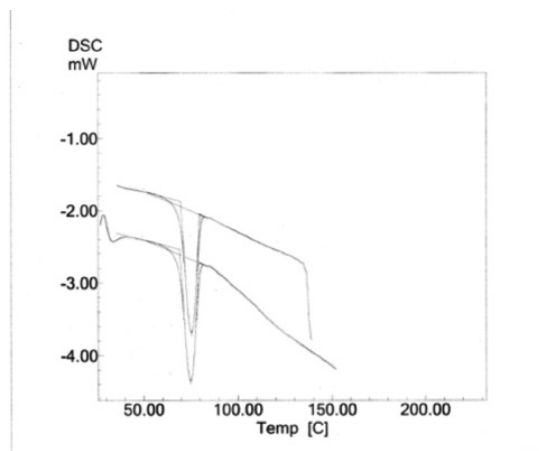


Figure 4. Differential scanning calorimetry thermograms of ibuprofen and its agglomerates

DSC: Differential scanning calorimetry

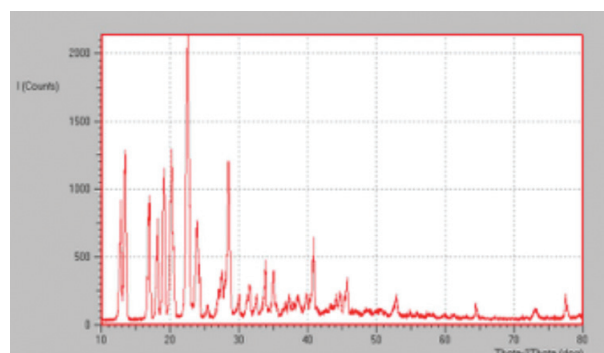


Figure 5a. X-ray diffraction spectra of ibuprofen

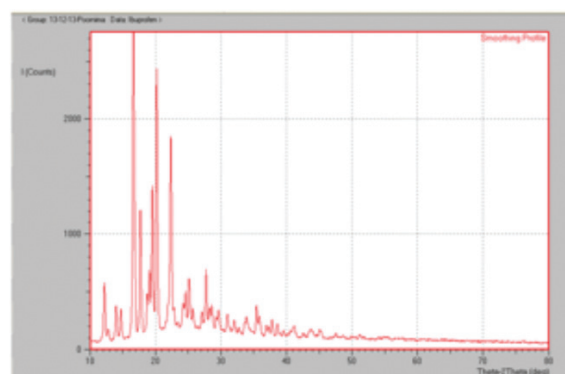


Figure 5b. X-ray diffraction spectra of spherical agglomerates of ibuprofen

does not undergo any polymorphic changes during the process of spherical agglomeration.

Micromeritic properties

Micromeritic properties such as bulk density, tapped density, angle of repose, and CI were determined and shown in Table 4. The bulk and tapped densities of the spherical agglomerates were lower than the corresponding value of the pure sample due to higher particle size and sphericity. The lower density is likely to be related to the intraparticle porosity and hence

the reduction in bulk density of the treated samples indicates a greater porosity within the agglomerated particles; similar findings were observed by Maghsoodi³⁰ and Gupta et al.⁴¹ CI for agglomerates was found to be lower when compared with the pure drug. This may be due to the formation of agglomerates. Fine particles with high surface to mass ratios are more cohesive than coarser particles, hence more influenced by gravitational force; similar findings were observed by Kumar et al.³³ and Viswanathan et al.³⁴ Decreased values of CI for agglomerates have better packability, indicating that they might be suitable for direct tableting; similar findings were observed by Maghsoodi³⁰ and Gupta et al.⁴¹ The flow properties of the crystals were reflected by the angle of repose. It was found that the angle of repose of the agglomerates was decreased when compared with pure ibuprofen. Such a decreased value indicates improvement in flowability, i.e., free flow of powder mass in comparison with the pure drug; similar findings were observed by Maghsoodi³⁰, Kumar et al.³³, Viswanathan et al.³⁴ and Gupta et al.⁴¹ Flowability of the powder was found to be decreased due to their formation of agglomerates. Here, the value of compressibility and angle of repose represents excellent and good flow of agglomerates, respectively, when compared with that of pure ibuprofen, which has very poor flow.

In vitro dissolution studies of agglomerates

The release of pure ibuprofen was less than that of ibuprofen agglomerates. The dissolution profile of agglomerates showed a significant ($p < 0.05$) difference when compared with pure drug. The reason for the faster dissolution may be due to the good wettability of the agglomerates, thus it was easily dissolved in the dissolution fluid, as reported by Jbilou et al.⁴² and Di Martino et al.⁴³ Ibuprofen agglomerates showed better dissolution than

Table 3. Comparative values of 2 θ and D values for pure drug and ibuprofen agglomerate

S. No	Pure drug		Ibuprofen crystals	
	Angle (2 θ)	D value (A $^\circ$)	Angle (2 θ)	D value (A $^\circ$)
1.	12.134	7.2877	12.222	7.23616
2.	14.546	6.0846	14.736	6.00634
3.	16.503	5.3671	16.66	5.31702
4.	17.546	5.0503	17.705	5.00559
5.	18.695	4.724	18.74	4.7313
6.	19.348	4.5838	19.52	4.5439

Table 4. Micromeritic properties of pure ibuprofen and agglomerates

No	Sample	Bulk density (g/cm 3)	Tapped density (g/cm 3)	CI (%)	Angle of repose ($^\circ$)
1.	Pure ibuprofen	0.833 \pm 2.31	0.55 \pm 1.9	33.9	40.6
2.	Ibuprofen Agglomerates	0.641 \pm 1.78	0.588 \pm 2.01	8.26	25.1

CI: Carr's index

the pure drug, which may lead to increased absorption rates and bioavailability, which is well correlated with the findings of Pawar et al.³⁹, Jbilou et al.⁴², Di Martino et al.⁴³, and Sano et al.⁴⁴ (Figure 6).

Evaluation of anti-inflammatory activity

Anti-inflammatory activity was tested for pure ibuprofen and agglomerates. Table 5 shows the results of paw edema and percentage inhibition of carrageenan-induced paw edema in rats treated with pure ibuprofen and agglomerates. An extremely significant ($p < 0.001$) inhibition of carrageenan-induced paw edema was observed in animals treated with ibuprofen agglomerates compared with the controls during the entire 5 hr duration of the study. Also, significant ($p < 0.05$) inhibition of carrageenan-induced paw edema was observed in animals treated with ibuprofen agglomerates compared with pure ibuprofen during the entire 5-h duration of the study (Table 5). This may be due to the increased dissolution of the agglomerates over pure drug, leading to better absorption and onset of drug action. Also, ibuprofen is a propionic acid derivative, its dissociation constant is 5.3; therefore it is easily absorbed in the acidic pH of the stomach because it is in an ionised form in acidic pH, as reported by Saritha et al.²² Moreover, due to the high wettability of agglomerates, the solubility of agglomerates was increased. Hence, agglomerates showed better anti-inflammatory activity over the pure drug. Therefore, the results of *in vivo* studies clearly demonstrate that ibuprofen agglomerates show better anti-inflammatory activity over pure drug, thus confirming the better therapeutic efficacy; the same phenomenon was reported by Saritha et al.¹⁶ and Liles and Flecknell.²³

An ulcerogenic potential study was performed for pure ibuprofen and agglomerates. Pure ibuprofen produced hemorrhagic steaks with higher intensity than the agglomerates. Pure ibuprofen-treated rats' stomachs showed hemorrhagic steaks with high intensity (severity score: 1.5), whereas agglomerate-treated rats' stomachs had red coloration (severity score: 0.5) (Figure 7). No ulcers were observed in the control rats' stomachs. From the ulcerogenic potential study, it can be concluded that ibuprofen agglomerates had improved ulcerogenic potential activity, which may be due to having better absorption and bioavailability than ibuprofen. Similar results were reported by Nagaraju et al.²⁷

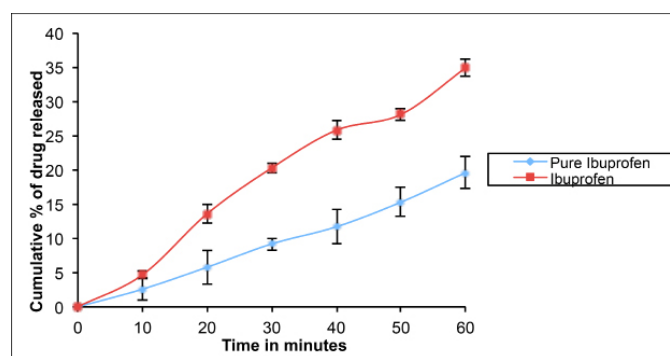


Figure 6. *In vitro* release profile of ibuprofen and its agglomerates

Table 5. Anti-inflammatory activity of pure and ibuprofen agglomerates

Group	Treatment	Time (hr)	Paw volume mean	% inhibition
Control	1% CMC suspension	5	0.51	--
Standard	20 mg (100 mg/Kg) pure ibuprofen	5	0.29	43.13
Test	20 mg (100 mg/Kg) ibuprofen agglomerates	5	0.14	72.54

CMC: Carboxymethylcellulose

**Figure 7.** Photographs of isolated stomach of rats for ulcerogenic potential studies

CONCLUSION

Ibuprofen agglomerates prepared using the simple spherical crystallization technique exhibited improved micromeritic properties and dissolution rate. FTIR, DSC, and XRD studies showed that there was no change in the crystal structure and polymorphism did not occur. Due to the significant improvement of micromeritic properties, this technique may be used for the formulation of ibuprofen tablets through direct compression. The agglomerates were found have better anti-inflammatory activity in rats when compared with pure drug due to improved solubility.

ACKNOWLEDGEMENTS

The authors are thankful to Granules India, Hyderabad, India for the gift sample of ibuprofen. We also thank the MNR educational trust and Sri Padmavathi Mahila Visva Vidyalayam for providing necessary facilities to carrying the work.

Conflict of Interest: No conflict of interest was declared by the authors.

REFERENCES

- Di Martino P, Di Cristofaro R, Barthelemy C, Joiris E, Palmieri Filippo G, Sante M. Improved compression properties of propyphenazone spherical crystals. *Int J Pharm.* 2000;197:95-106.
- Maghsoodi M. How spherical crystallization improves direct tableting properties: a review. *Adv Pharm Bul.* 2012;2:253-257.
- Nokhodchi A, Maghsoodi M. Preparation of spherical crystal agglomerates of naproxen containing disintegrants for direct tablet making by spherical crystallization technique. *AAPS PharmSciTech.* 2008;9:54-59.
- Muatlik S, Usha AN, Reddy MS, Ranjith AK, Pandey S. Improved bioavailability of aceclofenac from spherical agglomerates: development, *in vitro* and preclinical studies. *Pak J Pharm Sci.* 2007;20:218-226.
- Gupta VR, Mutalik S, Patel MM, Jani GK. Spherical crystals of celecoxib to improve solubility, dissolution rate and micromeritic properties. *Acta Pharm.* 2007;57:173-184.
- Varshosaz J, Tavakoli N, Salamat FA. Enhanced dissolution rate of simvastatin using spherical crystallization technique. *Pharm Dev Technol.* 2011;16:529-535.
- Pandey S, Patil AT. Preparation, evaluation and need of spherical crystallization in case of high speed direct tableting. *Curr Drug Deliv.* 2014;11:179-190.
- Kumar S, Chawla G, Bansal AK. Spherical crystallization of mebendazole to improve processability. *Pharm Dev Technol.* 2008;13:559-568.
- Maghsoodi M, Hassan-Zadeh D, Barzegar-Jalali M, Nokhodchi A, Martin G. Improved compaction and packing properties of naproxen agglomerated crystals obtained by spherical crystallization technique. *Drug Dev Ind Pharm.* 2007;33:1216-1224.
- Thati J, Rasmuson AC. On the mechanisms of formation of spherical agglomerates. *Eur J Pharm Sci.* 2011;42:365-379.
- Viswanathan CL, Kulkarni SK, Kolwankar DR. Spherical agglomeration of mefenamic acid and nabumetne to improve micromeritics and solubility: A technical note. *AAPS PharmSciTech.* 2006;7:48.
- Paradkar AR, Pawar AP, Chordiya JK, Patil VB, Ketkar AR. Spherical crystallization of celecoxib. *Drug Dev Ind Pharm.* 2002;28:1213-1220.
- Katta J, Rasmuson AC. Spherical crystallization of benzoic acid. *Int J Pharm.* 2008;348:61-69.
- Kovacic B, Vrečer F, Planinsek O. Spherical crystallization of drugs. *Acta Pharm.* 2012;62:1-14.
- Indian Pharmacopoeia, Ministry of Health and Family welfare, The Indian Pharmacopoeia commission, Ghaziabad, 2010:1482.
- Saritha D, Bose PSC, Reddy PS, Madhuri G, Nagaraju R. Improved dissolution and micromeritic properties of naproxen from spherical agglomerates: preparation, *in vitro* and *in vivo* characterization. *Braz J Pharm Sci.* 2012;48:667-676.

17. Maghsoodi M, Tajalli Bakhsh AS. Evaluation of physico-mechanical properties of drug-excipients agglomerates obtained by crystallization. *Pharm Dev Technol.* 2011;16:243-249.
18. Maghsoodi M, Yari Z. Effect of drying phase of the agglomerates prepared by spherical crystallization. *Iran J Pharm Res.* 2015;14:51-57.
19. Pawar A, Paradkar AR, Kadam SS, Mahadik KR. Effect of polymers on crystallo-co-agglomeration of ibuprofen-paracetamol: Factorial design. *Indian J Pharm Sci.* 2007;69:658-664.
20. Despande MC, Mahadik KR, Pawar AP, Paradkar AP. Evaluation of spherical crystallization as particle size enlargement technique for aspirin. *Indian J Pharm Sci.* 1997;59:32-34.
21. Usha AN, Mutalik S, Reddy MS, Ranjith AK, Kushtagi P, Udupa N. Preparation and, *in vitro*, preclinical and clinical studies of aceclofenac spherical agglomerates. *Eur J Pharm Biopharm.* 2008;70:674-683.
22. Saritha D, Bose CSP, Nagaraju R. Formulation and evaluation of self emulsifying drug delivery system (SEDDS) of Ibuprofen. *Int J Pharm Sci Res.* 2014;5:3511-3519.
23. Liles JH, Flecknell PA. The use of non-steroidal anti-inflammatory drugs for the relief of pain in laboratory rodents and rabbits. *Lab Anim.* 1992;26:241-255.
24. Rao CM, Ramesh KV, Biary KL, Kulkarni DR. Zinc complexes of NSAIDs abolish gastric ulceration propensity of parent drugs. *Indian Drugs.* 1990;28:64-67.
25. Hussain L, Akash MS, Naseem S, Rehman K, Ahmed KZ. Anti-ulcerogenic effects of salmalia malabarica in gastric ulceration-pilot study. *Adv Clin Exp Med.* 2015;24:595-605.
26. Rajashekhara N, Ashok BK, Sharma PP, Ravishankar B. Evaluation of acute toxicity and anti-ulcerogenic study of rhizome starch of two source plants of Tugaksheeree (*Curcuma angustifolia* Roxb. And *Maranta arundinacea* Linn.). *Ayu.* 2014;35:433-437.
27. Nagaraju R, Pratusha AP, Subhash Chandra Bose P, Khaza R, Bharathi K. Preparation and evaluation of famotidine polymorphs. *Curr Drug Discov Technol.* 2010;7:106-116.
28. Maghsoodi M, Hajipour A. Effect of binder liquid type on spherical crystallization. *Drug Dev Ind Pharm.* 2014;40:1468-1475.
29. Xia D, Ouyang M, Wu JX, Jiang Y, Piao H, Sun S, Zheng L, Rantanen J, Cui F, Yang M. Polymer mediated anti-solvent crystallization of nitrendipine: monodispersed spherical crystallization and growth mechanism. *Pharm Res.* 2012;29:158-169.
30. Maghsoodi M. Effect of process variables on physico-mechanical properties of the agglomerates obtained by spherical crystallization technique. *Pharm Dev Technol.* 2011;16:474-482.
31. Kulkarni PK, Subhash Chandra Bose P. Spherical agglomeration of nabumetone. *Indian J Pharm Educ Res.* 2007;41:18-23.
32. Bose CSP, Saritha D, Kumar VM, Kumar Dathrika S. Influence of various bridging liquids on spherical agglomeration of indomethacin. *Int J Res Pharm Sci.* 2011;2:147-157.
33. Kumar S, Chawla G, Bansal AK. Spherical crystallization of mebendazole to improve processability. *Pharm Dev Technol.* 2008;13:559-568.
34. Viswanathan CL, Kulkarni SK, Kolwankar DR. Spherical agglomeration of mefenamic acid and Nabumetone to improve micromeritics and Solubility: A Technical Note. *AAPS PharmSciTech.* 2006;7:48.
35. Kulkarni P, Dixit M. Preparation and characterization of spherical agglomerates of ibuprofen by neutralization method. *Int Res J Pharm.* 2010;1:305-313.
36. Florey K. Analytical profiles of drug substances and excipients. 1st ed. Elsevier India; New Delhi; 1984;13:222-224.
37. Kachrimanis K, Nikolakakis I, Malamataris S. Spherical crystal agglomeration of ibuprofen by the solvent-change technique in presence of methacrylic polymers. *J Pharm Sci.* 2000;89:250-259.
38. Kulkarni PK, Dixit M, Kini AG, Karthik M. Preparation and Characterization of spherical agglomerates of ibuprofen by solvent change method. *Scholars Research Library.* 2010;2:289-301.
39. Pawar AP, Paradkar AR, Kadam SS, Mahadik KR. Crystallo-co-agglomeration: a novel technique to obtain ibuprofen-paracetamol agglomerates. *AAPS PharmSciTech.* 2004;5:44.
40. Rasenack N, Muller BW. Properties of ibuprofen Crystallized Under Various Conditions: A Comparative Study. *Drug Dev Ind Pharm.* 2002;28:1077-1089.
41. Gupta VR, Mutalik S, Patel MM, Jani GK. Spherical crystals of celecoxib to improve solubility, dissolution rate and micromeritic properties. *Acta Pharm.* 2007;57:173-184.
42. Jbilou M, Ettabia A, Guyot-Hermann AM, Guyot JC. Ibuprofen Agglomerates Preparation by Phase Separation. *Drug Dev Ind Pharm.* 1999;25:297-305.
43. Di Martino P, Barthelemy C, Piva F, Joiris E, Palmieri GF, Martelli S. Improved dissolution behavior of fenbufen by spherical crystallization. *Drug Dev Ind Pharm.* 1999;25:1073-1081.
44. Sano A, Kuriki T, Handa T, Takeuchi H, Kawashima Y. Particle design of tolbutamide in the presence of soluble polymer or surfactant by spherical crystallization technique: improvement of dissolution rate. *J Pharm Sci.* 1987;76:471-474.



Development of Nanocochleates Containing Erlotinib HCl and Dexketoprofen Trometamol and Evaluation of *In Vitro* Characteristic Properties

Erlotinib HCl ve Deksketoprofen Trometamol İçeren Nanokohleatların Geliştirilmesi ve *In Vitro* Karakteristik Özelliklerinin Değerlendirilmesi

Özlem ÇOBAN¹, Zelihağül DEĞİM^{2*}

¹Karadeniz Technical University, Faculty of Pharmacy, Department of Pharmaceutical Technology, Trabzon, Turkey

²Biruni University, Faculty of Pharmacy, Department of Pharmaceutical Technology, İstanbul, Turkey

ABSTRACT

Objectives: Erlotinib HCl is a tyrosine kinase receptor inhibitor and an anticancer agent that was first approved by the FDA in 2004 for treatment of non-small-cell lung cancer and pancreatic cancer. Dexketoprofen trometamol is a NSAID, but recent studies showed that dexketoprofen trometamol also had an effect in carcinoma due to its inhibitor effects on prostaglandins. The combination of dexketoprofen and anti-cancer agents reduces pain caused by cancer by diminishing the tumors pressure, which causes necrosis; it also lowers the poor prognosis of cancer. Combination therapy will make life easier for patients, considering drug administration and dosing. Nanocochleates are new drug delivery systems that have not been examined as much as liposomes, but they have more advantages than liposomes.

Materials and Methods: In this study, erlotinib HCl and dexketoprofen trometamol were loaded into nanocochleates with various formulations and particle sizes/distributions, polydispersity indexes, and zeta potential analyses were performed. Transmission electron microscopy imaging was performed with the obtained optimal formulation and drug-release studies using Franz diffusion cells were conducted.

Results: As a result, drug carrier systems with a particle size of 196.42-312.33 nm and zeta potential greater than 15 mV were produced. The highest encapsulation efficiency for the main active ingredient, erlotinib HCl, was obtained in the KOH-1B formulation with 86.22±1.45%.

Conclusion: This study showed that the drugs were successfully loaded into the nanocochleates and the nanocochleates actively released the drugs.

Key words: Nanocochleate, erlotinib HCl, Franz diffusion cell

ÖZ

Amaç: Erlotinib HCl bir tirozin kinaz reseptör inhibitörü olup, FDA tarafından ilk kez 2004 yılında küçük hücreli olmayan akciğer kanseri ile pankreas kanserinin tedavisi için onaylanmış olan antikanserojen bir etkin maddedir. Deksketoprofen trometamol ise NSAİİ'dir. Ancak günümüzde prostaglandinler üzerindeki inhibitör etkisinden dolayı karsinomada da etkili olduğu yapılan çalışmalar ile gösterilmektedir. Bu nedenle günümüzde ayrı ayrı ürünler halinde kullanılan deksketoprofen ve antikanserojen madde kombine edildiğinde, hem hastaya alım kolaylığı sağlayarak sabit bir kan düzeyi sağlanabileceği hem de kansere bağlı ağrı ile tümörün basınç nekrozu yaratma ve kanser prognozunu kötü yönde artırma etkisinin azaltılması ve tümörün etkin bir şekilde tedavisinin mümkün olabileceği düşünülmüştür. Nanokohleatlar ise üzerinde lipozomlar kadar çok fazla çalışmanın yapılmadığı ancak lipozomlara kıyasla daha fazla avantaja sahip olan ilaç taşıyıcı sistemlerdir.

Gereç ve Yöntemler: Bu çalışmada, erlotinib HCl ve deksketoprofen trometamol çeşitli formülasyon çalışmaları ile nanokohleatlara yüklenmiş ve partikül büyüklüğü dağılımı, polidispersite indeksi ve zeta potansiyeli analizleri yapılmıştır. Elde edilen optimum formülasyon ile Franz difüzyon hücresinde salım çalışmaları ve geçirimli elektron mikroskobu görüntülemesi gerçekleştirilmiştir.

Bulgular: Yapılan çalışmalar sonucunda partikül büyüklüğü 196.42-312.33 nm aralığında ve zeta potansiyeli 15 mV'den büyük olan taşıyıcı sistemler üretilmiştir. Esas etkin madde olan erlotinib HCl için en yüksek yükleme verimliliği ise %86.22±1.45 ile KOH-1B formülasyonunda elde edilmiştir.

Sonuç: Çalışmalar sonucunda ilaçların nanokohleatlara başarılı bir şekilde yüklendiği ve yaklaşık %50 salım değerlerine ulaştığı tespit edilmiştir.

Anahtar kelimeler: Nanokohleat, erlotinib HCl, Franz difüzyon hücresi

*Correspondence: E-mail: zdegim@gmail.com, Phone:+90 535 302 68 45 ORCID-ID: orcid.org/0000-0003-2596-3615

Received: 03.02.2017, Accepted: 23.03.2017

©Turk J Pharm Sci, Published by Galenos Publishing House.

INTRODUCTION

Erlotinib hydrochloride (ERLO) is an epidermal growth factor receptor inhibitor that was approved by the United States Food and Drug Administration (FDA) in 2004 for the treatment of non-small-cell lung cancer and its anticancer effects promised hope in various preclinical models.¹ Tablet forms containing ERLO are available in the market² but when the FDA-Orange Book for the USA market or the electronic Medicines Compendium for European Union market were checked, there was no nanosystem with ERLO found. ERLO is slightly soluble in water. Aqueous solubility is dependent on pH and its solubility increases below pH 5.² ERLO has toxic effects such as diarrhea, skin rash, and fatigue, as well as toxic effects on pulmonary, hepatic and renal systems.³⁻⁶ In order to overcome these toxic effects, it is aimed to load this drug into a nano drug carrier system. In a study on healthy rats in the literature, no toxic effect with ERLO was observed compared with its free form when it was encapsulated in polymeric nanoparticles.⁷

Dexketoprofen trometamol (DEX) is water-soluble but it has also some oil-solubility; DEX is a salt of the S-isomer of the racemic non-steroidal anti-inflammatory drug (NSAID) ketoprofen.^{8,9} Although it inhibits cyclooxygenase (COX)-1 and COX-2 isoenzymes, it has partially selective activity for COX-1.^{10,11} Recent studies with NSAIDs have shown that this drug has a protective effect against breast and colorectal cancers, which are frequently observed worldwide.^{12,13} The underlying mechanism can be explained with angiogenesis by associated COX-derived prostaglandins.¹⁴ Taking all these observations into account, when DEX is used with ERLO, as a combination therapy, more effective cancer treatment can be obtained.

Cochleates are packaged lipidic structures, which are composed of negatively charged phospholipids in the presence of divalent counter ions such as Ca²⁺ and not containing water in the internal phase.¹⁵ It is thought that as the mechanism of formation, fusion occurs through Ca²⁺ followed by the leakage of the aqueous phase of the liposome, and the lipid layers are folded on each other to form solid spiral rods.^{15,16} Proteoliposome-derived cochleates are known to exhibit high immunogenicity when administered by intramuscular, oral, or intranasal routes. Previous studies have also supported the use of these constructs in the design and development of vaccines and adjuvants.¹⁷ In addition to this use, they are particularly effective in the oral use of hydrophobic drugs. Unlike liposomes, water is not present in their internal phases and they have a solid rod structure. Due to these constructions, they can protect trapped molecules against harsh environmental conditions such as pH, lipase degradation, and temperature. They are also resistant to lyophilization. Cochleates include phosphatidyl serine (PS), dioleoylphosphatidylserine (DOPS), phosphatidic acid, phosphatidylinositol (PI), phosphatidylglycerol as soy-based phospholipids either alone or as mixtures.¹⁶

The aim of this study was to load NSAIDs in combination with an anticancer drug to nanocochleate delivery systems, which is a new approach for cancer treatment. In this way, by targeting anticancer drug delivery systems directly to the tumor tissues,

adverse effects will be reduced, a low dose will provide more effective treatment, and combined drug administration will enhance treatment. Furthermore, the combination of an NSAID and an anticancer drug, which are currently used separately, will be more convenient for patients. Therefore, it was aimed to load ERLO, which is a hydrophobic drug, and DEX, a hydrophilic auxiliary drug, into nanocochleates and to characterize the system.

MATERIALS AND METHODS

Materials

DOPS and methoxy-poly(ethyleneglycol)2000-distearoylphosphatidylethanolamine (DSPE-PEG₂₀₀₀) were purchased from Avanti Polar Lipids, USA. Folic acid (FA), sodium acetate trihydrate, chloroform, and ethanol were from Sigma-Aldrich, Germany. ERLO was from Biotang, USA. DEX and calcium chloride dihydrate (CaCl₂·2H₂O) were purchased from Sigma. Acetic acid glacial was purchased from Fisher Scientific, UK. All chemicals were analytical grade and were used without further purification. Dialysis membrane (cellulose acetate molecular weight cut-off 12000 Da) was obtained from Sigma-Aldrich, USA.

Analytical method and calibration

Ultra-performance liquid chromatography (UPLC), which is highly sensitive, was preferred to determine the drug-loading capacity and the cumulative drug-release studies. Initially, ERLO and DEX were scanned using an ultraviolet spectrophotometer to determine their maximum absorbance wavelengths in distilled water containing ethanol (20%) and pH 3 acetate buffer, and they were found as 244 and 260 nm for ERLO and DEX, respectively. One milligram of ERLO and 1 mg of DEX were weighed separately and transferred into a 100 mL volumetric flask. Twenty milliliters of ethanol was added and the flask was sonicated to dissolve all the contents for 10 min, and then diluted up to 100 mL with distilled water. In addition, 1 mg of ERLO and 1 mg of DEX were weighed separately and transferred into a 100 mL volumetric flask. A portion of pH 3 acetate buffer was added and the flask was sonicated to dissolve all the contents for 10 min, and then diluted up to 100 mL with pH 3 acetate buffer. Finally, ERLO and DEX together, with a concentration of 10 µg/mL, was used as a stock solution. Solutions at concentrations ranging from 0.05 to 10 µg/mL were prepared by diluting the stock solution, samples were then analyzed using UPLC (6 replicates) and calibration curves were obtained. UPLC was found to be linear (r²=0.999) and reproducible for both mediums.

Development of ERLO and DEX-loaded nanocochleate formulations

The Bangham method was preferred because it was an easy method for preparing liposomes. In this context, DOPS, PEG-DSPE, FA, ERLO, and DEX were placed in a round-bottom flask, and chloroform was added to dissolve all the materials. The organic phase was evaporated at 42°C using a rotary evaporator. Distilled water was added and vortexed for 15 min

followed by ultrasonification for 1 hour. Six millimolar CaCl_2 was added dropwise to the liposome suspension with various ratios and vortexed for 30 min. Finally, the mixture was kept in a refrigerator at $+4^\circ\text{C}$ overnight. The formulation contents and the amounts of these ingredients are shown in Table 1.

Table 1. ERLO and DEX-loaded nanocochleate formulations

Formulations code	KOH-1A	KOH-1B	KOH-1C	KOH-1D
DOPS	10 mg	10 mg	10 mg	10 mg
DSPE-PEG ₂₀₀₀	10 mg	10 mg	10 mg	10 mg
FA	20 mg	20 mg	20 mg	20 mg
ERLO	6 mg	6 mg	6 mg	6 mg
DEX	3 mg	3 mg	3 mg	3 mg
Chloroform	5 mL	5 mL	5 mL	5 mL
6 mM CaCl_2	1:1	1:2	1:3	2:2

Determination of particle size distribution, polydispersity index and zeta potential of formulations, DOPS: Dioleoylphosphatidylserine, DSPE-PEG₂₀₀₀: Poly(ethyleneglycol)₂₀₀₀-distearoylphosphatidylethanolamine, FA: Folic acid, ERLO: Erlotinib hydrochloride, DEX: Dexketoprofen trometamol, CaCl_2 : Calcium chloride

The particle sizes of the formulations were measured using laser light scattering. A Malvern Zeta-Nanosizer instrument was used to measure particle size distribution, the polydispersity index, and zeta potential. Three parallel measurements were made and mean and standard deviation (SD) values were calculated.

Determination of encapsulation efficiency of formulations

In order to determine the encapsulation efficiency of the formulations, the formulations were first centrifuged at 18,000 rpm for 40 min and the supernatant fractions were analyzed to determine the amount of free drug. The amount of drug loaded into the formulation was determined by subtracting this value from the total amount of drug in the formulation and the values are given as percentages. Three parallel measurements were made and mean and SD values were calculated.

Transmission electron microscopy (TEM) analysis of the optimal formulation

TEM imaging was performed for the most appropriate formulation in terms of drug encapsulation efficiency, particle size distribution, polydispersity index, and zeta potential. These analyses were performed in the METU Central Laboratory. Prior to imaging, the samples were diluted 1:29 with distilled water.

Release studies using a Franz diffusion cell

Release studies were also performed using a Franz diffusion cell for the optimal formulation. In the release studies of the nanoparticulate systems containing ERLO, pH 3 acetate, pH 5.2 acetate, and pH 7.4 phosphate buffers were used as release media.^{18,19} When the release studies in the literature were considered, the most meaningful results were obtained in a pH 3 acetate medium; therefore, the pH 3 acetate buffer release medium was selected. The volume of the receptor medium was

2.5 mL, and the sample volume added to the donor phase was 1.5 mL. The diffusional area of the Franz cells was measured as 0.9 cm^2 . During the studies, the temperature of the medium was kept constant at $37\pm 0.2^\circ\text{C}$ and the stirring rate was maintained at 100 rpm. The experiment was conducted taking the entire sample from the receptor medium and replenished with fresh medium. When no release was observed the experiment was terminated. All samples were analyzed using UPLC.

RESULTS

Results of particle size distribution, polydispersity index and zeta potential studies

In vitro characterization studies, particle size distribution, polydispersity index, and zeta potential were investigated and the results are shown in Table 2.

Results of encapsulation efficiency studies

Determined encapsulation efficiencies are presented in Table 3.

TEM analysis image of the optimal formulation

As a result of the characterization studies, KOH-1B formulation, which had the highest encapsulation efficiency for drugs and the most suitable values in terms of PSD, PI and zeta potential, was determined as the optimal formulation. TEM imaging confirmed that a successful formulation was performed. A TEM image of the analysis is shown in Figure 1.

Release studies of the optimal formulation using a Franz diffusion cell

The release studies of the optimal formulation and the drug solution in the pH 3 acetate buffer for 48 hours resulted in 56.73% and 50.50% for ERLO and 47.83% and 81.89% for DEX, respectively. The results of the Franz cell diffusion studies are shown in Figure 2 and Figure 3.

Table 2. Results of the characterization studies

Formulation	PSD \pm SD (nm)	PI \pm SD	Zeta potential \pm SD (mV)
KOH-1A	312.33 \pm 31.93	0.349 \pm 0.076	-17.05 \pm 2.26
KOH-1B	218.90 \pm 13.14	0.285 \pm 0.07	-21.10 \pm 0.93
KOH-1C	211.43 \pm 13.21	0.300 \pm 0.131	-19.52 \pm 2.02
KOH-1D	196.42 \pm 9.71	0.196 \pm 0.021	-22.93 \pm 0.41

SD: Standard deviation

Table 3. Encapsulation efficiencies

Formulation	Encapsulation efficiency \pm SD (%)	
	DEX	ERLO
KOH-1A	48.54 \pm 1.47	84.38 \pm 0.79
KOH-1B	52.92 \pm 1.03	86.22 \pm 1.45
KOH-1C	47.43 \pm 0.98	85.55 \pm 1.17
KOH-1D	40.45 \pm 1.63	81.89 \pm 2.17

SD: Standard deviation, ERLO: Erlotinib hydrochloride, DEX: Dexketoprofen trometamol

When the kinetics of the release of drug solution and formulation were calculated, it was found that both formulations obeyed Hixson-Crowell kinetics for ERLO and DEX, and the correlation coefficients were 0.9984 and 0.9961 for ERLO and 0.9996 and 0.9993 for DEX, respectively. The kinetics results are shown in Table 4.

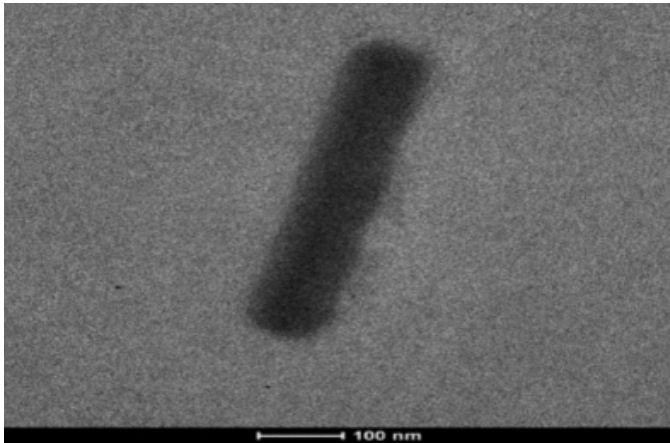


Figure 1. TEM image of the optimal formulation (x49,000)

TEM: Transmission electron microscopy

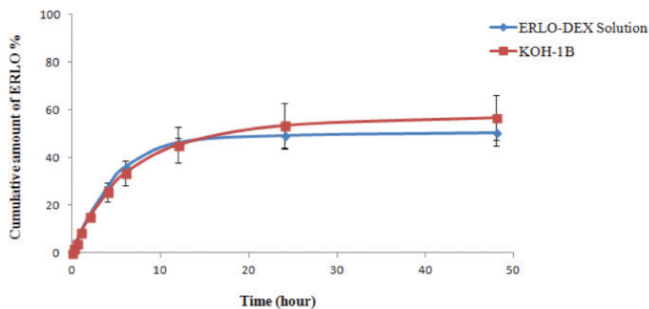


Figure 2. Franz cell diffusion release profiles of optimal formulation (◇) and drug solution (□) for ERLO at pH 3 acetate buffer (error bars represent standard deviations, n=3)

ERLO: Erlotinib hydrochloride, DEX: Dexamethasone trometamol

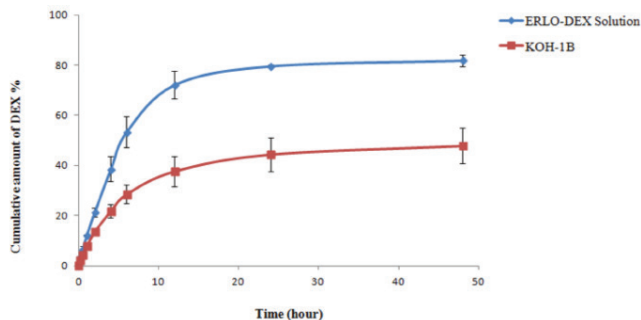


Figure 3. Franz cell diffusion release profiles of optimal formulation (◇) and drug solution (□) for DEX at pH 3 acetate buffer (error bars represent standard deviations, n=3)

ERLO: Erlotinib hydrochloride, DEX: Dexamethasone trometamol

Table 4. Correlation coefficients of various release kinetics

	Drug solution (ERLO-DEX solution)		Formulation (KOH-1B)	
	ERLO	DEX	ERLO	DEX
Zero-order	0.9975	0.9986	0.9947	0.9990
First-order	0.9096	0.9121	0.8889	0.9160
Higuchi	0.9783	0.9804	0.9801	0.9766
Hixson-Crowell	0.9984	0.9996	0.9961	0.9993
Korsmeyer-Peppas	0.9921	0.9941	0.9944	0.9921

ERLO: Erlotinib hydrochloride, DEX: Dexamethasone trometamol

DISCUSSION

Erlotinib is an effective agent in the treatment of many types of cancer, but mainly non-small-cell lung and pancreatic cancers. The studies show that erlotinib binds to human serum albumin while circulating in the bloodstream before going to the target site. This interaction can lead to some adverse effects such as rash, fatigue, and loss of appetite with oral intake of drug.²⁰ In addition to providing more effective treatment with lower doses, nanocarrier systems would prevent these toxic effects because of targeting. For this purpose, the preparation of drug delivery systems that selectively target cancer cells should be considered. Finally, we decided to use nanocochleates, which were discovered by D. Papahadjopoulos in 1975 as a drug-delivery system and began to be used in vaccine therapy in the 80's and 90's, because cochleate technology is known to be effective in the oral administration of hydrophobic drugs such as ERLO.¹⁷ Cochleates has been chosen for use as delivery system specifically for ERLO and DEX.

It is estimated that the pore size of blood vessels of tumor tissues is in the range of 400–600 nm. For this reason, the particle size of the carrier system should be 200 nm or less to reach the tumor tissue and to exploit the EPR effect.²¹ The nano-sized particles must have a certain zeta potential in order not to be aggregated; this value is reported as ± 30 mV.²² In this context, the developed carrier system should be evaluated in terms of particle size and zeta potential as well as encapsulation activities. Encapsulation efficiency, particle size distribution, polydispersity index, and zeta potential analyses were performed with four different purpose-made nanocochleate formulations. In considering the particle size results, it was found that the carrier systems had a size range of 196.42–312.33 nm. In addition to having small size, they also had suitable zeta potentials (more than 15 mV), which are a sign of stability. Although these results show a successful formulation design, the KOH-1B formulation had the highest encapsulation efficiency and was identified as the optimal formulation. KOH-1B formulation loaded with ERLO $86.22 \pm 1.45\%$, which has low water solubility and $52.92 \pm 1.03\%$ with DEX which is water soluble. This is possibly due to the lack of an aqueous phase in the structure of the nanocochleates and thus higher encapsulation efficiencies for hydrophobic drugs were achieved.

When CaCl_2 is used in a ratio of 1:1 or 2:2, Ca^{2+} ions are insufficient for a complete nanocochleate formation and a flabby spiral structure is formed. For this reason, only small amounts of DEX, which is a hydrophilic drug, can be loaded. When the CaCl_2 ratio is increased, a negatively charged zeta potential of the nanoparticles is observed. This can create a problem for the stability of carrier systems over time.

The release of active substances is important and *in vitro* release profiles provide information about the structure and behavior of the formulation, the possible interactions between the drug and the carrier system, and their effects on the rate and mechanism of drug release. Franz cell release studies are a useful method for determining *in vitro* release of the drug from micro- and nano-particles. This method is used to determine the release kinetics of various formulations including liposomes and nanoparticles.²³⁻²⁷ For this reason, Franz cell diffusion was preferred using a cellulose acetate membrane in our study. When the release profile of ERLO was considered, there was no significant difference between the nanocochleate and the drug solution, even though less drug was released from the drug solution. This is thought to be due to the dialysis membrane, which is hydrophilic, whereas ERLO is hydrophobic. This is because the ERLO has quickly reached saturation on surface of the membrane and the stagnant layer may be thick while in the solution phase and is held more strongly by the membrane. However, when it has been applied with a carrier system, ERLO has been slowly released to the receptor environment without reaching saturation on the membrane surface, and therefore the amount of released drug was still increasing with respect to the solution. For DEX, which has high water solubility, the situation is exactly the opposite; it quickly passes through the drug solution to the release environment because it has not reached any saturation on the surface of the hydrophilic membrane like itself. However, because it has been released from the carrier system, a lower release value is achieved compared with the drug solution.

When release kinetics were examined, it was determined that the drug solution and the formulation showed Hixson-Crowell release with the highest correlation coefficient. This model argues that drug release was achieved/controlled by diffusion. Drug release from cochleates cannot be achieved only through diffusion; the dissolution of the drug particles from the surface and opening of the cochleates may also enhance the dissolution and its rate.

CONCLUSION

When all the results are considered, it was observed that ERLO and DEX active materials were successfully loaded into the carrier system in combination and nano-sized carrier systems were obtained using the simple thin film method. TEM analysis also supported this result. *In vitro* release studies showed that our systems released the drugs.

Tablet formulations containing only ERLO are currently available, but serious adverse effects are observed with the systemic circulation passage when the free drug goes to the

target site. With our drug- delivery system, this difficulty will be avoided.

ACKNOWLEDGEMENTS

This study was supported by a research grant from The Scientific and Technological Research Council of Turkey (TÜBİTAK, Project Number: 213M675).

Conflict of Interest: No conflict of interest was declared by the authors.

REFERENCES

- Dowell J, Minna JD, Kirkpatrick P. Erlotinib hydrochloride. *Nat Rev Drug Discov.* 2005;4:13-14.
- Jawhari D, Alswisi M, Ghannam M, Al Halman J. Bioequivalence of new generic formulation of erlotinib hydrochloride 150 mg tablets versus Tarceva® in healthy volunteers under fasting conditions. *J Bioequiv Availab.* 2014;6:119-123.
- Vahid B, Esmaili A. Erlotinib-associated acute pneumonitis: Report of two cases. *Can Respir J.* 2007;14:167-170.
- Del Castillo Y, Espinosa P, Bodí F, Alcega R, Muñoz E, Rabassó, Castander D. Interstitial lung disease associated to erlotinib treatment: a case report. *Cases J.* 2010;3:59.
- Highlights of prescribing information: TARCEVA (erlotinib) tablets, for oral use (2016, October 18). Available from: https://www.accessdata.fda.gov/drugsatfda_docs/label/2016/021743s025lbl.pdf
- Saif MW. Hepatic failure and hepatorenal syndrome secondary to erlotinib safety reminder. *JOP.* 2008;9:748-752.
- Gregory M, Sheeba CJ, Kalaichelvan VK, Manavalan R, Neelakanta Reddy PN, Franklin G. Poly(D,L-lactic-co-glycolic acid) nanoencapsulation reduces erlotinib-induced subacute toxicity in rat. *J Biomed Nanotechnol.* 2009;5:464-471.
- Leman P, Kapadia Y, Herington. Randomised controlled trial of the onset of analgesic efficacy of dexketoprofen and diclofenac in lower limb injury. *Emerg Med J.* 2003;20:511-513.
- Sweetman BJ. Development and use of the quick acting chiral NSAID dexketoprofen trometamol (keral). *Acute Pain.* 2003;4:109-115.
- Balani M, Gawade P, Maheshgauri S, Ghole S, Shinde V, Sathe V. Results of two multicentric, comparative, randomized, parallel group clinical trials to evaluate the efficacy and safety of dexketoprofen trometamol in the treatment of dental pain and dysmenorrhoea in Indian patients. *Journal of Clinical and Diagnostic Research* 2008;2:1086-1091.
- Miranda HF, Noriega V, Sierralta F, Prieto JC. Interaction between dexibuprofen and dexketoprofen in the orofacial formalin test in mice. *Pharmacology Biochem Behav.* 2011;97:423-427.
- Khuder SA, Mutgi AB. Breast cancer and NSAID use: a meta-analysis. *Br J Cancer.* 2001;84:1188-1192.
- Sheehan KM, Sheehan K, O'Donoghue DP, MacSweeney F, Conroy RM, Fitzgerald DJ, Murray FE. The relationship between cyclooxygenase-2 expression and colorectal cancer. *JAMA.* 1999;282:1254-1257.
- Dannenber AJ, Altroki NK, Boyle JO, Dang C, Howe LR, Weksler BB, Subbaramaiah K. Cyclo-oxygenase 2: a pharmacological target for the prevention of cancer. *Lancet Oncol.* 2001;2:544-551.
- Miclea RD, Varma PR, Peng A, Balu-lyer SV. Development and characterization of lipidic cochleate containing recombinant factor VIII. *Biochim Biophys Acta.* 2007;1768:2890-2898.

16. Sankar VR, Reddy YD. Nanocochleate-a new approach in lipid drug delivery. *Int J of Pharm and Pharm Sci.* 2010;2:220-223.
17. Gil D, Bracho G, Zayas C, Del Campo J, Acevedo R, Toledo A, Lastre M, Pérez O. Strategy for determination of an efficient cochleate particle size. *Vaccine.* 2006;24(Suppl 2):92-93.
18. Srinivasan AR, Shoyele, SA. Influence of surface modification and the pH on the release mechanisms and kinetics of erlotinib from antibody-functionalized chitosan nanoparticles. *Ind Eng Chem Res.* 2014;53:2987-2993.
19. Mandal B. Design, development and evaluation of erlotinib-loaded hybrid nanoparticles for targeted drug delivery to nonsmall cell lung cancer. University of Tennessee Health Science Center. 2015:74-75.
20. Ye ZW, Ying Y, Yang XL, Zheng ZQ, Shi JN, Sun YF, Huang P. A spectroscopic study on the interaction between the anticancer drug erlotinib and human serum albumin. *J Inc Phenom Macrocyclic Chem.* 2014;78:405-413.
21. Mattheolabakis G, Rigas B, Constantinides PP. Nanodelivery strategies in cancer chemotherapy: biological rationale and pharmaceutical perspectives. *Nanomedicine (Lond).* 2012;7:1577-1590.
22. Singh R, Lillard JW Jr. Nanoparticle-based targeted drug delivery. *Exp Mol Pathol.* 2009;86:215-223.
23. Hua S. Comparison of *in vitro* dialysis release methods of loperamide-encapsulated liposomal gel for topical drug delivery. *Int J Nanomedicine.* 2014;9:735-744.
24. Aloisio C, Antimisiaris SG, Longhi MR. Liposomes containing cyclodextrins or meglumine to solubilize and improve the bioavailability of poorly soluble drugs. *Journal of Molecular Liquids.* 2017;229:106-113.
25. Derakhshandeha K, Fathi S. Role of chitosan nanoparticles in the oral absorption of Gemcitabine. *Int J Pharm.* 2012;437:172-177.
26. Degim Z, Mutlu NB, Yilmaz S, Eşsiz D, Nacar, A. Investigation of liposome formulation effects on rivastigmine transport through human colonic adenocarcinoma cell line (Caco-2). *Pharmazie.* 2010;65:32-40.
27. Ismail MF, ElMeshad AN, Salem NA. Potential therapeutic effect of nanobased formulation of rivastigmine on rat model of Alzheimer's disease. *Int J Nanomedicine.* 2013;8:393-406.



Development and Validation of a High-performance Liquid Chromatography–Diode-array Detection Method for the Determination of Eight Phenolic Constituents in Extracts of Different Wine Species

Çeşitli Şarap Örneklerinde Sekiz Fenolik İçeriğın Tayini için Bir HPLC-DAD Yönteminin Geliştirilmesi ve Geçerli Kılınması

© Ebru TÜRKÖZ ACAR^{1*}, © Mehmet Engin CELEP², © Mohammad CHAREHSAZ³, © Gülşah Selin AKYÜZ², © Erdem YEŞİLADA²

¹Yeditepe University, Faculty of Pharmacy, Department of Analytical Chemistry, İstanbul, Turkey

²Yeditepe University, Faculty of Pharmacy, Department of Pharmacognosy, İstanbul, Turkey

³Yeditepe University, Faculty of Pharmacy, Department of Pharmaceutical Toxicology, İstanbul, Turkey

ABSTRACT

Objectives: A new HPLC method was developed and validated for the determination of some phenolic compounds; gallic acid, chlorogenic acid, epigallocatechin, caffeic acid, vanillin, p-coumaric acid, rutin, and quercetin in some local wine and fruit wine samples.

Materials and Methods: Analyses were performed on a Zorbax Eclipse C18 column (4.6 x 150 mm, 3.5-µm particle size) using a gradient system. Mobile phase A was a 10-mM phosphoric acid solution and mobile phase B was methanol using a flow rate of 1 mL/min. Phenolic components were monitored using a DAD at three different wavelengths.

Results: The developed and validated method was generally linear between the 1-100 ppm concentration range. Recovery values were obtained in the range of 95-105% and repetitive. The method was successfully applied to investigate the phenolic profiles of different wine samples.

Conclusion: As a result of the study, an accurate, sensitive and reliable HPLC-DAD method was developed. The method was successfully used to determine the concentrations of antioxidant phenolic constituents from some local wine extracts.

Key words: Phenolic compounds, determination, wine, HPLC, validation

ÖZ

Amaç: Bu çalışmada amaç bazı yerel şarap ve meyve şarabı örneklerinde gallik asit, klorojenik asit, epigallokateşin, kafeik asit, vanilin, p-kumarik asit, rutin ve kersetin fenolik bileşiklerinin tayini için yeni bir HPLC yöntemi geliştirilmesi ve geçerli kılınmasıdır.

Gereç ve Yöntemler: Analizler, gradyan sistem kullanılarak bir Zorbax Eclipse C18 kolon (4.6 x 150 mm, 3.5-µm partikül boyutlu) üzerinde yürütülmüştür. Akış hızının 1 mL/min olduğu sistemde hareketli faz A 10-mM fosforik asit ve hareketli faz B metanol olarak belirlenmiştir. Fenolik bileşikler, üç farklı dalga boyunda bir DAD kullanılarak izlenmiştir.

Bulgular: Geliştirilen ve geçerli kılınan yöntemin 1-100 ppm derişim aralığında doğrusal cevap verdiği gözlenmiştir. Geri kazanım değerleri %95-105 değerleri arasındadır ve tekrarlanabilir sonuçlardır. Geliştirilen yöntem çeşitli şarap örneklerinde fenolik profili incelemek için uygulanmıştır.

Sonuç: Yapılan çalışma sonucunda doğru, hassas ve güvenilir ölçüm yapan bir HPLC-DAD yöntemi geliştirilmiş ve şarap özütlerinde, şarabın antioksidan özellik göstermesini sağlayan fenolik maddelerin derişimlerini tayin etmek için başarıyla kullanılmıştır.

Anahtar kelimeler: Fenolik bileşikler, tayin, şarap, HPLC, validasyon

*Correspondence: E-mail: ebruturkozacar@gmail.com, Phone: +90 530 381 65 20 ORCID-ID: orcid.org/0000-0002-8164-6617

Received: 03.11.2016, Accepted: 02.03.2017

©Turk J Pharm Sci, Published by Galenos Publishing House.

INTRODUCTION

Antioxidants are compounds that can delay or inhibit the oxidation of lipids or other molecules by inhibiting the initiation or propagation of oxidizing chain reactions.¹ Phenolic components, being secondary metabolites, are synthesized by different plants during regular development and show significant antioxidant activities and free radical scavenging properties.²⁻⁵ Epidemiologic studies showed that consumption of a healthy diet high in fruits and vegetables significantly increased the antioxidant capacity of plasma.⁶ Furthermore, these studies showed that there was an inverse relationship between the intake of fruit, vegetables, and cereals, and the incidence of coronary heart diseases and certain cancers.^{7,8} The same relationship was proposed for wine consumption by different researchers.⁸⁻¹³ Different fruits and vegetables show antioxidant properties.^{1,2,7,14} Among the natural antioxidants, red grape and its product wine have received much attention due to the high concentration and great variety of phenolic compounds.^{5,8}

Winemaking is one of the most ancient of man's technologies, known since the dawn of civilization, and has followed human and agricultural progress on the world.¹⁵ The earliest biomolecular archaeological evidence for plant additives in fermented beverages dates from the early Neolithic period in China and Anatolia, when different types of fruits and cereals were used to make wine such as grapes, rice, millet, and fruits.^{15,16} In earlier years in Egypt, a range of natural products, specifically herbs and tree resins were served with grape wine to prepare herbal medicinal wines.¹⁷ Many of the polyphenols and other bioactive compounds in the source materials are bonded to insoluble plant compounds. The winemaking process releases many of these bioactive components into aqueous ethanolic solution, thus making them more biologically available for absorption during consumption.¹⁸ Thus, winemaking releases beneficial components such as phenolic compounds of antioxidant fruits besides grapes. There has been increasing interest in fruit wines produced from different types of fruit. A non-grape fruit wine is a mixture composed of fruit juice, alcohol, and a wide range of components that may already be present in the fruit or synthesized during the fermentation process.¹⁹

The antioxidant potential of wine is closely related to its phenolic content, which may be affected by a number of factors, including grape variety, fermentation processes, vinification techniques, ageing, and geographic and environmental factors (soil type and climate).²⁰ According to the literature, there are different methods to determine the phenolic contents of the different wine samples such as high-performance liquid chromatography-mass spectrometry (HPLC-MS)^{3,8,10,21-23}, HPLC-diode-array detector (HPLC-DAD)^{5,9,11,12,24-27}, gas chromatography (GC)¹⁹, capillary electrophoresis (CE)²⁸, and spectrophotometric^{4,14,29,30} and electrochemical methods.^{9,31} These methods come with some advantages and disadvantages. Importantly, no studies have compared the phenolic profile of some local Turkish wines and fruit wines. In this study, a development and validation HPLC-DAD method is presented to evaluate the phenolic profile of some selected Anatolian wines and fruit wines.

MATERIALS AND METHODS

Chemicals and reagents

Standard materials of gallic acid (149-91-7) (1), chlorogenic acid (327-97-9) (2), epigallocatechin (989-51-5) (3), caffeic acid (331-39-5) (4), vanillin (121-33-5) (5), p-coumaric acid (501-98-4) (6), rutin (207671-50-9) (7) and quercetin (6151-25-3) (8) were purchased from Sigma-Aldrich Chemical Company (St. Louis, MO, USA). Ortho-phosphoric acid (85%) solution, ethanol (HPLC gradient grade) and methanol (HPLC gradient grade) were acquired from Merck (Darmstadt, Germany).

Ultrapure water for the preparation of the mobile phase (18.2 MW.cm at 25°C) was obtained by using Millipore Simplicity ultraviolet (UV) apparatus (Millipore, Molsheim, France).

Calibration, linearity, and quality control (QC) samples

The eight analytes stock solutions were prepared by dissolving a weighed amount of the standard substance in ethanol at a 1 mg/mL concentration value. All stock solutions were stored in a refrigerator at 4°C. Combined working solutions of mixed analytes at the concentrations of 5, 10, 20, 50, 100 µg/mL were obtained by dilution of the appropriate volume of stock solutions in volumetric flasks. Calibration curves were plotted, in triplicate, by analysing these freshly prepared standard solutions. Concentration values of the QC samples were as follows: the low-level concentration was 7.5 µg/mL, the medium-level concentration was 30 µg/mL, and the high level concentration was 80 µg/mL for each analyte.

Instruments and chromatographic conditions

Chromatographic analyses of phenolic compounds were performed using an Agilent 1260 HPLC system consisting of a quaternary pump model G1311B, an auto injector model G1329B, a thermostated column compartment model G1316A, and a DAD, model G4212B. The chromatograms were monitored and integrated by using Agilent ChemStation software. Chromatographic separations of the analytes were achieved on an Agilent Zorbax Eclipse XDB-C18 column (4.6 mm x 150 mm, 3.5-µm particle size) and the column was thermostated at 25±1°C during analysis. DAD signals for every analyte were selected according to their spectrums obtained from the Agilent ChemStation Software. Appropriate wavelengths were selected as: 214 nm for gallic acid, chlorogenic acid, and quercetin, 306 nm for vanillin, p-coumaric acid and rutin, and 333 nm for chlorogenic acid and caffeic acid. A gradient elution system was used to separate all analytes. For this purpose, two different mobile phases were used; Mobile phase A was 10 mM phosphoric acid solution and mobile phase B was methanol using a flow rate of 1 mL/min. The optimised gradient program was as follows: 0-15 min (0-60% B), 15-20 min (60-80% B), 20.0-22 min (80-100% B), 22-27 min (100-0% B) and 27-32 min (0% B). Samples were injected into the system as 10 µL.

Preparation of wine extracts

Both fruit wines and grape wines of Papazkarasi-type cultivar were purchased from local producers in Turkey. After removing the alcohol using a rotatory evaporator, the residual part of each

wine was lyophilized with a Christ Alpha 2-4 LD lyophilizer. The lyophilized extracts were dissolved in water at proper concentrations prior to experimentation.

RESULTS AND DISCUSSION

Optimization of chromatographic conditions

To achieve the best separation, different mobile phases were investigated such as buffers, organic solvents, and different concentrations and different mixtures of these solutions. For the reason that all substances analyzed should be in non-polar form, the analysis media was preferred as acidic. Accordingly, acetate buffer, phosphate buffer solution, and phosphoric acid solution were tried. The best separation performance was observed when the phosphoric acid solution was used. The concentration of phosphoric acid was investigated for column-filling material properties. Besides the concentration effect, the organic modifier effect was investigated by using methanol and acetonitrile. During this process, peak shape, peak height and separation ability of the investigated systems were evaluated. It was seen that 10 mM phosphoric acid solution was the most appropriate solution with methanol to separate the eight different phenol compounds. After determining the mobile phase components, different mixtures of these solutions at different rates were tested to achieve the best separation for all analytes through isocratic elution. However, gradient elution provided both the best separation of all analytes and the optimum analysis time. Therefore, 10 mM phosphoric acid solution was used as mobile phase A and methanol was used as mobile phase B for further experiments.

In addition, other chromatographic conditions such as flow rate, injection volume, and temperature were investigated. At the end of experiments, the optimum parameters were determined as 1 mL/min. for flow rate, 10 μ L for injection volume, and 25°C for temperature, together providing the best separation of the eight phenolic compounds. A chromatogram showing the separation of all analytes at optimized conditions is presented in Figure 1. As seen in this figure, all analytes were well separated from each other and can be observed individually.

Method validation

System suitability test

Before performing any validation experiments, researchers

should establish that the HPLC system procedure is capable of providing data of acceptable quality³² and make a system suitability test. System suitability is widely recognized as a critical component in chemical analysis and is frequently referred to in governmental regulations and guidance policies.³³ These tests are based on the concept that the equipment, electronics, analytical operations, and samples constitute an integral system that can be evaluated as a whole. Parameters related with system suitability test are investigated as follow: plate count (N) should be higher than 2000, tailing factors (T) should be equal to or lower than 2, resolution (R) between two peaks should be higher than 2, RSD value of retention time and area for six repetitions as repeatability should be equal or lower than 1% and capacity factor (k') should be higher than 2.³²

In light of this information, system suitability test results were investigated before the validation studies. For this purpose, a standard mixture was prepared containing 7.5 μ g/mL of gallic acid, chlorogenic acid, epigallocatechin, caffeic acid, vanillin, p-coumaric acid, rutin and quercetin. Six replicate analyses of this standard mixture were performed. All results obtained from chromatograms are shown in Table 1. It can be seen that all results were in the appropriate range and the optimized method was appropriate for the validation process.

Calibration curves

Different concentration values of each phenolic compound were investigated to determine the dynamic range for the

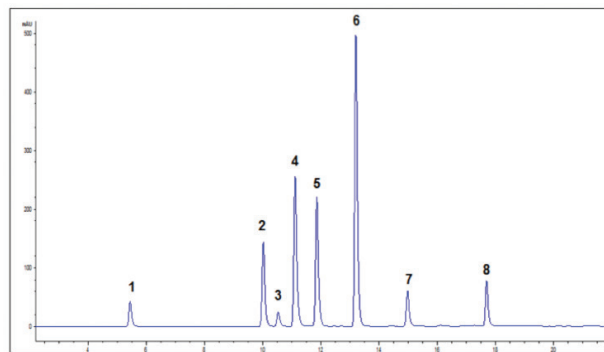


Figure 1. Obtained chromatogram of the 80 ppm standard mixture at 306 nm wavelength using the developed and optimized HPLC-DAD method. Gallic acid (1), chlorogenic acid (2), epigallocatechin (3), caffeic acid (4), vanillin (5), p-coumaric acid (6), rutin (7) and quercetin (8)

Table 1. System suitability test results for 7.5 μ g/mL of standard mixture (n=6)

Parameter	1	2	3	4	5	6	7	8
Retention time (min)	5.452	10.015	10.547	11.119	11.857	13.181	14.936	17.663
k' (≥ 2)	4.472	9.08	9.607	10.171	10.914	12.268	14.056	16.785
USP tailing (≤ 2)	0.635	0.785	1.324	0.923	1.101	1.139	1.016	1.285
N, theoretical number (≥ 2000)	7669	40347	55460	42850	55837	72625	91738	148468
Resolution (≥ 2)	20.37	2.763	2.845	3.548	6.785	9.018	14.234	30.749
RSD ($\leq 1\%$)	0.050	0.030	0.031	0.027	0.027	0.024	0.023	0.014

RSD: Relative standard deviation

method developed. For this purpose, standard solutions of each analyte as a mixture were prepared daily by diluting from the stock solution of compounds. Chromatograms obtained for each standard mixture were recorded and investigated to determine the calibration parameters of the method.

Limit of detection (LOD) and limit of quantification (LOQ) values of each substance were calculated by using calibration curve equations. As known, LOD is calculated by using the standard deviation (SD) of y-intercepts of regression lines. The sum of three times this SD value on the intercept of the calibration curve and intercept value 34 corresponds to the LOD signal value. In the same way, the sum of ten times this SD value on the intercept of calibration curve and intercept value corresponds to the LOQ signal value. Thus, LOD and LOQ values can be calculated using this approach. In this study, the limits of the developed method were determined using this calculation.

The calibration curve dynamic ranges and related method limits are shown in Table 2.

Accuracy

Accuracy studies for the developed method were performed by analyzing samples of known concentration in triplicate at three different levels as low, medium, and high-level in the dynamic range. For this purpose, standard mixtures of each compound at three different concentration values were prepared by diluting the stock solution and the concentration values were 7.5, 30, and 80 µg/mL. After analyzing these standard solutions, the results obtained were investigated and the calculated concentration values were compared with known concentration values as recovery. This comparison was made both for intra-day studies and inter-day studies. The results are presented in Table 3.

When Table 3 is investigated, it is seen that the recovery values are in the 95-105% range. This situation shows that the method is an accurate method.

Precision

Precision is the measure of the degree of repeatability of an analytical method under normal operation and is normally expressed as the percent relative SD (RSD) for a statistically significant number of samples. Table 3 also shows the precision of the method through the presentation of RSD values obtained from three repeated analyses of known amounts of standard at three different levels. For most of the components, these RSD values for intra-day studies were lower than 1%, which shows

that the method was very precise in intra-day studies, with the exception of gallic acid. When RSD values for inter-day studies were investigated, it was seen that RSD values for gallic acid, chlorogenic acid, and epigallocatechin were out of the limits. This situation indicates that these three substances should be analyzed using a daily calibration system. Unfortunately, the method developed cannot be precise for inter-day studies and analysts should work carefully and when preparing standard solutions, low- concentration values need particular attention.

Specificity

The specificity of the method was demonstrated by using spiked wine extract samples. For this purpose, each standard solution was spiked with the same wine extract and analyzed. It was observed that materials in wine extract samples did not present overlapping peaks with eight phenolic compounds. The peaks were also investigated by comparing UV spectrums obtained from chromatograms of the standard solution and chromatograms of the extracted wine samples.

Robustness and ruggedness

The robustness and ruggedness of the method were investigated by deliberately changing some analytic parameters in the range of $\pm 10\%$. The investigated parameters were injection volume, temperature, and concentration of phosphoric acid. Injection volume and temperature were parameters related with instrumentation and temperature was related with preparation of the mobile phase. Thus, both instrumental and personal error sources were investigated. Recovery values were calculated again for the new conditions and the results obtained are shown in Table 4. In general, when the obtained recovery values were investigated, it can be seen that the recovery values were appropriate to the 85-115 percentage rule. Especially at low concentration level, recovery values were affected by the changes. This means that if the analyte amount in the sample was at low level, the analyst should be more careful on analysis. The obtained recovery values were in the range between 88-105%, which shows that this method is robust.

Analysis of phenolic compounds in wine extract samples

The method developed and optimized was applied for analysis of eight different phenolic compound in different wine extract samples. One of the obtained chromatograms was presented in Figure 2. Table 5 shows the results for this analysis.

Table 2. Calibration curve parameters of the method developed for each analyte

	1	2	3	4	5	6	7	8
LOD (ppm)	0.99	0.62	0.14	0.09	0.04	0.05	0.42	0.04
LOQ (ppm)	3.32	2.06	0.48	0.30	0.13	0.16	1.40	0.12
Range (ppm)	5-100	2.5-100	1-100	1-100	1-100	1-100	2.5-100	1-100
Slope	60.959	25.018	63.616	51.415	36.368	75.341	8.3925	46.750
S _b	20.220	5.165	3.0640	1.525	0.488	1.186	1.174	0.587
R ²	0.9988	0.9988	0.9998	0.9999	0.9999	0.9999	0.9999	0.9999

LOD: Limit of detection, LOQ: Limit of quantification

Table 3. Results of accuracy and precision study for the developed method

Analyte	Concentration level	Intra-day variation		Inter-day variation	
		Accuracy	RSD	Accuracy	RSD
Gallic acid	L	112.99	1.26	105.28	8.70
	M	104.74	1.35	103.32	6.88
	H	99.02	1.05	100.57	2.98
Chlorogenic acid	L	98.54	0.51	96.96	10.06
	M	117.74	0.25	109.64	9.08
	H	98.57	0.21	107.95	8.62
Epigallocatechin	L	104.99	0.51	102.00	9.09
	M	105.76	0.34	104.06	1.75
	H	98.59	0.24	99.66	0.94
Caffeic acid	L	102.07	0.42	103.03	1.19
	M	99.38	0.08	99.38	0.14
	H	100.63	0.09	100.66	0.34
Vanillin	L	104.98	0.35	105.19	0.27
	M	100.25	0.06	100.44	0.16
	H	100.38	0.09	100.36	0.11
p-coumaric acid	L	104.80	0.30	104.98	0.15
	M	100.22	0.05	100.40	0.16
	H	100.49	0.10	100.48	0.09
Rutin	L	105.16	0.97	104.19	3.54
	M	100.38	0.23	100.71	0.54
	H	100.46	0.07	100.38	0.17
Quercetin	L	103.84	0.32	103.29	1.75
	M	101.42	0.67	101.20	0.22
	H	100.64	0.09	100.66	0.08

L: Low level QC (7.5 µg/mL), M: Medium level QC (30 µg/mL), H: High level QC (80 µg/mL), RSD: Relative standard deviation

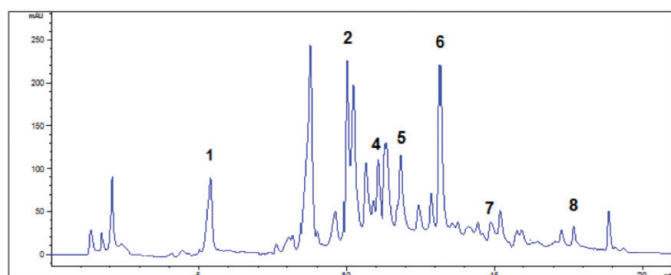


Figure 2. A sample HPLC chromatogram of black mulberry wine extract (visualized at 306 nm) Peaks: (1) gallic acid, (2) chlorogenic acid, (4) caffeic acid, (5) vanillin, (6) p-coumaric acid, (7) rutin, (8) quercetin

When the analysis results were investigated, it was seen that epigallocatechin could not be detected in these wine samples. If a comparison between the other phenolic compounds found in these wine samples is needed, it can be understood that black mulberry contains phenolic compounds, more than in other wine samples. Celep et al.²⁰ applied total phenolic content (TPC) and total antioxidant capacity (TOAC) tests to these wine samples and they showed that black mulberry wine had higher TPC and TOAC properties than other wine samples. Analysis results of the wine samples support these TPC and TOAC test results.

Table 4. Obtained recovery values during robustness-ruggedness studies. Results are expressed as the mean of triplicates \pm SD

Analyte	Conc. level	Injection volume		Temperature		Concentration of phosphoric acid	
		9 μ L	11 μ L	23°C	27°C	12 mM	8 mM
Gallic acid	L	92.03 \pm 1.20	97.42 \pm 0.20	104.00 \pm 2.01	98.50 \pm 0.92	91.93 \pm 0.44	89.86 \pm 0.79
	M	98.94 \pm 1.25	99.20 \pm 0.58	98.43 \pm 0.07	100.53 \pm 0.16	99.72 \pm 1.15	97.41 \pm 0.07
	H	99.80 \pm 0.25	99.42 \pm 0.09	99.38 \pm 0.10	99.99 \pm 0.10	101.45 \pm 1.23	104.08 \pm 0.26
Chlorogenic acid	L	100.43 \pm 3.41	99.99 \pm 1.84	96.74 \pm 1.22	96.20 \pm 0.92	92.48 \pm 0.05	90.65 \pm 0.09
	M	101.42 \pm 2.85	98.01 \pm 1.32	99.22 \pm 0.05	99.26 \pm 0.13	98.23 \pm 0.11	97.34 \pm 0.06
	H	98.14 \pm 1.45	99.54 \pm 0.13	99.44 \pm 0.05	99.68 \pm 0.11	101.59 \pm 0.87	103.82 \pm 0.28
Epigallocatechin	L	95.95 \pm 2.21	103.02 \pm 1.44	97.13 \pm 1.19	96.70 \pm 0.92	91.37 \pm 0.06	90.30 \pm 1.58
	M	99.60 \pm 0.36	97.35 \pm 0.22	99.02 \pm 0.02	99.31 \pm 0.09	97.20 \pm 0.08	98.42 \pm 0.02
	H	98.45 \pm 0.25	102.33 \pm 7.46	99.37 \pm 0.04	99.59 \pm 0.05	101.18 \pm 0.66	101.43 \pm 0.32
Caffeic acid	L	94.10 \pm 0.88	98.25 \pm 0.51	96.73 \pm 1.02	95.65 \pm 0.94	90.81 \pm 0.02	90.80 \pm 0.02
	M	99.79 \pm 0.40	99.07 \pm 0.58	99.22 \pm 0.02	99.24 \pm 0.09	97.98 \pm 0.16	97.88 \pm 0.16
	H	100.45 \pm 0.40	99.01 \pm 0.53	99.50 \pm 0.07	99.80 \pm 0.13	101.87 \pm 0.87	101.87 \pm 0.87
Vanillin	L	92.97 \pm 1.32	97.66 \pm 0.19	95.79 \pm 1.08	95.54 \pm 0.72	90.25 \pm 0.03	88.09 \pm 0.05
	M	100.28 \pm 0.50	98.95 \pm 0.62	99.16 \pm 0.07	99.32 \pm 0.12	97.97 \pm 0.10	96.93 \pm 0.05
	H	100.09 \pm 0.28	99.54 \pm 0.41	99.52 \pm 0.06	99.91 \pm 0.07	101.98 \pm 0.92	104.34 \pm 0.22
p-coumaric acid	L	93.21 \pm 1.56	97.43 \pm 0.36	96.24 \pm 0.85	95.74 \pm 0.95	90.80 \pm 0.17	88.89 \pm 0.05
	M	100.15 \pm 0.10	99.76 \pm 1.22	99.23 \pm 0.08	99.39 \pm 0.10	98.09 \pm 0.12	97.20 \pm 0.03
	H	99.83 \pm 0.18	99.36 \pm 0.13	99.49 \pm 0.05	99.78 \pm 0.12	101.85 \pm 0.86	103.98 \pm 0.25
Rutin	L	90.56 \pm 1.74	94.06 \pm 0.79	94.47 \pm 1.00	97.22 \pm 2.34	92.43 \pm 0.09	100.52 \pm 0.06
	M	101.21 \pm 1.06	99.64 \pm 1.23	99.35 \pm 0.03	99.16 \pm 0.06	98.44 \pm 0.13	96.65 \pm 0.02
	H	101.32 \pm 1.28	99.39 \pm 0.20	99.54 \pm 0.08	99.85 \pm 0.13	101.84 \pm 0.84	105.81 \pm 0.29
Quercetin	L	89.25 \pm 1.01	92.53 \pm 1.37	96.36 \pm 0.86	95.30 \pm 0.77	90.52 \pm 0.33	89.02 \pm 0.26
	M	99.28 \pm 0.95	99.42 \pm 1.25	98.84 \pm 0.02	99.23 \pm 0.43	97.97 \pm 0.15	97.18 \pm 0.05
	H	101.47 \pm 1.82	99.62 \pm 0.82	99.52 \pm 0.06	99.77 \pm 0.14	101.84 \pm 0.83	104.01 \pm 0.27

L: Low level, M: Medium level, H: High level

Table 5. Phenolic composition of the wine extracts using the developed method. Results are expressed as the mean of triplicates \pm SD and as μ g/mg sample

Analyte	Blueberry wine	Black mulberry wine	Cherry wine	Papazkarası wine
Gallic acid	1.2 \pm 0.070	1.66 \pm 0.085	0.73 \pm 0.014	0.20 \pm 0.028
Chlorogenic acid	nd	1.56 \pm 0.096	nd	nd
Epigallocatechin	nd	nd	nd	nd
Caffeic acid	0.06 \pm 0.010	0.32 \pm 0.003	0.12 \pm 0.009	0.48 \pm 0.080
Vanillin	0.02 \pm 0.001	0.59 \pm 0.016	0.02 \pm 0.003	0.01 \pm 0.003
p-coumaric acid	0.08 \pm 0.017	0.55 \pm 0.020	0.08 \pm 0.002	0.09 \pm 0.003
Rutin	0.33 \pm 0.015	0.91 \pm 0.012	0.19 \pm 0.006	0.17 \pm 0.005
Quercetin	0.08 \pm 0.004	0.33 \pm 0.008	0.08 \pm 0.005	0.01 \pm 0.001

nd: Not detected

CONCLUSION

This developed and validated method was applied successfully to determine the phenolic constituents of different wine samples. Our results were in good agreement with TPC and TOAC tests published previously. The method can also be used for the determination of the phenolic compounds of styrax liquids and different pekmez samples.

Conflict of Interest: No conflict of interest was declared by the authors.

REFERENCES

- Zheng W, Wang SY. Antioxidant Activity and Phenolic Compounds in Selected Herbs. *J Agric Food Chem*. 2001;49:5165-5170.
- Kahkönen MP, Hopia AI, Vuorela HJ, Rauha JP, Pihlaja K, Kujala TS, Heinonen M. Antioxidant Activity of Plant Extracts Containing Phenolic Compounds. *J Agric Food Chem*. 1999;47:3954-3962.
- Mirnaghi FS, Mousavi F, Rocha SM, Pawliszyn J. Automated determination of phenolic compounds in wine, berry, and grape samples using 96-blade solid phase microextraction system coupled with liquid chromatography-tandem mass spectrometry. *J Chromatogr A*. 2013;1276:12-19.
- Stratil P, Klejduš B, Kuban V. Determination of Total Content of Phenolic Compounds and Their Antioxidant Activity in Vegetables- Evaluation of Spectrophotometric Methods. *J Agric Food Chem*. 2006;54:607-616.
- Milano F, Giannetti V, Gobbi L, Recchia L, Tarola AM. Simultaneous Determination of Phenolic Compounds in Selected Italian Red Wines. *J Commodity Sci Technol Quality*. 2009;48:5-15.
- Cao G, Booth SL, Sadowski JA, Prior RL. Increases in human plasma antioxidant capacity after consumption of controlled diets high in fruit and vegetables. *Am J Clin Nutr*. 1998;68:1081-1087.
- Rice-Evans CA, Miller NJ, Paganga G. Antioxidant properties of phenolic compounds. *Trends Plant Sci*. 1997;2:151-159.
- Lingua MS, Fabani MP, Wunderlin DA, Baroni MV. From grape to wine: Changes in phenolic composition and its influence on antioxidant activity. *Food Chem*. 2016;208:228-238.
- Šeruga M, Novak I, Jakobek L. Determination of polyphenols content and antioxidant activity of some red wines by differential pulse voltammetry, HPLC and spectrophotometric methods. *Food Chem*. 2011;124:1208-1216.
- Dias FS, David JM, David JP. Determination of Phenolic Acids and Quercetin in Brazilian Red Wines from Vale do São Francisco Region Using Liquid-Liquid Ultrasound-Assisted Extraction and HPLC-DAD-MS. *J Braz Chem Soc*. 2016;27:1055-1059.
- Porgalı E, Büyüktuncel E. Determination of phenolic composition and antioxidant capacity of native red wines by high performance liquid chromatography and spectrophotometric methods. *Food Res Int*. 2012;45:145-154.
- Burin VM, Arcari SG, Costa LLF, Bordignon-Luiz MT. Determination of some phenolic compounds in red wine by RP-HPLC: Method Development and validation. *J Chromatogr Sci*. 2011;49:647-651.
- Peri P, Kamiloglu S, Capanoglu E, Ozcelik B. Investigating the Effect of Aging on the Phenolic Content, Antioxidant Activity and Anthocyanins in Turkish Wines. *J Food Process Pres*. 2015;39:1845-1853.
- Lin JY, Tang CY. Determination of total phenolic and flavonoid contents in selected fruits and vegetables, as well as their stimulatory effects on mouse splenocyte proliferation. *Food Chem*. 2007;101:140-147.
- Jagtap UB, Bapat VA. Wines from fruits other than grapes: Current status and future prospectus. *Food Bioscience*. 2015;9:80-96.
- Özdemir D. The demand for Turkish wine: estimates of the wine price elasticities. *Appl Econ Lett*. 2015;22:1355-1360.
- McGovern PE, Mirzoian A, Hall GR. Ancient Egyptian herbal wines. *P Natl Acad Sci U S A*. 2009;106:7361-7366.
- Shahidi F. Nutraceuticals and functional foods: Whole versus processed foods. *Trends Food Sci Tech*. 2009;20:376-387.
- Amidžić KD, Klaric I, Mornar A, Nigovic B. Evaluation of volatile compound and food additive contents in blackberry wine. *Food Control*. 2015;50:714-721.
- Celep E, Charehsaz M, Akyüz S, Acar ET, Yesilada E. Effect of *in vitro* gastrointestinal digestion on the bioavailability of phenolic components and the antioxidant potentials of some Turkish fruit wines. *Food Res Int*. 2015;78:209-215.
- Restivo A, Degano I, Ribechini E, Colombini MP. Development and Optimisation of an HPLC-DAD-ESI-Q-ToF Method for the Determination of Phenolic Acids and Derivatives. *PLOS ONE*. 2014;9:e88762.
- Kelebek H, Canbas A, Jourdes M, Teissedre PL. HPLC-DAD-MS Determination of Colored and Colorless Phenolic Compounds in Kalecik Karasi Wines: Effect of Different Vineyard Locations. *Anal Lett*. 2011;44:991-1008.
- Wang Y, Liu Y, Xiao C, Liu L, Hao M, Wang J, Liu X. Simultaneous determination of 15 phenolic constituents of Chinese black rice wine by HPLC-MS/MS with SPE. *J Food Sci*. 2014;79:1100-1105.
- Gouveia S, Castilho PC. Antioxidant potential of *Artemisia argentea* L'Hér alcoholic extract and its relation with the phenolic composition. *Food Res Int*. 2011;44:1620-1631.
- Huang Y, Lu WW, Chen B, Wu M, Li SG. Determination of 13 Phenolic Compounds in Rice Wine by High-Performance Liquid Chromatography. *Food Anal Method*. 2014;8:825-832.
- Salvatore E, Cocchi M, Marchetti A, Marini F, de Juan A. Determination of phenolic compounds and authentication of PDO Lambrusco wines by HPLC-DAD and chemometric techniques. *Anal Chim Acta*. 2013;761:34-45.
- Euterpio MA, Pagano I, Piccinelli AL, Rastrelli L, Crescenzi C. Development and validation of a method for the determination of (E)-resveratrol and related phenolic compounds in beverages using molecularly imprinted solid phase extraction. *J Agr Food Chem*. 2013;61:1640-1645.
- Dias F, Klassen A, Tavares MFM, David JM. Fast Determination of Phenolic Compounds in Brazilian Wines from Vale do São Francisco Region by CE. *Chromatographia*. 2013;76:559-563.
- Martelo-Vidal MJ, Vazquez M. Determination of polyphenolic compounds of red wines by UV-VIS-NIR spectroscopy and chemometrics tools. *Food Chem*. 2014;158:28-34.
- Medina MB. Determination of the total phenolics in juices and superfruits by a novel chemical method. *J Funct Food*. 2011;3:79-87.
- Chawla S, Rawal R, Kumar D, Pundir CS. Amperometric determination of total phenolic content in wine by laccase immobilized onto silver nanoparticles/zinc oxide nanoparticles modified gold electrode. *Anal Biochem*. 2012;430:16-23.
- Shabir GA. Validation of high-performance liquid chromatography methods for pharmaceutical analysis Understanding the differences and similarities between validation requirements of the US Food and Drug Administration, the US Pharmacopeia and the International Conference on Harmonization. *J Chromatogr A*. 2003;987:57-66.
- Briscoe CJ, Stiles MR, Hage DS. System suitability in bioanalytical LC/MS/MS. *J Pharm Biomed Anal*. 2007;44:484-491.
- Miller JH McB. Performance Parameters, Calculations and Tests, Method Validation in Pharmaceutical Analysis. In: Ermer J, Miller JH McB, eds. Darmstadt; Germany; 2005:170.



Orally-disintegrating Tablets in Fixed-dose Combination Containing Ambroxol Hydrochloride and Salbutamol Sulphate Prepared by Direct Compression: Formulation Design, Development and *In Vitro* Evaluation

Doğrudan Basım ile Hazırlanan Ambroksol Hidroklorür ve Salbutamol Sülfat İçeren Sabit Doz Kombinasyonu Oral-dağılan Tabletler: Formülasyon Tasarımı, Geliştirilmesi ve *In Vitro* Değerlendirilmesi

Deepak SHARMA^{1*}, Rajindra SINGH¹, Gurmeet SINGH²

¹Rayat Bahra Institute of Pharmacy, Department of Pharmaceutics, Hoshiarpur, Punjab, India

²ISF College of Pharmacy, Department of Pharmaceutics, Ghal Kalan, Moga, India

ABSTRACT

Objectives: To design a formulation and develop ODTs of AMB hydrochloride and salbutamol sulphate in combination for the treatment of respiratory disorders and perform an *in vitro* evaluation using superdisintegrants in combination with a suitable binder and excipients. Direct compression was used to prepare the tablets.

Materials and Methods: In the present research work, different concentrations of SSG as a superdisintegrant were used to optimize the concentration of SSG in the formulation of ODTs. Different concentrations of MCC and PVP K-30 were also studied along with the optimized SSG concentration. The tablets were evaluated for hardness, friability, weight variation, wetting time, *in vitro* DT, and percentage drug content uniformity. The optimized formulation was further evaluated in an *in vitro* release study, and drug-excipient compatibility and accelerated stability study.

Results: The optimized concentration of SSG was found as 4% on the basis of the lowest DT. The 1% concentration of MCC was selected as the optimum binder concentration on the basis of the lowest DT. ODTs passed all the quality control tests viz., weight variation, hardness, friability, *in vitro* DT, drug content (%) and wetting time. The formulation satisfied the requirements of the FDA for rapid-dissolving tablets and allowed more than 85% drug to be released within 30 min. The fourier transform infrared spectroscopy study revealed that there was no interaction between the drug and excipients. The accelerated stability study shows that formulation is quite stable at normal temperature and humidity conditions as well as at extreme temperature conditions.

Conclusion: By adopting a systematic formulation approach, ODTs of AMB hydrochloride and salbutamol sulphate in fixed-dose combination can be formulated using superdisintegrants in combination with appropriate binder and excipients; this was found to be economical and industrially feasible.

Key words: Orally-disintegrating tablets, sodium starch glycolate, *in vitro* disintegration time, ambroxol hydrochloride, salbutamol sulphate, optimization study

ÖZ

Amaç: Solunum bozukluklarının tedavisi için oral-dağılan AMB hidroklorür ve salbutamol sülfat kombinasyon tabletlerinin (ODT) geliştirilmesi ve kombine süper dağıtıcıların uygun bağlayıcı ve ekşiyanlar ile kombine kullanımı ile *in vitro* değerlendirmenin yapılmasıdır. Tabletleri hazırlamak için doğrudan basım kullanıldı.

Gereç ve Yöntemler: Bu araştırmada, oral dağılan tabletlerin formülasyonunda SNG konsantrasyonunu optimize etmek için farklı SNG konsantrasyonları süper dağıtıcı olarak kullanıldı. Farklı konsantrasyonlarda MCC ve PVP K-30 da optimize SNG konsantrasyonu ile birlikte çalışıldı. Tabletler, sertlik,

*Correspondence: E-mail: deepakpharmacist89@yahoo.com, Phone: +91 998 890 74 46 ORCID-ID: orcid.org/0000-0002-9445-1691

Received: 12.03.2017, Accepted: 13.04.2017

©Turk J Pharm Sci, Published by Galenos Publishing House.

kırılganlık, ağırlık değişimi, ıslanma süresi, *in vitro* dağılma süresi ve yüzde etken madde içerik tekdüzeliği açısından değerlendirildi. Optimize edilmiş formülasyon ayrıca *in vitro* salım çalışması ve etken madde-eksiptyan geçimliliği ve hızlandırılmış stabilite çalışmasıyla değerlendirildi.

Bulgular: En düşük dağılma süresine dayanarak SNG'nin optimum konsantrasyonu, %4 olarak bulundu. MCC'nin %1 konsantrasyonu, en düşük dağılma süresine dayanarak optimum bağlayıcı konsantrasyonu olarak seçildi. Oral dağılan tabletler, ağırlık değişimi, sertlik, kırılganlık, *in vitro* dağılma süresi, etken madde içeriği (%) ve ıslanma süresi gibi tüm kalite kontrol testlerini geçti. Formülasyon, hızlı çözünen tabletler için FDA şartlarını yerine getirdi ve %85'den fazla etken maddenin 30 dakika içinde salımını sağladı. Fourier dönüşümü kızıl ötesi spektroskopi çalışması, etken madde ve eksiptyanlar arasında herhangi bir etkileşimin olmadığını ortaya koymuştur. Hızlandırılmış stabilite çalışması, normal sıcaklık ve nem koşullarında ve aşırı sıcaklık koşullarında formülasyonun oldukça kararlı olduğunu göstermektedir.

Sonuç: Sistematik bir formülasyon yaklaşımı benimseyerek, sabit doz kombinasyonundaki AMB hidroklorür ve salbutamol sülfat ODT'leri, süper dağıtıcıların uygun bağlayıcı ve eksiptyanlar ile kombinasyonu kullanılarak formüle edilebilir; bunun ekonomik ve endüstriyel olarak uygulanabilir olduğu bulunmuştur.

Anahtar kelimeler: Oral dağılan tabletler, sodyum nişasta glikolat, *in vitro* dağılma süresi, ambroksol hidroklorür, salbutamol sülfat, optimizasyon çalışması

INTRODUCTION

In the late 80's, orally-disintegrating tablets (ODTs) or orodispersible tablets were developed and they were introduced to the market in early 90's. From that time, ODT dosage forms have become a well-known solution for geriatric or pediatric populations, which face difficulties in swallowing solid oral dosage forms.¹ ODTs disintegrate within a few seconds in the mouth of the patient and they are ideal for patients with dysphasia. As the saliva passes through the stomach, some drugs are absorbed from the mouth, pharynx, and esophagus, which ultimately lead to an increase in bioavailability of drug.² According to the definition by the Royal Spanish Pharmacopoeia, these tablets should disintegrate in less than 3 min. when tested at temperatures ranging between 35° and 39°C, simulating the temperature of the oral cavity. The others requirements with which these dose forms must comply is mechanical resistance, which is important from the handling point of view as well as for packaging and storage. ODTs must have ideal organoleptic characteristics.³ Orodispersible tablets are applicable for people who have difficulties in swallowing and for active people when water is not available, in the case of motion sickness, sudden episodes of coughing during the common cold, allergic conditions, and bronchitis. Due to this, these dose forms are increasingly being recognized in both industry and among academics. Orodispersible tablets are also called mouth-dissolving tablets, melt-in-mouth tablets, fast-dissolving tablets, rapid melts, porous tablets, quick dissolving, and so forth.⁴ Several newer disintegrants have been developed in more recent years, which are often called *super disintegrants*. These can be used at lower levels than conventionally used disintegrants. Swelling, porosity, capillary action, and deformation are the three major mechanisms and factors that affect the disintegration of tablets.⁵ Examples of superdisintegrants are croscarmellose, crospovidone, and sodium starch glycolate (SSG), which symbolize the example of crosslinked cellulose, crosslinked polymer, and a crosslinked starch, respectively. These are the commonly used synthetic origin super disintegrants.² There are various technological processes such as direct compression, freeze-drying, and molding, by which orodispersible tablets can be manufactured. The best way to manufacture ODTs is direct compression

because it is the right compromise among economical, manufacturing, and technological needs. To produce ODTs with satisfactory organoleptic, biopharmaceutical, and technological characteristics, it is important to select appropriate excipients that are able to produce the product with desired characteristics, efficacy, and pleasant mouth-feel.⁶ In the selection of excipients, those with rapid dissolution in water, low viscosity, sweet flavor, and high compressibility are considered. Due to the pleasant taste and ability to mask other flavors, sugars are most commonly used, which dissolve quickly in saliva because they are very soluble in water.³

Ambroxol (AMB) is a metabolite of bromhexine with similar actions and uses. It is chemically described as trans-4-[(2-amino-3,5-dibromobenzyl)amino]-cyclohexanol. AMB hydrochloride is an expectorant improver and a mucolytic agent used in the treatment of respiratory disorders such as bronchial asthma and chronic bronchitis, which are characterized by the production of excess or thick mucus. AMB hydrochloride has also been reported to have a cough-suppressing effect and anti-inflammatory action. It has been successfully used for decades in the form of its hydrochloride as a secretion-releasing expectorant in a variety of respiratory disorders.⁷ Salbutamol sulphate is a β -2 adrenergic agent with a greater bronchodilator effect and is useful in the treatment of asthma. Salbutamol sulphate must be given three to four times daily to maintain its bronchodilation effect due to the short half-life of 4-6 hrs.⁸

Formulations of the drugs chosen in fixed-dose combinations for the treatment of sudden allergic attacks and coughing are available in the market in conventional tablet and liquid dose forms. Due to sore throat conditions, pediatric patients experience difficulty in swallowing tablet-type dose forms. Liquid dose forms have their own limitations vis-a-vis stability and dose measurement perspectives. Hence, they do not comply with the prescription, which results in a high incidence of ineffective therapy and noncompliance. Therefore, in the present study, it was proposed to formulate a fixed-dose combination of AMB hydrochloride and salbutamol sulphate ODT by using direct compression with the aim of improving/enhancing patient convenience and compliance, reducing the lag time, and providing faster onset of action to immediately relieve respiratory disorders.

MATERIALS AND METHODS

Materials

AMB hydrochloride and salbutamol sulphate, which were used as the model drugs, were obtained from Trojan Pharma, Baddi, India as gift samples. Microcrystalline cellulose (MCC) as binder/disintegrant (Avicel PH-102) was received from NB Entrepreneurs, Nagpur, India, as a gift sample. Sodium saccharin, as a sweetening agent, was obtained from Loba Chemie, Mumbai, and talc as a glidant from Nice Chemicals Private Limited, Hyderabad, India. Sodium stearyl fumarate, as a lubricant, was purchased from Himedia. Polyvinylpyrrolidone (PVP) K-30, as a binder, was obtained from Himedia. SSG, as a superdisintegrant, (Primogel) and directly compressible mannitol (D-mannitol), as a diluent, were obtained from Qualikems Fine Chem Pvt. Ltd. All chemicals and reagents used in this research were of analytical grade.

Selection and optimization of excipients (Methodology)

The most important parameter that requires to be optimized in the development of ODTs is disintegration time (DT). ODTs were prepared through direct compression using different excipients such as binders and superdisintegrants. Various evaluation parameters such as friability, hardness, and DT were performed to select the best combination for formulation of ODTs. The combination with the lowest DT, optimum friability, and hardness was selected for further study.

Optimization of SSG

Various concentrations (1%, 2%, 4%, 6%, 8%, and 10%) of SSG were used in the preparation of ODTs to study the effect of concentration of superdisintegrants in the evaluation of the parameters of the tablets. A total of six formulations (F1-F6) were manufactured using direct compression as given in Table 1. For each specified formulation, the required quantity of each ingredient was taken. All the ingredients were passed through a no.60 mesh and co-ground in a pestle and mortar. Finally, talc and sodium stearyl fumarate were added and mixed for 5 min. The mixed blend of excipients was compressed into tablets using an 8-mm punch in a multi-punch tablet compression machine (Dhiman Industries, India).

Optimization of PVP K-30 or MCC (Avicel PH-102) with optimized concentration of SSG

In this method, the different concentrations of binder along with the optimized concentration of SSG were used to produce the tablets. A total of 14 formulations (B1-B14) were manufactured to study the effect of the type of binder with the optimized concentration of SSG as given in Table 2. For each specified formulation, the required quantity of each ingredient was taken. All the ingredients were passed through a no.60 mesh and co-ground in a pestle and mortar. Finally, talc and sodium stearyl fumarate were added and mixed for 5 min. The mixed blend of excipients was compressed into tablets using an 8-mm punch in a multi-punch tablet compression machine (Dhiman Industries, India).

Formulation of AMB hydrochloride, salbutamol sulphate ODTs

ODTs of AMB hydrochloride and salbutamol sulphate in fixed-dose combined-form were manufactured through direct compression. The required quantity of each ingredient was taken for formulation as shown in Table 3. Accurately-weighed quantities of AMB hydrochloride and salbutamol sulphate were taken and the optimized concentration of SSG and binder with excipients were co-ground in geometric progression in a dry and clean mortar. All ingredients were passed through a no.60 mesh. Finally, sodium stearyl fumarate and talc were added and mixed for 5 min. The mixed blend of excipients was compressed into tablets using an 8-mm punch in a multi-punch tablet compression machine (Dhiman Industries, India).

Evaluation parameters

Weight variation test

Twenty FDT tablets were selected at random from each formulation and weighed individually on a digital balance (Ohaus, USA). The individual weights were compared with the average weight for the determination of weight variation. To pass the weight variation test, tablets within the range of 80-250 mg should not deviate more than or less than ($\pm 7.5\%$) from its average weight according to Indian Pharmacopoeia (IP) limits.⁹

Table 1. Formula for one tablet (200 mg) of different concentrations of sodium starch glycolate

Ingredients	F1 (mg)	F2 (mg)	F3 (mg)	F4 (mg)	F5 (mg)	F6 (mg)
Ambroxol hydrochloride	7.5	7.5	7.5	7.5	7.5	7.5
Salbutamol sulphate	2	2	2	2	2	2
Sodium starch glycolate	2	4	8	12	16	20
Microcrystalline cellulose	2	2	2	2	2	2
Sodium stearyl fumarate	4	4	4	4	4	4
Talc	2	2	2	2	2	2
Sodium saccharin	3	3	3	3	3	3
Mint flavor	8	8	8	8	8	8
Mannitol	169.5	167.5	163.5	159.5	155.5	151.5

Table 2. Formula for one tablet (200 mg) for the optimization of PVP K-30 or MCC with optimized concentration of SSG

Ingredients	AMB HCl (mg)	SAL (mg)	SSG (mg)	PVP K-30 (mg)	MCC (mg)	SSF (mg)	Talc (mg)	SS (mg)	Mint Flavor	Mannitol (mg)
Formulation no.										
B1	7.5	2	8	2	-	4	2	3	8	163.5
B2	7.5	2	8	4	-	4	2	3	8	161.5
B3	7.5	2	8	6	-	4	2	3	8	159.5
B4	7.5	2	8	8	-	4	2	3	8	157.5
B5	7.5	2	8	10	-	4	2	3	8	155.5
B6	7.5	2	8	12	-	4	2	3	8	153.5
B7	7.5	2	8	14	-	4	2	3	8	151.5
B8	7.5	2	8	-	2	4	2	3	8	163.5
B9	7.5	2	8	-	4	4	2	3	8	161.5
B10	7.5	2	8	-	6	4	2	3	8	159.5
B11	7.5	2	8	-	8	4	2	3	8	157.5
B12	7.5	2	8	-	10	4	2	3	8	155.5
B13	7.5	2	8	-	12	4	2	3	8	153.5
B14	7.5	2	8	-	14	4	2	3	8	151.5

MCC: Microcrystalline cellulose, SSG: Sodium starch glycolate, PVP K-30: Polyvinylpyrrolidone K-30, AMB: Ambroxol, HCl: Hydrochloride, SAL: Salbutamol sulphate, SSF: Sodium stearyl fumarate, SS: Sodium saccharin

Table 3. Formula of ambroxol hydrochloride and salbutamol sulphate ODT

Ingredients	Formula for one tablet (200 mg)
Ambroxol hydrochloride	7.5
Salbutamol sulphate sodium	2
Starch glycolate	8
Microcrystalline cellulose	2
Sodium stearyl fumarate	4
Talc	2
Sodium saccharin	3
Mint flavor	8
Mannitol	163.5

ODT: Orally-disintegrating tablet

Hardness

To perform this test, tablets were placed between two anvils, the force to the anvils and the crushing strength that just caused the tablets to break was recorded. A Monsanto hardness tester was used to measure the hardness of the tablets. Three tablets from each formulation batch were tested randomly and the average reading was noted; the results are expressed as kg/cm².¹⁰

Thickness

The thickness of the tablets was determined using vernier caliper (Indian Caliper Industries, Ambala, India). Three

tablets from each batch were used, and the average value was calculated.¹¹

Friability

Twenty tablets from each formulation were accurately weighed and placed in the drum of a Roche friabilator (Campbell Electronics, Mumbai). The tablets were rotated at 25 rpm for a period of 4 min and then removed, dedusted, and accurately re-weighed (Ohaus, USA). Friability is expressed in terms of weight loss and was calculated as the percentage of the initial weight according to the IP specifications; friability under 1% was considered acceptable.¹²

$$\text{Percentage friability} = \frac{\text{Initial weight (W}_0\text{)} - \text{Final weight (W)}}{\text{Initial weight (W}_0\text{)}} \times 100$$

In vitro disintegration test

The DT of the tablet was measured in 900 mL of distilled water (37±2°C) using a Digital Tablet Disintegration Tester (Veego, India). The time in seconds taken for the complete disintegration of the tablet with no palpable mass in the apparatus was measured in seconds. Six tablets from each batch (formulation) were tested for the DT calculations.¹³

Wetting time

A piece of tissue paper folded twice was placed in a small Petri dish (ID 6.5 cm) containing 6 mL of distilled water. A tablet containing a small quantity of amaranth color was placed on the paper and the time for the upper surface of the tablet to become

completely red was measured. Three trials for each batch were performed.¹⁴

Drug content (%)

For the estimation of drug content (%), ten tablets were selected randomly and the average weight was calculated. The tablets were crushed in a mortar and an accurate weight equivalent 7.5 mg of AMB hydrochloride and 2 mg of salbutamol sulphate was weighed and dissolved in a suitable quantity of 6.8 pH phosphate buffers. The solution was sonicated, filtered, and suitably diluted and the drug content (%) was determined using the simultaneous equation method with a double-beam UV spectrophotometer (UV-1800 Shimadzu) at 244 nm and 276 nm wave-lengths, which correspond to AMB hydrochloride and salbutamol sulphate, respectively. Each sample was analyzed in triplicate. The tablets should comply with the IP specifications i.e. 85%-110%.¹⁵

In vitro drug release studies

In vitro drug release studies of all the formulations were performed using USP eight-stage dissolution testing apparatus-2 (paddle method) (Lab, India) at 50 rpm. Phosphate buffer pH 6.8 (500 mL) was used as the dissolution media with the temperature maintained at 37±0.5°C. Five milliliter samples were withdrawn at different intervals, diluted suitably, and analyzed at 244 nm and 276 nm. An equal volume of fresh dissolution medium was replaced to maintain the original volume. The in vitro release studies were performed in triplicate. Absorbance of these solutions was measured at their respective λ_{\max} .¹⁶ Cumulative percentage (%) drug release was calculated using the simultaneous equation method, which is given as:

$$\text{At 244 nm} \quad A_1 = 0.025_{A} + 0.0017_{S}$$

$$\text{At 276 nm} \quad A_2 = 0.0030_{A} + 0.0066_{S}$$

Where C_A is the concentration of AMB hydrochloride, and C_S is the concentration of salbutamol sulphate. By putting the values of absorbances A_1 and A_2 at their respective λ_{\max} , the concentrations of AMB hydrochloride and salbutamol sulphate were obtained in the sample solutions.¹⁷

Drug-excipient compatibility studies

This study generally includes fourier transform infrared spectroscopy (FTIR) and these are generally performed to confirm the drug- excipients compatibility. In order to determine the compatibility between pure drugs with the excipients used in formulation, the FTIR spectra of the physical mixture of the pure drugs and optimized ODT formulation were recorded on an

FTIR spectrophotometer (Bruker, USA) in the scanning range of 4000 to 600 cm^{-1} and the resolution was 1 cm^{-1} . FTIR scans were then evaluated for shifting and masking and the appearance of new peaks due to drug-excipient incompatibility.¹⁸

Accelerated stability studies

Accelerated stability studies were performed on the formulated ODTs (formulated in three primary batches), which were wrapped in aluminium foil and then stored in air-tight containers that were impermeable to solids, liquids, and gases, for a period of one month as prescribed by the ICH guidelines at a temperature of 40±2°C, at ambient humidity, as well as at room temperature (25±2°C). To achieve these types of storage conditions, we kept the sample in two stability chambers (Thermolab) to attain the above conditions. The tablets were withdrawn on the 15th and 30th day and analyzed for drug content (%), friability, hardness, and in vitro DT.¹⁹

RESULTS AND DISCUSSION

Optimization of superdisintegrant SSG

The results for the optimization of the superdisintegrant concentration in the ODTs are shown in Table 4. From the evaluation parameters, it was observed that SSG in 4% concentration was the optimum concentration for rapid tablet disintegration on the basis of the lowest DT observed with F3 formulation. The superdisintegrant action of SSG is exhibited by swelling and capillary action, which causes rapid disintegration of the tablets. Due to its hydrophilic nature, it rapidly absorbs water and swells up to 200-300% of their own weight. It is used in the concentration range of 4-8%. DT increases above 4% due to the gelling effect of SSG.²⁰

Optimization of PVP K-30 or MCC (Avicel PH-102) along with the optimized concentration of SSG

The results for optimization of different binders in the ODTs are given in Table 5. It was observed from the evaluation parameters that the DT of formulation B8 was further decreased and friability and hardness of the tablet complied with the IP limits. The lowest DT was observed in formulation B8 i.e. 1% MCC as compared with the B2 formulation i.e. 2% PVP K-30. The probable reason was that MCC has strong binding properties alongside its good disintegration, which is attributed to swelling or capillary action and high dilution potential. The strong binding property of MCC is a result of its plastic deformation under pressure. Generally, plastic deformation occurs if the crystal structure or shape is changed under compression against

Table 4. Evaluation parameters for the optimization of sodium starch glycolate

Evaluation parameters	F1 (1%)	F2 (2%)	F3 (4%)	F4 (6%)	F5 (8%)	F6 (10%)
*Weight variation (mg) ± SD	198±2.0	202±1.0	201±2.0	198±3.0	197±2.0	201±1.0
Friability (%) ± SD	0.8±0.1	0.8±0.2	0.1±0.1	0.3±0.1	0.1±0.1	0.1±0.1
*Hardness (kg/cm ²) ± SD	2.8±0.57	2.6±0.28	2.5±0.28	2.5±0.32	2.8±0.57	2.8±0.28
**Disintegration time (s) ± SD	65±1.74	48±1.35	34±1.86	45±2.36	72±1.76	90±2.64

IP: Indian Pharmacopoeia, SD: Standard deviation, *represents the average of 3 determinations, **represents the average of 6 determinations

Table 5. Evaluation parameters for the optimization of PVP K-30 or MCC (Avicel PH-102) with the optimized concentration of SSG

Evaluation parameters	*Weight variation (mg) ± SD	*Friability (%) ± SD	*Hardness (kg/cm ²) ± SD	**Disintegration time (s) ± SD
Formula no.				
B1	200±2.0	0.1±0.1	2.5±0.28	56±1.78
B2	201±1.0	0.2±0.1	2.0±0.28	40±1.67
B3	197±2.0	0.5±0.2	2.0±0.00	54±2.89
B4	199±3.0	0.3±0.2	3.0±0.76	71±2.40
B5	204±2.0	0.3±0.1	2.5±0.50	82±5.16
B6	202±2.0	0.8±0.3	2.5±0.50	95±5.77
B7	198±1.0	0.8±0.2	2.0±0.00	105±5.43
B8	201±1.0	0.1±0.1	2.5±0.50	36±2.13
B9	204±2.0	0.1±0.1	2.5±0.28	43±1.34
B10	197±3.0	0.2±0.2	2.5±0.28	55±1.10
B11	199±2.0	0.1±0.1	2.5±0.28	64±1.32
B12	203±2.0	0.1±0.25	2.5±0.28	78±2.08
B13	201±1.0	0.1±0.25	2.5±0.28	92±1.84
B14	202±1.0	0.1±0.25	2.5±0.28	103±1.73

SD: Standard deviation, PVP K-30: Polyvinylpyrrolidone K-30, MCC: Microcrystalline cellulose, SSG: Sodium starch glycolate, *represents the average of 3 determinations, **represents the average of 6 determinations

the intermolecular forces that restore crystal features to its original form.²¹ On the other hand, water-soluble materials such as PVP K-30 dissolve faster rather disintegrate. Therefore, as the optimum binder concentration, 1% MCC was selected for the final formulation of the AMB hydrochloride and salbutamol sulphate ODT. The study concluded that optimization of the binder: superdisintegrant concentration was essential for reducing the DT of the tablets.

Evaluation parameters for AMB hydrochloride & salbutamol sulphate ODT

ODTs were prepared through direct compression and evaluated for hardness, weight variation, friability, thickness, percentage drug content uniformity, and *in vitro* DT; the results of which are shown in Table 6. The weight variation of the formulated batches was shown to be within the acceptable IP limits. The drug content (%) was found to be AMB: 106.5±1.53%, SAL: 93.33±2.25%. The drug content (%) was found in the range of 85-115% of the label claim (IP acceptable limit). Tablets require a certain amount of hardness and resistance to friability to withstand mechanical shock in manufacture, packing, and shipping. Hardness was found to be 2.5±0.29 kg/cm². The friability of the tablets was found below 1%, indicating a good mechanical resistance of the tablets. The *in vitro* DT of the tablets was found to be less than 60 seconds as shown. The wetting time was good in practical terms for formulation. The formulated ODTs showed low DT, indicating the suitability of the formulation for being a mouth-dissolving tablet. From the *in vitro* release study, it was observed that 93.23±0.25% of AMB

Table 6. Evaluation parameters for ambroxol hydrochloride and salbutamol sulphate ODT

Evaluation parameters	Results
*Weight variation (mg) ± SD	201±2.0
*Thickness (mm) ± SD	3.63±0.06
*Hardness (kg/cm ²) ± SD	2.5±0.29
*Friability (%) ± SD	0.2±0.15
**Disintegration time (s) ± SD	34±1.14
*Wetting time (s) ± SD	26±1.53
*Drug content uniformity ± SD	AMB: 106.5±1.53 SAL: 93.33±2.25

SD: Standard deviation, ODT: Orally-disintegrating tablet, AMB: Ambroxol, SAL: Salbutamol sulphate, *represents the average of 3 determinations, **represents the average of 6 determinations

hydrochloride released in 20 min and 89.23±1.03% of salbutamol sulphate released in 12 min, indicating that the tablet complied with IP specifications i.e. 85%-110%, as given in Figure 1.

Drug-excipient compatibility studies

The FTIR spectra of pure drugs in combination and formulated ODT-containing drugs were obtained on an FTIR spectrophotometer. The FTIR results, as given in Figure 2 and Figure 3, indicated that there were no interaction between the drug and other excipients used in the formulation. The FTIR spectra of the physical mixture of AMB hydrochloride and salbutamol sulphate showed an intense band at 696.34 cm⁻¹,

1611.17 cm^{-1} , and 1279.00 cm^{-1} , corresponding to the presence of functional groups such as aliphatic bromo compound, secondary amine and secondary alcohol in AMB hydrochloride and at 1389.84 cm^{-1} , 1611.17 cm^{-1} , and 1389.84 cm^{-1} , corresponding to the presence of functional groups such as trimethyl, secondary amine, and phenol in salbutamol sulphate. The FTIR of AMB hydrochloride and salbutamol sulphate ODT formulation also showed intense absorption bands at 651.32 cm^{-1} , 1611.97 cm^{-1} , and 1280.03 cm^{-1} for AMB hydrochloride and at 1389.04 cm^{-1} , 1611.97 cm^{-1} , and 1389.04 cm^{-1} for salbutamol sulphate, indicating no changes in the functional groups and confirmed the undisturbed structures of AMB hydrochloride and salbutamol sulphate, which indicated no drug-excipient incompatibility, as shown in Figures 2 and 3.

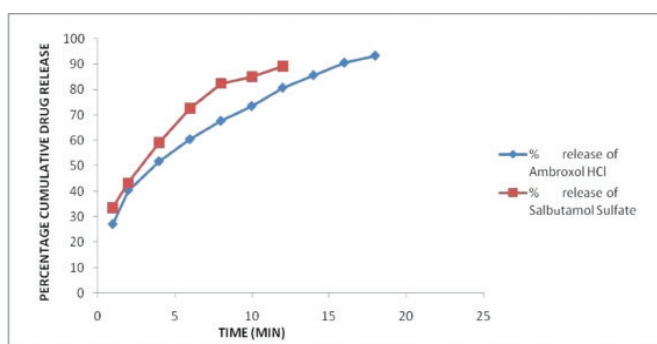


Figure 1. *In vitro* drug release profile of the ambroxol hydrochloride and salbutamol sulphate orally-disintegrating tablet

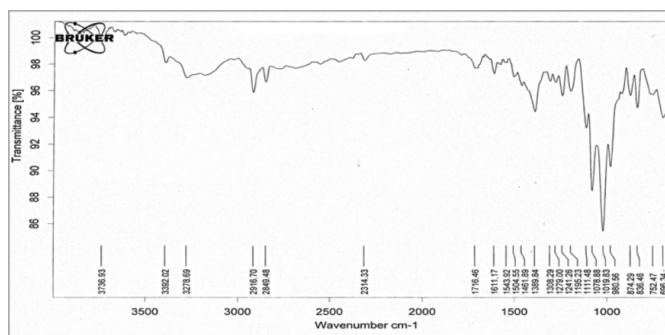


Figure 2. Fourier transform infrared spectroscopy spectra of the physical mixture of ambroxol hydrochloride, salbutamol sulphate, and blend

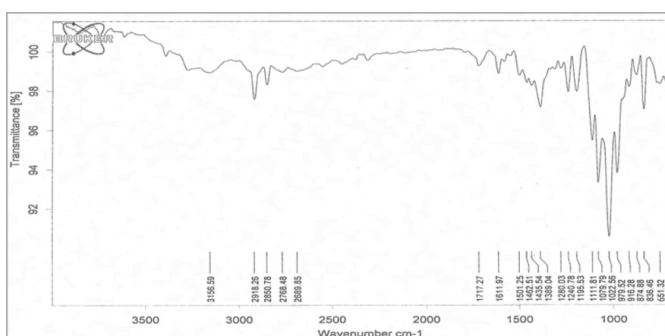


Figure 3. Fourier transform infrared spectroscopy spectra of ambroxol hydrochloride and salbutamol sulphate orally-disintegrating tablet formulation

Accelerated stability studies

Accelerated stability studies of the final optimized ODTs (prepared in three primary batches), which were wrapped in aluminium foil to simulate the Alu packing of drug products and then stored in air-tight containers impermeable to solids, liquids, and gases for a period of 1 month as prescribed by the ICH guidelines. The product was exposed to normal and extreme conditions of temperature and humidity. The stability data of the formulation are given in Table 7 and Table 8. The results of the stability study indicated that there was little difference observed in hardness, DT, drug content uniformity and friability before and after the storage period at room temperature and at ambient humidity, but at temperature of $40^{\circ}\text{C}\pm 2^{\circ}\text{C}$ and at ambient humidity. Hardness was found to be increased with time and prolonged the DT of the tablet.²² The probable reason was loss of moisture from tablets but in all cases, DT was within the specified IP limit (within 3 min.). This indicates that the formulation was fairly stable in both storage conditions. Statistical analysis (ANOVA) was also performed using the Graph Pad in Stat 3 statistical package for Windows. The stability data shown in the tables for the three primary batches of formulations were evaluated for drug content (%), friability, hardness, and disintegration time before and after stability testing, represented by the mean of three or six determinations \pm standard deviation. The statistical significance of the differences between the evaluation parameters of three primary batches was calculated using the Tukey-Kramer multiple comparison test, and the probability value of p smaller than 0.05 indicated a statistically significant difference.

CONCLUSION

The objective of the present investigations was achieved by preparing an orally-dissolving drug delivery system of AMB hydrochloride and salbutamol sulphate in fixed-dose combination with a faster onset of action by using an optimum amount of superdisintegrant SSG and binder MCC using direct compression. The optimization methods mentioned in the report were proved useful in the development of ODTs. The ODTs developed in this work will hopefully contribute to improving drug administration to patients with swallowing and chewing difficulties. The prepared ODTs passed all the quality control tests viz., weight variation, hardness, friability, *in vitro* DT, drug content (%), and wetting time. *In vitro* dissolution results were also studied. The ODT formulation satisfied the requirements of the Food and Drug Administration for rapid-dissolving tablets and allowed more than 85% of drug to be dissolved within 30 min. The FTIR study revealed that there was no interaction between drug and excipients. The accelerated stability study showed that the formulation was quite stable at normal temperature and humidity conditions, as well as at extreme temperature and humidity conditions. Thus, it is concluded that by adopting a systematic formulation approach, ODTs of AMB hydrochloride and salbutamol sulphate in fixed-dose combination can be formulated using superdisintegrants in combination with appropriate binder and excipients, which was found to be economical and industrially feasible.

Table 7. Accelerated stability data of the ambroxol hydrochloride and salbutamol sulphate ODT at temperature (40±2°C) and at ambient humidity

Time interval	Three primary batches								
	0 day			15 th day			30 th day		
Evaluation parameters	B-1	B-2	B-3	B-1	B-2	B-3	B-1	B-2	B-3
*Hardness (kg/cm ²) ± SD	2.7±0.29	2.5±0.00	2.5±0.00	2.9±0.29	2.7±0.29	2.8±0.29	3.0±0.29	3.2±0.29	3.2±0.29
*Friability (%) ± SD	0.2±0.1	0.3±0.1	0.2±0.1	0.5±0.2	0.4±0.1	0.3±0.1	0.3±0.1	0.2±0.1	0.3±0.1
*Drug content (%) ± SD	AMB- 90.8±3.36	AMB- 95.6±2.34	AMB- 93.8±1.24	AMB- 92.5±2.14	AMB- 93.5±2.67	AMB- 94.8±1.23	AMB- 91.3±1.98	AMB- 94.4±1.65	AMB- 95.7±3.63
	SAL- 104.7±1.97	SAL- 95.4±2.86	SAL- 97.7±3.97	SAL- 103±1.76	SAL- 98.6±2.07	SAL- 93.4±1.77	SAL- 97.8±2.97	SAL- 97.7±2.75	SAL- 94.2±2.43
**Disintegration time (s) ± SD	42±2.14	38±1.67	43±3.31	46±4.94	43±3.06	48±1.59	48±2.38	47±2.67	50±3.51

SD: Standard deviation, ODT: Orally-disintegrating tablet, AMB: Ambroxol, SAL: Salbutamol sulphate, *represents the average of n=3 determinations, **represents the average of n=6 determinations

Table 8. Accelerated stability data of the ambroxol hydrochloride and salbutamol sulphate ODT at room temperature and at ambient humidity

Time interval	Three primary batches								
	0 day			15 th day			30 th day		
Evaluation parameters	B-1	B-2	B-3	B-1	B-2	B-3	B-1	B-2	B-3
*Hardness (kg/cm ²) ± SD	2.7±0.29	2.5±0.00	2.5±0.00	2.7±0.29	2.3±0.29	2.5±0.00	2.5±0.00	2.5±0.29	2.3±0.29
Friability (%) ± SD	0.2±0.1	0.3±0.1	0.2±0.1	0.3±0.1	0.3±0.1	0.3±0.1	0.3±0.1	0.4±0.2	0.5±0.2
*Drug content (%) ± SD	AMB- 90.8±3.36	AMB- 95.6±2.34	AMB- 93.8±1.24	AMB- 96.8±4.23	AMB- 94.5±3.78	AMB- 96.8±2.31	AMB- 95.6±3.21	AMB- 94.4±3.14	AMB- 95.7±4.34
	SAL- 104.7±1.97	SAL- 95.4±2.86	SAL- 97.7±3.97	SAL- 100.3±4.13	SAL- 93.6±3.45	SAL- 98.4±2.54	SAL- 99.3±3.35	SAL- 92.7±1.42	SAL- 97.3±3.24
**Disintegration time (s) ± SD	42±2.14	38±1.67	43±3.31	42±3.97	41±4.52	47±1.66	46±2.83	44±2.52	48±3.75

SD: Standard deviation, ODT: Orally-disintegrating tablet, AMB: Ambroxol, SAL: Salbutamol sulphate, *represents the average of 3 determinations, **represents the average of 6 determinations

ACKNOWLEDGEMENTS

The authors highly acknowledge NB Entrepreneurs, Nagpur and Trojan Pharma, Baddi, India for providing gift samples of AVICEL PH-102 and drugs, and Rayat Bahra Institute of Pharmacy, Hoshiarpur Jalandhar for their efforts to facilitate the use of the necessary instruments and materials required during the entire course of this research work.

Conflict of Interest: No conflict of interest was declared by the authors.

REFERENCES

- Brniak W, Jachowicz R, Pelka P. The practical approach to the evaluation of methods used to determine the disintegration time of orally disintegrating tablets (ODTs). *Saudi Pharm J.* 2015;23:437-443.
- Pawar H, Varkhade C, Jadhav P, Mehra, K. Development and evaluation of orodispersible tablets using a natural polysaccharide isolated from *Cassia tora* seeds. *Integ Med Res.* 2014;3:91-98.
- Munoz H, Castan H, Clares B, Ruiz MA. Obtaining fast dissolving disintegrating tablets with different doses of melatonin. *Int J Pharm.* 2014;467:84-89.
- Kaur L, Bala R, Kanojia N, Nagpal M, Dhingra GA. Formulation development and optimization of fast dissolving tablets of aceclofenac using natural superdisintegrant. *ISRN Pharm.* 2014;2014:242504.
- Remya K, Beena P, Bijesh P, Sheeba A. Formulation development, evaluation and comparative study of effects of super disintegrants in cefixime oral disintegrating tablets. *J Young Pharm.* 2010;2:234-239.
- Segale L, Maggi L, Machiste EO, Conti S, Conte U, Grenier A, Bess C. Formulation design and development to produce orodispersible tablets by direct compression. *J Drug Del Sci Tech.* 2007;17:199-203.
- Bankar A, Bankar VH, Gaikwad PD, Pawar SP. Formulation design and optimization of sustained release tablet of ambroxol hydrochloride. *Int J Drug Del.* 2012;4:375-385.
- Aher SS, Songire PR, Saudagar RB. Formulation and evaluation of controlled release matrix tablet of albuterol sulphate. *Int J Curr Res.* 2016;8:35044-35050.

9. Comoglu T, Unal B. Preparation and evaluation of an orally fast disintegrating tablet formulation containing a hydrophobic drug. *Pharm Dev Technol.* 2015;20:60-64.
10. Malvey S, Kshirasagar N, Vishnu YV, Srikanth J. Formulation and evaluation of acyclovir orodispersible tablets using sublimation method. *J Gen Pract.* 2015;3:208.
11. Sharma D, Singh M, Kumar D, Singh G. Formulation development and evaluation of fast disintegrating tablet of salbutamol sulphate: A novel drug delivery for pediatrics and geriatrics. *J Pharm.* 2014;1-8.
12. Shoukri RA, Ahmed IS, Shamma RN. *In vitro* and *in vivo* evaluation of nimesulide lyophilized orally disintegrating tablets. *Eur J Pharm Biopharm.* 2009;73:162-171.
13. Sharma D, Singh M, Kumar D, Singh G, Rathore MS. Formulation development and evaluation of fast disintegrating tablets of ambroxol hydrochloride for pediatrics-A novel approach for drug delivery. *Indian J Pharma Edu Res.* 2014;48:40-48.
14. Bala R, Khanna S, Pawar PK. Formulation and optimization of fast dissolving intraoral drug delivery system for clobazam using response surface methodology. *J Adv Pharm Tech Res.* 2013;4:151-159.
15. Karthikeyan M, Umarul MA, Megha M, Shadeer HP. Formulation of diclofenac tablets for rapid pain relief. *Asian Pac J Trop Dis.* 2012;2(Suppl 1):308-311.
16. Earle RR, Ayalasomayajula LU, Venkatesh P, Naidu PG, Sagar SV, Vani BS. Formulation and evaluation of atenolol orodispersable tablets by coprocessed super-disintegration process. *Int J Adv Pharm.* 2016;5:46-51.
17. Sharma D, Kumar D, Singh M, Singh G, Rathore MS. Spectrophotometric method development and validation for simultaneous estimation of salbutamol sulphate and ambroxol hydrochloride in combined dosage Forms. *Int J Drug Dev Res.* 2013;5:124-132.
18. Sharma D. Formulation development and evaluation of fast disintegrating tablets of salbutamol sulphate for respiratory disorders. *ISRN Pharm.* 2013;2013:674507.
19. ICH Harmonised Tripartite Guideline. Cover Note for Revision of Q1A(R) Stability Testing of New Drug Substances and Products. Q1A(R2) 2003;pp.9. Available from: https://www.ich.org/fileadmin/Public_Web_Site/ICH_Products/Guidelines/Quality/Q1A_R2/Step4/Q1A_R2___Guideline.pdf
20. Mangal M, Thakral S, Goswami M, Ghai P. Superdisintegrants: An updated review. *Int J Pharm Pharm Sci Res.* 2012;2:26-35.
21. Al-khattawi A, Mohammed AR. Compressed orally disintegrating tablets: excipients evolution and formulation strategies. *Expert Opin Drug Deliv.* 2013;10:651-663.
22. Ahmad I, Shaikh RH. Effect of temperature and humidity on the disintegration time of packaged paracetamol tablet formulations. *Pak J Pharm Sci.* 1994;7:1-7.



A Simple Isocratic High-performance Liquid Chromatography Method for the Simultaneous Determination of Shikonin Derivatives in Some *Echium* Species Growing Wild in Turkey

Türkiye’de Yabani Yetişen Bazı *Echium* Türlerindeki Şikonin Türevlerinin Basit İzokratik HPLC Yöntemiyle Eşzamanlı Olarak Belirlenmesi

© Nuraniye ERUYGUR

Cumhuriyet University, Faculty of Pharmacy, Department of Pharmacognosy, Sivas;
Selcuk University, Faculty of Pharmacy, Department of Pharmacognosy, Konya, Turkey

ABSTRACT

Objectives: Dried roots of *Echium* species are used in Turkey for the treatment of wounds, inflammation, and depression. In this study, an reversed-phase-liquid chromatographic method with isocratic elution was developed to determine shikonin derivatives in *Echium* species.

Materials and Methods: The chromatographic separation and quantification was performed on a C18 column (ACE, 150 mm × 4.6 mm, 5 µm), with a mobile phase of acetonitrile and 0.1 M acetic acid (70: 30, v/v) at a flow rate of 1 mL/min, and ultraviolet detection at 520 nm.

Results: Linear behavior was observed over the investigated concentration range (2-500 ppm) for all analytes, with a correlation coefficient of >0.998. The proposed method was found to be specific and precise for the quantification of shikonin derivatives in *Echium* species.

Conclusion: The highest content of shikonin derivatives was observed in *E. italicum* L. compared with the other species studied herein, advocating the use of *E. italicum* L. roots as an alternate source for shikonin derivatives.

Key words: *Echium* sp., shikonin derivatives, HPLC

ÖZ

Amaç: Türkiye’de *Echium* türlerinin kurutulmuş kökleri yara, enflamasyon ve depresyon tedavisinde kullanılmaktadır. Bu çalışmada, *Echium* türlerinde bulunan şikonin türevlerinin içeriğini belirlemek için, ters faz yüksek performans sıvı kromatografisi izokratik elüsyon metodu geliştirilmiştir.

Gereç ve Yöntemler: Kromatografik ayırım ve miktar tayini, C18 (ACE, 150 mm × 4.6 mm, 5 µm) kolonda, asetoneitril, 0.1 M asetik asit (70: 30, v/v) mobil fazı ile 1 mL/min hızla, ultraviyole dedektörle 520 nm’de gerçekleştirilmiştir.

Bulgular: Tüm analitlerde incelenen konsantrasyon aralığında (2-500 ppm) lineer davranış gözlenmiş, korelasyon katsayısı >0,998 olarak bulunmuştur. Önerilen yöntemin, *Echium* türlerindeki şikonin türevlerinin incelenmesi için spesifik ve kesin olduğu bulunmuştur.

Sonuç: Şikonin türevlerinin en yüksek içeriği *E. italicum* L.’de gözlemlenmiştir ve bu da *E. italicum* L. köklerinin şikonin türevleri için, alternatif bir kaynak olarak kullanılmasını desteklemektedir.

Anahtar kelimeler: *Echium* sp., şikonin türevleri, HPLC

INTRODUCTION

Species of *Echium* occur abundantly as a flowering plant native to North Africa, mainland Europe, and the Macaronesian islands, but have also become invasive in southern Africa and Australia.

Out of the 60 species of this genus, nine are found in Turkey: *E. angustifolium*, *E. arenarium*, *E. italicum*, *E. glomeratum*, *E. orientale*, *E. parviflorum*, *E. plantagineum*, *E. russicum*, and *E. vulgare*.

*Correspondence: E-mail: neruygur@cumhuriyet.edu.tr, Phone: +90 544 552 19 82 ORCID-ID: orcid.org/0000-0002-4674-7009

Received: 13.01.2017, Accepted: 16.03.2017

©Turk J Pharm Sci, Published by Galenos Publishing House.

Based on the traditional documents on folk medicine, *Echium* sp. have been employed as diaphoretics, diuretics, expectorants, febrifuges, sedatives, analgesics, vulneraries, anxiolytics, and in the treatment of upper respiratory tract infections.¹⁻⁴ Pharmacologic studies have demonstrated that species of *Echium* possess antioxidant⁵⁻⁷, anti-inflammatory⁸, antibacterial^{9,10}, antiviral¹¹, antiproliferative¹²⁻¹⁴, analgesic¹⁵ and antidepressant¹⁶ activities. It is clinically proven as a useful and safe drug in patients with obsessive compulsive disorders.¹⁶⁻¹⁸ It is also reported that various extracts of *E. amoenum* have good antianxiety activity on *in vivo* models.¹⁹⁻²³ *Echium* species contain a variety of phytochemicals, including naphthoquinones, flavonoids, pyrrolizidine alkaloids, steroids, anthocyanins, fatty acids, amino acids, and essential oils. Many shikonin (S) derivatives (ShD) have been isolated from the roots of *Echium* plants. Naphthoquinones are a series of ShD such as S, acetylshikonin (AS), deoxyshikonin (DS), β , β -dimethylacrylshikonin (DMAS), isobutrylshikonin, isovalerylshikonin (IVS), and 2-methyl butrylshikonin (MBS).²⁴

S, R enantiomer of Alkannins, are lipophilic red pigments commonly known as isohexenylnaphthazarins. They are mostly found in more than 150 genus such as *Lithospermum*, *Echium*, *Onosma*, *Anchusa*, and *Cynoglossum* of the Boraginaceae family. Historically they were used as dyes by the ancient Greeks and Romans. S contains two parts structurally: the naphthazarine moiety (5, 8-dihydroxy-1, 4 naphthoquinone) and the chiral six-carbon side chain. It is readily sensitive to polymerization following treatment with acids, bases, heat, or light due to the naphthazarine core, and easily to oxidation by exposure to light or air just for the high chemical reactivity. Most of the ShD are present as ester derivatives linked with the hydroxyl group of the side chain, maintaining the naphthazarine moiety.²⁵ ShD have attracted the attention of many researchers due to their several potential pharmacologic activities such as antimicrobial, antitumor, wound healing, and antioxidants. S extracts obtained from *Lithospermum erythrorhizon* induced apoptosis against human colorectal carcinoma cells, HL60 cells, and HeLa cells by the mechanism of tumor suppression via signaling pathways that possibly involved reactive oxygen species, p53, p27, Bcl-2, caspase, and inhibition of DNA topoisomerase I/II and telomerase.²⁶⁻²⁸ A clinical study showed that ShD were efficacious in the treatment of patients with late-stage lung cancer who were inappropriate for other treatment.²⁹ Furthermore, the cream Helixderm®, made from S and derivatives, has been evaluated for wound healing activity in clinical trials undertaken at the Freie University and showed good results with granulation and epithelization.³⁰

In terms of the toxicologic effect of naphthoquinone compounds, it was reported that ShD did not induce any hematologic toxicity in animal models, which indicates that ShD may be safe for use *in vivo*³¹, whereas another report demonstrated toxicity in mice by intraperitoneal administration at a dose of 20 mg/kg for S, 41.0/22.75 mg/kg for AS, and 48 mg/kg for 3,3- β , β -DMAS. In

addition, toxicity has also been observed during *in vivo* testing for the antitumor effects of ShD.³²

Herbals and herbal drugs contain active ingredients present in the naturally occurring plant source in certain quantities, and the proportion between different constituents or active principles is a key quality parameter for the efficacy of the product. It is in this regard that the modern tools and techniques of analysis provide vital support and required evidence. According to our knowledge, there are no reports related to the phytochemical analyses of naphthoquinone derivatives in *Echium* sp. using high-performance liquid chromatography (HPLC) quantitatively. Thus, the aims of the present study were to quantify biologically active naphthoquinone derivatives in the ethanol extracts of the roots of four selected *Echium* species growing wild in Turkey.

EXPERIMENTAL

HPLC analysis of shikonin derivatives in different samples

Plant material and chemicals

E. italicum L., *E. vulgare* L., plant procured from 56 km north of Ankara, and *E. angustifolium* Miller., *E. parviflorum* Moench collected from the coast of Antalya province of Turkey, identified and authenticated by Dr. Gülderen Yılmaz, Assist. Professor, Ankara University, Faculty of Pharmacy, Department of Pharmaceutical Botany. A voucher specimen has been deposited in the Herbarium of Gazi University, Faculty of Pharmacy (GUE2991, GUE2992) and in the herbarium of Ankara University, Faculty of Pharmacy (AEF26023, AEF26024). The reference compounds were purchased from *Pureone biotechnology Co. Ltd*, China. Chemicals and reagents used in the study were of HPLC grade or analytical grade.

Extraction of plant samples

Extraction of crude plant extracts

The extraction procedure was performed as follows: the shade-dried and coarsely powdered roots of four *Echium* sp. (100 g) were extracted with 96% alcohol (2 × 750 mL) in a water bath with temperature of 40°C for 48 h. After cooling, the material was filtered and the residue was further extracted with ethanol (500 mL) twice. Following this procedure, all the extracts were pooled together, concentrated under vacuum using a rotavapor (Büchi, Switzerland) to afford the alcoholic extract, and then freeze-dried (Figure 1).

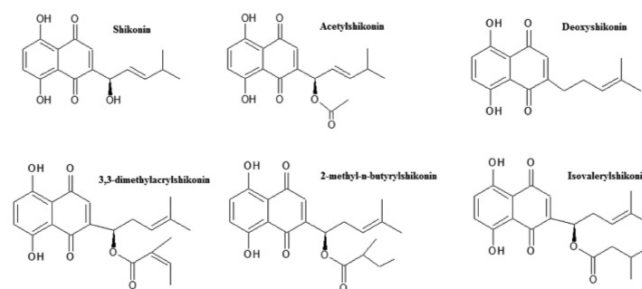


Figure 1. The structures of standard compounds

Identification of shikonin derivatives by thin-layer chromatography

Fifty milligrams of the ethanol extracts made from roots of four *Echium* species were taken into a set of 10 mL volumetric flasks separately and the volumes were completed to the mark with methanol. A 10- μ L aliquot of test samples of different extracts was applied to the TLC plate (aluminum foil-backed TLC plate coated with silica gel 60 F254, Merck, 0.2-mm layer thickness) separately. It was positioned 10 mm from the bottom of the plate, and then the plate was developed to a distance of about 9.5 cm using petroleum ether: ethyl acetate: acetic acid (85:15:1/v) as the mobile phase. The plates were then removed, air-dried, and the spots were visualized under an ultraviolet (UV) lamp at 254 nm after spraying 5% sulfuric acid reagent on the plate and heated at 105°C for about 5 min until the bands are clearly visible. The chromatogram obtained with test solution showed a band corresponding to those of ShD (Figure 2).

High-performance liquid chromatography

Instrumentation

An Agilent 1200 LC system (equipped with a G1311A pump, G1328B manual injector, G1322A degasser, G1316A column heater, and G1314B variable wavelength UV-detector) was employed (Agilent Technologies-Santa Clara, CA).

Chromatographic conditions

An ACE 5 C18 (150 mm \times 4.6 mm, 5 μ m) (Scotland) reversed-phase column was used as the stationary phase. An isocratic elution program was applied for chromatographic analysis. The mobile phase was a mixture of acetonitrile: 0.1 M acetic acid contained water=70:30 (pH: 2.82) with isocratic elution, filtered through a 0.45- μ m membrane filter (Millipore) and degassed by sonication for 30 min prior to use. The analysis was performed at a flow-rate of 1.0 mL/min. The injection volume was adjusted to 10 μ L. The temperature of the column was set to 25°C. The analysis was performed at 520 nm because the maximum UV absorbance for the analytes were obtained at this wavelength.

Preparation of test solution

The dry extracted samples were weighed and finely powdered. Approximately 100 mg of the ground powder was weighed carefully in the vials, then the sample was ultrasonically extracted with 15 mL methanol and 1 mL DMSO for about 30 min. After cooling, the volume was made up to 50 mL with the same solvent. Prior to analysis, the extraction solutions were filtered through a 0.45- μ m filter membrane (Merck, Millipore) and 10- μ L aliquot was injected into the HPLC system.

Preparation of standard solution

A standard stock solution of S, AS, DS, DMAS, MBS, and IVS was prepared by dissolving 1.0 mg of each compound in 10 mL of acetonitrile in a volumetric flask. For the determination of the limit of detection (LOD) and limit of quantification (LOQ), working standard solutions were prepared by further dilution of this stock solution with aqueous methanol.

Calibration curve

Linear calibration plots were obtained for the related standard compounds at six different concentration levels. After filtering through a 0.45- μ m membrane filter, 10 μ L of each concentration of the standard solution was injected into the HPLC system for analysis in triplicates. The regression equation and coefficient of correlation is given in Table 1.

Validation of method

LOD and LOQ were determined experimentally based on the signal-to-noise ratio until the average responses were approximately three (S/N=3) and ten times (S/N=10) that of the blank responses, respectively.

The accuracy of the method was ascertained by spiking the pre-analyzed samples with a known amount of standard solution prepared at three concentration levels (50, 100, and 150 ppm) in triplicate. The average percentage recovery was estimated by applying the values of the peak area to the regression equations of the calibration graph.

Precision test: The mixtures composed of S, DS, AS, DMAS, MBS, and IVS were taken and repeatedly injected six times to measure the peak areas respectively. The results are expressed as relative standard deviation (RSD).

The precision of the method (inter-day and intra-day variations of replicate determinations) was checked by injecting standard solution at different concentrations (12.5, 50, and 100 ppm) in triplicate on the same day and on five consecutive days. The results are reported in terms of RSD.

RESULTS AND DISCUSSION

Identification of active compounds by thin-layer chromatography (TLC)

The structures of the reference compounds analyzed using TLC are shown in Figure 1. The separation of four *Echium* species

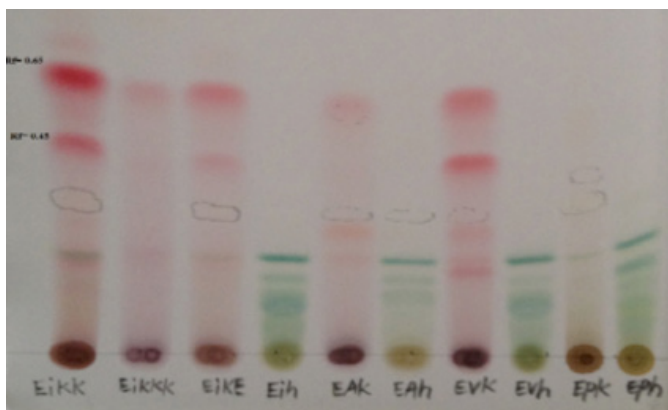


Figure 2. Thin layer chromatogram of four *Echium* species ethanol extracts from roots and aerial parts

EIKK: Chloroform extract of *E. italicum* roots, EIKKK: Chloroform extract of *E. italicum* root barks, EIKE: Ethanol extract of *E. italicum* roots, EIH: Ethanol extract of *E. italicum* aerial parts, EAK: Ethanol extract of *E. angustifolium* roots, EAH: Ethanol extract of *E. angustifolium* aerial parts, EVK: Ethanol extract of *E. vulgare* roots, EVH: Ethanol extract of *E. vulgare* aerial parts, EPK: Ethanol extract of *E. parviflorum* roots, and EPH: Ethanol extract of *E. parviflorum* aerial parts

root and aerial part ethanol extract with TLC are presented in Figure 2. A comparative chromatographic assessment showed the presence of the ShD in alcoholic extracts of roots of *E. italicum* L. *E. vulgare* L. and *E. angustifolium* Miller. The identification of the bands of ShD ($R_f=0.7-0.3$) in the sample extract was confirmed by overlaying their absorption with those of the standard compounds at 254 nm and 366 nm.

Optimization of HPLC

The critical aspects of developing a method in liquid chromatography are to provide good resolution between the studied compounds in the shortest analysis time. The current optimized conditions of HPLC with a C18 column and UV detector at 520 nm using isocratic mixture of acetonitrile and water as mobile phase achieved the best-resolved symmetric peaks for ShD. It was observed that the retention time of the reference standards was 4.176-16.58 min (Figure 3). The total run time of the ShD was found to be 20 min and the ShD in each extract could be observed on HPLC-UV chromatogram (Figure 4-7). This indicates that the present HPLC method is fast, specific, and convenient. The average retention time \pm SD for AS, S, DS, DMAS, MBS, and IVS was found to be 4.176 ± 0.003 , 8.752 ± 0.005 , 11.006 ± 0.004 , 15.059 ± 0.003 , 15.672 ± 0.004 and 16.584 ± 0.003 , respectively, for six replicates.

Validation of method

Calibration graphs were generated by plotting the linear regression of the peak area versus the corresponding analyte concentration; the calibration curve for each analyte was obtained using six concentration in the range of 2-500 ppm. The linear correlation coefficient (r^2) for all calibration curves was showing best linearity. The method was validated in terms of precision, accuracy, and other validation method parameters. The repeatability of the HPLC method and intermediate precisions for intra-day and inter-day variations are given in Table 1. The LOD value was found to be 0.19-2.01 ppm, which is the concentration that yields a signal-to-noise (S/N) ratio of 3:1. The LOQ value under the described conditions was 0.57-6.03

ppm with an S/N ratio of 10:1. This confirmed the sensitivity for the quantification of the compounds.

HPLC analysis of shikonin derivatives in different samples

The concentrations of the ShD in ethanol extracts of different

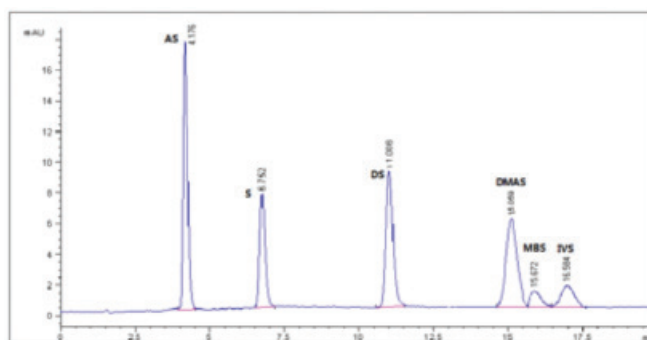


Figure 3. HPLC-UV chromatogram of reference standard mixtures prepared of 50 ppm

HPLC-UV: High-performance liquid chromatography-ultraviolet, AS: Acetylshikonin, S: Shikonin, DS: Deoxyshikonin, DMAS: β , β -dimethylacryshikonin, IVS: Isovalerylshikonin, MBS: 2-methyl butyrylshikonin

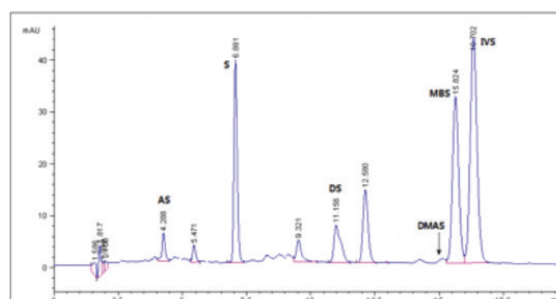


Figure 4. HPLC-UV chromatogram of ethanol extract of *E. italicum* L. root

HPLC-UV: High-performance liquid chromatography-ultraviolet, AS: Acetylshikonin, S: Shikonin, DS: Deoxyshikonin, DMAS: β , β -dimethylacryshikonin, IVS: Isovalerylshikonin, MBS: 2-methyl butyrylshikonin

Table 1. Validation parameters of the HPLC method for the determination of shikonin derivatives

Validation parameters	S	AS	DS	DMAS	MBS	IVS
Calibration range (ppm)	2-100	1-20	2-50	2-25	6.25-500	6.25-500
Correlation coefficient (r)	0.999	0.998	0.999	0.9996	1	0.999
Regression equation	$Y=5.761x + 0.333$	$Y=9.516x - 0.430$	$Y=7.509x - 3.424$	$Y=10.2x - 5.073$	$Y=2.920x - 1.794$	$Y=4.417x - 0.108v$
Limit of detection (ppm)	0.55	0.19	0.65	0.52	1.98	2.01
Limit of quantitation (ppm)	1.65	0.57	1.95	1.55	5.94	6.03
Method precision (RSD %)	1.12	2.012	1.464	1.87	1.58	2.72
Intermediate precision (RSD %)						
Interday (%)	1.11	1.25	0.98	1.28	1.76	0.87
Intraday (%)	1.26	2.36	1.45	2.11	2.95	1.93
Accuracy (RSD %)	2.67	2.08	3.03	4.24	2.62	2.96

S: Shikonin, AS: Acetylshikonin, DS: Deoxyshikonin, DMAS: 3,3- β , β -dimethylacryshikonin, MBS: 2-methyl-n-butrylshikonin, IVS: Isovalerylshikonin, ppm: Parts per million, RSD: Relative standard deviation

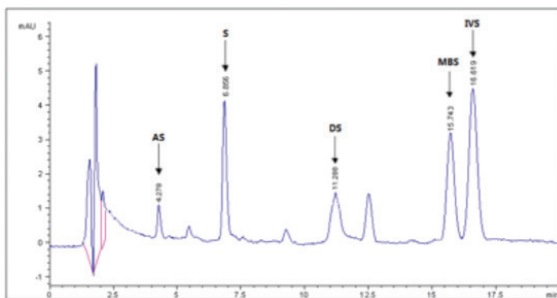


Figure 5. HPLC-UV chromatogram of ethanol extract of *E. vulgare* L. root
HPLC-UV: High-performance liquid chromatography-ultraviolet, AS: Acetylshikonin, S: Shikonin, DS: Deoxyshikonin, DMAS: β , β -dimethylacryshikonin, IVS: Isovalerylshikonin, MBS: 2-methyl butrylshikonin

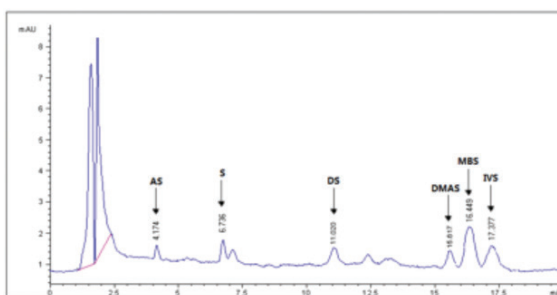


Figure 6. HPLC-UV chromatogram of ethanol extract of *E. angustifolium* Miller root

HPLC-UV: High-performance liquid chromatography-ultraviolet, AS: Acetylshikonin, S: Shikonin, DS: Deoxyshikonin, DMAS: β , β -dimethylacryshikonin, IVS: Isovalerylshikonin, MBS: 2-methyl butrylshikonin

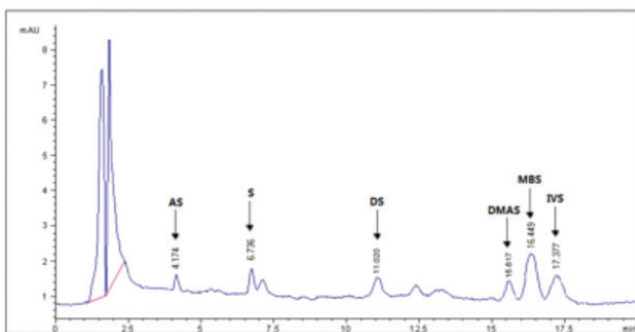


Figure 7. HPLC-UV chromatogram of ethanol extract of *E. parviflorum* Moench root

HPLC-UV: High-performance liquid chromatography-ultraviolet, AS: Acetylshikonin, S: Shikonin, DS: Deoxyshikonin, DMAS: β , β -dimethylacryshikonin, IVS: Isovalerylshikonin, MBS: 2-methyl butrylshikonin

Echium species were determined from the peak-area ratios using the equations of linear regression obtained from the calibration curves. Data for the concentration of ShD in ethanol extracts obtained from different *Echium* species growing wild in Turkey are presented in Table 2. As can be observed, the content of ShD was the highest in *E. italicum* L. compared with the other species.

CONCLUSIONS

S and derivatives are naturally occurring isohexenylnaphthazarine compounds, which are used as a red dye in drugs, cosmetics, and the textile industry in the Far East and Europe³³, and comprise the active ingredients of several pharmaceutical preparations because they exert potent biologic activities with wound healing, antimicrobial, cytotoxic, and antioxidant properties. However, these bioactive constituents become expensive due to their physical instability and tedious separation process. Therefore, it is important to develop a simple, fast, and sensitive method to evaluate S compounds in drugs, extracts, and pharmaceutical preparations. The implications of the current study are important because we have standardized the raw materials and preparations of the studied four *Echium* sp. roots for the first time. To the best of our knowledge, this is the first study to determine the amount of S and ShD in the four *Echium* sp. We developed a simple, accurate, fast, and reproducible HPLC method to quantify the active principles in *Echium* species. This method can be used for routine quality control analysis of this species. Although ShD are the main constituents of *Echium* sp. roots, the results of the current study also indicate that the maximum S derivative content in *Echium* species can be found in *Echium italicum* L. extract as compared with other studied extracts. Since most of the biologic activities such as antimicrobial, antiproliferative, antioxidant, analgesic, and antidepressant activities of *Echium* sp. roots can be attributed to ShD, the quantification of such compounds in the roots of these plants need to be considered as very important for the future use of preparations of these plants in several areas of clinical medicine. By using the optimized separation method described above, ShD can be detected in herbals or formulations prepared from Boraginaceae family plants, which are rich in naphthoquinone derivatives. We have demonstrated that the method is suitable for application in quality control of herbal formulations.

ACKNOWLEDGEMENT

The authors thank Osman Üstün, Uğur Tamer and Murat Şüküroğlu for helping with the research. The author would like

Table 2. Quantitative determination of shikonin derivatives in each *Echium* species

Content (w/w %)	S	AS	DS	DMAS	MBS	IVS
<i>E. italicum</i> L. root alcoholic extract	0.391	0.037	0.105	0.015	1.147	1.185
<i>E. vulgare</i> L. root alcoholic extract	0.053	0.040	0.022	0.004	0.162	0.121
<i>E. angustifolium</i> Millter root alcoholic extract	0.007	0.003	0.009	0.010	0.074	0.028
<i>E. parviflorum</i> Moench root alcoholic extract	0.007	0.003	0.008	n.d.*	0.023	0.015

*n.d.: Not detected, w/w: Weight by weight, AS: Acetylshikonin, DS: Deoxyshikonin, DMAS: 3,3- β , β -dimethylacrylshikonin

to thank Ali Çetin for his careful reading of the manuscript and helpful comments and suggestions. This work was supported by the Gazi University Academic Research Grants [grant number: GÜBAP 02-2010/2011].

Conflict of Interest: No conflict of interest was declared by the author.

REFERENCES

- Ahvazi M, Khalighi-Sigaroodi F, Charkhchian MM, Mojab F, Mozaffarian VA, Zakeri H. Introduction of medicinal plants species with the most traditional usage in Alamut region. *Iran J Pharm Res.* 2012;11:185-194.
- Çakılcıoğlu U, Turkoglu I. An ethnobotanical survey of medicinal plants in Sivrice (Elazığ-Turkey). *J Ethnopharmacol.* 2010;132:165-175.
- Chevallier A. *The Encyclopedia of Medicinal Plants.* Dorling Kindersley Limited, London; 1996.
- Grieve M. *A Modern Herbal 2.* Dover Publications. NewYork; 1982.
- Ferreira ICFR, Aires E, Barreira JCM, Estevinho LM. Antioxidant activity of Portuguese honey samples: Different contributions of the entire honey and phenolic extract. *Food Chemistry.* 2009;114:1438-1443.
- Niciforovic N, Mihailovic V, Maskovic P, Solujic S, Stojkovic a, Pavlovic Muratspahic D. Antioxidant activity of selected plant species; potential new sources of natural antioxidants. *Food Chem Toxicol.* 2010;48:3125-3130.
- Ranjbar A, Khorami S, Safarabadi M, Shahmoradi A, Malekirad AA, Vakilian K, Mandegary A, Abdollahi M. Antioxidant Activity of Iranian *Echium amoenum* Fisch & C.A. Mey Flower Decoction in Humans: A cross-sectional Before/After Clinical Trial. *Evid Based Complement Alternat Med.* 2006;3:469-473.
- Abed A, Minaiyan M, Ghannadi A, Mahzouni P, Babavalian MR. Effect of *Echium amoenum* Fisch. et Mey a Traditional Iranian Herbal Remedy in an Experimental Model of Acute Pancreatitis. *ISRN Gastroenterol.* 2012;2012:141548.
- Abolhassani M. Antibacterial Effect of Borage (*Echium amoenum*) on *Staphylococcus aureus*. *Braz J Infect Dis.* 2004;8:382-385.
- Karakas FP, Yildirim A, Türker A. Biological screening of various medicinal plant extracts for antibacterial and antitumor activities. *Turk J Biol.* 2012;36:641-652.
- Farahani M. Antiviral Effect Assay of Aqueous Extract of *Echium amoenum*-L against HSV-1. *Zahedan J Res Med Sci.* 2013;15:46-48.
- Conforti F, Ioele G, Statti GA, Marrelli M, Ragno G, Menichini F. Antiproliferative activity against human tumor cell lines and toxicity test on Mediterranean dietary plants. *Food Chem Toxicol.* 2008;46:3325-3332.
- Uysal H, Kizilet H, Ayar A, Taheri A. The use of endemic Iranian plant, *Echium amoenum*, against the ethyl methanesulfonate and the recovery of mutagenic effects. *Toxicol Ind Health.* 2015;31:44-51.
- Wassel G, el-Menshawi B, Saeed A, Mahran G, el-Merzabani M. Screening of selected plants for pyrrolizidine alkaloids and antitumor activity. *Pharmazie.* 1987;42:709.
- Heidari MR, Azad EM, Mehrabani M. Evaluation of the analgesic effect of *Echium amoenum* Fisch & C.A. Mey. extract in mice: possible mechanism involved. *J Ethnopharmacol.* 2006;103:345-349.
- Moallem SA, Hosseinzadeh H, Ghoncheh F. Evaluation of Antidepressant Effects of Aerial Parts of *Echium vulgare* on Mice. *JBMS.* 2007;10:189-196.
- Sayyah M, Kamalinejad M. A preliminary randomized double blind clinical trial on the efficacy of aqueous extract of *Echium amoenum* in the treatment of mild to moderate major depression. *Prog Neuropsychopharmacol Biol Psychiatry.* 2006;30:166-169.
- Sayyah M, Boostani H, Pakseresht S, Malaieri A. Efficacy of aqueous extract of *Echium amoenum* in treatment of obsessive-compulsive disorder. *Prog Neuropsychopharmacol Biol Psychiatry.* 2009;33:1513-1516.
- Gholamzadeh S, Zare S, Ilkhanipoor M. Evaluation of the anxiolytic effect of *Echium amoenum* petals extract, during chronic treatment in rat. *Research in pharmaceutical science.* 2007;2:91-95.
- Gholamzadeh S, Zare S, Ilkhanipoor M. Anxiolytic Effect of *Echium amoenum* During Different Treatment Courses. *Research Journal of Biological Sciences.* 2008;3:176-178.
- Gomes NG, Campos MG, Orfao JM, Ribeiro CA. Plants with neurobiological activity as potential targets for drug discovery. *Prog Neuropsychopharmacol Biol Psychiatry.* 2009;33:1372-1389.
- Rabbani M, Sajjadi SE, Vaseghi G, Jafarian A. Anxiolytic effects of *Echium amoenum* on the elevated plus-maze model of anxiety in mice. *Fitoterapia.* 2004;75:457-464.
- Shafaghi B, Naderi N, Tahmasb L, Kamalinejad M. Anxiolytic Effect of *Echium amoenum* L. in Mice. *Iranian Journal of Pharmaceutical Research.* 2002;1:37-41.
- Albrecht A, Vovk I, Simonovska B, Srbinoska M. Identification of shikonin and its ester derivatives from the roots of *Echium italicum* L. *J Chromatogr A.* 2009;1216:3156-3162.
- Wang R, Yin R, Zhou W, Xu DF, Li S. Shikonin and its derivatives: a patent review. *Expert Opin Ther Pat.* 2012;22:977-997.
- Hsu PC, Huang YT, Tsai ML, Wang YJ, Lin JK, Pan MH. Induction of apoptosis by shikonin through coordi native modulation of the Bcl-2 family, p27, and p53, release of cytochrome c, and sequential activation of caspases in human colorectal carcinoma cells. *J Agric Food Chem.* 2004;52:6330-6337.
- Gao D, Hiromura M, Yasui H, Sakurai H. Direct reaction between shikonin and thiols induces apoptosis in HL60 cells. *Biol Pharm Bull.* 2002;25:827-832.
- Wu Z, Wu LJ, Li LH, Tashiro S, Onodera S, Ikejima T. Shikonin regulates HeLa cell death via caspase-3 activation and blockage of DNA synthesis. *J Asian Nat Prod Res.* 2004;6:155-166.
- Guo XP, Zhang XY, Zhang SD. Clinical trial on the effects of shikonin mixture on later stage lung cancer. *Zhong Xi Yi Jie He Za Zhi.* 1991;11:598-599.
- Papageorgiou VP, Assimopoulou AN, Ballis AC. Alkannins and Shikonins: A New Class of Wound Healing Agents. *Curr Med Chem.* 2008;15:3248-3267.
- Su L, Liu LH, Wang Y, Yan G, Zhang Y. Long term systemic toxicity of shikonin derivatives in Wistar rats. *Pharm Biol.* 2014;52:486-490.
- Papageorgiou VP, Assimopoulou AN, Couldouros EA, Heapworth D, Nicolou KC. The Chemistry and Biology of Alkannin, Shikonin, and Related Naphthazarin Natural Products. *Angew Chem Int Ed.* 1999;38:270-300.
- Bozan B, Baser KHC, Kara S. Quantitative determination of naphthoquinones of *Arnebia densiflora* by TLC-densitometry. *Fitoterapia.* 1999;70:402-406.



Use of Water Soluble and Phosphorescent MPA-capped CdTe Quantum Dots for the Detection of Urea

Üre Tayini için Suda Çözünebilen ve Fosforesan MPA Kaplı CdTe Kuantum Noktacıklarının Kullanımı

✉ Tülay OYMAK^{1*}, ✉ Nusret ERTAŞ², ✉ Uğur TAMER²

¹Cumhuriyet University, Faculty of Pharmacy, Department of Analytical Chemistry, Sivas, Turkey

²Gazi University, Faculty of Pharmacy, Department of Analytical Chemistry, Ankara, Turkey

ABSTRACT

Objectives: To describe a method for the determination of urea in blood serum using urease enzyme and 3-MPA-capped CdTe quantum dots.

Materials and Methods: The method is based on the increase in pH of the solution as a result of the reaction between urea and urease, which causes an increase in the phosphorescence signal of MPA-CdTe quantum dots in the pH range of 2.5-5.0. Under the optimum conditions, the linear range of urea was 0.016-0.16 mM (1-10 mg/L) and the limit of detection based on 3 s/b was calculated as 0.003 mM (0.17 mg/L). The relative standard deviation was calculated as 3.4% at 4 mg/L urea concentration (n=7).

Results: The method was applied to human serum samples. The same samples were analyzed by an independent laboratory and the results were not statistically different, at 95% confidence level (F test).

Conclusion: The proposed method does not need sample pretreatment, is simple, selective, and cost-effective for the determination of urea in serum samples.

Key words: Phosphorescent quantum dots, MPA-capped CdTe, urea

ÖZ

Amaç: Bu çalışmada 3-MPA kaplı CdTe kullanılarak üre tayini için yöntem geliştirilmiştir.

Gereç ve Yöntemler: Yöntem üreaz enzimi ile ürenin reaksiyonu sonucu üretilen amonyakın ortam pH'sini değiştirmesi esasına dayanmaktadır. MPA kaplı CdTe'nin fosforesans sinyali pH 2.5-5.0 arasında üre konsantrasyonu ile doğrusal olarak artmaktadır. Optimum koşullar altında doğrusal aralık 0.016-0.16 mM (1-10 mg/L) gözlenebilir sınırı 3 s/b formülüne göre 0.003 mM (0.17 mg/L) olarak hesaplanmıştır. Bağıl standart sapma, 4 mg/L üre konsantrasyonunda %3.4 olarak hesaplanmıştır (n=7).

Bulgular: Yöntem serum numunesine başarılı bir şekilde uygulanmıştır. Aynı serum numuneleri bağımsız bir laboratuvar tarafından analiz edilmiş ve sonuçlarda %95 güven aralığında istatistiksel fark görülmemiştir (F testi).

Sonuç: Önerilen yöntem serumda üre tayini için, örnek ön hazırlığına ihtiyaç duymayan, basit, seçici ve düşük maliyetlidir.

Anahtar kelimeler: Fosforesan kuantum noktacı, MPA kaplı CdTe, üre

INTRODUCTION

Urea, which is an end product of protein metabolism and the main nitrogen component of urine, is an important biomarker monitored in blood and urine samples to diagnose renal and liver diseases. Urea concentrations above the normal level can be an indication of renal failure, urinary tract obstruction, and gastrointestinal bleeding.^{1,2} Conversely, low urea concentrations may be observed in hepatic failure, nephritic syndrome, and

cachexia. Therefore, it is essential to develop techniques for the determination of urea in blood. Conventional spectroscopic methods have been used for many years in clinical laboratories for the determination of urea in blood samples.³⁻⁵ However, these methods are time consuming due to sample pretreatment and an unsuitable real-time determination of urea. Urease-based biosensors are alternative methods for the determination of urea levels.⁶ To this end, a number of methods have

*Correspondence: E-mail: tulayoymak@cumhuriyet.edu.tr, Phone: +90 505 808 67 79 ORCID-ID: orcid.org/0000-0001-5820-1364

Received: 14.01.2017, Accepted: 23.03.2017

©Turk J Pharm Sci, Published by Galenos Publishing House.

been developed and reported such as potentiometry⁷⁻⁹, voltammetry^{10,11}, conductometry¹²⁻¹⁴, ion selective electrode¹⁵, and spectrometry.^{16,17}

Quantum dots (QDs) are superior to organic dyes with their size-tunable photonic properties, quantum yield, and stability against photobleaching.¹⁸⁻²¹ The luminescence properties of QDs are highly sensitive to changes on their surface. The majority of QD photoluminescent probes are based on the increasing or quenching of the photoluminescence signal, which is caused by chemical or physical interaction. Thus the selective determination of an analyte can be achieved via interaction with functionalized QD or non-functionalized QD.²²⁻²⁵

QDs have been widely used as biosensors in biotechnology.²⁴⁻²⁷ Recently, a few applications of QDs for the determination of urea appeared in the literature.^{6,17,24} All of these studies are based on the pH change upon the reaction of urea and urease. Although most previous studies have been focused on QDs as a fluorescence sensor, their long lifetime allows the use of the phosphorescence mode, which has more advantages than fluorescence; for example, the spectral interferences from biologic matrices can be easily prevented in the phosphorescence mode.^{6,28,29}

This study describes a simple and reliable analytical method for the determination of urea in biologic samples using 3-mercaptopropionic acid (MPA)-capped cadmium telluride (CdTe) QDs. The urea concentration was determined in serum samples by monitoring the increase in phosphorescence signal in the presence of urease.

EXPERIMENTAL

Materials

All the measurements were performed using analytical grade chemicals. Deionized water was used throughout the study. CdCl₂, H₂TeO₆, NaBH₄, NaOH, HCl, and urease were obtained from Merck, and the MPA was obtained from Fluka. Trisodium citrate was obtained from Riedel de Haen and ethanol was obtained from Sigma-Aldrich. Dilute solutions of the QD, urease, and urea were prepared daily.

Apparatus

A Varian, Cary Eclipse Luminescence spectrometer equipped with a xenon lamp was used for photoluminescence measurements. All instrumental parameters were controlled using the instrument software. The automatic filter selection mode for both excitation and emission monochromator was used to avoid scattered light. Excitation and emission spectral band passes were 20 nm for both monochromator. The detector voltage was set to 800 V. An Orion 720. A model pH/Ionmeter was used for pH adjustments. Deionized water with 18.2 MΩ.cm was obtained from Millipore Simplicity water purification system. A Nüve NF200 centrifuge and Nüve MK418 magnetic stirrer were used during the synthesis of the QDs. Unicam Mattson 1000 Fourier transform infrared (FTIR) spectrometer was used to obtain IR spectra of the modified QDs to confirm surface modification. The ultraviolet (UV) spectrum of QDs was obtained using a Shimadzu UV-

visible (VIS) spectrometer. Transmission electron microscopy (TEM) measurements were performed on a JEOL 2100 HRTEM instrument (JEOL Ltd., Tokyo, Japan). TEM samples were prepared by pipetting 10 µL of QD solution onto copper grids, which were allowed to stand for 10 min.

Synthesis of water-soluble MPA-CdTe QDs

MPA-CdTe QDs were synthesized using a modified method of Yuan et al.³⁰ In the method, 25 mL 0.64 mM CdCl₂ solution and 0.10 g of trisodium citrate was transferred into a single-necked flask. Then, 100 µL, 11.5 M MPA and 0.01 mmol Te (IV) were added respectively, with continuous stirring. The color of the solution becomes bright yellow with the addition of 50 mg of NaBH₄, and it is heated to 90°C for 1 hour with continuous stirring. After cooling, QDs were precipitated with ethanol, centrifuged and dried in vacuum. Each batch resulted in 80-100 mg of dry QD powder, and in order to have a constant QD concentration, a 75-mg portion of the QD powder was re-dissolved in water and diluted to 25 mL volume. At this stage, the pH of the QD solution was adjusted to 11.4 and heated to 96-100°C for a different period of time. An increase in particle size as well as fluorescence emission at longer wavelength was observed.

Procedure for urea determination

Ten milliliters of 3.0 mg/mL MPA-CdTe and 10 mL of 5 units/mL urease solutions were placed into a beaker and the pH was adjusted to 2.5 with 0.01 M HCl. The solution was transferred to a 25-mL volumetric flask and diluted to volume with deionized water. A series of standard solutions was prepared by transferring 1.0 mL of the mixture solution into a test tube and then various volumes of urea standard solution or 0.10 mL of serum samples were added. The volume was completed to 5.0 mL with deionized water. The solutions were mixed and allowed to stand for 10 min at laboratory temperatures. Measurements were performed using the phosphorescence mode with a 0.1 ms delay time and 3 ms gate time. Excitation wavelength was 300 nm and spectral band passes were 20 nm for both excitation and emission monochromators.

Samples

Human serum samples were collected from healthy volunteers. The samples were diluted 50 times with deionized water adjusted to pH 2 with 0.01 M HCl before the measurement procedure. The same samples were analyzed for urea using standard methods used in clinical laboratory in order to test the accuracy of the proposed method.

RESULTS AND DISCUSSION

Characterization of MPA-CdTe QDs

The QDs were characterized using fluorescence, UV-VIS, infrared spectroscopy, and TEM images. After the synthesis procedure (without thermal pretreatment), the QDs had fluorescence emission maximum at 505-510 nm with a full width at half maximum about 35 nm, and almost no phosphorescence signal, as shown in Figure 1. On the other hand, when this QD was heated to 90-100°C (pH 11.4) for different periods of

time, an increase in particle size as well as fluorescence and phosphorescence emission intensity was observed. Therefore, the heating period of three hours, which provided intense phosphorescence signal at longer wavelength, was selected to avoid fluorescence background emission from the biologic sample. The phosphorescence spectra of MPA-capped CdTe heated at different periods of time are shown in Figure 1.

The diameter of CdTe QD heated for 180 min (Figure 1) was calculated using the equation given below.²⁷

$$D = (9.8127 \times 10^{-7}) \lambda^3 - (1.7147 \times 10^{-3}) \lambda^2 + (1.0064) \lambda - 194.84$$

D is the diameter of the nanocrystals (nm); λ is the wavelength corresponding to absorbance maximum determined as 560 nm from the UV-VIS spectrum, as shown Figure 2a. Calculations showed that the diameter of the MPA-CdTe QDs was 3.34 nm. A TEM image of MPA-capped CdTe QDs is shown in Figure 2b.

FTIR spectroscopy was used to confirm the modification of CdTe QDs with MPA molecules. The spectra of free MPA and MPA-CdTe are given in Figure 3a, 3b. The two bands at 2666 and 2570 cm^{-1} , which is attributed to hydrogen bonding between acid and thiol groups, disappeared in the IR spectra of MPA capped-CdTe because the MPA is attached to QD through S-atoms. The small peaks that appeared at 2927, 2945, and 2854 cm^{-1} were attributed to the asymmetric and symmetric C-H stretching of methylene groups. The appearance of an intense peak at 1570 cm^{-1} can be attributed to asymmetric stretching of carboxylic acid.

The effect of pH and concentration of urease on phosphorescence intensity of MPA-capped CdTe QDs

pH is one of the important parameters that affects the photoluminescence intensity of the QDs. Therefore, the effect of the solution pH on the signal intensity of QD was studied using 0.5 mL of 0.04 M Britton-Robinson buffer between pH 2.5-8.0. It was observed that the phosphorescence signal increased linearly as the pH increased from 2.5 to 5.0, and decreased between pH 5.0-8.0. Therefore, a pH between 2.5-5.0 was selected for the determination of urea in the presence of QD and urease.

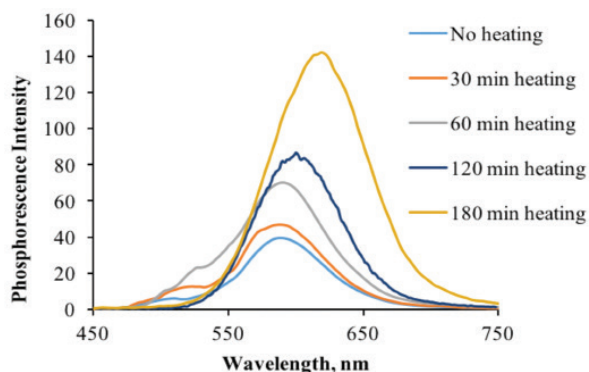


Figure 1. The effect of heating period on the phosphorescence signal of MPA-CdTe quantum dots. Excitation wavelength was 300 nm, heating periods 30, 60, 120, 180, 240 min at pH 11.4

MPA: 3-mercaptopropionic acid, CdTe: Cadmium telluride

Interestingly, the influence of pH on the fluorescence signal was different than the signal measured in the phosphorescence mode. The effect of pH on the photoluminescence intensity of MPA-CdTe QDs is shown Figure 4.

The effect of urease concentration was studied between 1-7.5 units/mL in the presence of 0.24 mg/L MPA-CdTe and 0.07 mM urea. The maximum signal enhancement was observed when the urease concentration was 5 units/mL, which was then used throughout the experiments.

Determination of urea

Determination of urea is based on the production of ammonia in the presence of urease.

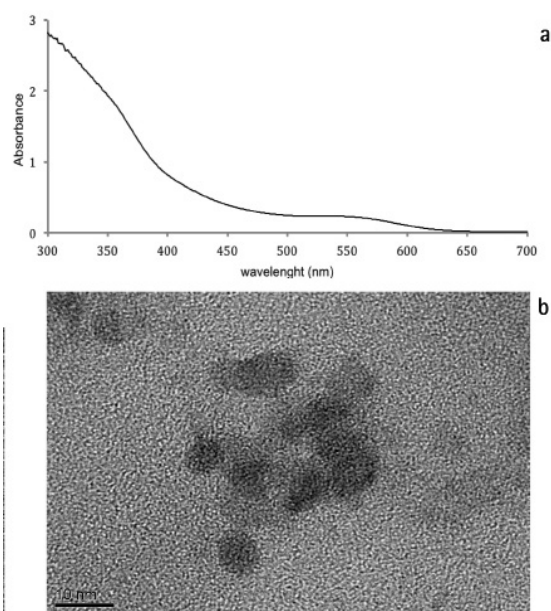


Figure 2. UV-VIS absorption spectrum of MPA-CdTe QDs given in Figure 1, the peak at 560 nm was used to calculate particle size (a) TEM image of the same QD (b)

UV-VIS: Ultraviolet visible, MPA: 3-mercaptopropionic acid, CdTe: Cadmium telluride, QDs: Quantum dots, TEM: Transmission electron microscopy

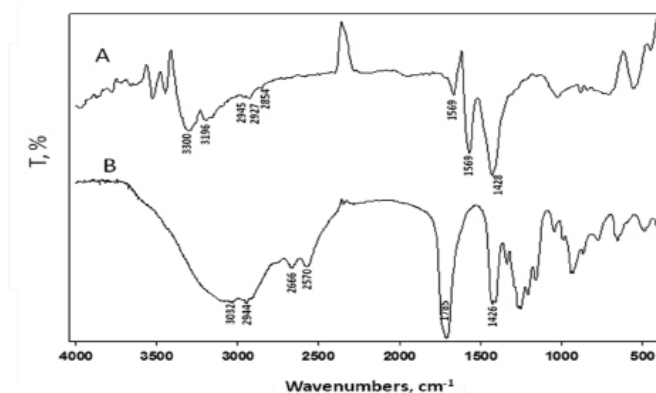


Figure 3. FTIR spectra of (a) MPA capped CdTe and (b) MPA alone

FTIR: Fourier transform infrared, MPA: 3-mercaptopropionic acid, CdTe: Cadmium telluride

The pH of the medium is increased depending on the degradation of urea by urease. Consequently, the phosphorescence signal increased throughout the pH 2.5-5.0 range with increasing urea concentration. In the optimum conditions (0.24 mg/mL CdTe-MPA, 5 units/mL urease and pH 2.5), the calibration was constructed by plotting $I-I_0$ versus urea concentration (I_0 : phosphorescence signal of CdTe-MPA I: phosphorescence signal of CdTe - MPA + 0.0016 - 0.16 mM urea). A linearity in phosphorescence signal was observed between 0.016 -0.16 mM urea concentrations. The phosphorescence signal with increasing urea concentration is shown Figure 5a. Although the fluorescence signal increased with urea concentration, the dynamic range was relatively narrow as shown in Figure 5b. The calibration curve based on phosphorescence signal is given in Figure 6.

The lifetime software of the instrument was used to obtain a decay curve for the phosphorescence emission and the data were used to construct a log intensity versus time graph. The lifetime of the QD was calculated using the $-1/\text{slope}$ of this linear line and found as 21.5 μs . (Figure 7).

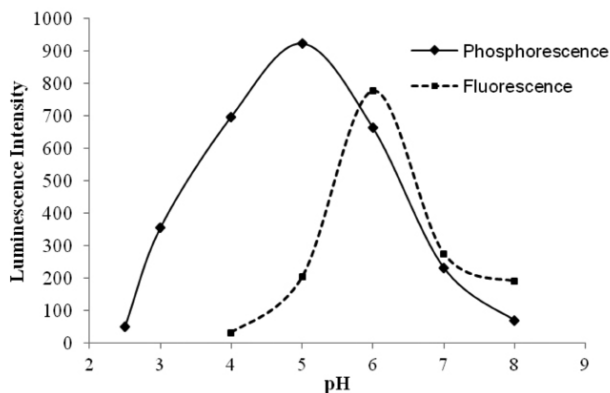


Figure 4. The effect of pH on luminescence intensity of MPA capped CdTe QDs. pH was adjusted using 0.5 mL of 0.04 M Britton-Robinson buffer and diluted to 2.5 mL

MPA: 3-mercaptopropionic acid, CdTe: Cadmium telluride, QDs: Quantum dots

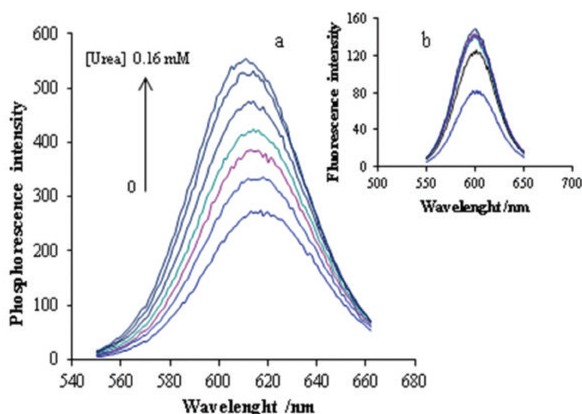


Figure 5. Enhancing photoluminescence signal with increasing urea concentration. Urea concentration 0-0.16 mM, urease concentration was 5 units/mL

The proposed method was compared with the methods in the literature. The limit of detection for the proposed method was lower or comparable with the methods such as fluorescence, amperometry, and potentiometry (Table 1). The analytical performance data of the method used for the determination of urea are given in Table 2. The proposed method is relatively simple and free from the interference from the biologic matrix because the phosphorescence signal was used.

Determination of urea in human serum

Serum samples obtained from university laboratory were analyzed for urea using the proposed method. In order to test the accuracy of the proposed method, the same samples were analyzed in a private clinical laboratory; the results of which are shown in Table 3. The precision in terms of percent relative standard deviation, for three parallel determinations, was less than 6.7% and the urea concentrations were consistent with those reported.

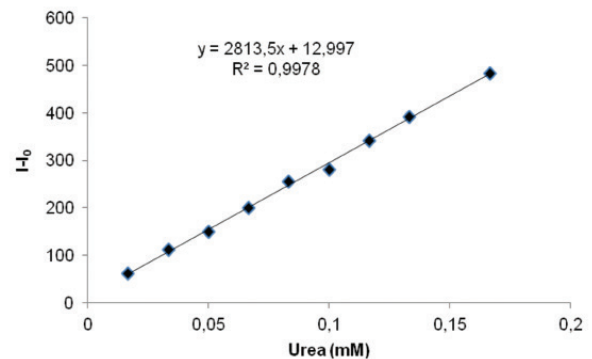


Figure 6. Calibration graph in the phosphorescence mode (I_0 : Phosphorescence signal of MPA-CdTe, I: Phosphorescence signal of MPA-CdTe + 0.016 - 0.16 Mm urea concentration)

MPA: 3-mercaptopropionic acid, CdTe: Cadmium telluride

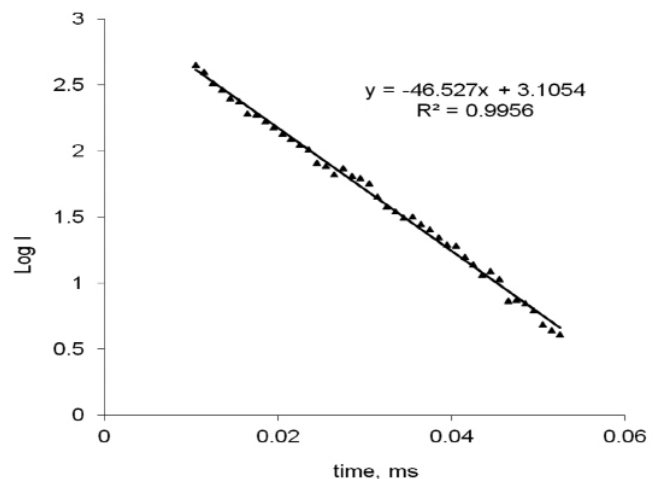


Figure 7. Lifetime measurements of the MPA-capped CdTe QDs, excitation and emission spectral band pass and the PMT voltage were 20 nm and 900 V, respectively

MPA: 3-mercaptopropionic acid, CdTe: Cadmium telluride, QDs: Quantum dots, PMT: Photomultiplier tube

Table 1. Comparison of proposed methods with the methods in literature used for urea determination

Method	Signal mechanism	Linear range, mM	LOD, mM	References
Fluorescence	CdSe/ZnS-Urease	0-10	-	17
Fluorescence	CdSe/ZnSe-MSA-Urease	0.01-100	0.01	24
Amperometry	PVC ammonium electrode	15-80	15	5
Potentiometry	Urease polyurethane-acrylate	0.2-0.6	0.2	9
Phosphorescence	Mn doped ZnS QDs-Urease	0.014-60	0.014	6
Phosphorescence	MPA capped CdTe-Urease	0.016-0.16	0.003	This work

LOD: Logarithm of odds, ZNS: Zinc selenide, CdSe: Cadmium selenium, MSA: Mannitol salt agar, PVC: Polyvinyl chloride, QDs: Quantum dots, MPA: 3-mercaptopropionic acid

Table 2. Analytical performance data of the method used for urea determination (n=7)

Linear range	0.016-0.16 mM
LOD	0.003 mM
SD	0.13
RSD %	3.4%
RE %	-1.0

LOD: Logarithm of odds, SD: Standard deviation, RSD: Relative standard deviation, RE: Relative error

Table 3. Comparison of the urea concentration found in serum samples (n=3)

Sample	Found (\pm s), mM	
	CdTe-MPA	Results from the private clinical laboratory*
Human serum 1	2.3 \pm 0.08	2.50 \pm 0.03
Human serum 2	2.5 \pm 0.02	2.50 \pm 0.08
Human serum 3	2.1 \pm 0.06	2.16 \pm 0.08

*Blood urine nitrogen test based on a spectrophotometric method, CdTe: Cadmium telluride, MPA: 3-mercaptopropionic acid

CONCLUSION

It was shown that water-soluble and phosphorescent MPA-CdTe QDs can be used for the determination of urea in human blood serum samples. The proposed method is based on enzymatic degradation of urea by urease. In addition, the use of phosphorescence prevents interference such as scatter and autofluorescence from the sample matrix. Compared with conventional room temperature phosphorimetric methods, phosphorescent QDs provide a simpler methodology because no additional chemicals such as heavy atoms and oxygen removal processes are necessary. The results show that the proposed method is accurate, selective, rapid, and simple for urea determination in serum samples and can be applied to other biologic samples.

Conflict of Interest: No conflict of interest was declared by the authors.

REFERENCES

- Chen JC, Chou JC, Sun TP, Hsiung SK. Portable urea biosensor based on the extended-gate field effect transistor. *Sens. Sens Actuators B Chem.* 2003;91:180-186.
- Azadbakht A, Gholivand MB. Covalent attachment of Ni-2,3-pyrazine dicarboxylic acid onto gold nanoparticle gold electrode modified with penicillamine- CdS quantum dots for electrocatalytic oxidation and determination of urea. *Electrochimica Acta.* 2014;125:9-21.
- Usman Ali SM, Ibutoto ZH, Salman S, Nur O, Willander M, Danielsson B. Selective determination of urea using urease immobilized on ZnO nanowires. *Sens Actuators B Chem.* 2011;160:637-643.
- Alizadeh T, Akbari A. A capacitive biosensor for ultra-trace level urea determination based on nano-sized urea-imprinted polymer receptors coated on graphite electrode surface. *Biosens Bioelectron.* 2013;43:321-327.
- Campanella L, Mazzei F, Sammartino MP, Tommasetti M. New enzyme sensors for urea and creatinine analysis. *Bioelectrochemistry.* 1990;23:195-202.
- Bi L, Dong X, Yu Y. Room-temperature phosphorescence sensor based on manganese doped zinc sulfide quantum dots for detection of urea. *J Lumin.* 2014;153:356-360.
- Eggenstein C, Borchardt M, Diekmann C, Gründig B, Dumschat C, Cammann K, Knoll M, Spener F. A disposable biosensor for urea determination in blood based on an ammonium-sensitive transducer. *Biosens Bioelectron.* 1999;14:33-41.
- Soldatkin AP, Montoriol J, Sant W, Martelet C, Jaffrezic-Renault N. A novel urea sensitive biosensor with extended dynamic range based on recombinant urease and ISFETs. *Biosens Bioelectron.* 2003;19:131-135.
- Lakard B, Herlem G, Lakard S, Antoniou A, Fahys B. Urea potentiometric biosensor based on modified electrodes with urease immobilized on polyethylenimine films. *Biosens Bioelectron.* 2004;19:1641-1647.
- Mizutani F, Yabuki S, Sato Y. Voltammetric enzyme sensor for urea using mercaptohydroquinone-modified gold electrode as the base transducer. *Biosens Bioelectron.* 1997;12:321-328.
- Luo YC, Do JS. Urea biosensor based on PANi(urease)-Nafion/Au composite electrode. *Biosens Bioelectron.* 2004;20:15-23.
- Lee WY, Kim SR, Kim TH, Lee KS, Shin MC, Park JK. Sol-gel-derived thick-film conductometric biosensor for urea determination in serum. *Anal Chim Acta.* 2000;404:195-203.

13. Castillo-Ortega MM, Rodriguez DE, Encinas JC, Plascencia M, Méndez-Velarde FA, Olayo R. Conductometric uric acid and urea biosensor prepared from electroconductive polyaniline-poly(n-butyl methacrylate) composites. *Sens Actuators B Chem.* 2002;85:19-25.
14. Chaudhari PS, Gokarna A, Kulkarni M, Karve MS, Bhoraskar SV. Porous silicon as an entrapping matrix for the immobilization of urease. *Sens Actuators B Chem.* 2005;107:258-263.
15. Huang CP, Li YK, Chen TM. A highly sensitive system for urea detection by using CdSe/ZnS core-shell quantum dots. *Biosens Bioelectron.* 2007;22:1835-1838.
16. Tsai HC, Doong RA. Preparation and characterization of urease-encapsulated biosensors in poly(vinyl alcohol)-modified silica sol-gel materials. *Biosens Bioelectron.* 2007;23:66-73.
17. Duong HD, Rhee JI. Use of CdSe/ZnS luminescent quantum dots incorporated within sol-gel matrix for urea detection. *Anal Chim Acta.* 2008;626:53-61.
18. Weng J, Song X, Li L, Qian H, Chen K, Xu X, Cao C, Ren J. Highly luminescent CdTe quantum dots prepared in aqueous phase as an alternative fluorescent probe for cell imaging. *Talanta.* 2006;70:397-402.
19. Zhang Y, Zhang H, Guo X, Wang H. L-Cysteine-coated CdSe/CdS core-shell quantum dots as selective fluorescence probe for copper(II) determination. *Microchem J.* 2008;89:142-147.
20. Singh SB, Limaye MV, Lalla NP, Kulkarni SK. Copper-ion-induced photoluminescence tuning in CdSe nanoparticles. *J Lumin.* 2008;128:1909-1912.
21. Liang J, Huang S, Zeng D, He Z, Ji X, Ai X, Yang H. CdSe quantum dots as luminescent probes for spirinolactone determination. *Talanta.* 2006;69:126-130.
22. Frigerio C, Ribeiro DS, Rodrigues SS, Abreu VL, Barbosa JA, Prior JA, Marques KL, Santos JL. Application of quantum dots as analytical tools in automated chemical analysis: a review. *Anal Chim Acta.* 2012;735:9-22.
23. Murphy CJ. Optical sensing with quantum dots. *Anal Chem.* 2002;74:520A-526A.
24. Huang CP, Li YK, Chen TM. A highly sensitive system for urea detection by using CdSe/ZnS core-shell quantum dots. *Biosens Bioelectron.* 2007;22:1835-1838.
25. Yu D, Wang Z, Liu Y, Jin L, Cheng Y, Zhou J, Cao S. Quantum dot-based pH probe for quick study of enzyme reaction kinetics. *Enzyme Microb Technol.* 2007;41:127-132.
26. Wang YQ, Ye C, Zhu ZH, Hu YZ. Cadmium telluride quantum dots as pH-sensitive probes for tiopronin determination. *Anal Chim Acta.* 2008;610:50-56.
27. Fortes PR, Frigerio C, Silvestre CI, Santos JL, Lima JL, Zagatto EA. Cadmium telluride nanocrystals as luminescent sensitizers in flow analysis. *Talanta.* 2011;84:1314-1317.
28. He Y, Wang HF, Yan XP. Exploring Mn-doped ZnS quantum dots for the room-temperature phosphorescence detection of enoxacin in biological fluids. *Anal Chem.* 2008;80:3832-3837.
29. Wu P, He Y, Wang HF, Yan XP. Conjugation of glucose oxidase onto Mn-doped ZnS quantum dots for phosphorescent sensing of glucose in biological fluids. *Anal Chem.* 2010;82:1427-1433.
30. Yuan J, Guo W, Yin J, Wang E. Glutathione-capped CdTe quantum dots for the sensitive detection of glucose. *Talanta.* 2009;77:1858-1863.



Calcium Mobilization and Inhibition of Akt Reduced the Binding of PEO-1 Cells to Fibronectin

Ca²⁺ Mobilizasyonu ve Akt İnhibisyonu ile PEO-1 Hücrelerinin Fibronektine Bağlanmasında Azalma

© Seda Mehtap SARI KILIÇASLAN^{1*}, © Aysun AYRIM², © Elif APAYDIN³, © Zerrin İNCESU⁴

¹Anadolu University, Faculty of Education, Department of Primary Education, Eskişehir, Turkey

²Eskişehir Osmangazi University, Institute of Life Sciences, Eskişehir, Turkey

³Anadolu University, Institute of Life Sciences, Eskişehir, Turkey

⁴Anadolu University, Faculty of Pharmacy, Department of Biochemistry, Eskişehir, Turkey

ABSTRACT

Objectives: To investigate the effects of intracellular calcium (Ca²⁺) mobilization, β -catenin and Akt signal pathways after the binding of metastatic ovarian cells to fibronectin.

Materials and Methods: The expression levels of $\alpha 4\beta 1$ and $\alpha v\beta 6$ integrin were determined using $\alpha 4$, $\beta 1$, αv , and $\beta 6$ antibodies using flow cytometry on PEO-1 cells. The effect of [Ca²⁺]_i on cell adhesion capacity was investigated using RTCA after stimulating PEO-1 cells using thapsigargin and tunicamycin. The binding rate of PEO-1 cells to fibronectin was also investigated in the presence of either different concentrations of cardamonin, which inhibits the accumulation of β -catenin, or different concentrations of FPA 124, which is a specific inhibitor for the PKB/Akt signal pathway, using RTCA.

Results: RTCA analysis results showed that increasing [Ca²⁺]_i through leakage of the calcium pool was strongly effective on PEO-1 cell binding to fibronectin. Extracellular calcium influx also reduced the binding of PEO-1 cells. Cell binding to fibronectin was also inhibited with a ratio of 64% in the presence of 100 μ M cardamonin compared with untreated control cells. Finally, it was found that PKB/Akt inhibition with 15 μ M FPA 124 decreased the binding of PEO-1 cells to fibronectin with a ratio of 88% compared with untreated control cells.

Conclusion: PEO-1 cell binding to fibronectin via integrins could be related to intracellular Ca²⁺ mobilization and Akt signaling.

Key words: Fibronectin, calcium, tunicamycin, ovarian cancer

ÖZ

Amaç: Metastatik ovaryum kanser hücrelerinin fibronektine bağlanmasından sonra, hücre içi Ca²⁺ mobilizasyonu, β -katenin ve Akt sinyal yollarının etkilerinin araştırılmasıdır.

Gereç ve Yöntemler: $\alpha 4\beta 1$ ve $\alpha v\beta 6$ integrinlerin ekspresyon düzeyleri $\alpha 4$, $\beta 1$, αv ve $\beta 6$ antikorları kullanılarak akım sitometrisi ile PEO-1 hücrelerinde tespit edilmiştir. [Ca²⁺]_i'un hücre adezyon kapasitesine etkisi, PEO-1 hücrelerinin thapsigargin ve tunicamisin ile uyarılmasından sonra RTCA kullanılarak araştırıldı. PEO-1 hücrelerinin fibronektine bağlanma oranı β -kateninin toplanmasını inhibe eden farklı kardamonin konsantrasyonları varlığında veya PKB/Akt sinyal yolu için spesifik inhibitör olan FPA 124'ün farklı konsantrasyonları için RTCA kullanılarak araştırıldı.

Bulgular: RTCA analiz sonuçları kalsiyum depolarından sızmasıyla artan [Ca²⁺]_i'un PEO-1 hücrelerinin fibronektine bağlanmasını güçlü bir şekilde etkilediğini göstermiştir. Hücre dışı kalsiyum akımı PEO-1 hücrelerinin bağlanmasını azaltmıştır. 100 μ M kardamonin varlığında muamele edilmemiş kontrol hücrelerine göre hücrenin fibronektine bağlanması %64 oranında inhibe olmuştur. Son olarak, 15 μ M FPA 124 ile PKB/Akt inhibisyonu da PEO-1 hücrelerinin fibronektine bağlanmasını %88 oranında düşürdüğü bulunmuştur.

Sonuç: PEO-1 hücrelerinin integrinler aracılığı ile fibronektine bağlanmasının hücre içi Ca²⁺ mobilizasyonu ve Akt sinyali ile ilgili olabilir.

Anahtar kelimeler: Fibronektin, kalsiyum, tunicamisin, ovaryum kanseri

*Correspondence: E-mail: smskilicaslan@anadolu.edu.tr, Phone: +90 222 335 0580 / 3433 ORCID-ID: orcid.org/0000-0001-7547-5519

Received: 13.01.2017, Accepted: 06.04.2017

©Turk J Pharm Sci, Published by Galenos Publishing House.

INTRODUCTION

The cell adhesion molecules, integrins, activate outside-in signaling pathways necessary for cell invasion by mediating attachment between cells and the extracellular matrix (ECM). The integrins participate in cell morphology, migration, proliferation, differentiation, survival^{1,2}, as well as apoptosis. Integrin-mediated cell attachment is necessary for cancer cell metastasis and invasion. Moreover, ECM-integrin signaling is said to have survival advantage in different types of cancer cells against many chemotherapeutic treatments.² Studies on this topic are usually based on integrin expressions. Signal transduction mechanisms of integrins in ovarian cells, however, have not yet been explicitly investigated.

Cell-ECM adhesiveness is generally increased in human cancers, which allows cancer cells to destroy the histologic structure. Reduced cell-ECM adhesiveness is also important for cancer invasion and metastasis.³ Moreover, some studies showed that the adhesion capacity of highly metastatic cells could be reduced by inhibiting integrin expression or modifies the process that leads metastatic cells to anoikis, which is programmed cell death that is induced upon cell detachment from ECM.^{4,5} αv integrin subunit-inhibition or αv -knockdown was shown to inhibit the colonogenic and migratory ability of human prostate cancer cells *in vitro* and *in vivo*.^{4,6} Accordingly, αv integrin is said to be a promising target for cancer therapy strategies.

Ovarian cancer cells can spread in cell form or spherul form from the surface of the ovary. Therefore, metastatic ovarian cells should survive and proliferate without ECM binding. The microenvironment of cells is dynamic and contains survival factors such as cytokines, growth factors, hormones, proteases, and ECM proteins that regulate tumor cell migration, invasion, survival, and spherul forms.⁷ In particular, fibronectin and vitronectin (ECM proteins) induce the formation of spheroids, adherence, and disaggregation of ovarian cancer cells. These proteins, which are disintegrated by metalloproteinase-2, increase the adhesion of ovarian cancer cells to the peritoneal region that is the nascent stage of metastasis.⁸

β -catenin is a multi-functional protein involve in the Wnt signal pathway, as well as adhesion via E-cadherin in epithelial cells.⁹ In normal epithelial cells, β -catenin binds to the E-cadherin- α -catenin complex in adherent junctions. In the presence of Wnt signaling, however, β -catenin accumulates in the cytoplasm and then translocates to the nucleus due to activation of a large number of target genes including LEF/TCF genes.¹⁰ These activated genes are attributed to the development of some diseases, especially various types of human cancers. A number of studies showed that accumulation of β -catenin was also effective in creating a suitable microenvironment for cancer progression.^{11,12}

Recently, it has been shown that Akt is one of the most effective regulatory proteins in the β -catenin accumulation process. In particular, N-cadherin adhesion can lead to phosphatidylinositol 3-kinase (PI3K) mediated activation of Akt, and that might stimulate the β -catenin signaling pathway.¹³

Moreover, the Akt protein also phosphorylates glycogen synthase kinase 3 beta (GSK3 β) and leads to inactivating the function of GSK3 β . In this case, stabilization and accumulation of β -catenin is induced.¹⁴

The current study aimed to investigate the role of increased Ca²⁺ via tunicamycin (TN) treatment and β -catenin-Akt signaling on the binding of metastatic ovarian cancer cells (PEO-1) to fibronectin. We investigated the expression levels of integrins that play an active role in PEO-1 binding to fibronectin using flow cytometry and immunofluorescence staining. Using real-time cellular analysis (RTCA), we showed that increasing cytoplasmic calcium in PEO-1 cells influenced cell adhesion. Inhibition of the accumulation of β -catenin and Akt signaling using specific inhibitors led to inhibition of PEO-1 adhesion to fibronectin. These results suggest a link between the adhesion of PEO-1 ovarian cells and Ca²⁺ mobilization, and the function of Akt and β -catenin.

MATERIALS AND METHODS

Cell culture

The PEO-1 human ovarian cancer cell line was purchased from Public Health England (10032308) and cultured in RPMI 1640, 10% fetal bovine serum, 2 mM sodium pyruvate, and 2 mM glutamine.

Detection of integrin expression

Expression levels of αv , $\alpha 4$, $\beta 1$, and $\beta 6$ integrin were determined using specific antibodies with flow cytometry on PEO-1 cells. The cells were incubated with a 1:200 dilution of primary antibodies against integrin subunits, subsequently washed in PBS, and incubated with a 1:200 FITC-conjugated secondary antibody for 30 min at 4°C. Control cells contained either a primary antibody or an FITC secondary antibody. After washing, all samples were analyzed using a flow cytometer (Becton Dickinson, FACS Aria II, Canada).

Localization of integrins on cell membrane

The localization of integrins was detected using fluorescence microscopy. Coverslips were coated with 50 μ g/mL fibronectin. The cells were then seeded, washed with PBS, and fixed with 4% formaldehyde, washed again and then permeabilized with 0.1% Tween-20. After washing with PBS, the cells were treated with 1% bovine serum albumin (BSA). The cells were treated with specific primary integrin antibodies (1:200 dilution) overnight at +4°C, then with the FITC-conjugated secondary antibody (1:300 dilution) for 1 h at +4°C. No primary antibody was added in the control group. After washing the coverslips, they were mounted on microscope slides. The slides were examined using fluorescence microscopy and monitored.

Binding assays

The binding rate of PEO-1 cells to fibronectin

RTCA was used for real-time and time-dependent analysis of binding of PEO-1. RTCA measures changes in electrical

impedance as cells attach and spread in multi-well plates covered with a gold microelectrode array.¹⁵ Electrode impedance is displayed and recorded as “cell index” values, which reflects the biologic status of the monitored cells, including the cell number, cell viability, morphology, and cell adhesion.¹⁶

Sixteen-well plates were coated with different concentrations (1 µg/mL, 5 µg/mL, 10 µg/mL, 15 µg/mL, 25 µg/mL, 50 µg/mL, 100 µg/mL) of fibronectin, except the control wells. The wells were washed with PBS and then blocked with 1% BSA to inhibit non-specific binding. After a background impedance measurement, 5×10^4 cells/well were seeded. Impedance was monitored at 15-min intervals for 24 h. The rate of cell adhesion was calculated according to the normalized cell index (NCI) or cell index formula.

NCI = (impedance at time point n - impedance in the absence of cells) / nominal impedance value.

CI = (resistance measured at a time point - resistance measured without the cell) / 15Ω.

The role of [Ca²⁺]_i on PEO-1 cell adhesion capacity

Integrins on the cell surface were activated using fibronectin (50 µg/mL). The effect of [Ca²⁺]_i on cell adhesion capacity was investigated using RTCA after stimulating PEO-1 cells with IP₃-independent intracellular calcium release, thapsigargin (TG) (50 nM, 100 nM, 500 nM, 1 µM, 2 µM), and extracellular calcium channel blocker TN (0,5-1-5-10-20 µg/mL). PEO-1 cells were treated with 5, 20, 35 mM EGTA [ethylene glycol-bis(β-aminoethyl ether)-N,N,N',N'-tetraacetic acid], which is Ca²⁺ chelator, to create a non-calcium environment. Measurement of cell adhesion was conducted for 24 h.

The role of cardamonin and Akt on the binding ability of PEO-1 cells

Sixteen-well plates were prepared as mentioned above. After the wells were coated with 50 µg/mL fibronectin, the plates were seeded with 5×10^4 PEO-1 cells and transferred into RTCA for 2 h incubation before monitoring. After that, the cells were treated with different concentrations of cardamonin (3,13 µM, 6,25 µM, 12,5 µM, 25 µM, 50 µM, 100 µM), an inhibitor β-catenin, and FPA 124 (5 µM, 15 µM, 25 µM, 35 µM), an Akt signal pathway inhibitor. The cells were monitored at 30-min intervals for a period of 24 h. Uncoated wells were used as a control group together with the wells containing no inhibitor.

RESULTS

Expression and localization of integrins on the surface of PEO-1 cells

The expression and localization of α4, β1, αv, and β6 integrin subunits were investigated using flow cytometry and immunofluorescence staining. The results of the flow cytometric analysis are given in Figure 1. The expression levels of αv, α4, β6, and β1 were in a descending order with respect to expression level. The expression level of the αv integrin subunit was found to be abundant compared with the others.

PEO-1 cells were incubated with specific primary integrin antibodies and the localization of integrin subunits was demonstrated using fluorescence microscopy (Figure 2). PEO-1 cells showed low but detectable level of β6 integrin subunit localization, whereas cells exhibited considerable amounts of α4, αv, and β1 localizations over the whole cell as labelled with specific antibodies.

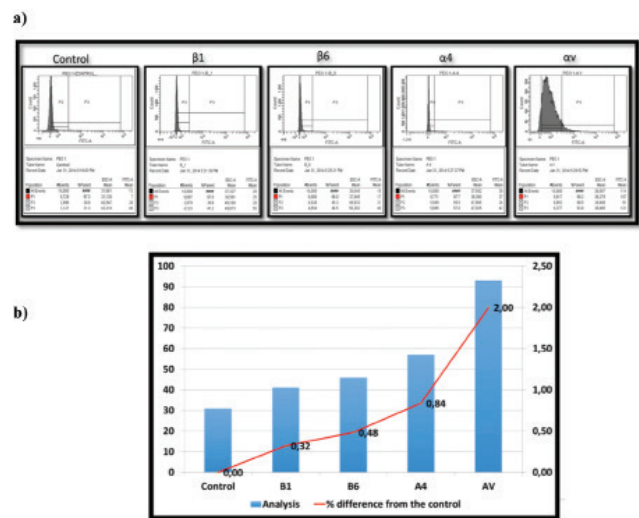


Figure 1. Flow cytometric analysis of α4, β1, αv and β6 integrin subunits expression (a), and percentage of integrin subunits expressions (b) on the surface of human ovarian cancer PEO-1 cell line. (a) Cells were first treated with α4, β1, αv and β6 primary antibodies, except the controls, and then FITC conjugated secondary antibodies. (b) The left axis is expression level, the right axis is the percentage differences from the control group. Expression levels of α4, β1, αv and β6 are higher by about 32%, 48%, 84%, and 200% than the control group, respectively

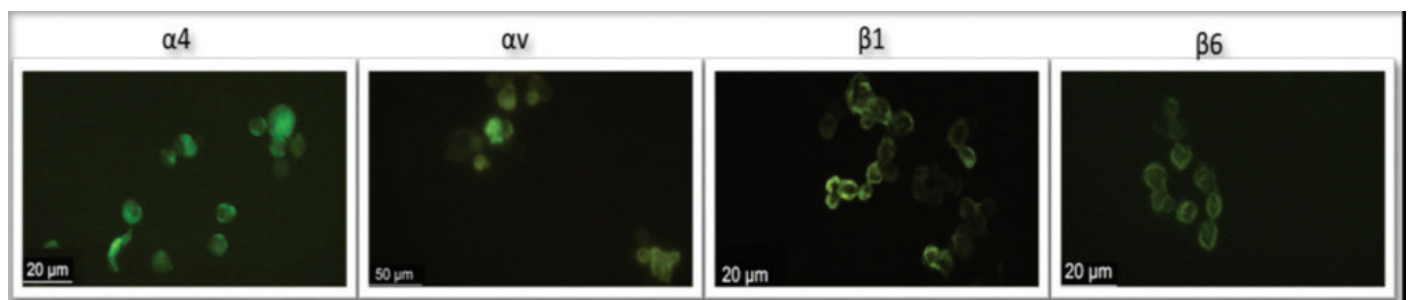


Figure 2. Immunofluorescence staining of human ovarian cancer PEO-1 cells for α4, αv, β1 and β6 integrin subunits. The cells were labelled with various primary integrin antibodies at 37°C for 1 h. After that, PEO-1 cells were incubated with FITC-conjugated secondary antibody

The binding rate of PEO-1 cells to fibronectin

PEO-1 cells were examined using RTCA to determine the binding of cells in various concentrations (1-100 µg/mL) of fibronectin. The results, shown in Figure 3, indicate that PEO-1 cells bound to fibronectin at all concentrations compared with the control cells. The cells showed a higher percentage of binding to 50 µg/mL fibronectin (cell index 5-6 at 24 h), whereas low-concentration fibronectin (1 µg/mL) supported little cell adhesion. The result suggests that 50 µg/mL fibronectin would be a suitable concentration for use in further studies.

Effects of calcium on PEO-1 cell binding

Figure 4 depicts that the involvement of Ca²⁺ increases in the mechanism of cell adhesion to fibronectin. PEO-1 cells were plated onto 16-well plates that were previously coated with 50 µg/mL fibronectin in the presence or absence of various concentrations of TN, TG or EGTA. The results demonstrated that integrin-mediated PEO-1 adhesion to fibronectin was reduced by Ca²⁺ mobilization from both the extracellular and intracellular Ca²⁺ pool. The addition of all Ca²⁺ mobilization compounds resulted in a decrease in CI down to zero at the 24 h time point because of the cells becoming rounded and detaching from the well bottom.

Figure 4a demonstrates that the change in cell index occurred within the first few hours of exposing PEO-1 cells to all concentrations of TN. The rate of adhesion of PEO-1 cells to fibronectin decreased in a dose-dependent manner. TN concentrations of 0.5 and 1 µg/mL indicated no effects on PEO-1 adhesion ability as compared with the control cells. The proportion of adherent cells reduced to a minimal level by the presence of 20 µg/mL TN. The results suggest that extracellular calcium mobilization reduced the adhesion of highly metastatic PEO-1 cells to fibronectin, and might induce anoikis of PEO-1 cells; however, the latter remains unclear.

The addition of all concentrations of TG reduced cell adhesion to fibronectin in a time-dependent manner as compared with the control cells (CI: 0.4) (Figure 4b). After 24-h incubation, even the addition of the lowest concentration (50 nM) of TG decreased the attachment of PEO-1 cells to fibronectin to zero. The results suggest that the adhesion of PEO-1 cells to fibronectin was decayed by the inhibition of the endoplasmic reticulum pump via TG treatment.

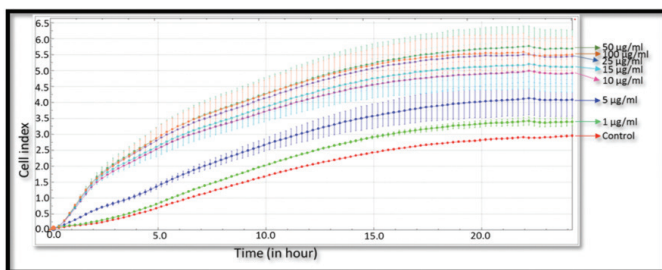


Figure 3. The binding ability of PEO-1 cells to fibronectin by RTCA. PEO-1 cells were allowed to incubate for 24 h on 16-well plates coated with 1-50 µg/mL fibronectin concentrations. The control wells were not coated with fibronectin. As mentioned in the Materials and Methods section, impedance was monitored at 15-min intervals for 24 h

Treatment of PEO-1 cells with various concentrations of EGTA also reduced the rate of adhesion within 5 h and then remain unchanged (Figure 4c).

The role of the PKB/Akt signal pathway on PEO-1 cell binding to fibronectin

FPA-124 was used to inhibit the protein kinase B (PKB)/Akt signal pathway. The impact of inhibiting PKB/Akt on cell binding was tested with different concentrations (5 µM, 15 µM, 25 µM, 35 µM) of FPA 124 (Figure 5). The percentage of the impact of different FPA-124 concentrations on cell binding at 24 h in PEO-1 is given in Figure 5b.

Figure 5a demonstrates the attachment of the control cells (without FPA-124; CI: 1.9). The cell index of the group treated with 5 µM FPA-124 inhibitor is close to that of control group (CI: 1.4 after 24-h incubation). Increasing the concentration of inhibitor by about three times showed the different effects on PEO-1 cell attachment to fibronectin. For the first few hours, cell attachment to fibronectin increased after adding 15 µM FPA inhibitor; however, longer incubation times reduced the binding of PEO-1 cells to the background level (CI: 0.3). The results suggest that FPA inhibitors might cause rapid focal contacts between cell-fibronectin in a dose dependent manner. Higher

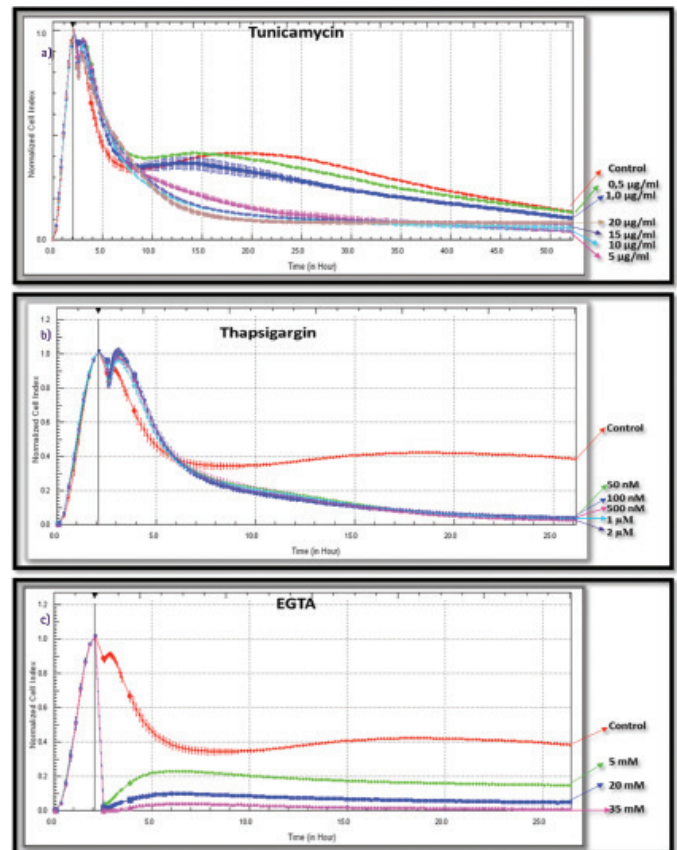


Figure 4. Effects of TN, TG and EGTA on PEO-1 binding to 50 µg/mL fibronectin after 24 h. (a) PEO-1 cells were treated with 0.5-1-5-10-20 µg/mL of TN; (b) with 50-100-500 nM-1-2 µM TG and (c) with 5-20-35 mM of EGTA for 24 h after being plated onto 50 µg/mL fibronectin. The rate of cell adhesion was calculated according to the NCI formula

concentrations of FPA-124 (25 and 35 μM) inhibited the binding of cells to fibronectin immediately after being added to the culture medium.

The role of cardamomin on PEO-1 cell binding to fibronectin

The effects of cardamomin on PEO-1 cell binding to fibronectin were investigated using RTCA and adding various concentrations (3.13, 6.25, 12.5, 25, 50 and 100 μM) of cardamomin. The results are shown in Figure 6a and b. The addition of 100 μM

cardamomin to the cells inhibited cell binding to fibronectin by about 64%. With the exception of 3.13- μM cardamomin treatment, all other concentrations of cardamomin inhibited cell binding to fibronectin as compared with the control cells plated on uncoated wells. Treatment of cells with the lowest concentration (3.13 μM) of cardamomin stimulated the rate of cell binding to fibronectin at around 13% as compared with the control cells. The results showed that the degradation of β -catenin in the cytoplasm by cardamomin had an important role in PEO-1 cell binding to fibronectin.

DISCUSSION

Adhesion and integrin activation are important to metastasize ovarian cancer cells onto the peritoneal mesothelial surface of the abdominal cavity¹⁷, and in the resistance to anoikis of epithelial ovarian cancer spheroids. It has been reported that some binding proteins might be involved in the implantation of ovarian cancer metastasis.¹⁸ CD44 in particular, which is a receptor for the ECM protein hyaluronic acid, plays a crucial role in mediating the mesothelial binding of ovarian cancer cells and β 1 integrins such as α 5 β 1 integrin (a receptor for fibronectin), α 3 β 1 (a receptor for fibronectin, collagen and laminin) and α v (a receptor for fibronectin and vitronectin) expressed by ovarian cancer cells; and ovarian cancer cell binding to peritoneal mesothelium.¹⁸ In our experiment, we found that the expression level of α v was two-fold higher than in the control group in PEO-1 cells. The other integrin expression levels of α 4, β 1, and β 6 subunits were higher at around 32%, 48%, and 84%, respectively, than in the control group. The α v β 1 fibronectin receptor most likely contributes to integrin-mediated binding of PEO-1 cells. These results are consistent with previous findings. Carduner et al.¹⁹ reported that α v had an important role in ovarian cancer progression. Lessan et al.²⁰ informed that β 1 integrin may responsible for adhesion of ovarian cancer cells.

Fibronectin has been detected in ovarian cancer cell metastases and is also present in ascites.^{21,22} Fibronectin contributes to the formation, adhesion, and disaggregation of ovarian cancer cell spheroids.²³ Therefore, the investigation of the binding capacity of ovarian cancer cells to fibronectin should be useful for targeted therapies. The binding studies herein suggest that PEO-1 cells could be able to adhere to fibronectin in a dose dependent-manner and the maximum binding rate was reached after adhesion of cells to 50 $\mu\text{g}/\text{mL}$ fibronectin. The binding capacity of PEO-1 cells was also measured in the presence or absence of calcium because integrin-mediated cell adhesion is regulated by extracellular Ca²⁺ ions²⁴, and an increased calcium concentration in the cytoplasm is essential for various signal transduction pathways such as proliferation and apoptosis and thus is also crucial in cancer.²⁵ TN induces endoplasmic stress by inhibiting glycosylation and leads to the accumulation of unfolded proteins. Endoplasmic stress has a critical role in regulating cell death.²⁶ Our results clearly indicated that increased calcium levels in the cytoplasm of PEO-1 cells by either extracellular or intracellular stores was essential for the binding of these cells to fibronectin. Increasing intracellular calcium in PEO-1 cells reduced cell adhesiveness and also

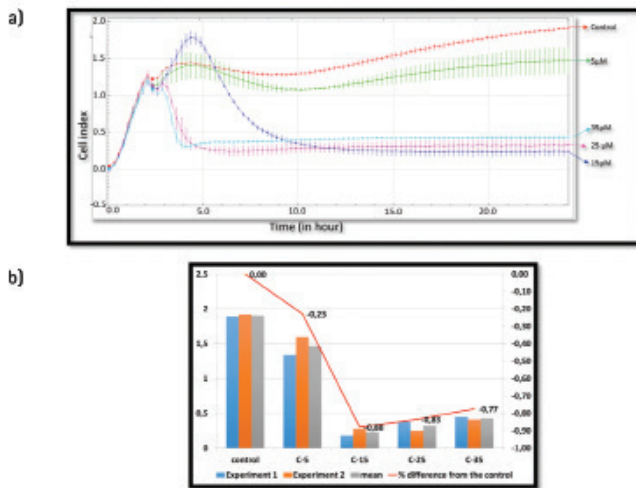


Figure 5. The role of PKB/Akt molecules on PEO-1 cell binding to fibronectin (a) and the impact of different FPA-124 concentrations on cell binding at 24 h (b). 16-wells plates were prepared as described in Materials and Methods. Various concentrations (5-35 μM) of FPA-124 inhibitor were added to each well. No inhibitor was added to the control groups. (b) The left axis is the cell index at 24 h, the right axis is the percentage differences from the control group

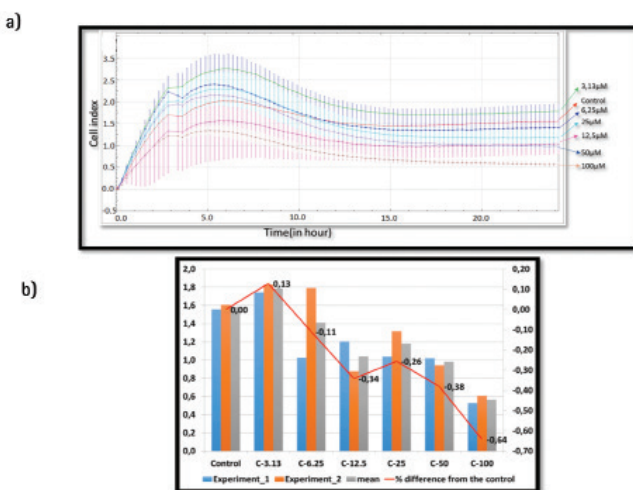


Figure 6. The effect of cardamomin on binding of PEO-1 cells to fibronectin (a) and the percentage of the impact of different cardamomin concentrations on PEO-1 cell binding to fibronectin at 24 h (b). Wells were coated with 50 $\mu\text{g}/\text{mL}$ fibronectin at +4°C overnight. The cells were transferred into each well and then incubated with cardamomin (concentration range between 3.13 μM and 100 μM) for 24 h. The results represented are the means of the two wells. (b) The left axis is the cell index at 24 h, the right axis is the percentage differences from the control group

might have caused programmed cell death induced after cell detachment from the ECM.

PKB/Akt is a serine/threonine kinase that has an important role in cell survival, cell proliferation, invasion, and adhesion to the ECM in various types of cells such as human umbilical vein endothelial cells²⁷, breast cancer cell²⁸, and lung adenocarcinoma.²⁹ The overexpression of PI3K/Akt-related genes has been observed in ovarian cancer tissues.³⁰ Moreover, fibronectin adhesion promotes metastatic behavior on these types of cancer cells through the focal adhesion kinase-PI3K/Akt pathway.³¹ Xing et al.³² suggested that Akt activation promoted by fibronectin might have a critical role in cell survival. In the present study, inhibition of PKB/Akt with the FPA inhibitor decreased the rate of adhesion of PEO-1 cells to fibronectin in a dose dependent manner, suggesting that PKB/Akt participates in the signaling of adhesion in these cells.

In the present study, we found that the inhibition of β -catenin by cardamonin reduced PEO-1 cell binding to fibronectin. β -catenin is an activated downstream signal molecule from Akt, and Akt-mediated phosphorylation of β -catenin results in its accumulation in the cytosol and translocation into the nucleus, thus upregulating genes related to cell proliferation such as c-Myc, cyclin D1 and D2.³³ The function of β -catenin may be necessary for the adhesive and signaling responses required for cancer. The inhibition of β -catenin activity causes suppression of several cancer hallmarks, which might be useful as a putative drug target.³⁴ Pramanik et al.³⁵ found that inhibition of β -catenin signaling blocked pancreatic tumor growth. Verma et al.³⁶ showed that small interfering RNAs directed against β -catenin reduced β -catenin-dependent gene expression and growth of colon cancer cells. In this study, we found that the binding ability of PEO-1 ovarian cells to fibronectin decreased with treatment of 100 μ M cardamonin, suggesting that β -catenin might be involved in the adhesion process of PEO-1 cells to fibronectin as well as Akt. This process could be mediated by integrin, especially the α v subunit, but further experiments are required to investigate the role of the α v subunit under these circumstances.

CONCLUSION

In conclusion, PEO-1 cell binding to fibronectin via integrins could be related to intracellular Ca²⁺ mobilization and Akt signaling. However, the sensitivity of these cells against anoikis still remains to be investigated.

ACKNOWLEDGEMENTS

This work was funded by grants from the Anadolu University (Project No. 1308S303 and 1301S011). The authors wish to thank Anadolu University, Medicinal Plants, Drugs and Scientific Research Center (AÜBİBAM) for technical support. Earlier versions of this paper were presented at the 40th FEBS Congress, The Biochemical Basis of Life, Berlin, Germany, July 4-9, 2015 and at the International Multidisciplinary Symposium on Drug Research and Development, Eskişehir, Turkey, 15-17 October, 2015. The abstract of this paper was published at the FEBS Journal, 282 (Suppl 1), 286, July 2015.

Conflict of Interest: No conflict of interest was declared by the authors.

REFERENCES

- Manso AM, Kang SM, Ross RS. Integrins, Focal Adhesions and Cardiac Fibroblasts. *J Investig Med.* 2009;57:856-860.
- Aoudjit F, Vuori K. Integrin Signalling in Cancer Cell Survival and Chemoresistance. *Chemotherapy Res and Pract.* 2012;2012:1-16.
- Hirohashi S, Kanai Y. Cell adhesion system and human cancer morphogenesis. *Cancer Sci.* 2003;94:575-581.
- van den Hoogen C, van der Horst G, Cheung H, Buijs JT, Pelger RC, van der Pluijm G. Integrin α v expression is required for the acquisition of a metastatic stem/progenitor cell phenotype in human prostate cancer. *Am J Pathol.* 2011;179:2559-2568.
- Paoli P, Giannoni E, Chiarugi P. Anoikis molecular pathways and its role in cancer progression. *Biochimica et Biophysica Acta-Molecular Cell Research.* 2013;1833:3481-3498.
- Lu JG, Li Y, Li L, Kan X. Overexpression of osteopontin and integrin α v in laryngeal and hypopharyngeal carcinomas associated with differentiation and metastasis. *J Cancer Res Clin Oncol.* 2011;137:1613-1618.
- Puiffe ML, Le Page C, Filali-Mouhim A, Zietarska M, Ouellet V, Tonin PN, Chevrette M, Provencher DM, Mes-Masson AM. Characterization of ovarian cancer ascites on cell invasion, proliferation, spheroid formation, and gene expression in an *in vitro* model of epithelial ovarian cancer. *Neoplasia.* 2007;9:820-829.
- Kenny HA, Kaur S, Coussens LM, Lengyel E. The initial steps of ovarian cancer cell metastasis are mediated by MMP-2 cleavage of vitronectin and fibronectin. *J Clin Invest.* 2008;118:1367-1379.
- Bodnar L, Stanczak A, Cierniak S, Smoter M, Cichowicz M, Kozłowski W, Szczylik C, Wiczorek M, Lamparska-Przybylska M. Wnt/ β -catenin pathway as a potential prognostic and predictive marker in patients with advanced ovarian cancer. *J of Ovarian Research.* 2014;7:16-26.
- Hur J, Jeong S. Multitasking β -catenin: From adhesion and transcription to RNA regulation. *Animal Cell Systems.* 2013;17:299-305.
- Uchino M, Kojima H, Wada K. Nuclear beta-catenin and CD44 upregulation characterize invasive cell populations in non-aggressive MCF-7 breast cancer cell. *BMC Cancer.* 2010;10:414-417.
- Chau WK, Ip CK, Mak AS. C-Kit mediates chemoresistance and tumor-initiating capacity of ovarian cancer cells through activation of Wnt/ β -catenin-ATP-binding cassette G2 signaling. *Oncogene.* 2012;31:103-107.
- Tran NL, Adams DG, Vaillancourt RR, Heimark RL. Signal transduction from N-cadherin increases Bcl-2. Regulation of the phosphatidylinositol 3-kinase/Akt pathway by homophilic adhesion and actin cytoskeletal organization. *J Biol Chem.* 2002;277:32905-32914.
- Sharma M, Chuang WW, Sun Z. Phosphatidylinositol 3-kinase/Akt stimulates androgen pathway through GSK3 β inhibition and nuclear beta-catenin accumulation. *J Biol Chem.* 2002;277:30935-30941.
- Rahim S, Üren A. A real time electrical impedance based technique to measure invasion of endothelial cell monolayer by cancer cells. *J Vis Exp.* 2011;50:2792-2797.
- Zhang JD. 2016. Available from: <https://www.bioconductor.org/packages/devel/bioc/vignettes/RTCA/inst/doc/aboutRTCA.pdf>.
- Sawada K, Mitra AK, Radjabi AR, Bhaskar V, Kistner EO, Tretiakova M, Jagadeeswaran S, Montag A, Becker A, Kenny HA. Loss of E-cadherin promotes ovarian cancer metastasis via α 5-integrin, which is a therapeutic target. *Cancer Res.* 2008;68:2329-2339.

18. Strobel T, Cannistra S. B1-Integrins partly mediated binding of ovarian cancer cells to peritoneal mesothelium *in vitro*. *Gynecologic Oncology*. 1999;73:362-367.
19. Carduner L, Leroy-Dudal J, Picot CR, Gallet O, Carreiras F, Kellouche S. Ascites-induced shift along epithelial-mesenchymal spectrum in ovarian cancer cells: enhancement of their invasive behaviour partly dependant on av integrins. *Clinical and Experimental Metastasis*. 2014;31:675-688.
20. Lessan K, Aguiar DJ, Oegema T, Siebenson L, Skubitz AP. CD44 and β 1 integrin mediate ovarian carcinoma cell adhesion to peritoneal mesothelial cells. *Am J Pathol*. 1999;154:1525-1537.
21. Bignotti E, Tassi RA, Calza S, Ravaggi A, Bandiera E, Rossi E, Donzelli C, Pasinetti B, Pecorelli S, Santin AD. Gene expression profile of ovarian serous papillary carcinomas: identification of metastasis-associated genes. *Am J Obstet Gynecol*. 2007;196:245.
22. Wilhelm O, Hafter R, Copenrath E, Pflanz M, Schmitt M, Graeff H. Fibrin-fibronectin compounds in human ovarian tumor ascites and their possible relation to the tumor stroma. *Cancer Res*. 1988;48:3507-3514.
23. Mitra AK, Sawada K, Tiwari P, Mui K, Gwin K, Lengyel E. Ligand-independent activation of c-Met by fibronectin and α (5) β (1)-integrin regulates ovarian cancer invasion and metastasis. *Oncogene*. 2011;30:1566-1576.
24. Tsaktanis T, Kremling H, Pavsic M, von Stackelberg R, Mack B, Fukumori A, Steiner H, Vielmuth F, Spindler V, Huang Z, Jakubowski J, Stoecklein NH, Luxenburger E, Lauber K, Lenarcic B, Gires O. Cleavage and cell adhesion properties of human epithelial cell adhesion molecule (HEPCAM). *The Journal of Biological Chemistry*. 2015;290:24574-24591.
25. Giorgi C, Bonova M, Pinton P. Inside the tumor: p53 modulates calcium homeostasis. *Cell Cycle*. 2015;147:933-934.
26. Nami B, Donmez H, Kocak N. Tunicamycin-induced endoplasmic reticulum stress reduces *in vitro* subpopulation and invasion of CD44+/CD24- phenotype breast cancer stem cells. *Exp Toxicol Pathol*. 2016;68:418-426.
27. Hwang HJ, Chung HS, Jung TW, Ryu JY, Hong HC, Seo JA, Kim SG, Kim NH, Choi KM, Choi DS, Baik SH, Yoo HJ. The dipeptidyl peptidase-IV inhibitor inhibits the expression of vascular adhesion molecules and inflammatory cytokines in HUVECs via Akt- and AMPK-dependent mechanisms. *Mol Cell Endocrinol*. 2015;405:25-34.
28. Leung HW, Wang Z, Yue GG, Zhao SM, Lee JK, Fung KP, Leung PC, Lau CB, Tan NH. Cyclopeptide RA-V inhibits cell adhesion and invasion in both estrogen receptor positive and negative breast cancer cells via PI3K/AKT and NF- κ B signaling pathways. *Biochim Biophys Acta*. 2015;1853:1827-1840.
29. Piegeler T, Schlapfer M, Dulli RO, Schwartz DE, Borgeat A, Minshall RD, Beck-Schimmer B. Clinically relevant concentrations of lidocaine and ropivacaine inhibit TNF α -induced invasion of lung adenocarcinoma cells *in vitro* by blocking the activation of Akt and focal adhesion kinase. *Br J Anaesth*. 2015;115:784-791.
30. Gwak H, Kim S, Dhanasekaran DN, Song YS. Resveratrol triggers ER stress-mediated apoptosis by disrupting N-linked glycosylation of proteins in ovarian cancer cells. *Cancer Lett*. 2016;371:347-353.
31. Yousif NG. Fibronectin promotes migration and invasion of ovarian cancer cells through up-regulation of FAK-PI3K/Akt pathway. *Cell Biol Int*. 2013;38:85-91.
32. Xing H, Weng D, Chen G, Tao W, Zhu T, Yang X, Meng L, Wang S, Lu Y, Ma D. Activation of fibronectin/PI-3K/Akt2 leads to chemoresistance to docetaxel by regulating survivin protein expression in ovarian and breast cancer cells. *Cancer Lett*. 2008;261:108-119.
33. Fang D, Hawke D, Zheng Y, Xia Y, Meisenhelder J, Nika H, Mills GB, Kobayashi R, Hunter T, Lu Z. Phosphorylation of beta-catenin by AKT promotes beta-catenin transcriptional activity. *J Biol Chem*. 2007;282:11221-11229.
34. Luu HH, Zhang R, Haydon RC, Rayburn E, Kang Q, Si W, Park JK, Wang H, Peng Y, Jiang W, He TC. Wnt/beta-catenin signalling pathway as a novel cancer drug target. *Curr Cancer Drug Targets*. 2004;4:653-671.
35. Pramanik KC, Fofaria NM, Gupta P, Ranjan A, Kim SH, Srivastava SK. Inhibition of β -catenin signaling suppresses pancreatic tumor growth by disrupting nuclear β -catenin/TCF-1 complex: critical role of STAT-3. *Oncotarget*. 2015;6:11561-11574.
36. Verma UN, Surabhi RM, Schmaltieg A, Becerra C, Gaynor RB. Small Interfering RNAs Directed against β -Catenin Inhibit the *in vitro* and *in vivo* Growth of Colon Cancer Cells. *Clin Cancer Res*. 2003;9:1291-1300.



Synthesis and Evaluation of Vanillin Derivatives as Antimicrobial Agents

Vanilin Türevlerinin Antimikrobiyal Ajanlar Olarak Sentezi ve Değerlendirilmesi

✉ Rakesh YADAV*, ✉ Dharamvir SAINI, ✉ Divya YADAV

Banasthali University, Faculty of Pharmacy, Rajasthan, India

ABSTRACT

Objectives: The present work involves the synthesis of novel acetyl vanillin derivatives and evaluation for their anti-microbial potential against *Escherichia coli*.

Materials and Methods: The titled compounds were prepared by reacting acetyl nitro vanillin with different substituted amines (Schiff base). The starting material acetyl nitro vanillin was synthesized by reacting acetyl vanillin with fuming nitric acid which in turn was prepared from 4-hydroxy-3-methoxybenzaldehyde (vanillin).

Results: The chemical structures of the synthesized compounds were confirmed on the basis of their spectral data (FT-IR, UV/Visible, ¹H-NMR, Mass spectra).

Conclusion: All the synthesized compounds were tested *in vitro* for antimicrobial activity and compound F & I showed significant activity as compared to the standard drug.

Key words: Vanillin, antimicrobial activity, Schiff bases, ciprofloxacin

ÖZ

Amaç: Mevcut çalışma, yeni asetil vanilin türevlerinin sentezini ve *Escherichia coli*'ye karşı antimikrobiyal potansiyelinin değerlendirilmesini içerir.

Gereç ve Yöntemler: Başlıktaki bileşikler, asetil nitro vanilinin farklı ikame edilmiş aminler (Schiff baz) ile reaksiyona sokulmasıyla hazırlandı. Başlangıç malzemesi asetil nitro vanilin, asetil vanilinin, sırasıyla 4-hidroksi-3-metoksibenzenaldehyden (vanilin) hazırlanan dumanlı nitrik asit ile reaksiyona sokulmasıyla sentezlenmiştir.

Bulgular: Sentezlenen bileşiklerin kimyasal yapıları, spektral verilerine (FT-IR, UV/Görünür, ¹H-NMR, Kütle spektrumu) dayanarak teyit edildi.

Sonuç: Sentezlenen tüm bileşikler, antimikrobiyal aktivite için *in vitro* olarak test edildi ve bileşik F & I, standart ilaçla karşılaştırıldığında önemli aktivite gösterdi.

Anahtar kelimeler: Vanilin, antimikrobiyal aktivite, Schiff bazları, siprofloksasin

INTRODUCTION

Antimicrobial agents like penicillins, cephalosporins, tetracyclines, nitrobenzene derivatives, macrolide antibiotics (erythromycin, roxithromycin etc.), polypeptide antibiotics (polymixin-B, Bacitracin etc.), nicotinic acid derivatives derived from the various sources are currently available in the market. But microbial resistance in most of the pathogenic bacteria to these drugs repeatedly appears. In order to check this consequential medical problem, the extension of newer varieties of antimicrobial agents is a prominent task.¹ Vanillin (4-hydroxy-

3-methoxybenzaldehyde), a dietary flavoring agent, has been reported to show antioxidant and anti-mutagenic activities, and has also been proved to be an anti carcinogen against a variety of chemical and physical agents.^{2,3}

Vanillin is considered to be one of the most widely appreciated flavoring compounds. In spite of its flavor qualities, vanillin exhibits the antimicrobial potential and has been used as a natural food preservative.⁴ Many natural compounds, including phenolic compounds derived from plants, exhibit strong antimicrobial properties and therefore have the potential to be applied to food

*Correspondence: E-mail: rakesh_pu@yahoo.co.in, Phone: +01438228365 ORCID-ID: orcid.org/0000-0002-8932-5076

Received: 30.03.2017, Accepted: 13.04.2017

©Turk J Pharm Sci, Published by Galenos Publishing House.

products as novel preservatives.⁵ It is investigated that vanillin primarily affects the cytoplasmic membrane of the food-related bacteria *Escherichia coli*, *Lactobacillus plantarum* and *Listeria innocua*. The antimicrobial activity of vanillin and related derivatives was found to be dependent on the time of exposure, concentration and the target organism. The inhibitory action of vanillin is more effective against non-lactic Gram-positive than Gram-negative bacteria.⁶ The minimal inhibitory concentrations of vanillin is bacteriostatic in contrast to the more potent phenolic antimicrobials such as carvacrol and thymol, which are bactericidal.^{7,8}

The mode of action of nearly all antimicrobials can be classed into one or more of the following groups: (a) reaction with the cell membrane, (b) inactivation of essential enzymes, or (c) destruction or inactivation of genetic material.⁹ Phenolic compounds are hydrophobic in nature and are therefore regarded as membrane active.¹⁰

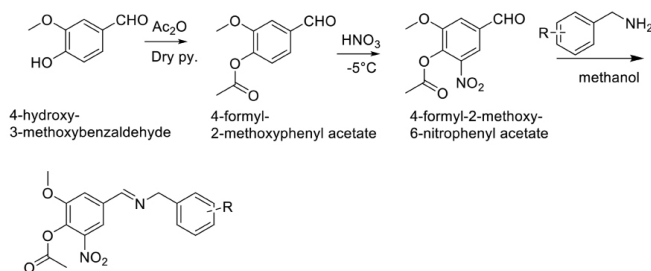
On the basis of these observations we tried our efforts to synthesize some nitro vanillin derivatives, starting with vanillin, which possess minimum microbial resistance and better activity. We now report the synthesis of these new compounds and resulting structure activity relationships for zone inhibition.

EXPERIMENTAL

All reagents and chemicals were used as obtained from the commercial supplier without further purification. All moisture sensitive reactions were carried out under dry nitrogen atmosphere. Column chromatography was carried out using silica gel 60-120 mesh size and distilled solvents. Thin layer chromatography (TLC) analyses were performed on precoated silica gel plates (GF254, Merck). Infrared (IR) spectra were recorded on BRUKER ALPHA using ATR technique. Proton nuclear magnetic resonance (¹H-NMR) spectra were recorded on a BRUKER AVANCE II 400 MHz spectrometer in deuterated solvents. The chemical shifts are reported in δ (ppm) relative to internal standard tetramethylsilane and coupling constants J are given in Hertz. Mass spectrometry was conducted using Agilent 1100 LC has been coupled with Bruker mass spectrometer model Esquire 3000.

RESULTS

The designed compounds on the basis of various literature reports were synthesized according to the following synthetic Scheme 1. The starting material vanillin was used to afford



Scheme 1.

the targeted compounds A-J, with a series of reaction. The completion of reaction was monitored with the help of TLC at each step. The compounds were characterized for physical parameters and tabulated in Table 1.

The chemical structures of the synthesized compounds were confirmed using various spectral techniques such as IR, NMR, Mass etc. are mentioned in the experimental part.

The acetylation of vanillin was confirmed with presence of carbonyl peak in IR at $\sim 1695\text{ cm}^{-1}$ and resonance of methyl protons at $\sim 2.29\text{ ppm}$ in ¹H-NMR. Further nitration of compounds was confirmed by appearance of IR peak at $\sim 1540\text{ cm}^{-1}$ in various derivatives (A-J). Substitution of various amines was confirmed by the presence of IR peak at $\sim 1370\text{ cm}^{-1}$ whereas proton resonance at $\sim 8.5\text{ ppm}$ in all the synthesized compounds.

Although the compounds showed significant activity as compared to the standard but compounds F (fluorine substituted) and I (pyridine substituted) showed similar inhibition ($25\text{ }\mu\text{g/mL}$) as compared to ciprofloxacin ($10\text{ }\mu\text{g/mL}$). This study revealed that there must be proper electron withdrawing substituents at *para* position of the substituted amines to have potent activity.

Experimental work

General method for preparation of acetyl vanillin

Vanillin (3.2 mmol) was dissolved in dichloromethane (DCM) (5-6 mL) and acetic anhydride (3.84 mmol) and dry pyridine (3.84 mmol) were added to this solution under anhydrous conditions. This mixture was stirred for 3-4 hrs at room temperature. Completion of reaction is detected by TLC in 1:1 Hexane: Ethyl acetate. The solvent DCM was evaporated and the mixture was poured on crushed ice. Precipitates obtained were filtered and rinsed with water, dried the precipitate and re-crystallized from 95% ethanol.

General method for preparation of acetyl nitro vanillin

Acetyl vanillin (2.59 mmol) was dissolved in 5 mL of DCM. This mixture was kept in -5 to -10°C ice bath and stirred. When clear solution is obtained, 2 mL of fuming nitric acid was added to this reaction mixture then stirred for 1-2 hr at room temperature. For work up add ice cold water was added, the precipitate was obtained, this obtained precipitate filtered washed and dried. TLC taken in 1:1 Hexane: Ethyl acetate.

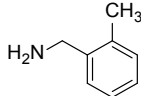
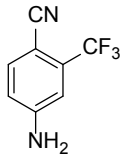
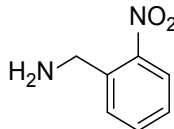
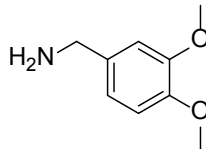
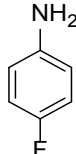
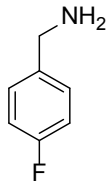
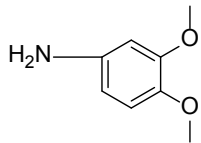
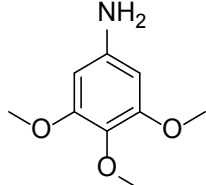
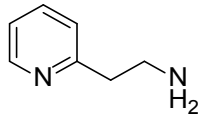
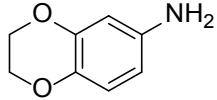
General method for preparation of Schiff bases

Equimolar mixture of acetyl nitro vanillin (0.418 mmol) was dissolved in 25 mL of ethanol and then various amines (A-J) (0.428 mmol) were added to the mixture and stirred for 2-3 hrs at ambient temperature. The completion of reaction was detected by the TLC in 1:1 Hexane: Ethyl acetate. Solvent evaporated and oily compounds were collected.

2-Methoxy-4-(((2-methylbenzyl)-imino)-methyl)-6-nitrophenyl acetate (A)

¹H-NMR: δ 2.29 (s, 3H, CH₃), 2.38 (s, 3H, CH₃), 3.83 (s, 3H, O-CH₃), 4.87 (s, 2H, CH₂-N), 7.16-7.10 (tt, $J=5.2, 5.0, 5.0, 5.2$ 3H, CH₂-Ar), 7.34 (d, $J=7.2, 1\text{H}$, CH-Ar), 8.05 (s, 2H, CH-Ar) and 8.65 (s, 1H, CH=N-) ppm. ESI-MS (m/z): 342. IR: 1467, 1643, 1695, 1019, 1538, 1371, 1597.

Table 1. Physical constant of Schiff bases

S. No.	Code	R=Amine	M.F.	M. Wt. g/mol	M.P.	Yield
1	A		$C_{18}H_{18}N_2O_5$	342.35	Oily mass	60%
2	B		$C_{18}H_{12}F_3N_3O_5$	407.31	Oily mass	40%
3	C		$C_{17}H_{15}N_3O_7$	373.09	Oily mass	35%
4	D		$C_{19}H_{20}N_2O_7$	388.38	Oily mass	52%
5	E		$C_{16}H_{13}FN_2O_5$	332.29	Oily mass	47%
6	F		$C_{17}H_{15}FN_2O_5$	346.31	Oily mass	34%
7	G		$C_{18}H_{18}N_2O_7$	374.35	Oily mass	58%
8	H		$C_{19}H_{20}N_2O_8$	404.38	Oily mass	53%
9	I		$C_{17}H_{17}N_3O_5$	343.34	Oily mass	37%
10	J		$C_{18}H_{16}N_2O_7$	372.33	Oily mass	46%

4-(((4-Cyano-3-(trifluoromethyl)-phenyl)-imino)-methyl)-2-methoxy-6-nitro-phenyl acetate (B)

¹H-NMR: δ 2.18 (s, 3H, CH₃), 3.73 (s, 3H, O-CH₃), 6.27 (s, 2H, CH-Ar), 7.19 (s, 1H, CH-Ar), 7.48 (s, 1H, CH-Ar), 8.08 (s, 1H, CH-Ar) and 8.11 (s, 1H, CH=N-) ppm. ESI-MS (m/z): 407. IR: 2218, 1643, 1696, 1021, 1541, 1359, 1609, 1171.

2-Methoxy-6-nitro-4-(((2-nitrobenzyl)-imino)-methyl)-phenyl acetate (C)

¹H-NMR: δ 2.23 (s, 3H, CH₃), 3.61 (s, 3H, O-CH₃), 4.80 (s, 2H, CH₂-N), 7.16- 7.10 (tt, *J*=5.2, 5.0, 5.0, 5.2 3H, CH₂-Ar), 7.31 (d, *J*=7.2, 1H, CH-Ar), 8.15 (s, 2H, CH-Ar) and 8.23 (s, 1H, CH=N-) ppm. ESI-MS (m/z): 373. IR: 1467, 1592, 1651, 1025, 1524, 1343.

4-(((3,4-Dimethoxybenzyl)-imino)-methyl)-2-methoxy-6-nitrophenyl acetate (D)

¹H-NMR: δ 2.28 (s, 3H, CH₃), 3.83 (s, 9H, O-CH₃), 4.87 (s, 2H, CH₂-N), 6.68 (d, *J*=7.2, 1H, CH-Ar), 6.76 (d, *J*=8.8, 1H, CH-Ar), 6.90 (s, 1H, CH-Ar), 8.05 (s, 2H, CH-Ar), 8.74 (s, 1H, CH=N-). ESI-MS (m/z): 388. IR: 1467, 1591, 1654, 1022, 1541, 1336.

4-(((4-Fluorophenyl)-imino)-methyl)-2-methoxy-6-nitrophenyl acetate (E)

¹H-NMR: δ 2.28 (s, 3H, CH₃), 3.83 (s, 3H, O-CH₃), 7.24 (d, *J*=7.6, 2H, CH₂-Ar), 7.32 (d, *J*=6.2, 2H, CH-Ar), 8.05 (s, 2H, CH-Ar), 8.66 (s, 1H, CH=N-). ESI-MS (m/z): 332. IR: 1593, 1658, 1006, 1545, 1384, 1609, 1154.

4-(((4-Fluorobenzyl)-imino)-methyl)-2-methoxy-6-nitrophenyl acetate (F)

¹H NMR: δ 2.28 (s, 3H, CH₃), 3.83 (s, 3H, O-CH₃), 4.87 (s, 2H, CH₂-N), 7.17 (d, *J*=7, 2H, CH₂-Ar), 7.22 (d, *J*=6, 2H, CH-Ar), 8.05 (s, 2H, CH-Ar), 8.65 (s, 1H, CH=N). ESI-MS (m/z): 346. IR: 1507, 1652, 1090, 1062, 1546, 1385, 1438, 1120.

4-(((3,4-Dimethoxyphenyl)-imino)-methyl)-2-methoxy-6-nitrophenyl acetate (G)

¹H-NMR: δ 2.28 (s, 3H, CH₃), 3.83 (s, 9H, O-CH₃), 6.78-6.76 (d, *s*, *J*=4.8, 2H, CH₂-Ar), 7.88 (d, *J*=10.0, 1H, CH-Ar), 8.05 (s, 2H, CH-Ar), 8.66 (s, 1H, CH=N). ESI-MS (m/z): 374. IR: 1467, 1655, 1593, 1024, 1545, 1384, 1609.

2-Methoxy-6-nitro-4-(((3,4,5-trimethoxyphenyl)-imino)-methyl)-phenyl acetate (H)

¹H-NMR: δ 2.28 (s, 3H, CH₃), 3.83 (s, 12H, O-CH₃), 6.63 (s, 2H, CH-Ar), 8.05 (s, 2H, CH-Ar), 8.66 (s, 1H, CH=N-). ESI-MS (m/z): 404. IR: 1650, 1721, 1005, 1545, 1385, 1596.

2-Methoxy-6-nitro-4-(((2-(pyridin-2-yl)-ethyl)-imino)-methyl)-phenyl acetate (I)

¹H NMR: δ 2.29 (s, 3H, CH₃), 3.26 (t, *J*=7.0, 2H, N-CH₂CH₂), 3.83 (s, 3H, O-CH₃), 3.87 (t, *J*=7.1, 2H, CH₂-N), 7.25-7.20 (m, *J*=4.7, 8.0, 1.4, 4.7, 2H, CH-Ar), 7.58 (t, *J*=4.5, 6.1, 1H, CH-Ar), 8.05 (s, 2H, CH-Ar), 8.44 (d, *J*=9.8, 1H, CH-Ar), 8.65 (s, 1H, CH=N). ESI-MS (m/z): 343. IR: 1655, 1590, 1001, 1538, 1368, 1435.

4-(((2, 3-Dihydrobenzo-[b][1,4]-dioxin-6-yl)-imino)-methyl)-2-methoxy-6-nitro-phenyl acetate (J)

¹H NMR: δ 2.28 (s, 3H, CH₃), 3.83 (s, 3H, O-CH₃), 4.28 (s, 4H, CH₂-O), 6.78 (d, *J*=5.8, 2H, CH-Ar), 6.89 (d, *J*=9.1, 1H, CH-Ar), 8.05 (s, 2H, CH-Ar), 8.66 (s, 1H, CH=N-). ESI-MS (m/z): 372. IR: 1656, 1597, 1017, 1535, 1426.

Table 2. Antimicrobial activity of ciprofloxacin and synthesized compounds (A-J) on *E. coli*

S. No.	Micro-organism→ Sample↓	<i>E. coli</i>
		Zone of inhibition Mean (mm)
1	Ciprofloxacin (µg/mL)	
	30	20±0.15
	20	18±0.13
2	10	15±0.19
	Drug-A (µg/mL)	
	100	10±0.04
3	50	8±0.11
	25	6±0.08
	Drug-B (µg/mL)	
4	100	6±0.11
	50	6±0.16
	25	6±0.02
5	Drug-C (µg/mL)	
	100	6±0.19
	50	6±0.11
6	25	6±0.05
	Drug-D (µg/mL)	
	100	16±0.11
7	50	10±0.03
	25	08±0.01
	Drug-E (µg/mL)	
8	100	20±0.14
	50	15±0.13
	25	7±0.08
9	Drug-F (µg/mL)	
	100	15±0.03
	50	13±0.13
10	25	11±0.05
	Drug-G (µg/mL)	
	100	15±0.01
11	50	8±0.17
	25	6±0.09
	Drug-H (µg/mL)	
12	100	10±0.06
	50	8±0.05
	25	6±0.10
13	Drug-I (µg/mL)	
	100	15±0.11
	50	13±0.16
14	25	10±0.02
	Drug-J (µg/mL)	
	100	14±0.04
15	50	11±0.11
	25	6±0.08

Antimicrobial activity

Bacterial cultures

Bacterial cultures were procured from microbial culture collection, National Centre for Cell Science, Pune, Maharashtra, India. The lyophilized cultures of bacterial strains upon culturing in nutrient broth for 24-48 hrs at 37°C in an incubator resulted into turbid suspension of activated live bacterial cell ready to be used for microbiological study. The *E. coli* (Bact-1) used for antimicrobial studies was found to be active using well diffusion method (100 µL). From the broth of respective revived cultures of bacteria, loop full of an inoculum was taken and streaked on to the nutrient agar medium and incubated again at same culture conditions and duration that yielded the pure

culture colonies on to the surface of the agar culture that are successfully stored in refrigerated conditions at 4°C as stock culture to be used for further experimentation.

Anti-biogram studies

The antimicrobial activity of the synthesized compound against bacterial pathogens was used under present study. The synthesized compounds (A-J) were prepared in various concentrations (100, 50 and 25 µg/mL) and applied on to the test organism using well diffusion method. Results of the experiment are being concluded in the Table 2, which clearly shows the anti-microbial activity of synthesized compound out of the bacterial strains used in the present work (Figure 1).

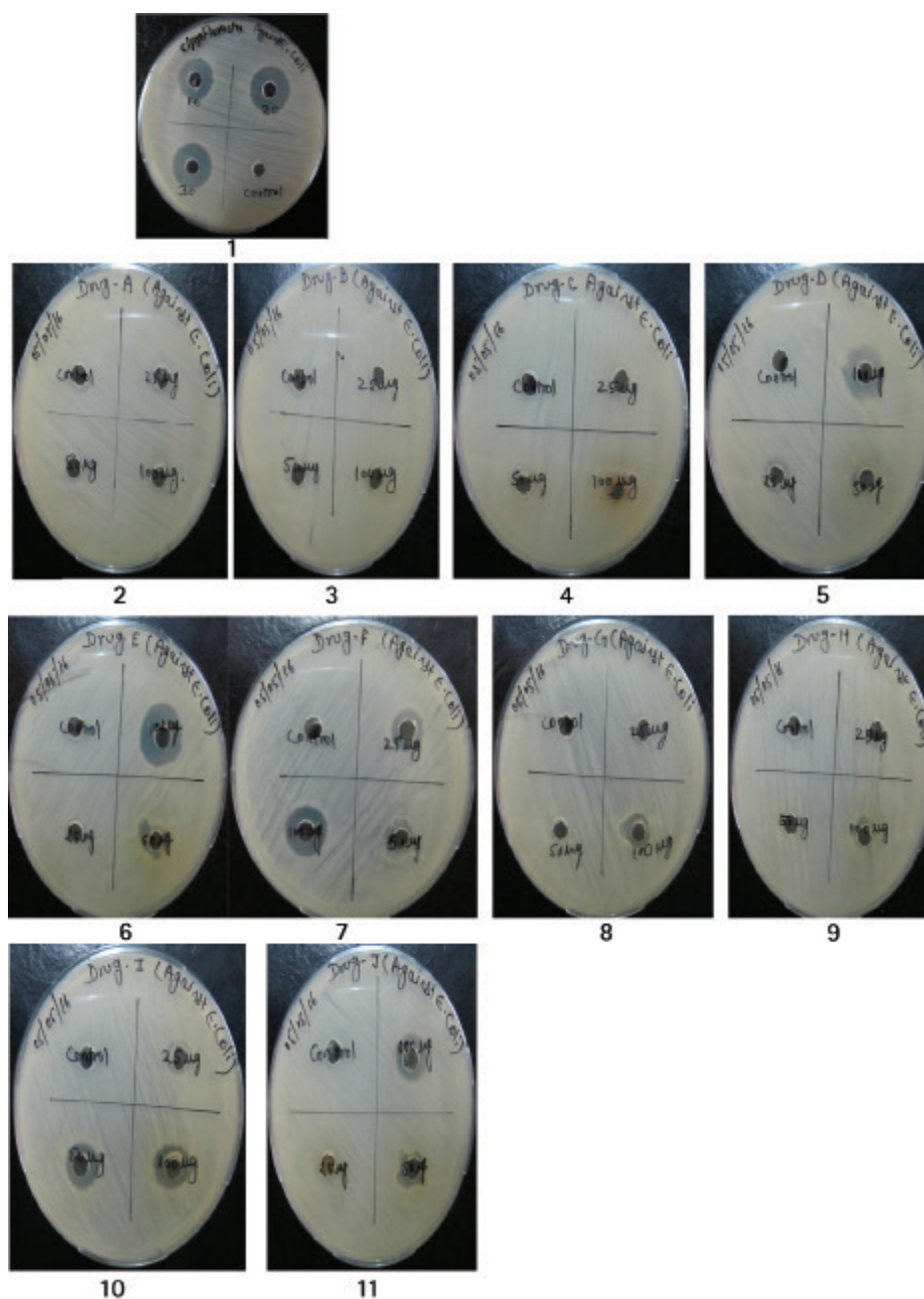


Figure 1. Antimicrobial activity of synthesized compounds (A-J) against *E. coli*

CONCLUSIONS

We have reported a simple synthetic method of vanillin related derivatives. The reactions occurred very fast, in mild condition, using reasonable reagents and solvents with moderate yield. The antimicrobial activity of the synthesized compounds was effectively screened against *E. coli*. The compounds bearing electron withdrawing substituents (F & I) showed significant activity as compared to standard. The outcome of the work will be valuable for further studies in term of toxicity effect and quantity structure activity relationship to improve their biological and pharmacological properties.

ACKNOWLEDGEMENTS

Authors are thankful to the Vice-chancellor, Banasthali Vidyapith, Banasthali, India for providing constant support for research work. The financial assistance from DST-CURIE and MHRD, New Delhi is duly acknowledged.

Conflict of Interest: No conflict of interest was declared by the authors.

REFERENCES

1. Leeb M. Antibiotics: a shot in the arm. *Nature*. 2004;431:892-893
2. Hocking MB. Vanillin: synthetic flavoring from spent sulfite liquor. *J Chem Educ*. 1997;74:1055-1059.
3. Evans JD, Martin SA. Effects of thymol on ruminal microorganisms. *Curr Microbiol*. 2000;41:336-340.
4. Kamat JP, Ghosh A, Devasagayam TP. Vanillin as an antioxidant in rat liver mitochondria: Inhibition of protein oxidation and lipid per oxidation induced by photosensitization. *Mol Cell Biochem*. 2000;209:47-53.
5. Beuchat LR, Golden DA. Antimicrobials occurring naturally in foods. *Food Tech*. 1989;43:134-142.
6. Jay JM, Rivers, GM. Antimicrobial activity of some food flavoring compounds. *J Food Saf*. 1984;6:129-139.
7. Ultee A, Gorris LG, Smid EJ. Bactericidal activity of carvacrol towards the food-borne pathogen *Bacillus cereus*. *J Appl Microbiol*. 1998;85:211-218.
8. Sikkema J, de Bont JA, Poolman B. Interactions of cyclic hydrocarbons with biological membranes. *J Biol Chem*. 1994;269:8022-8028.
9. Sikkema J, de Bont JA, Poolman B. Mechanisms of membrane toxicity of hydrocarbons. *Microbiol Rev*. 1995;59:201-222.
10. Cox SD, Mann CM, Markham JL, Bell HC, Gustafson JE, Warmington JR, Wyllie SG. The mode of antimicrobial action of the essential oil of *Melaleuca alternifolia* (tea tree oil). *J Appl Microbiol*. 2000;88:170-175.



The Structural, Crystallinity, and Thermal Properties of pH-responsive Interpenetrating Gelatin/Sodium Alginate-based Polymeric Composites for the Controlled Delivery of Cetirizine HCl

Setirizin HCl'nin Kontrollü Salımı için pH Duyarlı İnterpenetrasyon Jelatin/Sodyum Aljinat-esaslı Polimerik Kompozitlerin Yapı, Kristalinite ve Termal Özellikleri

Samrin AFZAL¹, Samiullah KHAN^{2*}, Nazar Mohammad RANJHA¹, Aamir JALIL¹, Amina RIAZ¹, Malik Salman HAIDER¹, Shoaib SARWAR¹, Fareha SAHER¹, Fahad NAEEM¹

¹Bahauddin Zakariya University, Faculty of Pharmacy, Multan, Pakistan

²The Islamia University of Bahawalpur, Faculty of Pharmacy and Alternative Medicine, Punjab, Pakistan

ABSTRACT

Objectives: The present work aimed to design and synthesize pH-sensitive cross-linked Ge/SA hydrogels using different ratios of each polymer, and to investigate the effect of each polymer on dynamic, equilibrium swelling, and *in vitro* release pattern of cetirizine hydrochloride, which was selected as a model drug.

Materials and Methods: These gelatin and sodium alginate hydrogels were prepared at room temperature through free radical polymerization using glutaraldehyde as a crosslinker. These polymeric composites were used as model systems to envisage various important characterizations. The *in vitro* release pattern of drug was investigated in three different mediums (phosphate buffer solution of pH 1.2, 5.5, 7.5 whose ionic strength was kept constant). Various structure property relationships that affect its release behavior were determined such as swelling analysis, porosity, sol-gel analysis, average molecular weight between crosslinks (M_c), solvent interaction parameter (χ), volume fraction of polymer (V_{2s}) and diffusion coefficient. The structural, crystallinity, and thermal stability were confirmed using FTIR, XRD, and DSC analysis.

Results: These hydrogels showed maximum swelling at pH 1.2. Zero-order, first-order, Higuchi, and Peppas models were applied to demonstrate the release pattern of drug. The release of drug occurred through non-Fickian diffusion or anomalous mechanism. Porosity was found increased with an increase in concentration of both polymers, and porosity decreased when the concentration of the crosslinker was increased. Gel fraction increased with an increase in concentration of SA, Ge, and glutaraldehyde.

Conclusion: The prepared pH sensitive hydrogels can be used as a potential carrier for the sustained delivery of cetirizine hydrochloride.

Key words: pH responsive, dynamic swelling, cetirizine HCl, *in vitro* release, controlled delivery

ÖZ

Amaç: Bu çalışmada, her bir polimerin farklı oranları kullanılarak pH duyarlı çapraz bağlı jelatin/sodyum aljinat hidrojenlerinin tasarlanması ve sentezlenmesi ve her bir polimerin dinamik, kararlı şişme ve model etken madde olarak seçilen setirizin hidroklorürün *in vitro* salım profiline etkisinin araştırılması amaçlanmıştır.

Gereç ve Yöntemler: Bu jelatin ve sodyum aljinat hidrojenleri, oda sıcaklığında, çapraz bağlayıcı olarak glutaraldehitin kullanımıyla serbest radikal polimerizasyonu ile hazırlandı. Bu polimerik kompozitler, çeşitli önemli karakterizasyonları öngörmek için model sistemler olarak kullanıldı. Etken maddelerin *in vitro* salım modeli üç farklı ortamda (pH 1.2, 5.5, 7.5 iyonik kuvveti sabit tutulan fosfat tampon çözeltisi) araştırıldı. Solunum analizi, gözeneklilik, sol-jel analizi, çapraz bağlar arasındaki ortalama molekül ağırlığı (M_c), çözücü etkileşim parametresi (χ), polimerin hacim fraksiyonu (V_{2s}) ve difüzyon gibi salım davranışını etkileyen çeşitli yapı özellik ilişkileri belirlendi. FTIR, XRD ve DSC analizi kullanılarak yapı, kristalinite ve termal stabilite doğrulandı.

*Correspondence: E-mail: Sami_pharmacist99@hotmail.com, Phone: +923339952522 ORCID-ID: orcid.org/0000-0001-7004-9393

Received: 02.04.2017, Accepted: 20.04.2017

©Turk J Pharm Sci, Published by Galenos Publishing House.

Bulgular: Bu hidrojeller pH 1.2'de maksimum şişme gösterdi. Etken madde salım modelini göstermek için sıfır derece, birinci derece, Higuchi ve Peppas modelleri uygulandı. Etken madde salımı, non-Fick difüzyon veya anomolus mekanizmasıyla gerçekleşti. Her iki polimer konsantrasyonundaki artışla porozitenin arttığı ve çapraz bağlayıcı konsantrasyonu arttıkça gözenekliliğin azaldığı bulundu. Sodyum aljinat, jelatin ve glutaraldehit konsantrasyonunda artış ile jel fraksiyonu artmıştır.

Sonuç: Hazırlanan pH'ya duyarlı hidrojeller, setirizin hidroklorür sürekli salımı için potansiyel bir taşıyıcı olarak kullanılabilir.

Anahtar kelimeler: pH'ya duyarlı, dinamik şişme, setirizin HCl, *in vitro* salım, kontrollü salım

INTRODUCTION

Modern research is oriented towards site-targeted and controlled release of drug. Various peptides and proteins have emerged in response to several advancements in genetics and biotechnology. Proper drug delivery systems for successful treatment are very necessary.¹ Hydrogels have earned much significance in this regard.

Hydrogels are three-dimensional networks that have the ability to absorb a considerable amount of water.² The water-absorbing ability depends upon the nature of the aqueous environment and polymer composition.³ Hydrogels have found extensive applications as drug delivery systems, contact lenses, wound dressings, and artificial lung and joint biomaterials. They are involved in catheterization and endoscopy to reduce surface friction for the comfort of patients.^{4,5} Hydrogels have the ability to protect drugs from aggressive environments e.g., the presence of certain enzymes and low pH of the stomach.

Natural polysaccharides play a vital role in developing solid dose forms for drug delivery.⁶ Natural polymers are generally cheap and have attracted the attention of researchers to prepare natural polymer-based hydrogels.⁷ In the present study, gelatin and sodium alginate (SA) were used to prepare hydrogels. Both of these natural polymers are biodegradable and are employed for sustained release of drug because they are degraded within the human body.⁸

Gelatin is a product of protein prepared by hydrolyzing collagen (skin and connective tissues).⁹ Amino acids including proline, glycine and hydroxy-proline are present in higher amounts in gelatin and others to a lesser extent include aspartic acid, alanine, arginine and glutamic acid.¹⁰ Gelatin contains (-NH₂) and (-COOH) as ionizing groups that swell at both lower and higher pH, and this property makes it the best option to develop hydrogels for sustained drug delivery. The formation of thermo-reversible gels (100%) is also one of the properties of gelatin and it can be seen when gelatin is cooled below 35°C. Gels formed by gelatin are mostly stronger because of the presence of increased concentration of pyrrolidines. In order to form a gel, gelatin has the capacity to absorb ten times its weight of water. Gelatin is insoluble in organic solvents (alcohol, CCl₄, ether and benzene). Gelatin can be used as a binding agent, a thickening agent, and an encapsulating agent.

SA belongs to a group of agents that were studied extensively and these agents were made of stiff linear polysaccharides. SA belongs to the most commonly used gel-forming agent obtained from seaweed. They contain residues of β-1, 4-linked D-mannuronic acid and α-1, 4-linked L-glucuronic acid. They also have free -OH and -COOH groups for chemical modification.

It can be used in the preparation of wound dressings because they have the ability to form a gel when in contact with moisture due to the formation of a strong hydrophilic gel.¹¹ Hence, it is nontoxic, biocompatible, and non-carcinogenic.^{12,13} These are the polysaccharides that can be used as chelators, emulsifiers, and suspending agents, and can also be used to prepare membranes.^{14,15}

Aldehydes with lower molecular weight such as formaldehyde and glutaraldehyde (GA) are used to harden gelatin¹⁶ and crosslinking occurs through formation of Schiff bases. These bases are formed when (-NH₂) free groups in gelatin react with glutaraldehyde.¹⁷ Swelling of hydrogels is greatly affected by the concentration of the crosslinker. Hydrogels with a higher degree of crosslinking swell less than those with a lower quantity of crosslinker.

Cetirizine dihydrochloride (CTZ HCl) is a potent second-generation histamine H₁ antagonist that is effective in the treatment of allergic rhinitis, chronic urticaria, and pollen-induced asthma. It is rapidly absorbed from the GI tract following oral administration with peak plasma concentrations achieved in about 1 hour. Unlike first-generation histamine H₁ antagonists, cetirizine is less able to cross the blood-brain barrier and induce drowsiness. However, some serious adverse effects such as somnolence, fatigue, dry mouth, and insomnia have been reported with CTZ HCl. Therefore, in order to control the toxicity associated with this drug, the delivery system needs to be modified. Figure 1 indicates the chemical structure of CTZ HCl.

The main objective of the current study was to prepare pH-sensitive Ge/SA hydrogels for sustained delivery of an antihistaminic drug (CTZ HCl) to the gastrointestinal tract. By developing these stimuli-responsive polymeric hydrogel systems, the main idea was to provide controlled delivery and metabolism of the drug, and in turn, to reduce the adverse effects associated with this drug. The hydrogel samples were developed to achieve the following objectives: 1) To synthesize different hydrogel samples with different feed composition ratios and degree of crosslinking; 2) To investigate the effect of composition and crosslinking ratio on dynamic and equilibrium swelling behavior in phosphate buffer solutions of variable pH values; 3) To investigate the effect of pH and composition on release of model drug in phosphate buffer solutions of variable pH values and to confirm the controlled delivery of model drug (CTZ HCl); 4) To evaluate sol-gel fraction analysis, porosity measurement, networking parameters, and the diffusion coefficient; 5) To evaluate the best release mechanism by applying various mathematical release models; 6) To confirm the

network structure of the hydrogels by various characterization tools such as Fourier transform infrared (FTIR) spectroscopy, X-ray diffraction (XRD), and differential scanning calorimetric (DSC) were used to investigate the stability of the hydrogel samples.

MATERIALS AND METHODS

Materials

Gelatin type B from bovine skin (Ge) ($M_w \sim 402.47 \text{ gmol}^{-1}$) (purity 98%) (Merck, Germany) and sodium alginate (Merck, Germany) were used as polymers. GA was obtained from Merck-Schuchardt. Acetic acid (AA), which was used as catalyst, was obtained from Merck-Schuchardt. Cetirizine HCl was gifted by Hamaz Pharma, Multan, Pakistan. Potassium bromide (KBr) of FTIR grade was purchased from Fisher Scientific (UK). Potassium dihydrogen phosphate, sodium hydroxide, and sodium chloride were used as received. All chemicals used were of analytical grade. Double-distilled water was used for the preparation of the hydrogels and buffer solutions.

Synthesis of pH-sensitive gelatin/sodium alginate (Ge/SA) hydrogels

Ge/SA hydrogels crosslinked with GA was prepared at room temperature using free radical polymerization as reported earlier with minor modifications.¹⁸ Briefly, both polymers were taken in different concentrations. SA solution was made by adding the desired quantity of SA in bidistilled water at 60°C for 1 hr. The SA solution was then cooled down. An aqueous solution of gelatin was made with the addition of a weighed quantity of gelatin in a 3% solution of AA at a temperature of 40°C. The gelatin solution was placed at room temperature and then added to the SA solution and stirred for 45 min. Varying quantities of GA were added to this homogeneous mixture. Double-distilled

water was added to make the final weight up to 50 grams. The final homogeneous mixture was poured into 16-mm internal diameter test tubes (Pyrex) with 150 mm length. The oxygen was removed from the glass tubes by nitrogen bubbling for 15 to 20 min. Oxygen can hinder the normal polymerization process. The tubes were capped and placed at room temperature for 72 hours. After complete polymerization and gel formation, hydrogel in cylindrical form was removed from tubes after 72 hours. Each cylinder was cut into 5-mm length discs. These discs were dried at room temperature. After drying these discs, they were extensively washed with ethanol-water mixture (40:60) for complete removal of unreacted material. Throughout this time span, the ethanol/water mixture was replaced every day until its pH became equal to the pH of the water/ethanol mixture. Finally, the synthesized Ge/SA discs were placed first at room temperature and afterwards in an oven under vacuum at 45°C until solid, reaching a stable mass. These gelatin and SA hydrogels were stored in a vacuum desiccator for future use.¹⁸ The various formulations of SA/Ge hydrogels are given in Table 1. Figure 2 indicates the presumptive structure of Ge/SA hydrogels.

Swelling behavior of synthesized hydrogels

Preparation of buffer solutions

Phosphate buffer solutions of (pH 1.2, 5.5, 6.5, and 7.5) were prepared using potassium dihydrogen phosphate (KH_2PO_4). The buffering agent concentration was 0.05 M. A 0.2 M solution of HCL and NaOH was used to adjust the pH of these solutions. In order to maintain the ionic strength of these buffer solutions to $I=0.65 \text{ M}$, NaCl was added.

Dynamic swelling studies

The swelling analysis was preceded in 100 mL USP PBS of pH 1.2, 5.5, 6.5, and 7.5. Pre-weighed dried hydrogel discs were allowed to swell in different pH solutions (1.2, 5.5, 6.5, and 7.5) at room temperature i.e. 25-30°C. The swollen discs were removed from the desired pH solutions at predetermined regular time intervals. The discs were first blotted with filter paper to

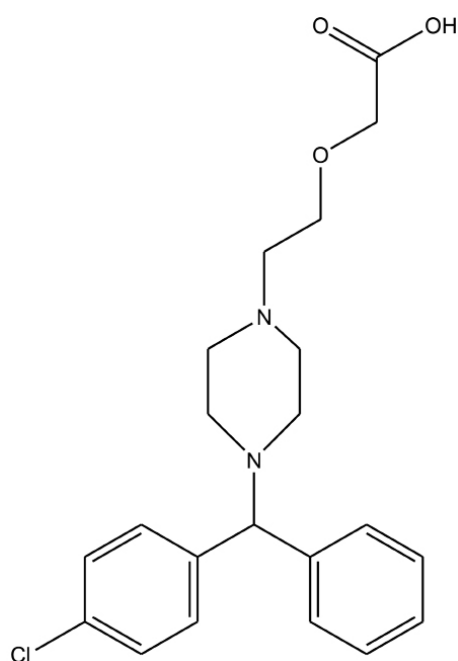


Figure 1. Structure of cetirizine hydrochloride

Table 1. Feed composition of various formulations of Ge/SA hydrogels

Sample codes	Gelatin (g)/100 g solution	SA (g)/100 g solution	Ge: SA	GA (g)/100 g solution
S1	10.5	1.0	91.30/8.70	0.345
S2	10.5	1.5	87.5/12.5	0.360
S3	10.5	2	84/16	0.375
S4	10	2	83.33/16.67	0.360
S5	11	2	84.61/15.39	0.390
S6	12	2	85.71/14.29	0.42
S7	11	2	84.61/15.39	0.455
S8	11	2	84.61/15.39	0.487
S9	11	2	84.61/15.39	0.52

Ge/SA: Gelatin/sodium alginate

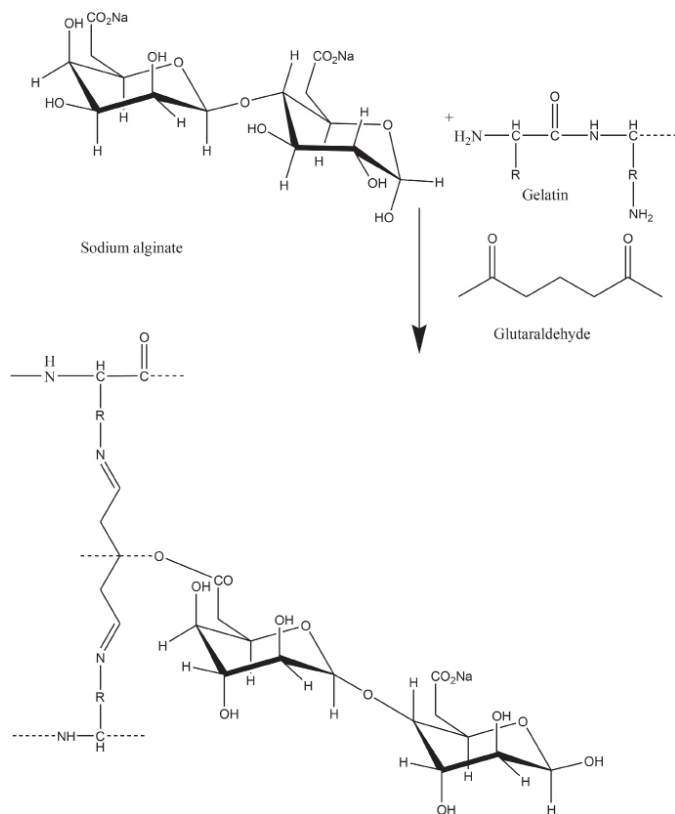


Figure 2. Proposed structure of Ge/SA hydrogel cross-linked with glutaraldehyde

remove excess solution and then weighed and positioned in the same bath solution. These studies were performed for about 8 hours. The underlying relation denoted by (1) was used to determine the swelling ratio of the synthesized disc.^{18,19}

$$q = \frac{W_t - W_d}{W_d} \quad (1)$$

Where W_t =mass of swollen gel at time t . W_d =original mass of dried hydrogel and q =the swelling coefficient.

Equilibrium swelling studies

Equilibrium swelling studies were conducted by allowing the hydrogel discs to swell till they attained a constant weight and reached a state of equilibrium. The discs at higher pH absorbed much more water and became fragile and had to be handled carefully to avoid breakage.

The following equation provided the means to determine Q_{eq} .¹⁹

$$S_{(Eq)} = \frac{W_h}{W_d} \quad (2)$$

W_h represents the mass of swollen gel at equilibrium, and W_d stands for original mass of dried hydrogel.

Diffusion coefficient

Diffusion coefficient (DC) represents the quantity of substance diffusing across a unit area through a concentration gradient in unit time. DC is dependent on the amount and nature of chemicals in the polymer. The following equation was used for the determination of DC:²⁰

$$D = \pi \left(\frac{h \cdot \theta}{4 \cdot q_{eq}} \right)^2 \quad (3)$$

Where q_{eq} = swelling of gel at E_q , θ = slope of the linear part of the swelling curves, h =original thickness of gel before swelling and DC represents diffusion coefficient of the hydrogels.

Physicochemical characterization of Ge/SA hydrogels

For the evaluation of the structure and properties of the hydrogel, we performed the following characterizations:

Volume fraction of the polymer

Polymer volume fraction is the quantity of fluid absorbed and retained by the gel in its swollen state.^{21,22} The following equation was used to determine the volume fraction of the polymer:

$$V_{2s} = \left[1 + \frac{d_p}{d_s} \left(\frac{M_a}{M_b} - 1 \right) \right]^{-1} \quad (4)$$

Where, polymer density (gm/mL) is denoted with d_p and solvent density is denoted by d_s . M_a and M_b are the masses taken in (g) of the swollen and dry hydrogels respectively. (V_{2s}) units are mL/mol.

Determination of solvent interaction parameter (χ)

The solvent interaction parameter χ was calculated by using the Flory–Huggins theory.^{23,24} These parameters were used to determine whether the polymers were compatible with the molecules of the surrounding fluid. According to this theory, the following equation (5) was used to determine χ :

$$\chi = \frac{\ln(1 - V_{2s}) + V_{2s}}{V_{2s}^2} \quad (5)$$

V_{2s} =the volume fraction of swollen hydrogel in its equilibrium state.

Molecular weight between the crosslinks

The Flory–Rehner theory was used to analyze this parameter. It can be predicted for Ge/SA hydrogels by knowing the molecular weight between the crosslinks. It suggested that M_c values were amplified by increasing the swelling ratios of Ge/SA gels. The following relation was used to determine M_c .^{24,25}

$$M_c = \frac{d_p V_s (V_{2s}^{1/3} - V_{2s} / 2)}{\ln(1 - V_{2s}) + V_{2s} + \chi V_{2s}^2} \quad (6)$$

Where, ρ_p denoted the density of the polymer and ρ_s represents the density of the solvent. $V_{2,s}$ =the volume fraction of the swollen gel and χ =Flory–Huggins parameters.

Cross-linked density (N)

This is defined as the number of links between two cross-linked chains. In order to measure N, the following equation was used:²⁶

$$N = \frac{2M_c}{M_r} \quad (7)$$

M_r =Molecular weight of the repeating unit and was determined using the following equation:

$$M_r = \frac{m_{SA}M_{SA} + m_{Ge}M_{Ge} + m_{GA}M_{GA}}{m_{SA} + m_{Ge} + m_{GA}} \quad (8)$$

Here, m_{SA} , m_{Ge} , m_{GA} are the feed masses of SA, gelatin, and GA, respectively. M_{SA} , M_{Ge} , and M_{GA} are the molar masses of SA, gelatin and GA.

Sol-gel analysis

The uncrosslinked polymer from the gel structure was determined using sol-gel analysis. For this purpose, unwashed samples were cut into 3-4 mm discs. The prepared sample discs were placed at room temperature for complete drying and afterwards in a vacuum oven at 45°C to an invariable weight. The weighed discs were placed for Soxhelt extraction at 85°C minimum for up to 4 hours. This process of extraction removes the uncrosslinked polymer from the hydrogel. The extracted hydrogels were placed in the oven at 45°C for drying until a constant weight was achieved. The gel fraction was measured by taking into consideration the initial dry weight (W_0) and extracted dry gel (W_1) weight using the following equation.^{20,26}

$$\text{Sol fraction (\%)} = \left[\frac{W_0 - W_1}{W_0} \right] \times 100 \quad (9)$$

$$\text{Gel fraction (\%)} = (100 - \text{Sol fraction}) \quad (10)$$

Measurement of porosity

This is the measure of the presence of voids over the total volume of hydrogels between 0-1 and in the form of percentage as 0-100%. The dried gelatin/SA hydrogels were submerged in absolute ethanol for one night and excess ethanol was blotted using filter paper. The blotted hydrogels were then weighed and porosity was determined using the following equation:

$$\text{Porosity} = \frac{(M_2 - M_1)}{\rho V} \times 100 \quad (11)$$

Here, M_1 =weight of the hydrogel before placing in absolute ethanol, M_2 =weight obtained after immersion in ethanol. ρ stands for density of absolute ethanol. V =the volume of hydrogel.²⁰

Preparation of drug-loaded hydrogels

Loading and release studies of CTZ HCl were performed on Ge/SA hydrogel samples that had maximum swelling. The discs were loaded with drug by dipping them in a 1% w/v aqueous solution of CTZ HCl. The desired solution of CTZ HCl was made by dissolving the drug in water. The discs were allowed to remain in the CTZ HCl solution till equilibrium swelling was achieved. The swollen hydrogels were removed and first dried by placing them at room temperature, followed by oven drying at 46°C to a consistent weight.¹⁸

Measuring cetirizine hydrochloride loading

Three methods were used to measure the amount of CTZ HCl loaded in the Ge/SA hydrogels.²⁰ The equation used to determine the amount of cetirizine loaded by weight method is shown below:

$$\text{Amount of drug} = W_D - W_d \quad (12)$$

$$\text{Drug Loading\%} = \frac{W_D - W_d}{W_d} \times 100 \quad (13)$$

In this equation, W_d =weight of dry hydrogels before the loading of drug and W_D is the weight of drug-loaded dried gels.

In the swelling method, the weighed hydrogel disc was placed in CTZ HCl solution until reaching equilibrium swelling. The hydrogels loaded with drug were removed and weighed once more after removing excess fluid with blotting paper to determine the amount of absorbed drug solution. The difference in weight of the gels gave the volume of cetirizine hydrochloride loaded or entrapped in the Ge/SA hydrogels. The amount of CTZ HCl was calculated from the volume.

In the extraction method, the drug was determined by repeatedly extracting the weighed amount of loaded gels in the presence of distilled water. In each turn, 25 mL of new distilled water was added until there was no drug left in the solution. The quantity of CTZ HCl was measured using a spectrophotometer. Quantities of drug present in all parts of the extract were added and this provided the means to measure the total drug loaded.

Release studies of Cetirizine hydrochloride

An *in vitro* dissolution test was used to determine the release of CTZ HCl freely soluble in water, which involved the use of dissolution apparatus 2 in association with UV-spectrophotometer (IRMECO, UV-Vis U2020). The pulsatile drug release profile of drug at equal intervals of time was obtained in the dissolution medium, which comprised various pH values (1.2, 5.5, and 7.5). The weighed Ge/SA gel discs were placed in 900 mL dissolution medium at 37±2°C. The prepared medium was kept stirring at 100 rpm to evenly distribute the released drug in the medium. The CTZ HCl release study was conducted at 229 nm for up to 12 hours. Each time, 5 mL of dissolution medium was taken for UV analysis to verify the concentration of drug. The withdrawn solution was replaced with the same amount of new 0.05 M PBS.¹⁸

Analyzing the pattern of drug release

In order to evaluate the drug release data zero order, first order, the Higuchi and Korsmeyer–Peppas models were employed. To achieve controlled release of drug, it is necessary that the drug diffuses faster than the swelling of the gel. The equations employed for the above-mentioned models are:

$$\text{Zero-order kinetics: }^{27} F_t = K_0 t \quad (14)$$

F_t is the fraction of release of drug in time t and K_0 is the zero-order release constant.

$$\text{First-order kinetics: }^{27} \ln(1-F) = -K_1 t \quad (15)$$

F represents the fraction of drug release in time t and K_1 is the first-order release constant.

$$\text{Higuchi model: } F = K_2 t^{1/2} \quad (16)$$

F represents fraction of drug release in time t and K_2 is the Higuchi constant.

$$\text{Korsmeyer–Peppas model: } M_t/M_\infty = K_3 t^n \quad (17)$$

M_t is the mass of water absorbed at time t , M_∞ is the quantity of water at equilibrium, K_3 describes the swelling mechanism^{28,29}, and n is the release exponent.

Characterization of Ge/SA hydrogels

Differential scanning calorimetry

Differential scanning calorimetry was performed in the DSC unit (Netzsch DSC 200 PC Phox, Germany). The samples were heated in a closed aluminum pan at a temperature of 40°C/min. Nitrogen was used as a purge gas with a flow rate of 50 mL/min.²⁰

X-ray diffraction analysis

XRD for drug loaded and unloaded hydrogel was performed using Bruker D8 Discover (Germany) apparatus. Measurement conditions included target (CuK α), voltage (35 KV), and current (35 mA). A system of diverging, receiving, and anti-scattering slits of 1°, 1°, 1°, and 0.15°, respectively, was used. The percentage crystallinity was determined using the equation below:²⁰

$$\% \text{ Crystallinity} = \text{Crystalline area} / \text{Total area} \times 100 \quad (18)$$

Fourier transformed infra-red (FTIR) spectroscopic analysis

Cross-linked hydrogel samples were crushed with pestle in an agate mortar. The crushed material was mixed with KBr (Merck IR spectroscopy grade) in 1:100 proportions and dried at 40°C. The mixture was compressed to a 12-mm semi-transparent disk by applying a pressure of 65 kN (pressure gauge, Shimadzu) for 2 min. The FTIR spectra over the wavelength range 4500–400 cm⁻¹ were recorded using an FTIR spectrometer (FT-IR 8400 S, Shimadzu).¹⁸

Statistical analysis

For the statistical analysis of data, Student's t-test was used to compare the results and to determine the statistical significant/non-significant interpretation at 95% confidence interval; p values less than 0.05 were considered as significantly different. Data are presented as mean \pm standard deviation (SD).

RESULTS AND DISCUSSION

Effect of pH on swelling and drug release of Ge/SA hydrogels

Prepared hydrogels containing SA and Ge were used to investigate the pH responsive behavior in phosphate buffer solutions of various pH values. The hydrogels were sensitive to pH; their swelling was dependent on pK_a and pH of the swelling medium. The prepared hydrogels contained both NH₂ (amine) and -COOH (carboxylic group), known as polyampholytic gels. These hydrogels showed the maximum swelling in pH 1.2 solution and the second highest swelling in pH buffer 7.5. Swelling of hydrogels was maximal at pH 1.2 because of protonation of -NH₂ groups and then these amine groups were ionized. Electrostatic repulsion of similar charges was the main cause of swelling in the hydrogels.³⁰ At pH 7.5, (-COOH) groups present in both SA and Ge were changed to (COO⁻) groups, resulting in anion-anion repulsion that eventually increased the swelling of the hydrogels. The results of swelling studies (dynamic and equilibrium swelling) are shown in Table 2, which showed that the swelling of the hydrogels were decreased

Table 2. Dynamic and equilibrium swelling values of Ge/SA hydrogels using GA as a crosslinker

Sample code	Dynamic swelling coefficient				Equilibrium swelling coefficient			
	pH 1.2	pH 5.5	pH 6.5	pH 7.5	pH 1.2	pH 5.5	pH 6.5	pH 7.5
S ₁	4.298	3.515	3.45	3.78	10.64	4.33	x	x
S ₂	4.26	3.373	3.346	3.75	9.9	4.31	x	x
S ₃	4.129	3.305	3.32	3.704	9.6	3.915	x	x
S ₄	4.411	3.62	3.73	3.803	10.70	4.93	x	x
S ₅	4.379	3.65	3.74	3.918	11.15	4.99	x	x
S ₆	4.59	3.68	3.79	3.928	12.98	5.11	x	x
S ₇	4.31	3.54	3.63	3.64	11.00	5.00	x	x
S ₈	4.29	3.53	3.63	3.603	10.52	4.805	x	x
S ₉	3.8	3.5	3.511	3.56	9.70	3.915	5.8	x

x: Sample broken, Ge/SA: Gelatin/sodium alginate, GA: Glutaraldehyde

when the pK_a value of the swelling medium was less than that of the polymer. These synthesized SA/Ge hydrogels can swell at both acidic and basic pHs. Therefore, they can be used for the sustained delivery of drug.

For loading of CTZ HCl, hydrogel samples were selected that showed maximum swelling. CTZ HCl was selected as a model drug because of its solubility in water. Hydrogel samples prepared with different degrees of crosslinking agents (S_7 - S_9) and with increased quantities of gelatin (S_4 - S_7) were selected for the loading of drug. Table 3 shows the amount of loaded drug in the selected samples.

In order to determine the effect of pH on CTZ HCl release, the loaded hydrogel samples were immersed in solutions of pH 1.2, 5.5, and 7.5. A dissolution apparatus was used to determine the release of drug. The maximum amount of drug was released when the hydrogels were immersed in a pH 1.2 solution and the second highest release of drug was observed at pH 7.5; the minimum amount of drug was released in a pH 5.5 solution. Table 4 refers to the effect of pH of the dissolution medium on percentage drug release of Ge/SA hydrogels.

Effect of Ge concentration on swelling and drug release from Ge/SA hydrogels

Gelatin is a natural polymer and its concentration was changed in different hydrogel samples, ranging from 10, 11, and 12 g/100 g in Ge/SA hydrogels with GA as a crosslinker. Three samples with different concentrations of Ge (S_4 to S_6) were synthesized and used to analyze the effect of gelatin on dynamic and equilibrium swelling and on the release of CTZ HCl from the hydrogels. It was observed that with an increase in gelatin content, an increase in drug release and swelling occurred. This increase is suggested to be due to the presence of ionizable (NH_2) and ($COOH^-$) groups, which increase the spaces between the polymer chains, and swelling of hydrogels was increased due to hydrostatic repulsion.³¹ Figure 3 indicates the effect of different concentrations of Ge on dynamic swelling coefficient of Ge/SA hydrogels in PBS of various pH values. The quantity of drug release from these hydrogels was observed via dissolution. When the quantity of gelatin was increased, an increase in drug release was observed. The drug release increased from 78.15% to 81.28% in pH 1.2, 49.86% to 52.31% in

Table 3. Amount of cetirizine hydrochloride loaded in formulations of Ge/SA hydrogels

Sample codes	Amount of CTZ HCl loaded (g/g of dry gel)	
	By swelling	By extraction
S_4	0.078	0.0715
S_5	0.082	0.0798
S_6	0.083	0.0802
S_7	0.078	0.0750
S_8	0.073	0.0699
S_9	0.06225	0.0604

Ge/SA: Gelatin/sodium alginate, CTZ HCl: Cetirizine dihydrochloride

pH 5.5, and 66.72% to 70.21% in pH 7.5. Figure 4-6 indicates the effect of different concentrations of Ge on the *in vitro* release of CTZ HCl as a function of time from Ge/SA hydrogels in PBS of various pH values.

Sodium alginate effect on swelling and on drug release from Ge/SA hydrogels

The concentrations of SA used in the preparation of hydrogels were 1, 1.5, and 2 g/100 g of the sample solution (S_1 to S_3) with a constant amount of gelatin and GA. A decrease in swelling was observed with an increase in the SA content. This decrease was due to the presence of pores in the matrix of the SA, which hindered the diffusion of water into SA/Ge hydrogels. Bajpai et al.³², also experienced a similar pattern for hydrogels prepared with SA. Figure 7 refers to the impact of SA on the dynamic swelling coefficient of Ge/SA hydrogels in PBS of variable pH values.

Effect of crosslinker quantity on swelling behavior and drug release from Ge/SA hydrogels

The extent of crosslinking was a major factor that affected the swelling and CTZ HCl release properties of hydrogels. To highlight this factor, hydrogels prepared with different

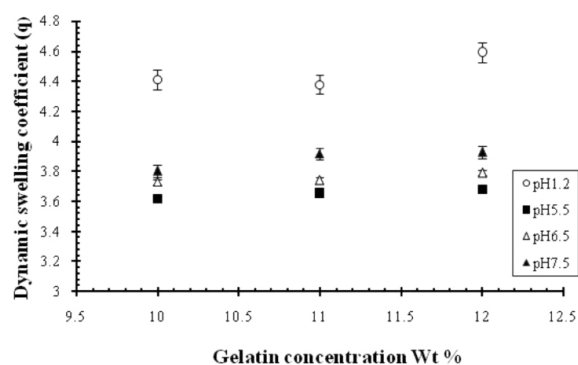


Figure 3. Dynamic swelling behavior of SA/Ge hydrogels with different concentrations of Ge (S_4 - S_6), keeping the concentration of SA and GA constant in solutions of various pHs (1.2, 5.5, 6.5, and 7.5)

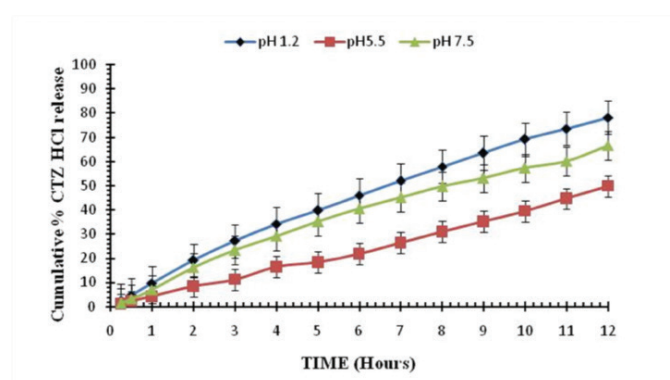


Figure 4. Pulsatile cumulative percentage drug release of CTZ HCl from Ge/SA hydrogels (10/2 g) in phosphate buffer solutions of various pH values. Each point represents the mean \pm standard deviation of $n=3$ experiments

CTZ HCl: Cetirizine dihydrochloride

concentrations (S_7 to S_9) of GA (3.5%, 3.75%, and 4%) while keeping the quantity of both the polymers constant (SA/Ge = 2/11g). When increased quantities of crosslinker was used, dense networks were produced with shrunken mesh size and a tighter structure. This resulted in minimal spaces for the entrance and accommodation of water and swelling decreased.³³ Figure 8 refers to the effect of GA on the dynamic swelling coefficient of Ge/SA hydrogels in PBS of variable pH values. Drug release from hydrogels is dependent on swelling and samples with the minimum amount of crosslinker showed maximum swelling and drug release. When the quantity of crosslinker was increased, the drug release was decreased from 85.56% to 80.06% in pH 1.2, 51.02% to 48.96% in 5.5, and 72.86% to 69.01% in pH 7.5, respectively. Figures 9-11 indicate the effect of different concentrations of GA on the *in vitro* release of CTZ HCl as a function of time from Ge/SA hydrogels in PBS of various pH values.

Molecular weight between crosslinks (M_c) and solvent interaction parameters

The concentration of gelatin has a direct relation with M_c values. An increase in gelatin concentration enhanced the M_c values. Higher swelling is due to the presence of (-COOH) and (-NH₂) groups in Ge. X and $V_{2,5}$ values increased by increasing the concentration of SA and crosslinker and decreased with an increase in the concentration of gelatin. The M_c value has a direct relation with gelatin concentration and is inversely proportional to the SA and GA concentration. The values of the structural parameters are elaborated in Table 5.

Diffusion coefficient of polymers (D)

The diffusion coefficient is an indirect method to determine the amount of solute diffused in the polymer network of the hydrogel. It can be better measured using Fick's law of diffusion. The diffusion coefficient was found to be decreased when increased concentrations of SA and GA were used. The diffusion coefficient increased with increasing concentrations of gelatin because swelling increases with increased concentrations of gelatin. Table 5 indicates the values of D .

Sol-gel analysis

Sol-gel analysis was performed to determine the uncrosslinked polymer concentration in the hydrogel. Different compositions of SA/Ge were used to determine the effect of polymers and

Table 4. Cetirizine hydrochloride released (%) from various formulations of Ge/SA hydrogels

Sample Codes	pH 1.2	pH 5.5	pH 7.5
S_4	78.15	49.86	66.72
S_5	79.52	50.21	67.87
S_6	81.28	52.31	70.21
S_7	85.56	51.02	72.86
S_8	83.85	49.53	70.99
S_9	80.06	48.96	69.01

Ge/SA: Gelatin/sodium alginate

degree of crosslinking on the gel fraction of the hydrogels. The gel fraction increased with an increase in concentrations of SA, Ge, and GA, and the sol fraction was decreased. This mechanism was observed due to enhanced grafting, and

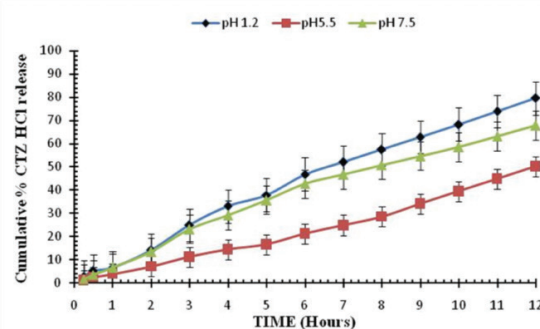


Figure 5. Pulsatile cumulative drug release of CTZ HCl from Ge/SA hydrogels (11/2 g) in phosphate buffer solutions of various pH values. Each point represents the mean \pm standard deviation of n=3 experiments

CTZ HCl: Cetirizine dihydrochloride, Ge/SA: Gelatin/sodium alginate

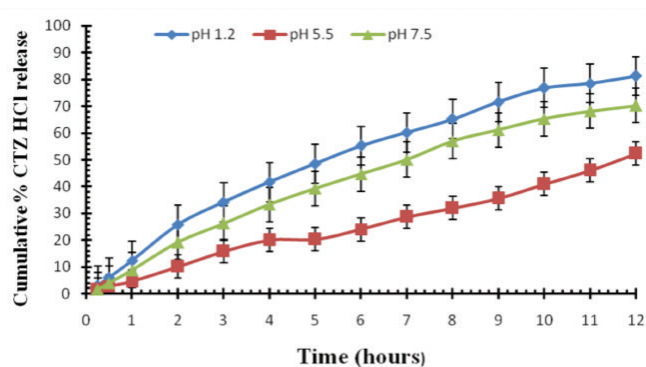


Figure 6. Pulsatile cumulative percentage drug release of CTZ HCl from Ge/SA hydrogels (12/2 g) in phosphate buffer solutions of various pH values. Each point represents the mean \pm standard deviation of n=3 experiments

CTZ HCl: Cetirizine dihydrochloride, Ge/SA: Gelatin/sodium alginate

Table 5. Flory-huggins network parameters of Ge/SA hydrogel

Sample codes	Amount of GA %	Gel fraction %	Sol fraction (%)	Porosity %
S_1	3.00	81.64	18.36	10.21
S_2	3.00	82.50	17.50	12.01
S_3	3.00	83.23	16.77	13.65
S_4	3.00	87.10	12.90	14.66
S_5	3.00	89.90	10.10	21.45
S_6	3.00	91.81	8.91	28.25
S_7	3.50	89.96	10.04	24.66
S_8	3.75	91.12	8.88	20.10
S_9	4.00	93.30	6.70	10.54

Ge/SA: Gelatin/sodium alginate, GA: Glutaraldehyde

increased concentrations of polymers (SA and Ge) and crosslinker resulted in extensive crosslinking; this mechanism was not observed with lower concentrations of these agents. Similar findings were reported by Ranjha and Mudassir²⁷, who prepared hydrogels composed of chitosan and acrylic acid. Natural polymers showed an increase in gel fraction at higher concentrations. Table 6 indicates the gel fraction (%) of Ge/SA hydrogels.

Porosity

It was analyzed that by increasing the concentration of SA and gelatin in the hydrogel, the porosity increased. Porosity increases because both SA and Ge increase the viscosity of the resulting solution. Viscous solutions have the capability to prevent the escape of bubbles from the solution. Viscous solutions also limit the movement of free radicals and result in impaired polymerization, and as a result, porosity increases.

By increasing the concentration of GA, porosity decreases. Increased crosslinker concentration causes the shrinkage in mesh size of the resulting gels, lesser pores are formed, and eventually porosity decreases. Figures 12-14 indicate the effect of variables on porosity percentage of Ge/SA hydrogels. Ranjha and Mudassir²⁷ used chitosan to prepare hydrogels and

their results showed that chitosan formed a viscous solution that entrapped the bubbles, which lead to voids in the hydrogel matrix. Table 6 indicates the porosity (%) of Ge/SA hydrogels.

Cetirizine hydrochloride release mechanism

When hydrogels are immersed in water, they swell due to diffusion of water molecules in the polymeric network. This swelling of hydrogels leads to the release of drug, which in this case was CTZ HCl. The most appropriate method to determine best model for drug is based on values of the regression coefficient denoted by r . The model should have an r value close to one.

Regression coefficient values (r) with different concentrations of Ge and GA are given in Tables 7 and 8. The r values of the Higuchi model at various Ge and GA concentrations showed greatest linearity and the CTZ HCl release mechanism was found to be diffusion controlled.

The effect of varying amounts of Ge and GA on the release exponent (n) at different pH solutions is shown in Tables 9 and 10. All the values lie between 0.5-1.0 and no n value is above or below this range, which shows non-fickian behavior at various pHs (1.2, 5.5, and 7.5). This means that CTZ HCl release from

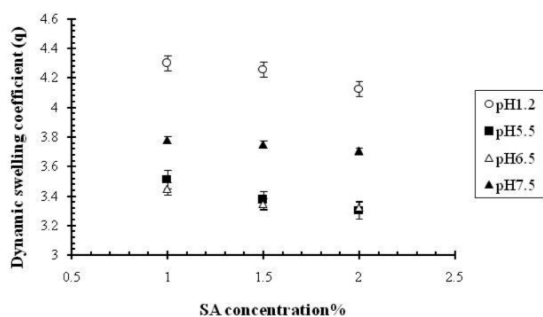


Figure 7. Dynamic swelling behavior of SA/Ge hydrogels with different concentrations of SA (S_1 - S_3), keeping concentrations of Ge and GA constant in various pH solutions (1.2, 5.5, 6.5, and 7.5)

SA: Sodium alginate

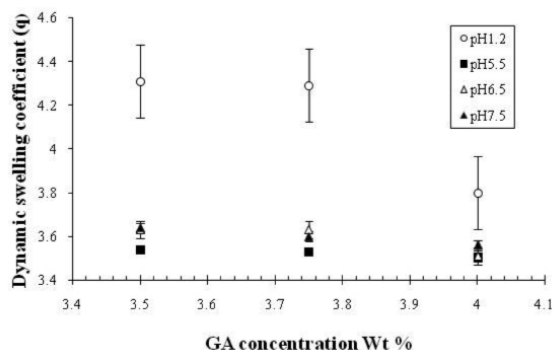


Figure 8. Dynamic swelling behavior of SA/Ge hydrogels with different concentrations of GA (S_7 - S_9), keeping SA and Ge constant at solutions of various pH (1.2, 5.5, 6.5, and 7.5)

GA: Glutaraldehyde

Table 6. Gel fraction and porosity percentage of various formulations of Ge/SA hydrogels

Sample codes	$V_{2,s}$	χ	M_c	M_r	q	$D \times 10^{-5} \text{ (cm}^2 \text{ sec}^{-1}\text{)}$
S_1	0.01237	-0.5021	379.0811	327.0548	10.64	0.017051
S_2	0.01461	-0.5065	268.6011	323.353	9.9	0.015598
S_3	0.01627	-0.5069	208.9656	319.89	9.6	0.04494
S_4	0.01789	-0.5077	182.6242	317.1373	10.7	0.031071
S_5	0.01280	-0.5062	210.5662	322.4706	11.15	0.037747
S_6	0.00811	-0.5060	280.9112	327.1765	12.98	0.038721
S_7	0.01307	-0.5225	502.5351	315.7327	11	0.52161
S_8	0.01330	-0.5341	422.0532	312.5146	10.52	0.045609
S_9	0.01401	-0.5347	371.2564	309.3912	9.7	0.032161

Ge/SA: Gelatin/sodium alginate

Table 7. Effect of various concentrations of Ge on drug release kinetics of Ge/SA hydrogel in varying pH solutions using GA as a crosslinker

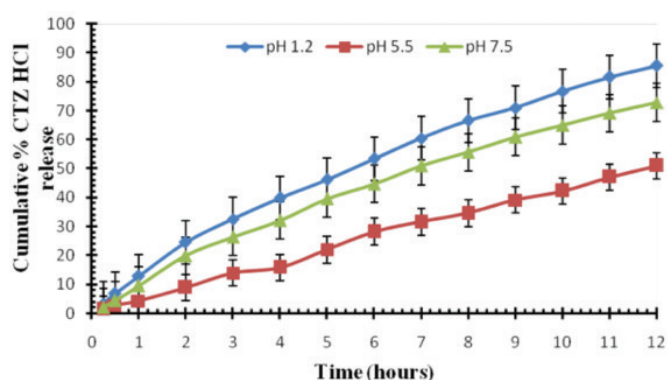
Sample codes	Ge contents	pH	Zero-order kinetics		First-order kinetics		Higuchi model	
			K_0 (h ⁻¹)	R ²	K_1 (h ⁻¹)	R ²	K_2 (h ⁻¹)	R ²
S ₄	10	1.2	6.324	0.990	0.122	0.991	0.270	0.998
		5.5	4.024	0.997	0.054	0.981	0.167	0.954
		7.5	5.426	0.989	0.089	0.998	0.233	0.999
S ₅	11	1.2	6.658	0.992	0.128	0.988	0.283	0.990
		5.5	4.014	0.993	0.054	0.969	0.165	0.930
		7.5	5.692	0.986	0.094	0.998	0.244	0.996
S ₆	12	1.2	6.500	0.968	0.14	0.998	0.282	0.999
		5.5	4.053	0.991	0.056	0.974	0.170	0.959
		7.5	5.821	0.983	0.103	0.998	0.251	0.998

Ge/SA: Gelatin/sodium alginate, GA: Glutaraldehyde

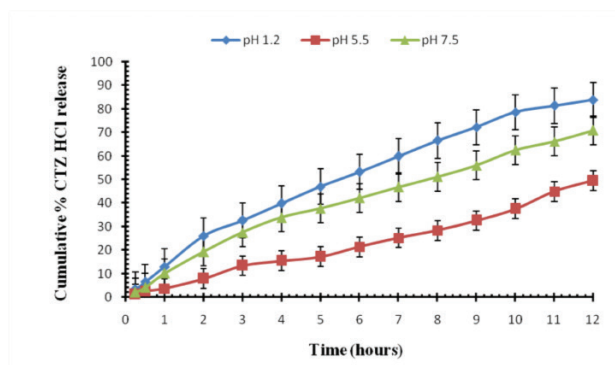
Table 8. Effect of various quantities of GA on drug release kinetics of Ge/SA hydrogel in solution of various pH values

Samples no	GA contents	pH	Zero-order kinetics		First-order kinetics		Higuchi model	
			K_0 (h ⁻¹)	R ²	K_1 (h ⁻¹)	R ²	K_2 (h ⁻¹)	R ²
S ₇	3.5%	1.2	6.754	0.988	0.153	0.990	0.290	0.999
		5.5	4.262	0.999	0.058	0.994	0.179	0.972
		7.5	5.853	0.988	0.106	0.998	0.251	0.999
S ₈	3.75%	1.2	6.695	0.981	0.150	0.992	0.288	0.998
		5.5	3.860	0.990	0.052	0.968	0.160	0.942
		7.5	5.502	0.984	0.097	0.995	0.236	0.997
S ₉	4%	1.2	6.212	0.996	0.127	0.992	0.265	0.993
		5.5	3.877	0.989	0.054	0.999	0.166	0.997
		7.5	5.508	0.991	0.095	0.998	0.235	0.997

Ge/SA: Gelatin/sodium alginate, GA: Glutaraldehyde

**Figure 9.** Pulsatile cumulative percentage drug release of CTZ HCl from Ge/SA hydrogels (11/2 g) using 3.5% GA in phosphate buffer solutions of various pH values. Each point represents the mean \pm standard deviation of n=3 experiments

CTZ HCl: Cetzirizine dihydrochloride

**Figure 10.** Pulsatile cumulative percentage drug release of CTZ HCl from Ge/SA hydrogels (11/2 g) using 3.75% GA in phosphate buffer solutions of various pH values. Each point represents the mean \pm standard deviation of n=3 experiments

CTZ HCl: Cetzirizine dihydrochloride

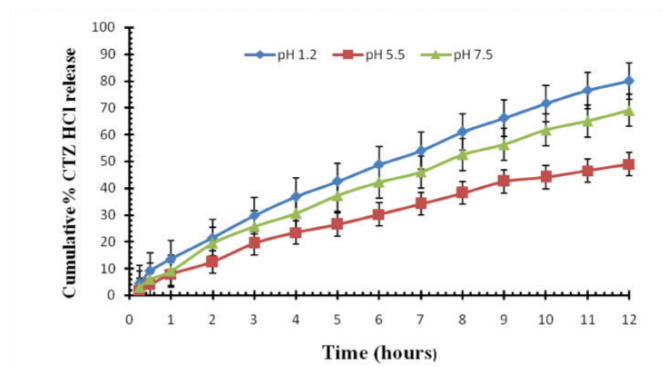


Figure 11. Pulsatile cumulative percentage drug release of CTZ HCl from Ge/SA hydrogels (11/2 g) using 4% GA in phosphate buffer solutions of various pH values. Each point represents the mean \pm standard deviation of $n=3$ experiments

CTZ HCl: Cetirizine dihydrochloride

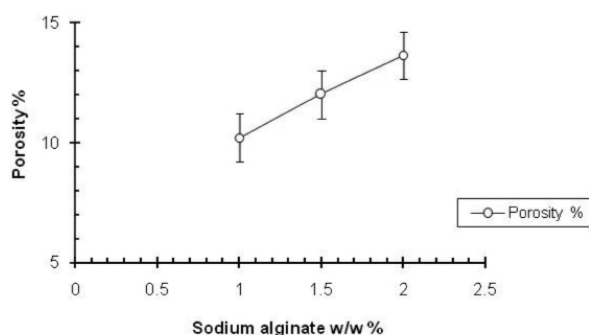


Figure 12. Effect of different concentrations of SA (1, 1.5, and 2 g) on the porosity percentage of Ge/SA hydrogels

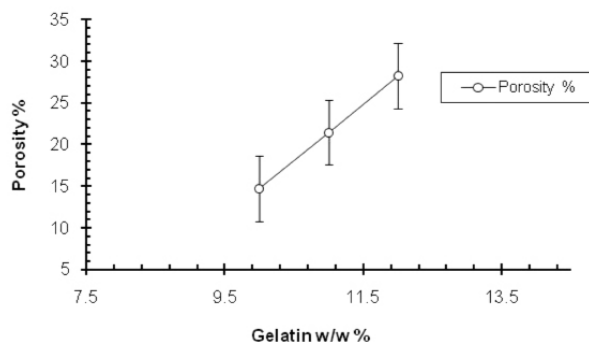


Figure 13. Effect of different concentrations of Ge (10, 11, and 12 g) on the porosity percentage of Ge/SA hydrogels

hydrogels is due to the swelling and relaxation of polymers, which, in this case, were Ge and SA.

Characterization of Ge/SA hydrogels

Differential scanning calorimetry

DSC thermograms of pure drug, unloaded, and drug-loaded hydrogels are presented in Figure 15. The thermograms of DSC clearly indicate a sharp melting peak of CTZ HCl at about 201.3°C, followed by a decomposition peak at about 260°C. The drug-

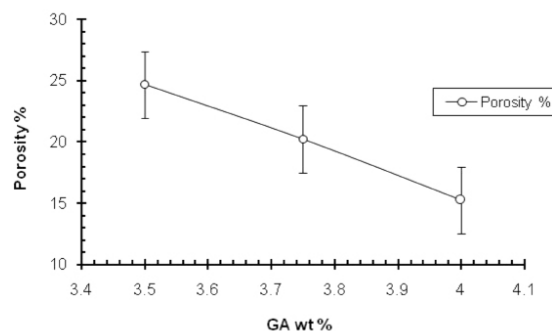


Figure 14. Effect of different concentrations of GA (3.5, 3.75, and 4%) on the porosity percentage of Ge/SA hydrogels

GA: Glutaraldehyde

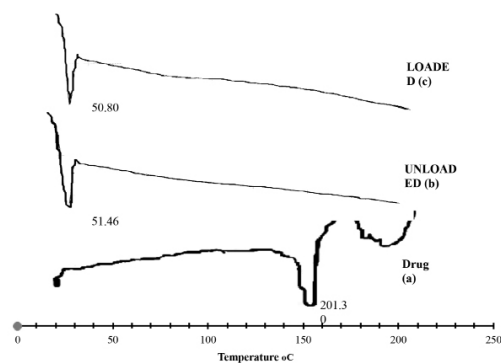


Figure 15. DSC thermogram of a) Pure drug b) Unloaded and c) Drug-loaded hydrogel

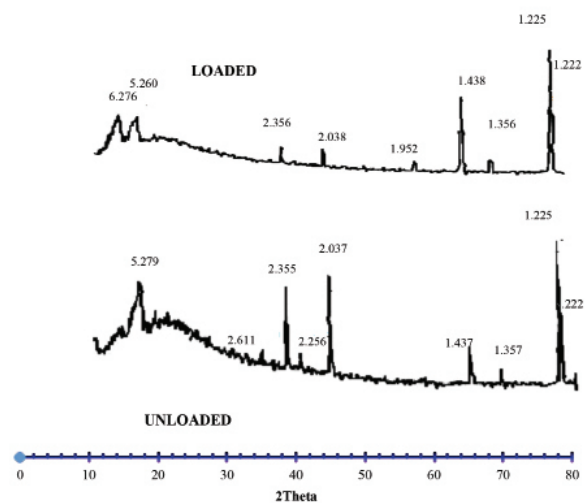


Figure 16. XRD patterns of loaded and unloaded Ge/SA hydrogels

loaded hydrogel showed an absence of drug melting peak, which indicates molecular dispersion of drug in the prepared hydrogels. The unloaded sample showed no endothermic transitions due to the rigid polymer network structure because of chain entanglement. The prepared hydrogels were found to be stable.

X-ray diffraction (XRD) analysis

The XRD pattern of the Ge/SA hydrogel and drug-loaded Ge/SA hydrogel is depicted in Figure 16. The diffractogram of the unloaded Ge/SA hydrogel indicated peaks at $\sim 16.780^\circ$, 38.180° , 44.440° , 64.820° , 69.200° , 77.940° , and 78.180° (2θ), and the diffractogram of the drug-loaded Ge/SA hydrogel indicated peaks at $\sim 16.840^\circ$, 38.160° , 44.420° , 64.800° , 69.220° , 77.940° , and 78.180° (2θ). These values were nearly the same as those of the Ge/SA hydrogel sample without drug, which means that there was no apparent interaction reported between drug and hydrogel.

FTIR spectroscopic analysis

The FTIR spectra of the Ge/SA hydrogels are shown in Figure 17. The FTIR spectra of SA/Ge indicates the characteristic absorption peaks observed at 3274 cm^{-1} typical for hydroxyl stretching and a peak at 1637 cm^{-1} , which corresponds to a stretch of C=O. Peaks at 1521 , 1458 , 1408 , and 1349 cm^{-1} in the SA spectrum indicate the anti-symmetric stretch and symmetric stretch of $-\text{COO}^-$ in associated carboxylic acid salt. Two other

interactions in the C-O stretch of C-OH groups can be found at 1030^{-1} , 1080 cm^{-1} , and the peak at 1248 cm^{-1} corresponds to the anti-symmetric stretching of C-O-C.

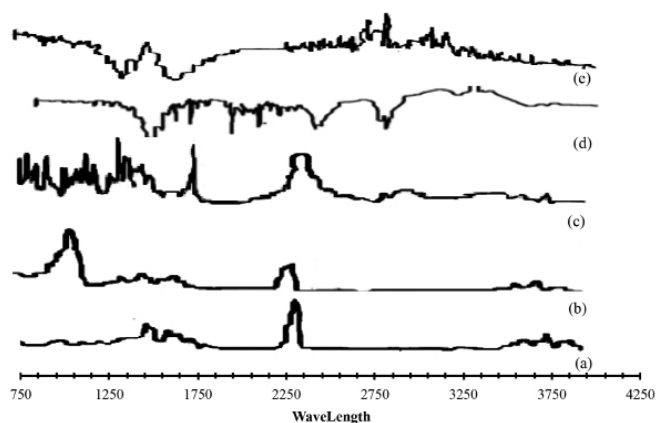


Figure 17. FTIR of a) Gelatin b) Sodium alginate c) Cetirizine hydrochloride d) Unloaded and e) Loaded samples

Table 9. Effect of Ge concentration on drug release mechanism of Ge/SA hydrogels in buffer solutions of various pH

Samples no	Ge contents	pH	Release exponent (n)	R ²	Order of release
S ₄	10	1.2	0.863	0.999	Non-fickian
		5.5	0.967	0.998	Non-fickian
		7.5	0.927	0.989	Non-fickian
S ₅	11	1.2	0.933	0.990	Non-fickian
		5.5	0.944	0.994	Non-fickian
		7.5	0.953	0.995	Non-fickian
S ₆	12	1.2	0.799	0.988	Non-fickian
		5.5	0.917	0.990	Non-fickian
		7.5	0.889	0.988	Non-fickian

Ge/SA: Gelatin/sodium alginate, GA: Glutaraldehyde

Table 10. Effect of GA concentration on the release kinetics of drug from Ge/SA hydrogels when placed in various pH solutions

Sample codes	GA contents	pH	(Release exponent) "n"	R ²	Release order
S ₇	3.5%	1.2	0.781	0.998	Non-fickian
		5.5	0.965	0.997	Non-fickian
		7.5	0.854	0.990	Non-fickian
S ₈	3.75%	1.2	0.784	0.992	Non-fickian
		5.5	0.952	0.990	Non-fickian
		7.5	0.830	0.980	Non-fickian
S ₉	4%	1.2	0.702	0.999	Non-fickian
		5.5	0.777	0.996	Non-fickian
		7.5	0.784	0.999	Non-fickian

Ge/SA: Gelatin/sodium alginate, GA: Glutaraldehyde

CONCLUSION

pH-sensitive hydrogels composed of SA and Ge were prepared in the presence of GA as a crosslinker at room temperature. The swelling ratio of cross-linked hydrogels was more in acidic media than in basic media. The gel fraction increased as the concentration of Ge, SA, and GA increased. Cetirizine hydrochloride was loaded as a model drug. Hydrogels with higher content of Ge showed the highest swelling and drug release. In contrast, a decreasing trend in drug release was observed with an increasing degree of crosslinking. The analysis of drug release showed that CTZ HCl was released from Ge/SA hydrogels by non-fickian diffusion. FTIR analysis showed the successful formation of cross-linked structure. XRD pattern analysis showed the crystalline nature of Ge/SA hydrogels. DSC analysis confirmed the thermal stability of the Ge/SA hydrogels over an extended temperature range. The results showed that the prepared hydrogels were a suitable candidate for sustained delivery of drug.

ACKNOWLEDGEMENTS

The authors highly acknowledge Department of Pharmacy, Bahauddin Zakariya University Multan for providing us the laboratory facilities.

Conflict of Interest: No conflict of interest was declared by the authors.

REFERENCES

- Kikuchi A, Okano T. Pulsatile drug release control using hydrogels. *Adv Drug Deliv Rev.* 2002;54:53-77.
- Peppas NA, Bures P, Leobandung W, Ichikawa H. Hydrogels in pharmaceutical formulations. *Eur J Pharm Biopharma.* 2000;50:27-46.
- Peppas, NA, Khare, AR. Preparation, Structure and diffusional behavior of hydrogels in controlled release. *Adv Drug Del Rev.* 1993;11:1-35.
- Chaterji S, Kwon IK, Park K. Smart polymeric gels, redefining the limits of biomedical devices. *Prog Poly Sci.* 2007;32:1083-1122.
- Ranjha, NM, Mudassir J, Akhtar N. Methyl methacrylate-co-itaconic acid (MMA-co-IA) hydrogels for controlled drug delivery. *J Sol-Gel Technol.* 2008;47:23-30.
- Sutar PB, Mishra RK, Pal K, Banthia AK. Development of pH sensitive polyacrylamide grafted pectin hydrogel for controlled drug delivery system. *J Mater Sci Mater Med.* 2008;19:2247-2253.
- Yu H, Xioa C. Synthesis and properties of novel hydrogels from oxidized konjac glucomanna crosslinked gelatin for *in vitro* drug delivery. *Carbohydr Poly.* 2008;72:479-489.
- Kurisawa M, Yui N. Dual-stimuli-responsive drug release from interpenetrating polymer Network-structured hydrogels of gelatin and dextran. *J Control Release.* 1998;54:191-200.
- Hago EE, Li X. Interpenetrating Polymer Network Hydrogels Based on Gelatin and PVA by Biocompatible Approaches: Synthesis and Characterization. *Adv Mat Sci Eng.* 2013;2013:1-8.
- Willam JR. *Pharmaceutical necessities. Remington "science and practice of pharmacy".* 21st ed. Chapter 55 page 2006:1074.
- Boateng JS, Matthews KH, Stevens HN, Eccleston GM. Wound Healing Dressings and Drug Delivery Systems: A Review. *J Pharm Sci.* 2008;9:2892-2923.
- Thomas A, Harding KG, Moore K. Alginates from wound dressings activate human macrophages to secrete tumour necrosis factor-alpha. *Biomaterials.* 2000;21:1797-1802.
- Paul W, Sharma CP. In *Encyclopedia of Surface and Colloid Science*, Marcel Dekker: New York; 2004.
- Rowley JA, Madlambayan G, Mooney DJ. Alginate hydrogels as synthetic extracellular matrix materials. *Biomaterials.* 1999;20:45-53.
- Martinsen A, Storrø I, Skjårk-Braek G. Alginate as immobilization material: III. Diffusional properties. *Biotechnol Bioeng.* 1992;39:186-194.
- Mees CEK, James TH. *The hardening of Gelatin and Emulsions.* Macmillan; New York; 1966:77.
- Hennink WE, van Nostrum CF. Novel crosslinking methods to design hydrogels. *Adv Drug Del Rev.* 2002;54:13-36.
- Khan S, Ranjha NM. Effect of degree of cross-linking on swelling and on drug release of low viscous chitosan/poly(vinyl alcohol) hydrogels. *Polym. Bull.* 2014;71:2133-2158.
- Bukhari SMH, Khan S, Rehanullah M, Ranjha NM. Synthesis and Characterization of Chemically Cross-Linked Acrylic Acid/Gelatin Hydrogels: Effect of pH and Composition on Swelling and Drug Release. *Int J Poly Sci.* 2015;2015:1-15.
- Jalil A, Khan S, Naeem F, Haider MS, Sarwar S, Riaz A, Ranjha NM. The structural, morphological and thermal properties of grafted pH-sensitive interpenetrating highly porous polymeric composites of sodium alginate/acrylic acid copolymers for controlled delivery of diclofenac potassium. *Desig Monomers Poly.* 2016;20:308-324.
- Mudassir J, Ranjha NM. Dynamic and equilibrium swelling studies: crosslinked pH sensitive methyl methacrylate-co-itaconic acid (MMA-co-IA) hydrogels. *J Poly Res.* 2007;15:195-203.
- Shi XN, Wang WB and Wang AQ. Effect of surfactant on porosity and swelling behaviors of guar gum-g-poly (sodium acrylate-co-styrene)/attapulgit superabsorbent hydrogels. *Colloids Surf B Biointerfaces.* 2011;88:279-286.
- Lin CC, Metters AT. Hydrogels in controlled release formulations: Network design and mathematical modeling. *Adv Drug Del Rev.* 2006;58:1379-1408.
- Naeem F, Khan S, Jalil A, Ranjha NM, Riaz A, Haider MS, Sarwar S, Saher S, Afzal S. pH responsive cross-linked polymeric matrices based on natural polymers: effect of process variables on swelling characterization and drug delivery properties. *Bioimpacts.* 2017;7:179-194.
- Peppas NA, Hilt JZ, Khademhosseini A, Langer R. Hydrogels in biology and medicine: From molecular principles to bionanotechnology. *Adv Mater.* 2006;18:1345-1360.
- Alla SGA, El-Din HMN, El-Naggar AWM. Structure and swelling release behavior of poly (vinyl pyrrolidone) (PVP) and acrylic acid (AAc) copolymer hydrogels prepared by gamma irradiation. *Eur Poly J.* 2007;43:2987-2998.
- Ranjha NM, Mudassir J. Swelling and aspirin release study: cross-linked pH sensitive vinyl acetate-co-acrylic acid (VAC-co-AA) hydrogels. *Drug Dev Ind Pharm.* 2008;34:512-521.
- Korsmeyer RW, Gurny R, Doelker E, Buri P, Peppas NA. Mechanism solute release from porous hydrophilic polymers. *Int J Pharm.* 1983;15:25-35.

29. Higuchi T. Mechanism of sustained action medication. Theoretical analysis of rate of release of solid drugs dispersed in solid matrices. *J Pharm Sci.* 1963;52:1145-1149.
30. Lin Y, Chen Q, Luo H. Preparation and characterization of N-(2-carboxybenzyl) chitosan as a potential pH- sensitive hydrogel for drug delivery. *Carbohydr Res.* 2007;342:87-95.
31. Bader RA, Herzog KT, Kao WJ. A Study of Diffusion in Poly(ethyleneglycol)-Gelatin Based Semi-Interpenetrating Networks for Use in Wound Healing. *Polym Bull (Berl).* 2008;62.
32. Bajpai J, Mishra S, Bajpai, AK. Dynamics of controlled release of potassium nitrate from a highly swelling binary polymeric blend of alginate and carboxymethyl cellulose. *J Appl Poly Sci.* 2007;106:961-972.
33. Praday M, Kopecek J. Hydrogels for site-specific oral delivery. Poly[(acrylic acid)-co-(butyl acrylate)] crosslinked with 4,4'-bis(methacryloylamino) azobenzene. *Macromol Chem.* 1990;191:1887-1897.



In Vitro Protection by *Crataegus microphylla* Extracts Against Oxidative Damage and Enzyme Inhibition Effects

Crataegus microphylla Ekstrelerinin Oksidatif Hasara Karşı *In Vitro* Koruma ve Enzim İnhibisyonu Etkileri

© Gülin RENDA¹, © Arzu ÖZEL^{2*}, © Burak BARUT², © Büşra KORKMAZ¹, © Nurettin YAYLI¹

¹Karadeniz Technical University, Faculty of Pharmacy, Department of Pharmacognosy, Trabzon, Turkey

²Karadeniz Technical University, Faculty of Pharmacy, Department of Biochemistry, Trabzon, Turkey

ABSTRACT

Objectives: *Crataegus* species have been used as food and also in folk medicine for the treatment of various diseases. The present study aimed to make investigations on the biologic properties of different extracts prepared from *Crataegus microphylla* C. Koch, which was collected from Turkey.

Materials and Methods: Dried leaf, stem bark, and fresh fruit samples of *C. microphylla* were separated and ethanol extract, acidified (0.5% HCl, pH: 2.5) ethanol extract, ethanol:water (1:1) extract, methanol extract, acidified (0.5% HCl, pH: 2.5) methanol extract, methanol:water (1:1) extract, water extract, and acidified (0.5% HCl, pH: 2.5) water extract were prepared for each. Various biologic effects such as the prevention of oxidative DNA damage, acetylcholinesterase, tyrosinase, α -glucosidase inhibition, and antioxidant effects with 2,2-diphenyl-1-picrylhydrazyl (DPPH) radical scavenging, PRAP, and FRAP assays of these extracts at different concentrations were studied.

Results: Acidified methanol extract of stem barks exhibited the highest acetylcholinesterase and tyrosinase inhibitions among the other extracts with IC_{50} values of $204.02 \pm 0.95 \mu\text{g/mL}$ and $37.30 \pm 0.27 \mu\text{g/mL}$, respectively. Acidified ethanol extract of leaves was the most efficient extract against α -glucosidase, giving an IC_{50} of $15.78 \pm 0.14 \mu\text{g/mL}$. The IC_{50} value of the acidified ethanol extract for DPPH was $9.89 \pm 0.09 \mu\text{g/mL}$. Methanol extracts of leaves and stem barks at the dose of $125 \mu\text{g/mL}$ exhibited significant protective activity against DNA strand scission by hydroxyl radicals ($\cdot\text{OH}$) on supercoiled pBR322 DNA.

Conclusion: Acidified methanol or ethanol extracts prepared with stem bark and leaf from *C. microphylla* have potential antioxidant, hypoglycemic, and neuroprotective effects.

Key words: DPPH, FRAP, hawthorn, PRAP, Rosaceae

ÖZ

Amaç: *Crataegus* türleri gıda olarak ve halk arasında çeşitli hastalıkların tedavisinde kullanılmaktadır. Bu çalışma Türkiye'den toplanan *Crataegus microphylla* C. Koch'tan hazırlanan farklı ekstraktların biyolojik özelliklerini araştırmayı amaçlamaktadır.

Gereç ve Yöntemler: Kurutulmuş yaprak, gövde kabuğu ve taze meyve örnekleri ayrıldı ve etanol ekstresi, asitlendirilmiş (%0.5 HCl, pH: 2.5) etanol ekstresi, etanol:su (1:1) ekstresi, metanol ekstresi, asitlendirilmiş (%0.5 HCl, pH: 2.5) metanol ekstresi, metanol:su (1:1) ekstresi, su ekstresi ve asitlendirilmiş (%0.5 HCl, pH: 2.5) su ekstresi hazırlandı. Ekstrelerin oksidatif DNA hasarının önlenmesi, asetilkolinesteraz, tirozinaz, α -glukozidaz inhibisyonu ve antioksidan aktivitesi 2,2-difenil-1-pikrilhidrazil (DPPH) radikal süpürme, PRAP ve FRAP gibi çeşitli biyolojik aktiviteleri farklı konsantrasyonlarda araştırılmıştır.

Bulgular: Gövde kabuklarından asitlendirilmiş metanol ekstraktı sırasıyla $204.02 \pm 0.95 \mu\text{g/mL}$ ve $37.30 \pm 0.27 \mu\text{g/mL}$ IC_{50} değerleri ile diğer ekstreler arasında en yüksek asetilkolinesteraz ve tirozinaz inhibisyonu göstermiştir. Yaprakların asitlendirilmiş etanol ekstresi, α -glukozidaz enzimine karşı $15.78 \pm 0.14 \mu\text{g/mL}$ ile en düşük IC_{50} değerini göstermiştir. DPPH için asitlendirilmiş etanol ekstraktının IC_{50} değeri $9.89 \pm 0.09 \mu\text{g/mL}$ bulunmuştur. $125 \mu\text{g/mL}$ dozunda yaprakların ve gövde kabuklarının metanol ekstreleri, süpersarmal pBR322 DNA üzerinde hidroksil iyonu ($\cdot\text{OH}$) tarafından DNA sarmalının kesilmesine karşı önemli koruma aktivitesi sergiledi.

Sonuç: *C. microphylla* gövde kabuğu ve yaprak ile hazırlanan asitlendirilmiş metanol veya etanol ekstrelerinin potansiyel antioksidan, hipoglisemik ve nöroprotektif etkileri bulunmaktadır.

Anahtar kelimeler: DPPH, FRAP, alıç, PRAP, Rosaceae

*Correspondence: E-mail: arzuozel@ktu.edu.tr, Phone: +90 462 377 88 03 ORCID-ID: orcid.org/0000-0001-7381-5575

Received: 03.03.2017, Accepted: 11.05.2017

©Turk J Pharm Sci, Published by Galenos Publishing House.

INTRODUCTION

The *Crataegus* genus (Rosaceae) has approximately 200 species worldwide and 24 species in Turkey.^{1,2} All plant species in this genus have the common name "Hawthorn".³ *Crataegus microphylla* C. Koch is one of the wild edible fruits in Turkey.⁴ *Crataegus* species have been used as food and also in folk medicine for the treatment of different heart diseases and diabetes for hundreds of years.^{3,5,6} Fruits of the *Crataegus* species are used for stimulating digestion, improving blood circulation, and for the treatment of diarrhea, abdominal pain, amenorrhea, hypertension, and hyperlipidemia in Chinese traditional medicine.³ In addition, products that include the extracts of some *Crataegus* species are consumed as natural health products in Europe, Asia, and North America.^{7,8} Epidemiologic studies and associated meta-analyses showed that long-term consumption of plant polyphenols in diet protected against the development of cancers, cardiovascular diseases, diabetes, osteoporosis, and neurodegenerative diseases.⁹⁻¹³

In addition to its ethnopharmacologic use, the preventive effect of *C. microphylla* fruit extract against genotoxicity induced by methyl methanesulfonate has been investigated in human cultured blood lymphocytes and found to reduce the oxidative stress and genotoxicity induced by toxic compounds. This activity is attributed to its phenolic content and antioxidant potential.¹⁴

By the results of many pharmacologic studies performed with extracts and isolated constituents of *Crataegus* species, flavonoids and proanthocyanidins were found to be responsible for the cardiovascular protective activity of the plant.⁸ With phytochemical studies, D-sorbitol, apigenin, naringenin, eriodictoyl, vitexin, vitexin-4'-*O*-rhamnoside, hesperetin, luteolin, luteolin 7-*O*-glucoside, quercetin, and hyperoside have been isolated from *C. microphylla*.¹⁵⁻¹⁸ Hyperoside was found to be the major compound in leaves and flowers of *C. microphylla*.¹⁷

Oxidative stress is involved in several neurodegenerative disease and degenerative disorders such as cancer, arteriosclerosis, and diabetes.¹⁹ As the accepted consent, the phenolic content determines the antioxidative properties of plant species, and polyphenols play a role in the prevention of chronic human diseases.⁹ The prevention of DNA damage, antioxidant activity, and total phenolic and flavonoid contents of extracts of new sources are very important in explaining their biochemical properties and behavior. In particular, studies of inhibition of these enzymes and prevention of DNA oxidative damage will also enlighten researchers to perform further studies in terms of neurodegenerative enzyme inhibition, anti-diabetic activity, and preventing the conversion to mutagenic forms with various extracts from *C. microphylla*.

In this study, prevention of oxidative DNA damage, acetylcholinesterase (AChE), tyrosinase, α -glucosidase inhibition behaviours and antioxidant effects: 2,2-diphenyl-1-picrylhydrazyl (DPPH) radical scavenging effect, phosphomolybdenum-reducing antioxidant power (PRAP), ferric-reducing antioxidant power (FRAP) with total phenolic and total flavonoid contents of the *C. microphylla* leaves, stem barks and fruits that were extracted with ethanol, methanol, and water were investigated. The biologic evaluation of the aerial part extracts of *C. microphylla* was investigated for the first time in this work.

EXPERIMENTAL

Plant material and sample preparation

Leaf, stem bark (B), and fruit of *C. microphylla* were collected from Kale, Gümüşhane-Turkey, in September 2015. A voucher specimen was deposited at the Hacettepe University, Faculty of Pharmacy, Herbarium (Voucher No: HUEF 15021).

Dried leaf (L), B and fresh fruit (F) samples of *C. microphylla* were separated and 50 g of L, B, and F was extracted with 250 mL of various solvents to obtain ethanol extract (1), acidified (0.5% HCl, pH: 2.5) ethanol extract (2), ethanol:water (1:1) extract (3), methanol extract (4), acidified (0.5% HCl, pH: 2.5) methanol extract (5), methanol:water (1:1) extract (6), water extract (7), and acidified (0.5% HCl, pH: 2.5) water extract (8) for each, respectively. Extractions were performed in a shaker for 4 h x 3 times, for each sample. Extracts were filtered and evaporated under reduced pressure using a rotary evaporator. Crude extracts were kept in a refrigerator at +4°C until used. All of the extracts in Table 1 were tested in all assays.

Table 1. The codes and yields (w/w) of the extracts prepared with various solvents of leaf, bark and fruit from *C. microphylla*

	Codes	Yields (w/w)
Leaf in EtOH	L1	16.2
Leaf in EtOH, pH 2.5	L2	15.8
Leaf in EtOH:H ₂ O (1:1)	L3	23.2
Leaf in MeOH	L4	20.6
Leaf in MeOH, pH 2.5	L5	17.6
Leaf in MeOH:H ₂ O (1:1)	L6	24.6
Leaf in H ₂ O	L7	10.2
Leaf in H ₂ O, pH 2.5	L8	18.2
Bark in EtOH	B1	5.8
Bark in EtOH, pH 2.5	B2	7.4
Bark in EtOH:H ₂ O (1:1)	B3	9.1
Bark in MeOH	B4	10.0
Bark in MeOH, pH 2.5	B5	8.3
Bark in MeOH:H ₂ O (1:1)	B6	9.6
Bark in H ₂ O	B7	7.3
Bark in H ₂ O, pH 2.5	B8	6.8
Fruit in EtOH	F1	10.9
Fruit in EtOH, pH 2.5	F2	10.0
Fruit in EtOH:H ₂ O (1:1)	F3	6.3
Fruit in MeOH	F4	10.7
Fruit in MeOH, pH 2.5	F5	9.8
Fruit in MeOH:H ₂ O (1:1)	F6	5.7
Fruit in H ₂ O	F7	8.6
Fruit in H ₂ O, pH 2.5	F8	9.5

*L: Leaf, B: Bark, F: Fruit, w/w: Weight per weight

Enzyme inhibitions

Acetylcholinesterase inhibition

AChE inhibition was examined using the method described by Ellman et al.²⁰ and Ingkaninan et al.²¹ Galantamine was used as the positive control. All extracts (L1-8, B1-8 and F1-8) at various concentrations were separately added to a 96-well microplate and incubated for 15 min at 25°C. Absorbance was measured at 412 nm using a 96-well microplate reader. Inhibition of AChE was calculated using Formula 1, in which A_{control} is the activity of enzyme without extract (solvent in buffer pH=8) and A_{sample} is the activity of enzyme with extract at various concentrations. The inhibitory concentrations of 50% of AChE (IC_{50}) values were calculated from the graph of the percentage inhibition against extract concentrations.

$$\text{Formula 1. Inhibition (\%)} = \left[\frac{A_{\text{sample}} - A_{\text{control}}}{A_{\text{control}}} \right] \times 100$$

Tyrosinase inhibition

Tyrosinase inhibition was examined using the method described by Masuda et al.²² Kojic acid was used as the positive control. The tyrosinase inhibition percentage of all extracts (L1-8, B1-8 and F1-8) (20 μ L) at various concentrations was calculated using Formula 1. The inhibitory concentration of 50% of tyrosinase (IC_{50}) values was calculated from the graph of the percentage inhibition against extract concentrations.

α -glucosidase inhibition

α -glucosidase inhibition was examined using the method described by da Silva Pinto et al.²³ Acarbose was used as the reference drug. The α -glucosidase inhibition percentage of all extracts (L1-8, B1-8 and F1-8) at various concentrations was calculated using Formula 1. The inhibitory concentration of 50% of α -glucosidase (IC_{50}) values was calculated from the graph of the percentage inhibition against extract concentrations.

Antioxidant activities

Determination of total phenolic contents

The Folin-Ciocalteu reagent was used to determine the total phenolic content according to the method described by Kähkönen et al.²⁴ Gallic acid was also used as standard compound. The total phenolic contents of all extracts (L1-8, B1-8 and F1-8) were expressed as mg gallic acid equivalents (GAE) per g of dry weight sample.

Determination of total flavonoid contents

The total flavonoid content was measured by using the aluminum nitrate assay (Chang et al.²⁵ 2002). Quercetin was used as the standard compound. The total flavonoid contents of all extracts (L1-8, B1-8 and F1-8) were expressed as mg quercetin equivalents (QE) per g of dry weight sample.

DPPH radical scavenging assay

The DPPH radical scavenging activities of all extracts (L1-8, B1-8 and F1-8) were examined using the method described by Blois compared with gallic acid and ascorbic acid as the reference compounds.²⁶ The absorbance of the sample (A_{sample})

was measured at 517 nm. An assay mixture without samples was used as a control (A_{control}). The inhibition percentage was calculated using Formula 2. The scavenging concentrations of 50% of DPPH (SC_{50}) values were calculated from the graph of the percentage inhibition against extract concentrations.

Formula 2.

$$\text{Scavenging effects (\%)} = \left[\frac{(A_{\text{control}} - A_{\text{sample}})}{A_{\text{control}}} \right] \times 100$$

PRAP assay

PRAP of all L1-8, B1-8 and F1-8 extracts were examined using phosphomolybdic acid.²⁷ The PRAP of extracts was expressed as mg QE per g of dry weight sample.

FRAP assay

FRAP of all L1-8, B1-8 and F1-8 extracts was examined using the method described by Oyaizu.²⁸ The ferric-reducing power of extracts was expressed as butylated hydroxyanisole equivalents (BHA-E) per g of dry weight sample.

Prevention of DNA oxidative damage

The protective effects of all L1-8, B1-8 and F1-8 extracts of *C. microphylla* against DNA oxidative damage induced by hydroxyl radical were monitored by the conversion of pBR322 to open circular form according to Yeung et al.²⁹ Total volume of reaction mixture (10 μ L) contained Tris-HCl buffer (pH 7.0), supercoiled plasmid pBR322 DNA (250 ng), 1 mM $FeSO_4$, 2% H_2O_2 and 125 μ g/mL of extracts. The mixtures were incubated at 37°C for 1 h. The reaction was stopped by adding 5 μ L of loading buffer (0.2% bromophenol blue, 4.5% sodium dodecyl sulfate, 0.2% xylene cyanol, 30% glycerol). The mixtures were then loaded on 0.8% agarose gel containing EB 1 mg/mL in TAE (Tris-acetate-EDTA). Electrophoresis was carried out at 100 V for 90 min. and the resulting image was visualized with BioRad Gel Doc XR system.

Statistical analysis

The experiments were performed in triplicate and the results are expressed as the mean \pm standard deviation. The statistical analysis was performed with SPSS 15.0 for Windows and Microsoft Excel for Windows 10. The differences between the extracts were evaluated using one-way analysis of variance followed by Duncan's multiple range tests. $P < 0.05$ was considered statistically significant.

RESULTS

Enzyme inhibition

AChE inhibition results of extracts of leaf, stem bark and fruit from *C. microphylla* are presented in Table 2. All of the extracts had low AChE inhibition values when compared with galanthamine with IC_{50} values of 7.34 ± 0.09 μ g/mL. However, among the tested extracts, B5 and B2 exhibited the highest AChE inhibitions with IC_{50} values of 204.02 ± 0.95 μ g/mL and 230.58 ± 3.18 μ g/mL, respectively. Some of the extracts (L8, B3, B7, F1, F3, F4, F6, F7 and F8) were inactive against AChE enzyme.

The results of the tyrosinase enzyme inhibitory effect of the extracts are given in Table 2. The lowest IC₅₀ values of the extracts indicate a higher inhibition effectiveness. All of the extracts from *C. microphylla* exhibited promising activity against tyrosinase compared with kojic acid. Methanol and ethanol extracts of stem bark of *C. microphylla* displayed remarkable tyrosinase inhibitory activities with IC₅₀ values of lower than 50 µg/mL. The B2 extract exhibited the highest tyrosinase inhibition with IC₅₀ values of 37.30±0.27 µg/mL (p<0.05), and B5 inhibited tyrosinase with IC₅₀ values of 37.41±0.17 µg/mL.

In this work, IC₅₀ values of α-glucosidase inhibition of *C. microphylla* extracts are presented in Table 2. A lower IC₅₀

Table 2. IC₅₀ (µg/mL) of acetylcholinesterase, tyrosinase and α-glucosidase inhibitory activities of leaf, bark, and fruit extracts from *C. microphylla*

Samples*	AChE	Tyrosinase	α-glucosidase
L1	349.14±1.34 ^a	59.19±0.14	90.35±1.32
L2	472.81±3.77	51.30±0.26	^b 15.78±0.14
L3	355.83±1.84	70.71±0.16	258.13±2.41
L4	932.83±2.31	49.31±0.13	191.36±1.92
L5	382.20±2.84	43.74±0.28	^b 29.92±0.26
L6	324.77±1.72	52.42±0.73	57.80±0.94
L7	513.35±2.37	145.80±0.51	167.94±1.36
L8	nd	142.42±1.42	270.64±2.42
B1	314.83±2.50	38.79±0.82	465.60±2.26
B2	230.58±3.18	^b 37.41±0.17	^b 38.25±0.51
B3	nd	41.52±0.35	164.95±1.32
B4	538.31±1.52	38.25±0.62	367.65±2.42
B5	204.02±0.95	^b 37.30±0.27	^b 39.63±0.62
B6	630.21±2.52	40.32±0.21	68.31±0.22
B7	nd	155.90±1.47	256.76±2.35
B8	298.41±1.36	144.47±0.31	^b 46.02±0.52
F1	nd	129.34±0.46	nd
F2	301.77±2.25	139.37±0.32	624.22±2.48
F3	nd	85.77±0.41	nd
F4	nd	62.11±0.58	465.12±3.42
F5	434.53±3.27	56.02±0.21	250.94±1.95
F6	nd	147.29±0.52	nd
F7	nd	165.75±0.47	nd
F8	nd	149.83±0.69	731.81±3.26
Galantamine	7.34±0.09	-	-
Kojic acid	-	24.01±0.02	-
Acarbose	-	-	31.92±0.08

*L: Leaf, B: Bark, F: Fruit, ^aValues expressed are means ± SD, ^b(p<0.05), nd: Not detected, AChE: Acetylcholinesterase

value indicates strong inhibitory activity. L2, L5, B2, B5 and B8 extracts exhibited significant (p<0.05) α-glucosidase inhibition as shown in Table 2. IC₅₀ values of L2, L5, B2, B5 and B8 extracts were found to 15.78±0.14, 29.92±0.26, 38.25±0.51, 39.63±0.62 and 46.02±0.52 µg/mL, respectively. On the other hand, F1, F3, F6, and F7 extracts had no α-glucosidase inhibition effects. All of the data of α-glucosidase inhibition indicated that L2, L5, B2, B5, and B8 extracts of *C. microphylla* could be effective hypoglycemic agents.

Antioxidant activities

The total phenolic contents of various extracts of *C. microphylla* leaves, stem barks, and fruits were determined from the gallic acid standard curve ($y=1.9251x + 0.3125$, $R^2=0.9967$) and expressed as mg GAE/g dry weight. The total phenolic contents of *C. microphylla* stem barks and leaves were in the range of 13.22±0.38 to 132.26±1.83 mg GAE/g dry weight and 30.93±0.64 to 85.26±1.60 mg GAE/g dry weight, whereas extracts of fruits exhibited 5.00±0.18 to 57.28±1.35 mg GAE/g dry weight as shown in Figure 1. B1 (123.11±2.38), B2 (132.26±1.83), B4 (111.84±2.19), B5 (120.40±2.89), and B6 (112.46±2.13) extracts contained more than 100 mg GAE/g dry weight. On the other hand, B7 and F8 extracts exhibited the lowest total phenolic contents (13.22±0.38, 5.00±0.18 and 14.89±0.73 mg GAE/g dry weight).

Total flavonoid contents of leaf, stem bark, and fruit extracts from *C. microphylla* were determined from the quercetin standard curve ($y=12.632x \pm 0.509$, $R^2=0.9981$) as shown in Figure 2. The total flavonoid contents expressed as mg QE/g dry weight found in our extracts ranged from 0.97±0.09 to 63.34±0.92 mg QE/g dry weight. Total flavonoid contents of leaf extract from *C. microphylla* appeared higher than other extracts. The highest total flavonoid content was found in the L1 (63.34±0.92 mg QE/g dry weight) extract, followed by the L2 (56.25±0.73 mg QE/g dry weight), L4 (52.89±0.47 mg QE/g dry weight), L5 (49.39±1.03 mg QE/g dry weight), and L6 (50.53±0.92 mg QE/g dry weight) extracts. Stem bark extracts of *C. microphylla* were in the range of 0.97±0.09 to 4.78±0.24 mg QE/g dry weight.

Among the tested extracts, B2 (9.89±0.09 µg/mL), B5 (10.47±0.29 µg/mL), B1 (11.94±0.07 µg/mL) and L2 (12.29±0.07 µg/mL)

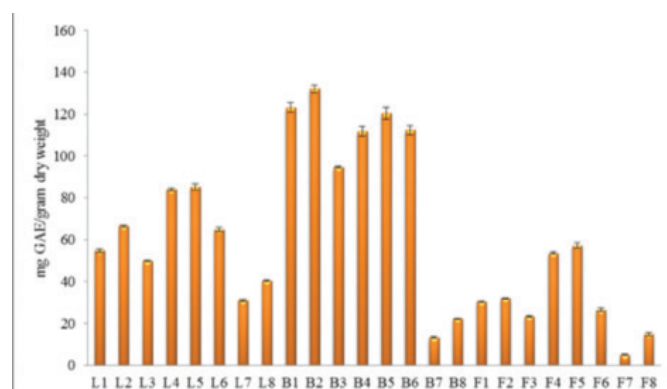


Figure 1. Total phenolic contents of the extracts

*L: Leaf, B: Bark, F: Fruit

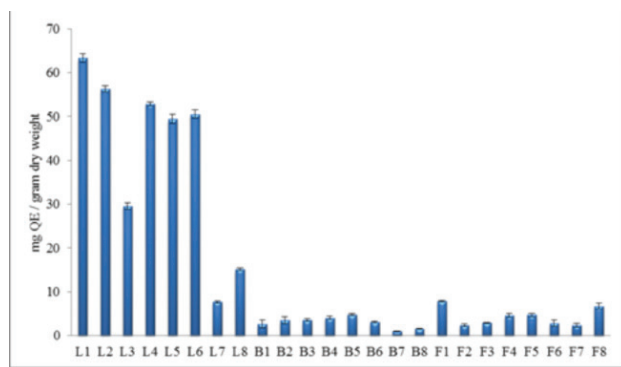


Figure 2. Total flavonoid contents of the extracts

*L: Leaf, B: Bark, F: Fruit

($p < 0.05$) extracts showed the highest scavenging activity in this assay as shown in Table 3. The IC_{50} values of ethanol, acidified ethanol, methanol, and acidified methanol extracts of leaf and stem bark of *C. microphylla* were found lower than $70 \mu\text{g/mL}$. In the leaf, stem bark, and fruit extracts of *C. microphylla*, F7 extract showed the lowest DPPH radical scavenging activities. F5 extract exhibited the highest scavenging activities among the leaf extracts with $123.50 \pm 1.31 \mu\text{g/mL}$.

PRAP of leaf, stem bark, and fruit extracts from *C. microphylla* were determined from the quercetin standard curve ($y = 0.0066x \pm 0.5295$, $R^2 = 0.9986$) as shown in Table 3. B2, B5, and B4 extracts displayed the highest reducing activities with 368.37 ± 2.41 , 324.69 ± 3.69 and $247.75 \pm 2.73 \text{ mg QE/g dry weight}$,

Table 3. DPPH radical scavenging, phosphomolybdenum-reducing antioxidant power (PRAP) and ferric-reducing antioxidant power (FRAP) assay values of leaf, bark, and fruit extracts from *C. microphylla*

Sample*	DPPH radical scavenging [SC_{50} values of extracts ($\mu\text{g/mL}$)]	PRAP (mg QE/g dry weight)	FRAP (mg BHAE/g dry weight)
L1	23.42 ± 0.19^a	98.54 ± 1.35	165.58 ± 0.33
L2	12.29 ± 0.07	138.93 ± 1.42	214.87 ± 0.72
L3	20.77 ± 1.38	149.76 ± 0.42	227.00 ± 2.32
L4	17.94 ± 1.40	82.12 ± 0.57	222.04 ± 4.95
L5	15.79 ± 0.38	117.83 ± 2.52	197.07 ± 1.66
L6	42.83 ± 0.72	42.91 ± 0.93	205.58 ± 0.88
L7	149.12 ± 2.41	34.86 ± 0.36	123.69 ± 3.22
L8	91.40 ± 1.42	35.40 ± 0.39	140.29 ± 1.45
B1	11.94 ± 0.14	179.89 ± 1.63	191.77 ± 2.78
B2	9.89 ± 0.09	368.37 ± 2.41	240.62 ± 1.03
B3	34.04 ± 0.52	151.10 ± 1.58	216.20 ± 1.64
B4	18.84 ± 0.38	247.75 ± 2.73	224.30 ± 4.11
B5	10.47 ± 0.29	324.69 ± 3.69	232.26 ± 1.83
B6	65.52 ± 1.41	221.54 ± 2.51	199.70 ± 1.55
B7	140.92 ± 2.51	40.84 ± 0.93	59.20 ± 1.52
B8	60.06 ± 0.93	41.44 ± 0.83	57.24 ± 0.77
F1	177.11 ± 1.58	34.88 ± 0.25	60.28 ± 2.44
F2	164.63 ± 1.79	38.24 ± 0.49	62.84 ± 1.75
F3	206.16 ± 2.69	32.45 ± 0.41	53.11 ± 0.81
F4	131.53 ± 1.44	37.39 ± 0.18	76.29 ± 1.69
F5	123.50 ± 1.31	42.80 ± 0.15	87.28 ± 2.05
F6	219.97 ± 2.48	29.44 ± 0.17	35.39 ± 0.99
F7	669.21 ± 3.94	25.68 ± 0.82	25.00 ± 2.38
F8	600.70 ± 2.07	28.63 ± 0.41	34.99 ± 1.42
GA	68.14 ± 0.18	-	-
AA	54.01 ± 0.13	-	-

*L: Leaf, B: Bark, F: Fruit, ^aValues expressed are means \pm SD, ^b($p < 0.05$), BHAE: Butylated hydroxyanisole equivalents, QE: Quercetin equivalents, DPPH: 2,2-diphenyl-1-picrylhydrazyl

respectively; F7 extract indicated the lowest activity 25.68 ± 0.82 mg QE/g dry weight dry weight.

The results of the ability to reduce Fe^{3+} to Fe^{2+} are presented in Table 3. Stem bark and leaf extracts have a strong ferric reducing power. B2 and B5 extracts demonstrated the highest ferric reducing activity with 240.62 ± 1.03 mg BHA/g dry weight and 232.26 ± 1.83 mg BHA/g dry weight, respectively; F7 extract exhibited the lowest activity 25.00 ± 2.38 mg BHA/g dry weight.

Prevention of DNA oxidative damage

It is known that when circular plasmid DNA is subjected to electrophoresis, the fastest to migrate is the supercoiled Form I, the slowest moving is the open circular Form II, and the linear Form III runs in between the other two forms.³⁰ Prevention of DNA oxidative damage by *C. microphylla* is shown in Figure 3. The assay revealed that there was a formation of Form II and Form III because of hydroxyl radicals, as shown in Lane 2 on Figure 3.

However, with the addition of extracts, the conversion of supercoiled pBR322 DNA to open circular and linear forms decreased except with F8 extract at $125 \mu\text{g/mL}$. L4 and B4 extracts exhibited the highest preventative effect of DNA oxidative damage at $125 \mu\text{g/mL}$. The results proved that the prevention of DNA oxidative damage results were compatible with the radical scavenging assay.

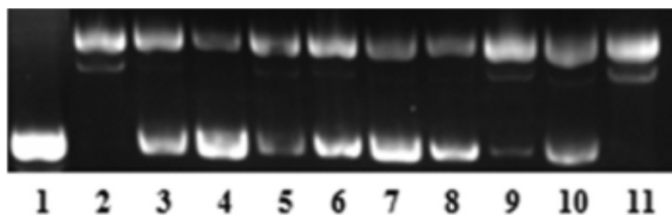


Figure 3. Protective effect of ethanol, methanol and water extracts of leaf, stem bark and fruit from *C. microphylla* in DNA oxidative damage assay. Lane 1: DNA control; Lane 2: DNA + 2% H_2O_2 + 1 mM FeSO_4 ; Lane 3: DNA + 2% H_2O_2 + 1 mM FeSO_4 + L1; Lane 4: DNA + 2% H_2O_2 + 1 mM FeSO_4 + L4; Lane 5: DNA + 2% H_2O_2 + 1 mM FeSO_4 + L7; Lane 6: DNA + 2% H_2O_2 + 1 mM FeSO_4 + B1; Lane 7: DNA + 2% H_2O_2 + 1 mM FeSO_4 + B4; Lane 8: DNA + 2% H_2O_2 + 1 mM FeSO_4 + B7; Lane 9: DNA + 2% H_2O_2 + 1 mM FeSO_4 + F1; Lane 10: DNA + 2% H_2O_2 + 1 mM FeSO_4 + F4; Lane 11: DNA + 2% H_2O_2 + 1 mM FeSO_4 + F7.

*L: Leaf, B: Bark, F: Fruit

DISCUSSION

Alzheimer's disease (AD) is one of the most frequent forms of dementia among older people.³¹ Although AChE inhibitors such as tacrine, donepezil, galantamine, and rivastigmine are important in the treatment for AD, they have adverse effects including gastrointestinal problems.^{32,33} Considering all the extracts, stem bark extracts, which had promising results at AChE inhibition, presented higher phenolic content than the other extracts (Figure 1). Recent studies have shown that antioxidants could scavenge oxygen radicals and could also attenuate inflammation pathways, and also pointed toward an association between AD and

inflammatory processes as well as antioxidant activity.³⁴ From this point of view, it is stated that the use of antioxidants could be considered in the treatment of AD.³⁵

Parkinson's disease (PD) is one of the neurodegenerative diseases caused by dopaminergic neuron deficiency in the brain.³⁶ Methanol and ethanol extracts from *C. microphylla* had higher inhibition activity than water extracts of *C. microphylla* due to total phenolic contents. There is a positive correlation between phenolic content and tyrosinase inhibition.³⁷ These results showed that, extracts of *C. microphylla*, especially B5 extract, had promising neuroprotective potential due to AChE and tyrosinase inhibition.

α -Glucosidase is a key enzyme in the hydrolysis of oligosaccharide and contributes to the formation of glucose.³⁸ It is important to find a new α -glucosidase inhibitor for DM, such as natural products with low toxicity and adverse effects.

Organic solvents such as methanol and ethanol are known to be efficient for the extraction of phenolics. Besides, water is a good choice because it is used to make infusions and decoctions in herbal medicine. Also, acidified extraction systems were shown to be more efficient, especially for the hydrolysis of bound phenolic compounds.^{39,40} Due to the fact that many solvents may extract different compounds from plant tissues, we wanted to compare the results. The hydrolysis process was done with acidification and aglycones were obtained with acidified extracts (L2, 5, 8; B2, 5, 8; F2, 5, 8) (Table 1).

When we compared the extracts that were prepared with the same solvents, total phenolic contents of the acidified ones were found to be higher than the non-acidified ones (Figure 1). The total phenolic content of L2 was found to be higher than L1, L5 was higher than L4, and L8 was higher than L7. The same results were also obtained with B and F series (Figure 1).

Similar to our findings, it was reported that methanol extract of *C. microphylla* leaves indicated scavenging activity to $92.82 \pm 0.79\%$ at $500 \mu\text{g/mL}$.⁴¹ According to Sharifi et al.⁴², IC_{50} values of methanol extract of *C. microphylla* were found as $13.01 \pm 0.2 \mu\text{g/mL}$.

The efficiency of an antioxidant extract was reported to be dependent on the pH of the solvents, as well as the solubility of antioxidant compounds by the solvents used for the extraction.⁴³ Besides, methanol, ethanol, and water, which are commonly used solvents for extraction, and acidified alcohols are also widely used for extraction to release aglycone by chemical hydrolysis under acidic conditions.⁴⁴ These results confirm that higher contents of total phenolic displayed higher DPPH free radical scavenging activities. All data showed that there was a relationship between the total phenolic and radical scavenging activities.

The results showed that methanol and ethanol extracts of leaf and bark from *C. microphylla* had more effective phosphomolybdenum-reducing power than its water extract. The B2 and B5 extracts with higher reducing power showed a positive correlation with phosphomolybdenum-reducing power assay.

Prevention of DNA oxidative damage was based on the ability of

extracts (L1-8, B1-8 and F1-8) from *C. microphylla* to protect the supercoiled pBR322 DNA against damage caused by hydroxyl radicals ($\cdot\text{OH}$). The antioxidant activity of 50% aqueous methanolic extract of whole plant of *C. microphylla* was studied before with an *in vitro* study and found to have moderate antioxidant activity.⁴⁵ However, there are no previous works on the AChE, tyrosinase, α -glucosidase inhibitory effects and oxidative DNA damage protective effects of various extracts of *C. microphylla*. In this context, it was aimed to compare the extractability of compounds that serve a function in the activity by various solvents.

CONCLUSION

This study presented the potential AChE, tyrosinase, α -glucosidase inhibitory effects, total phenolic, total flavonoid contents, the antioxidant effects, and prevention of oxidative DNA damage of leaf, stem bark and fruit of various extracts (L1-8, B1-8 and F1-8) from *C. microphylla*. Concurrently, the correlation between the antioxidant activity and the DNA damage protective effects of the extracts (L1-8, B1-8 and F1-8) was described. Our results can be evaluated as a preliminary work for the use of *C. microphylla* extracts in herbal products.

Conflict of Interest: No conflict of interest was declared by the authors.

REFERENCES

- Dönmez AA. The Genus *Crataegus* L. (Rosaceae) with special reference to hybridisation and biodiversity in Turkey. *Turk J Bot.* 2004;28:29-37.
- Dönmez AA. A new species of *Crataegus* (Rosaceae) from Turkey. *Bot J Linn Soc.* 2005;148:245-249.
- Chang Q, Zhong Z, Harrison F, Chow MS. Hawthorn. *J Clin Pharmacol.* 2002;42:605-612.
- Browicz K. *Crataegus* L. In: PH Davis, ed. *Flora of Turkey and the East Aegean Islands*, Edinburgh University Press; Edinburgh; 1972;4:133-147.
- Kumar D, Arya V, Bhat ZA, Khan NA, Prasad DN. The genus *Crataegus*: chemical and pharmacological perspectives. *Rev Bras Farmacogn.* 2012;22:1187-1200.
- Rastogi S, Pandey MM, Rawat AK. Traditional herbs: a remedy for cardiovascular disorders. *Phytomedicine.* 2016;23:1082-1089.
- Edwards JE, Brown PN, Talent N, Dickinson TA, Shipley PR. A review of the chemistry of the genus *Crataegus*. *Phytochemistry.* 2012;79:5-26.
- Assessment report on *Crataegus* spp., folium cum flore, European Medicines Agency Committee on Herbal Medicinal Products (HMPC), EMA/HMPC/159076/2014, Accessed on: 13 October 2014.
- Pandey KB, Rizvi SI. Plant polyphenols as dietary antioxidants in human health and disease. *Oxi Med Cell Longev.* 2009;2:270-278.
- Abidi E, Habib J, Yassine A, Chahine N, Mahjoub T, Ellak A. Effects of methanol extracts from roots, leaves, and fruits of the Lebanese strawberry tree (*Arbutus andrachne*) on cardiac function together with their antioxidant activity. *Pharm Biol.* 2016;54:1035-1041.
- Graf BA, Milbury PE, Blumberg JB. Flavonols, flavones, flavanones, and human health: epidemiological evidence. *J Med Food.* 2005;8:281-290.
- Arts IC, Hollman PC. Polyphenols and disease risk in epidemiologic studies. *Am J Clin Nutr.* 2005;81:317-325.
- Palma-Duran SA, Vlassopoulos A, Lean M, Govan L, Combet E. Nutritional intervention and impact of polyphenol on glycohemoglobin (HbA1c) in non-diabetic and type 2 diabetic subjects: Systematic review and meta-analysis. *Crit Rev Food Sci Nutr.* 2017;57:975-986.
- Hosseinimehr SJ, Azadbakht M, Tanha M, Mahmodzadeh A, Mohammadifar S. Protective effect of hawthorn extract against genotoxicity induced by methyl methanesulfonate in human lymphocytes. *Toxicol Ind Health.* 2011;27:363-369.
- Strain HH. Sources of d-sorbitol. *J Am Chem Soc.* 1937;59:2264-2266.
- Meriçli AH, Melikoğlu G. Investigations on Turkish *Crataegus* species. *Acta Pharm Turcica.* 2002;44:169-173.
- Melikoğlu G, Bitiş L, Meriçli AH. Flavonoids of *Crataegus microphylla*. *Nat Prod Res.* 2004;18:211-213.
- Tajali AA, Khazaeipool M. Effects of height and organs on flavonoids of *Crataegus microphylla* C. Koch in Iran *Int J Biosci.* 2012;2:54-58.
- Moyo MS, Amoo O, Ncube B, Ndhlala AR, Finnie JF, Van Staden J. Phytochemical and antioxidant properties of unconventional leafy vegetables consumed in Southern Africa. *S Afr J Bot.* 2013;84:65-71.
- Ellman GL, Courtney KD, Andres V Jr, Feather-stone RM. A new and rapid colorimetric determination acetylcholinesterase activity. *Biochem Pharmacol.* 1961;7:88-95.
- Ingkaninan K, de Best CM, van der Heijden R, Hofte AJ, Karabatak B, Irth H, Tjaden UR, van der Greef J, Verpoorte R. High-performance liquid chromatography with on-line coupled UV, mass spectrometric and biochemical detection for identification of acetylcholinesterase inhibitors from natural products. *J Chromatogr A.* 2000;872:61-73.
- Masuda T, Yamashita D, Takeda Y, Yonemori S. Screening for tyrosinase inhibitors among extracts of seashore plants and identification of potent inhibitors from *Garcinia subelliptica*. *Biosci Biotech Biochem.* 2005;69:197-201.
- da Silva Pinto M, Kwon YI, Apostolidis E, Lajolo FM, Genovese MI, Shetty K. Functionality of bioactive compounds in Brazilian strawberry (*Fragaria x Ananassa* Duch.) cultivars: evaluation of hyperglycemia and hypertension potential using *in vitro* models. *J Agric Food Chem.* 2008;56:4386-4392.
- Kähkönen MP, Hopia AI, Vuorela HJ, Rauha JP, Pihlaja K, Kujala TS, Heinonen M. Antioxidant Activity of Plant Extracts Containing Phenolic Compounds. *J Agr Food Chem.* 1999;47:3954-3962.
- Chang CC, Yang MH, Wen MH, Wen HM, Chern JC. Estimation of total flavonoid content in propolis by two complementary colorimetric methods. *J Food Drug Anal.* 2002;10:178-182.
- Blois MS. Antioxidant determinations by the use of a stable free radical. *Nature.* 1958;181:1199-1200.
- Falcioni G, Fedeli D, Tiano L, Calzuola I, Mancinelli L, Marsili V, Gianfranceschi G. Antioxidant activity of wheat sprouts extract *in vitro*: inhibition of DNA oxidative damage. *J Food Sci.* 2002;67:2918-2922.
- Oyaizu M. Studies on products of browning reactions-antioxidative activities of browning reaction prepared from glucosamine. *Jpn J Nut.* 1986;44:307-315.
- Yeung SY, Lan WH, Huang CS, Lin CP, Chan CP, Chang MC, Jeng JH. Scavenging property of three cresol isomers against H_2O_2 , hypochlorite, superoxide and hydroxyl radicals. *Food Chem Toxicol.* 2002;40:1403-1413.
- Özel A, Barut B, Demirbaş Ü, Biyiklioglu Z. Investigation of DNA binding, DNA photocleavage, topoisomerase I inhibition and antioxidant activities of water soluble titanium(IV) phthalocyanine compounds. *J Photochem Photobiol B.* 2016;157:32-38.

31. Lewis WG, Green LG, Grynszpan F, Radic Z, Carlier PR, Taylor P, Finn MG, Sharpless KB. Click chemistry in situ: acetylcholinesterase as a reaction vessel for the selective assembly of a femtomolar inhibitor from an array of building blocks. *Angew Chem Int Engl*. 2002;41:1053-1057.
32. Tian T, Weng L, Wang S, Weng X, Zhang L, Zhou X. Cationic tetrapyrrolic macromolecules as new acetylcholinesterase inhibitors. *J Porphyr Phthalocyanines*. 2009;13:893-902.
33. Zengin G, Nithiyanantham S, Locatelli M, Ceylan R, Uysal S, Aktumsek A, Kalai Selvi P, Maskovic P. Screening of *in vitro* antioxidant and enzyme inhibitory activities of different extracts from two uninvestigated wild plants: *Centranthus longiflorus* subsp. *longiflorus* and *Cerintho minor* subsp. *auriculata*. *Eur J Integr Med*. 2016;8:286-292.
34. Ferreira A, Proença C, Serralheiro MLM, Araujo ME. The *in vitro* screening for acetylcholinesterase inhibition and antioxidant activity of medicinal plants from Portugal. *J Ethnopharmacol*. 2016;108:31-37.
35. Gibson GE, Huang HM. Oxidative stress in Alzheimer's disease. *Neurobiol Aging*. 2005;26:575-578.
36. Bao K, Dai Y, Zhu ZB, Tu FJ, Zhang WG, Yao XS. Design synthesis biphenyl derivatives mushroom tyrosinase inhibitors. *Bioorg Med Chem*. 2010;18:6708-6714.
37. Choi HK, Lim YS, Kim YS, Park YS, Lee CH, Hwang KW, Kwon DY. Free-radical-scavenging and tyrosinase-inhibition activities of Cheonggukjang samples fermented for various time. *Food Chem*. 2008;106:564-568.
38. Majouli K, Hlila MB, Hamdi A, Flamini G, Jannet HB, Kenani A. Antioxidant activity and α -glucosidase inhibition by essential oils from *Hertia cheirifolia* (L.). *Ind Crop Prod*. 2016;82:23-28.
39. Acosta-Estrada BA, Gutierrez-Urbe JA, Serna-Saldivar SO. Bound phenolics in foods, a review. *Food Chem*. 2014;152:46-55.
40. Mushtaq M, Sultana B, Anwar F, Batool S. Antimutagenic and antioxidant potential of aqueous and acidified methanol extracts from citrus limonum fruit residues. *J Chil Chem Soc*. 2015;60:2979-2983.
41. Artun FT, Karagöz A, Özcan G, Melikoğlu G, Anıl S, Kultur S, Sutlupinar N. *In vitro* evaluation of antioxidant activity of some plant methanol extracts. *J BUON*. 2016;21:720-725.
42. Sharifi N, Sourı E, Ziai SA, Amin G, Amanlou M. Discovery of new angiotensin converting enzyme (ACE) inhibitors from medicinal plants to treat hypertension using an *in vitro* assay. *DARU*. 2013;21:74.
43. Kutlu T, Durmaz G, Ateş B, Yılmaz İ, Çetin MŞ. Antioxidant properties of different extracts of black mulberry (*Morus nigra* L.). *Turk J Biol*. 2011;35:103-110.
44. Nollet LML, Toldra F. *Handbook of Analysis of Active Compounds in Functional Foods*, CRC Press; Boca Raton; 2012.
45. Serteser A, Kargioğlu M, Gök V, Bağcı Y, Ozcan MM, Arslan D. Determination of antioxidant effects of some plant species wild growing in Turkey. *Int J Food Sci Nutr*. 2008;59:643-651.



Composition of Volatile Oil of *Iris pallida* Lam. from Ukraine

Iris pallida Lam'ın Uçucu Yağı Bileşimi Ukrayna

© Olga MYKHAILENKO

National University of Pharmacy, Department of Botany, Kharkiv, Ukraine

ABSTRACT

Objectives: To qualitatively and quantitatively study the composition of essential oil from the dried rhizomes and leaves of *Iris pallida* Lam. from Ukraine for the first time.

Materials and Methods: Essential oils obtained by steam distillation were investigated using gas chromatography–mass spectrometry.

Results: The essential oils were obtained from the leaves and rhizomes by yielding 0.03% and 0.20%, respectively. The analysis of the oil resulted in the identification of 26 components in the leaves and 18 components in the rhizomes. The dominant terpenes in the essential oil of the leaves of *I. pallida* were squalene (6%), hexahydrofarnesylacetone (8%) and neophytadiene (up to 6%). Among them, myristic acid (56%), capric acid (14.50%), lauric acid (15.42%), α -irone (2.85%) were found as the dominant compounds of the essential oil of the rhizomes of *I. pallida*. α -irone and γ -irone contents are accepted as the most significant criteria of the commercial quality of Iris essential oil. The compounds β -damascenone and squalene were identified for the first time in plants of the genus *Iris*.

Conclusion: *I. pallida* of Ukraine can be recommended as an additional source of raw materials for essential oil from the rhizomes and as a source of bioactive substances.

Key words: *Iris pallida*, essential oil, rhizomes, leaves, gas chromatography–mass spectrometry analysis

ÖZ

Amaç: *Iris pallida* Lam kurutulmuş rizom ve yapraklarından elde edilen esansiyel yağın nitel ve nicel bileşimi Ukrayna'dan ilk kez okundu.

Gereç ve Yöntemler: Buhar distilasyonu ile elde edilen uçucu yağlar, gaz kromatografisi-kütle spektrometresi ile araştırıldı.

Bulgular: Uçucu yağlar, sırasıyla %0.03 ve %0.20 verimle yapraklardan ve köksüzlerden elde edildi. Yağ analizleri yapraklarda 26 bileşen ve rizomlarda 18 bileşenin tanımlanmasına neden oldu. *I. pallida* yapraklarının uçucu yağdaki baskın terpenler skualen (%6), heksahidrofarnesilaseton (%8) ve neofitadien (%6'ya kadar) idi. *I. pallida* rizomlarının temel yağlarının baskın bileşikleri arasında miristik asit (%56), kaprik asit (%14.50), lorik asit (%15.42) ve α -irone (%2.85) bulunmuştur. İris esansiyel yağının ticari kalitesinin en önemli kriteri olarak α -irone ve γ -irone içeriği kabul edilmektedir. β -Damascenon, skualen gibi bileşikler, ilk kez *Iris* cinsindeki bitkilerde tanımlandı.

Sonuç: Ukrayna *I. pallida*'nın florası, rizomlardan esansiyel yağ için ham maddelerin ek bir kaynağı olarak ve biyoaktif maddeler kaynağı olarak tavsiye edilebilir.

Anahtar kelimeler: *Iris pallida*, uçucu yağ, rizomlar, yapraklar, gaz kromatografisi-kütle spektrometresi analizi

INTRODUCTION

Iris L. is the largest and the most complicated genus of the *Iridaceae*. The genus includes more than 300 *Iris* species. The range of the genus now extends to all continents of the northern hemisphere, their distribution covers Europe, the Middle East, and northern Africa, Asia, and across North America.^{1,2} *Iris*es are used in traditional medicine and aromatherapy, and many

of them are common ornamental plants.³ Sixteen species of *Iris* genus inhabit Ukraine.⁴

Some species of this genus, such as *Iris versicolor* L., *Iris variegata* L., *Iris florentina* L., and *Iris germanica* L. have gained great attention from cosmetic and perfume industries^{5,6} due to their violet-like smell caused by irone-type compounds. The essential oil of *Iris* is included in perfumes and lotions of

*Correspondence: E-mail: zolya85@gmail.com, Phone: +38572656829 ORCID-ID: orcid.org/0000-0003-3822-8409

Received: 08.02.2017, Accepted: 11.05.2017

©Turk J Pharm Sci, Published by Galenos Publishing House.

higher quality, such as "Iris Ganach" (Guerlain), "Extravagance d'Amarige" (Givenchy), "Dia pour Femme" (Amouage), "Les Exclusifs de Chanel 28 La Pausa" (Chanel), "Ghost summer breeze" (Ghost), and others.

There are several medicines and dietary supplements on the pharmaceutical market that are based on the presented *Iris*es. Rhizomes of *Iris pseudacorus* L. are used as part of the collecting on M.N. Zdenko (Ukraine; Russian Federation) and "Pancreophile" ("Fytolynyya SmartMed", Ukraine)^{7,8}, also, *I. versicolor* is included in homeopathic medicines "Iris-plus" (Doctor N, Russian Federation)⁹ and «Kaliris – ЕДІАС-114» (EDAC holding company, Russian Federation), which are used for the treatment of papillomatosis of the bladder, chronic pancreatitis, anti-acid gastritis, and peptic ulcers of the stomach. In addition, the rhizomes of *I. versicolor* make up part of the complex drug Mastodynon (Bionorica SE, Germany), which is used for violations of the menstrual cycle, mastopathy, and premenstrual syndrome.¹⁰ "Orris (Iris) Herbasol Extract PG" was created based on the rhizome of *Iris pallida* (Lipoid Cosmetic, Switzerland) for use in cosmetology for skin and hair.¹¹ Rhizomes of *I. germanica* make up part of the general tonic drug "Original grosser Bittner balsam" (Richard Bittner AG, Austria).¹² Therapeutic and prophylactic drugs were created from the leaves of *Iris lacteal* for patients cancer such as "Vitonk" (multivitamin product) and "Laktir" (to reduce adverse effects during chemotherapy and radiation sickness) (Russian Federation).^{9,13}

Iris species have an immense medicinal importance and are used in the treatment of cancer, inflammation, and bacterial and viral infections. Numerous scientific papers on their use in treatment were published covering a variety of their pharmacologic activities, and the presence of flavones, flavone C-glycosides^{14,15}, isoflavones, terpenoids, xanthenes, or simple phenolics, stilbenes and quinones in their extracts were demonstrated within recent years.^{16,17}

Many kinds of *Iris*es have been valued for their medicinal properties in traditional use, especially in India¹⁸ and China^{14,19}, where more than 30 species have been used in folk herbal medicines. *Iris*es were reported to have various biologic properties, including having potent antiulcer, anticancer, antioxidant, piscicidal activities^{15,18}, and cytotoxic, anti-inflammatory, and antibacterial activity.^{14,17,20-22}

Continuing the study of the component composition of the essential oil of *Iris* plants²³⁻²⁹, we chose *I. pallida* Lam. as the subject of the study. "Orris root" (*I. pallida*, *I. germanica*, *I. florentina*) is used to obtain the essential oil in Mediterranean countries.^{6,21,22,30}

I. pallida is a perennial herb, the rhizome is creeping and thick. Its leaves are broadly-ensiform, 30–60 cm long, the perianth is pale-purple with a yellow beard. Rhizomes contain isoflavones-irigenin, iristectorigenin A, nigricin, nigricanin, irisflorentin, iriskumaonin methyl ether, irilone, iriflogenin, and others.^{14,15,17,21} The essential oil (about 0.1%), known as "Orris butter", consists of about 85% myristic acid, with irone (odiferous constituent with violet-like odor), γ -dihydro-irones, ionone, methyl myristate^{22,30}, and other substances such as fat, resin, starch, mucilage, bitter

principle, glycoside-iridin, and small amount of tannin.^{11,17} The essential oil of the rhizome strengthens the immune system, and has a regenerating effect.⁶ The extract of the roots of *I. pallida* was formerly used as a diuretic, expectorant, remedy for coughs, and chronic diarrhea.^{18,21} The chemical composition of the essential oil of *I. pallida* from Ukraine is lacking. Studying the chemical composition of *I. pallida* is interesting in terms of increasing the harvesting of raw base materials.

The objective of the present work was to determine the component composition of the essential oil of the rhizomes and leaves of *I. pallida* from Ukraine using chromatography-mass spectrometry.

MATERIALS AND METHODS

Plant material

The subjects of the study were rhizomes and leaves of *I. pallida* Lam. (*Iridaceae*) (Figure 3), that were prepared in September, 2015, in the Luhansk region (village Kremennaya, Ukraine). Analysis and estimation of the results were performed with air-dried raw materials. Voucher specimens were deposited in the Herbarium of the Pharmacognosy Department and Botany Department in The National University of Pharmacy, Kharkiv, Ukraine.

Preparation of volatile oils and extracts

The essential oil of the rhizomes and leaves of *I. pallida* was obtained by steam distillation for 12 hours in an apparatus consisting of a 25-mL round-bottomed flask, a reflux condenser, and a water bath. The method allows isolation of the essential oil from the plant material with trace quantities of essential oil.^{23,31,32}

A weighed sample of material (0.5 g) was placed in a 20.0-mL vial. The internal standard tridecane was added in terms of 50 μ g of the substance per a certain quantity of a plant sample. Ten milliliters of water were added to the sample and volatile compounds were distilled using steam for 2 hours under reflux. In the process of distillation, the volatile material was adsorbed on the inner surface of the reflux condenser. After the cooling system, the adsorbed material was washed by slow addition of 3.0 mL of ultra-pure pentane Fluka 76869 (content of microimpurities is 1.0 mg by 1.0l) in a dry vial on 10.0 mL. Washout was concentrated by blowing (100 mL/min) high-purity nitrogen until the volume of extract was 10.0 μ L, and which was fully collected using a chromatographic syringe.³³

Chromatographic conditions

The constituent composition of the rhizomes and leaves of the plant was studied using gas chromatography-mass spectrometry (GC/MS) on an Agilent Technologies 6890 with a 5973 mass-spectrometric detector. Introduction of the sample (2.0 μ L) into the chromatographic column was executed according to the *splitless* mode without stream splitting. The speed of sample introduction was 1.2 mL/min within 0.2 min. The chromatographic column was capillary DB-5 (30 m \times 0.25 mm \times 0.50 μ m). Mobile phase: helium, gas flow rate 1.2 mL/min. The temperature of the sample introduction heater was 250°C. The temperature-controlled chamber was programmable from 50 to 320°C with a rate of 4 degree/min.

Identification of components

For the identification of components, data from the mass-spectra libraries NIST05^{34,35} and WILEY 2007³⁶ with a total number of spectra of more than 470.000 were used, combined with the identification programs AMDIS and NIST.

The method was used for quantitative calculations of the internal standard.^{31,32,37} The calculation of component content C (mg/kg) was made using the following formula:

$$C = P_1 \cdot 50 \cdot 1000 / P_2 \cdot M$$

Where: P₁–peak area of tested substance; P₂–peak area of standard; 50–mass of internal standard (µg), injected into the sample; m–sample mass (g). The relative component content was defined as the percentage of the total amount.

RESULTS

In our previous research work, we reported the component composition of the essential oil of several *Iris*es from Ukraine (*Iris hungarica*, *I. pseudacorus*, *Iris pseudacorus f. alba*, *I. versicolor*, *I. germanica*)²³⁻²⁷ and Azerbaijan (*Iris medwedewii*, *Iris carthaliniae*).²⁹ Monoterpene ketone α-irone and triterpenoid squalene were identified in all samples. These substances can be used as markers in the chemotaxonomy and chemosystematics of plants of the genus *Iris* for further studies. Among the other components of the essential oil of *Iris*es, different norterpeneoids such as β-ionone-5,6-epoxide, β-ionone, *trans*-2,6-γ-irone, β-isometilionone, β-damascenone were defined in practically all *Iris* species. Among the other substances in the oil of *Iris*es were neophytadiene, eugenol, α-terpineol, germacrene D, terpinen-4-ol, hexahydrofarnesylacetone, farnesylacetone, phenylacetaldehyde, geranilacetone, 2-methoxy-4-vinylphenol. Also, *Iris* oil contains a large proportion of myristic acid (near 50–80%), other fatty acids (e.g., caprylic, capric, lauric, palmitic) and their esters.

The component composition of *Iris*es of Azerbaijan flora is considerably different, probably because *I. medwedewii* and *I. carthaliniae* are typical representatives of stony dry steppes, they grow in warmer climate, different from the steppe, marsh and forest *Iris* species of Ukraine flora. Sesquiterpenes β-farnesene, germacrene D, *trans*-caryophyllene, δ-cadene, spathulenol, caryophyllene oxide, α- and β-cadinol, α-copaene have been identified in both *Iris* species.²⁹ Calamenene was present only in *I. medwedewii*, and α- and β-bisabolene epoxides were found only in *I. carthaliniae*. Therefore, the component composition of the oil of these *Iris*es is similar to the oil composition of the rhizomes of *Iris nigricans* of Jordan³⁸, the rhizomes of *Iris sofarana*, and of the flowers of *Iris kerneriana* from Turkey.³⁹

The aim of this work was to determine the component composition of the essential oil of *I. pallida* using chromatography-MS; 0.03% and 0.20% of the oil yield was obtained from the air-dried leaves and rhizomes of *I. pallida*, respectively, through steam distillation. Using GC/MS analysis, 26 compounds were found in the essential oil from the leaves and 18 compounds from rhizomes of *I. pallida*. The essential oil included terpenoids¹², their oxygenated derivatives (alcohols, ketones, aldehydes,

esters), aromatic compounds¹¹, higher hydrocarbons⁶, and higher acids of their esters.^{8,40} The constituents of the essential oil that were obtained from the rhizomes and leaves of *I. pallida* are shown with their percentages and relative retention indices in Table 1 and in Figure 1, 2.

Table 1. Percentage chemical composition of the essential oil of *Iris pallida* rhizomes and leaves

Compound	RRI	Leaves	Rhizome
Phenylacetaldehyde	1001	1.72	-
6-Methyl-3,5-heptadien-2-one	1067	0.11	-
Decanal	1174	0.24	-
Caprylic acid	1220	-	1.72
α-Ethylidene phenylacetaldehyde	1221	0.21	-
Indole	1242	1.55	-
2-Methoxy-4-vinylphenol	1275	1.50	0.25
β-Damascenone	1334	0.39	-
4-Isobutylphenone	1384	15.08	-
3-Phenylpyridine	1400	0.40	-
Geranilacetone	1411	1.16	-
β-Ionone 5,6-epoxide	1435	0.76	-
β-Ionone	1438	0.86	-
Capric acid	1439	-	14.50
Dihydro-β-Irone	1466	-	0.25
α-Irone	1493	-	2.85
<i>trans</i> -2,6-γ-Irone	1498	-	1.22
Megastigmatrienone 1	1499	0.11	-
Megastigmatrienone 2	1515	0.52	-
β-Isometilionone	1522	-	0.21
Benzophenone	1550	31.84	1.11
Lauric acid	1630	-	15.42
Tridecanoic acid	1680	-	0.21
Myristic acid, methyl ester	1700	-	0.17
Myristic acid	1794	0.88	56.00
Hexahydro farnesyl acetone	1802	8.05	-
Neofitadien	1807	5.65	-
<i>epi</i> -Manoil oxide	1973	0.84	-
Palmitic acid	1983	-	1.13
Heneicosane	2100	-	0.23
Tricosane	2300	4.65	0.89
Tetracosane	2400	1.76	-
Pentacosane	2500	7.78	2.29
Heptacosane	2700	4.05	0.59
Squalene	2758	6.12	0.69
Nonacosane	2800	3.13	-
Cerotic acid, methyl ester	2815	0.64	-

The symbol “-” means that the compound was not identified

The essential oil of the leaves of *I. pallida* consists of alkanes (21.37%), aromatic compounds (6.26%), ketones (47.66%), sesquiterpenes (10.06%), diterpenes (5.9%), triterpenes (6.12%), accompanied by relatively smaller amounts of monoterpenes (1.16%) and fatty acids (0.88%).

The dominant terpenes in the essential oil of the leaves of *I. pallida* were squalene (6%), hexahydrofarnesylacetone (8%), and neophytadiene (up to 6%). Among the other compounds of the essential oil of the leaves were β -ionone (0.86%) and β -ionone-5,6-epoxide (0.76%), β -damascenone (0.39%), geranylacetone (1.16%), *epi*-maloiloxide (0.84%), ketones megastigmatrienone-1 (0.11%), and megastigmatrienone-2 (0.52%), 4-isobutylacetophenone (15.08%).

The major components of the essential oil of *I. pallida* rhizomes were fatty acids (89%), alkanes (8.29%), aromatic compounds (1.36%), sesquiterpenes (4.53%), and triterpenes (0.69%); monoterpenes and diterpenes were not found. The main saturated aliphatic mono-carboxylic acids were caprylic (1.72%), capric (14.50%), lauric (15.42%), tridecanoic (0.21%), palmitic (1.13%), and myristic (56%) acids. Among the sesquiterpenes were α -irone (2.85%), dihydro- β -irone (0.25%), *trans*-2,6- γ -irone (1.22%), and β -isometilionone (0.21%). Triterpenoids were represented only by squalene.

DISCUSSION

I. pallida Lam. (Figure 3) of the Ukrainian flora was chosen for the study, it had a sufficient resource base.

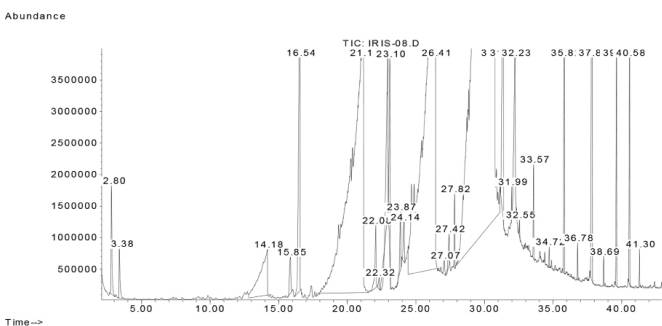


Figure 1. Chromatograms of GC-MS analysis of essential oil of rhizomes of *Iris pallida*

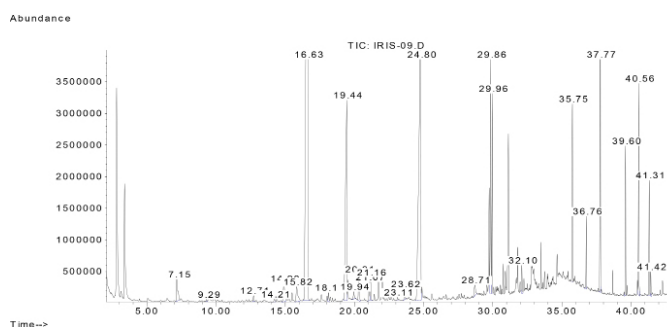


Figure 2. Chromatograms of GC-MS analysis of essential oil of leaves of *Iris pallida*

According to the classification of Rodionenko² (1987), *I. pallida* belongs to the group of Bearded Irises (*Barbatae* are the species with flowers, bearing a beard of multicellular hairsprings on the outer perianth lobes) from the *Iris* section of the series *Elatae* Lawrence. *I. pallida* is not endemic for our region because it entered the territory of Ukraine through introduction.⁴ It is widely cultivated.^{3,4}

The essential oil from "Orris roots" (*I. pallida*, *I. florentina* and *I. germanica*)^{17,22} is used in perfume industries^{5,6} and in aromatherapy.^{41,42} Rhizomes are harvested, dried, and aged for three to five years. During this time, fats and oils in the roots undergo degradation and oxidation, which produces many fragrant compounds that are invaluable in perfumery, whose scent is similar to violets.^{6,30,39} The essential oil from *Irises* is obtained through steam distillation.^{38,39,43} The volatile components of *I. pallida* from Ukraine were not studied.

Through GC/MS analysis of the volatile constituents of the rhizome (Figure 1), 18 components were identified, among which fatty acids and their esters predominated with caprylic (1.72%), capric (14.50%), lauric (15.42%), tridecanoic (0.21%), palmitic (1.13%), methyl myristate (0.17%) and myristic (56%) acids. The oil of the leaves is shown only by myristic acids (0.88%). Thus, it was consistent with data in the literature, which noted that myristic acid was the major compound (and/or always present) in the *Iris* species.^{17,22-24,29} Fatty acids are known to have antioxidant, antifungal, anti-inflammatory, and immunomodulatory properties⁴³, they are involved in metabolism, positively affect digestion, and create favorable conditions for beneficial intestinal microorganisms for their life activity.⁴⁴ In addition, palmitic and myristic acids are saturated fatty acids involved in the synthesis of prostaglandins and stability of cellular membranes. It has been found that lauric acid possesses antibacterial, antitumor, antimycobacterial, and antiviral activities.^{43,45} The composition of fatty acids and their esters gives us the possibility to investigate the use of *Iris* rhizome extracts for medical purposes.

The prevalence of fatty acids and their esters, as well as aliphatic hydrocarbons and their derivatives in the volatile constituents of leaves and rhizomes seems to be a common feature among the species of *Iris*.^{22-29,38,39,43}



Figure 3. General view of the living plants and drawing of *Iris pallida*

Monoterpenoid α -irone was detected to make up 2.85% of the total essential oil of *I. pallida* rhizomes. It is known that ketone α -irone is an indicator of the authenticity of iris oil.⁶ The presence of irones, homologues, and ionones, was reported mainly in the rhizomes of *I. pallida*, *I. germanica*, and *I. florentina*.^{21,30,46}

For comparison, the essential oil of the dried rhizomes of Syrian wild *I. germanica*⁴³ and fresh rhizomes of *I. nigricans*³⁸ have been established to contain α -irone at only 0.25% and 1.42%, respectively, using GC/MS. In the essential oil from fresh rhizomes of *I. florentina*, α -irone and γ -irone are absent⁴⁶, but at that time, the content of α -irone in the dry rhizome and essential oil of *I. florentina* were found as high (4.21%).

In the present study, norterpenoids and their derivatives were observed in the essential oil of the leaves and rhizomes of *I. pallida* for the first time. Their compositions differed. The highest percentage of norterpenoids was obtained in the rhizomes (9.06%) with much smaller amounts (2.01%) in the leaves.

The largest variety of component norterpenoids was found in the oil of *I. pallida* rhizomes. α -Dihydro- β -irone (0.25%), *trans*-2,6- γ -irone (1.22%) and β -isomethylionone (0.21%) were identified only in the rhizome. The availability of irones and ionones in the raw material determines the characteristic smell of violets of iris and their mucolytic action.²² Various compositions of norterpenoids were found in the leaves of *I. pallida*. Among them, β -damascenone (0.39%), β -ionone (0.86%), and β -ionone-5,6-epoxide (0.76%) were identified.

The analysis of the essential oil of the leaves of *I. pallida* led to the identification of 26 compounds, in which the ketones benzophenone and 4-isobutylphenone constituted the major compounds, accounting for 31.84% and 15.08% of the total oil composition, respectively. Regarding the volatile constituents of the leaves, aromatic compounds, ketones, and aldehydes, together with other aliphatic hydrocarbon compounds showed a high prevalence in the total oil composition.

The highest percentage of terpenes of squalene was observed in the essential oil of the leaves of *I. pallida* (6.12%), and the smallest content of squalene was in the essential oil of rhizomes (0.69%). In addition, sesquiterpenoids hexahydrofarnesylacetone (8.05%) and geranyl acetone (1.16%) were detected in *Iris* leaves, which exhibit an antimicrobial and cytotoxic activity, according to the latest pharmacologic studies.^{13,40,47}

Moreover, diterpenes neophytadiene, and *epi*-manoil oxide, with ketones megastigmatrienone-1, megastigmatrienone-2, 4-isobutylphenone were only indicated in the oil of the leaves and their content was 5.65, 0.84, 0.11, 0.52, and 15.08%, respectively, as illustrated in Figure 2.

A high content (21.37%) of alkanes was detected in the essential oil of *Iris* leaves. Its existence is caused by the fact that they are the part of the wax cuticle that covers the leaves and rhizomes of a plant, and volatile components from the raw materials are distilled off by steam, together with terpenoids.

The leaves and rhizomes of *I. pallida* contain 2-methoxy-4-vinylphenol, benzophenone, squalene, myristic acid, and

some saturated hydrocarbons. The chemical composition of the essential oils of the leaves of *I. pallida* was studied for the first time. Also, squalene and β -isometilionone were identified for the first time in the essential oil of *I. pallida* rhizomes. The variable composition of biologically-active compounds in the essential oil provides a basis for further study of *I. pallida* and as a promising source of raw materials for producing valuable essential oils.

CONCLUSIONS

Qualitative and quantitative analysis of the components of the essential oil of *I. pallida* from Ukraine was conducted using chromatography-MS for the first time. Rhizomes of *I. pallida* are characterized by the high content of essential oil (0.20%), distinguished by a rich chemical composition. Sixteen volatile components of the essential oil of rhizomes and 26 components of the leaves were found. Dihydro- β -irone, α -irone, *trans*-2,6- γ -irone, β -isometilionone, benzophenone, and others were found in the essential oil of *Iris* rhizomes. The dominant terpenes in the essential oil of *Iris* leaves were 4-isobutylphenone, benzophenone, hexahydrofarnesyl acetone, neofitadien, squalene.

Iris oil is recommended in aromatherapy for bronchial inflammation and coughing^{41,42}, and it is used in mixtures for skin care. The essential oil of iris normalizes brain function, and has a detoxifying, diuretic, expectorant, and strengthening effect on the immune system. Phytochemical studies have shown the prospects for further pharmacologic study of iris.⁹ The chemical composition of biologically active substances, including the presence of irones in the rhizomes of *I. pallida* could have industrial significance⁶; irones constitute an expensive natural ingredient of the cosmetic industry. *I. pallida* of Ukraine flora can be recommended as an additional source of raw materials for essential oil from rhizomes.

ACKNOWLEDGEMENTS

The author would like to express their gratitude to the acting Senior Researcher, Head of Department of the Floriculture of Botanical Garden of Kharkiv National University named after V. N. Karazin, Cand. Biol. Sci. Orlova T. G. for helping in the determination of the systematic classification of the plant, and to Professor of Pharmacognosy department of National University of Pharmacy, D.Sc. in Pharmacy, Vladimir M. Kovalyov, for his advice and participation in the discussion.

Conflict of Interest: No conflict of interest was declared by the authors.

REFERENCES

1. Goldblatt P, Manning JC. The *Iris* family: natural history and classification. Portland; Timber Press; 2008:336.
2. Rodionenko GI. The genus *Iris* L. (questions of morphology, biology evolution and systematics). London; British Iris Society; 1987:222.
3. Karpenko VP. Introduction history of species and varieties of genus *Iris* L. in Ukraine against the background of global trends. Umans'kiy National'nyi Universytet sadivnytstva visnyk; 2015;2:85-91.

4. Mosyakin SL, Fedoranchuk MM. Vascular plants of Ukraine. A nomenclatural checklist, In: Mosyakin SL, ed. Kiev; 1999:346.
5. Lawless J. The illustrated encyclopedia of essential oils. Publ. Element Books Ltd; Reissue edition; 1995:256.
6. Niir Board. Modern technology of perfumes, flavours and essential oils. 2nd ed. National Institute of Industrial Research; 2004:282-283.
7. Lekarstvennoe rastytelnoe surie. Pharmacognosy, Posobyie. In: Yakovlev GP, Holynovoy KF, eds. SPb; SpetsLyt; 2004:765.
8. Medicinal preparations of Ukraine. In: Chernykh VP, Zupanets IA, eds. Kharkiv, Publishing of the NFUU; Golden Pages; 2005:512.
9. Tihomirova LI, Bazarnova NG, Mikushina IV, Dolganova ZV. Pharmacological-biochemical rationale for the practical use of some representatives of the genus *iris* l. (review). Rastitelnye Resursy; 2015;3:25-34.
10. Gordeeva G. Application of the drug Mastodinone with functional deviation in the reproductive system. Reproductive Health of a Woman. 2002;3:47-51.
11. Henriette's Herbal Homepage: <http://www.henriettes-herb.com/eclectic/kings/iris-vers.html>
12. Patudin AV, Mishchenko VS, Nechaev NP, Kosmodemyanskiy LV. Homeopathic medicines (reference book for doctors, pharmacists and pharmacists). Moscow, Astral; 1999:252.
13. Minina SA, Pryakhina NI, Chemesova II, Chizhikov DV. A pediatric medicinal preparation containing an extract of the milk-white iris (*Iris lactea*). Pharm Chem J. 2008;42:37-39.
14. Wang H, Cui Y, Zhao C. Flavonoids of the genus *Iris* (*Iridaceae*). Mini Rev Med Chem. 2010;10:643-661.
15. Iwashina T, Ootani S. Flavonoids of the genus *Iris*; structures, distribution and function: review. Ann Tsukuba Bot Gard. 1998;17:147-183.
16. Kaššák P. Secondary metabolites of the chosen genus *Iris* species. Acta Univ Agric Silv Mendelianae Brun. 2012;60:269-280.
17. Kukula-Koch W, Sieniawska E, Widelski J, Urjin O, Głowniak P, Skalicka-Woźniak K. Major secondary metabolites of *Iris* spp. Phytochem Rev. 2015;14:51-80.
18. Khare CP. Indian medicinal plants. Heidelberg: Springer-Verlag; Berlin; 2007:836.
19. Waddick JW, Yu-tang Z. *Iris* of China. Portland, Oregon; Timber Press; 1992:192.
20. Zatylnikova OA, Osolodchenko TP, Kovalev VN. Antimicrobial activity of extracts of *Iris pseudacorus* L. Annals of Mechnikov's Institute. 2010;4:43-47.
21. Roger B, Jeannot V, Fernandez X, Cerantola S, Chahboun J. Characterisation and quantification of flavonoids in *Iris germanica* L. and *Iris pallida* Lam. resinoids from Morocco. Phytochem Anal. 2012;23:450-455.
22. Deng G, Zhang X, Wang Y, Lin Y, Chen X. Chemical Composition and Antimicrobial Activity of the Essential Oil of *Iris pallida* Lam. Chemistry and Industry of Forest Products. 2008;28:7-12.
23. Zatylnikova OA, Kovalev VN, Kovalev SV. The study of yellow iris essential oils' components. Rastitelnye Resursy. 2013;49:233-240.
24. Kovalev VN, Mikhailenko OA, Vinogradov BA. Aromatic Compounds and Terpenoids of *Iris hungarica*. Chem Nat Compd. 2014;50:161-162.
25. Mykchailenko OA, Kovalyov VN, Kovalyov SV. Chromatography-mass spectrometric study of bioactive substances of rhizomes with roots of *Iris pseudacorus* f. *alba*. Farmaciya of Kazakhstan. 2015;3:38-41.
26. Mykhailenko OA. Analysis of essential oil of leaves of *Iris germanica* L. Science and Practice 2015: abstracts of the 6th International Pharmaceutical Conference (November 5-6th, 2015). Kaunas Lithuania. 2015;30-31. Available from: <http://botanika.vdu.lt/wp-content/uploads/2015/11/konferencijos-med%C5%BElagoje.pdf>
27. Mykhailenko OA, Kovalev VN. Chemical composition of essential oil from leaves of *Iris versicolor*. 6th International Symposium on the Chemistry of Natural Compounds (November 21-23th, 2013). Tashkent-Bukhara, Republic of Uzbekistan. 2013;280. Available from: https://drive.google.com/file/d/10XqiXqrVKacT8V24739wcuBgKIJVOQxq/viewhttp://www.academia.edu/25814098/ACETYLCHOLINESTERASE_INHIBITING_CHARACTERES_OF_Salvia_spp
28. Mykhailenko OA, Kovalev VN. Aromatic compounds and terpenoids of essential oil of several *Iris* species. IV International Scientific Conference of Young Researchers (April 29-30th, 2016). Azerbaijan, Baku. 2016;1:187-188. Available from: http://www.academia.edu/25636164/%C4%B0C%4%B0M%4%B0D%4%BOPLOMAT%4%B0YA_M%4%B0C%4%B0R_D%4%BOPLOMAT%4%B0YANIN_FORMASI_K%4%B0M%4%B0_pp_784-786
29. Isaev DI, Mikhailenko OA, Gurbanov GM, Kovalev VN. Constituents of Essential Oils from Azerbaijan *Iris medwedewii* and *I. carthaliniae* Rhizomes. Chem Nat Compd. 2016;52:748-750.
30. Bicchi C, Rubiolo P, Rovida C. Analysis of constituents of *Iris* rhizomes. Part II. Simultaneous SFE of irones and iridals from *Iris pallida* L. rhizomes. Flavour Fragr J. 1993;8:261-267.
31. Chernogorod LB, Vinogradov BA. Essential oils of some *Achillea* L. species, containing fragranol. Rastit. Resur. 2006;42:61-68.
32. Golembiovska O, Tsurkan A, Vynogradov B. Components of *Prunella vulgaris* L. Grown in Ukraine. J Pharmacogn Phytochem. 2014;2:140-146.
33. Bicchi C, Brunelli C, Cordero C, Rubiolo P, Galli M, Sironi A. Direct resistively heated column gas chromatography (Ultrafast module-GC) for high-speed analysis of essential oils of differing complexities. J Chromatogr A. 2004;1024:195-207.
34. NIST Mass Spec Data Center SES. Mass Spectra, 6th ed. National Institute of Standards and Technology; Gaithersburg MD; 2005.
35. NIST Mass Spec Data Center SES. Retention Indices, 6th ed. National Institute of Standards and Technology; Gaithersburg MD; 2005.
36. WILEY 2007. Available from: http://www.wiley.com/legacy/annual_reports/ar_2007/
37. State Pharmacopoeia of Ukraine. State Enterprise: Scientific and Expert Pharmacopoeial Centre. 1ed. Kharkov; 2001:556.
38. Al-Jaber HI. Variation in essential oil composition of *Iris nigricans* Dinsm. (*Iridaceae*) endemic to Jordan at different flowering stages. Arab J Chem. 2016;9:1190-1196.
39. Başer KHC, Demirci B, Orhan IE, Kartal M, Sekeroglu N, Sener B. Composition of Volatiles from Three *Iris* Species of Turkey. J of Essential Oil Rese. 2011;23:66-71.
40. Wagner H, Bladt S. Plant drug analysis. Berlin; Springer; 2001:384.
41. Nikolaevskii VV. Aromatherapy. Guide. Moscow; Meditsina; 2000:336.
42. Fischer-Rizzi S. Complete aromatherapy handbook: essential oils for radiant health. Sterling publishing company, Inc; USA; 1990:240.
43. Almaarri K, Abou Zedan TA, Albatat N. Chemical analysis of essential oils of some Syrian wild *Iris* species. Am J Biochem Mol Biol. 2013;3:38-49.
44. Gunstone FD. Fatty acids and lipid chemistry. London; Blackie Academic and Professional; 1996:547.
45. Plant lipids: biology, utilization and manipulation. In: Denis J, ed. Murphy. Wiley-Blackwell; 2005:403.
46. Kara N, Baydar H. Scent components in essential oil, resinoids and absolute of iris (*Iris florentina* L). Anadolu Tarım Bilim Derg. 2014;29:70-74.
47. Wren RC. Potter's New Cyclopaedia of Botanical Drugs and Preparations. London; C.W. Daniel Company Ltd; 1988:384.



Development and Characterization of Insulin-loaded Liposome-chitosan-Nanoparticle (LCS-NP) Complex and Investigation of Transport Properties Through a Pancreatic Beta Tc Cell Line

İnsülin Yüklü Lipozom-Kitosan-Nanopartikül (LCS-NP) Kompleksinin Geliştirilmesi ve Karakterizasyonu ve Pankreatik Beta Tc Hücre Hattından Geçiş Özelliklerinin Araştırılması

© Merve ÇELİK TEKELİ, © Çiğdem YÜCEL*, © Sedat ÜNAL, © Yeşim AKTAŞ

Erciyes University, Faculty of Pharmacy, Department of Pharmaceutical Technology, Kayseri, Turkey

ABSTRACT

Objectives: In recent years, studies on oral use have increased rapidly due to the restrictive aspects of parenteral administration of indispensable peptide-structured insulin in the rapidly growing worldwide treatment of diabetes. The aim of the study was to examine the development of a novel insulin-loaded LCS-NP complex, and its characterization and efficacy on pancreatic cells responsible for insulin release.

Materials and Methods: Blank liposomes and insulin-loaded LCS-NPs were prepared using dry film hydration and ionotropic gelation methods, respectively. The LCS-NP complex was prepared by mixing liposomes/NPs in a 2:1 (w/w) ratio. The cytotoxic effects of the various concentrations of insulin and formulation components on the pancreatic cell line were determined using a 3-(4,5-dimethylthiazol-2-yl)-2,5 diphenyl tetrazolium bromide assay and quantities to be used in the formulation were determined. Particle size, zeta potential, encapsulation efficiency, *in vitro* release profile and release kinetics, and transport properties of the prepared complex were investigated.

Results: The newly developed insulin-loaded LCS-NP complex had a particle size of $2.85\pm 0.035 \mu\text{m}$ and zeta potential of $8.11\pm 1.025 \text{ mV}$. The encapsulation yield was found as $48\pm 1.1\%$. *In vitro* insulin release from the complex was $80.9\pm 2.71\%$. Insulin transport from β Tc cells was 30.50% . Permeability coefficients ($\log k$) were calculated as -1.280 ± 0.070 for the insulin solution and -1.020 ± 0.062 for the insulin-loaded complex.

Conclusion: This study suggests that insulin could be successfully loaded into the newly developed LCS-NP complex, and it is thought that this complex carries an effective formulation potential for long-term efficacy in the treatment of diabetes.

Key words: Insulin, diabetes, chitosan nanoparticle, liposome-chitosan-nanoparticle complex

ÖZ

Amaç: Son yıllarda dünya çapında hızla artan diyabet tedavisinde vazgeçilmez peptid yapılı insülinin parenteral uygulamalarının kısıtlayıcı yönleri nedeniyle oral kullanıma yönelik çalışmalar hızla sürmektedir. Çalışmada amaç, insülin yüklü yeni geliştirilen LCS-NP komplekslerinin geliştirilmesi, karakterize edilmesi ve insülin salımından sorumlu pankreatik hücreler üzerinde etkinliğinin incelenmesidir.

Gereç ve Yöntemler: Boş lipozomlar film hidrasyon metodu ile, insülin yüklü kitozan NP'ler ise iyonik jelasyon metodu ile hazırlanmış ve fosfolipit/ NP 2:1 oranında karıştırılması ile kompleksler hazırlanmıştır. İnsülinin çeşitli konsantrasyonları ve formülasyon bileşenlerinin pankreatik hücre hattı üzerinde sitotoksik etkileri 3-(4,5-dimethylthiazol-2-yl)-difenil tetrazolium bromid testi ile belirlenmiş ve formülasyonda kullanılacak miktarları belirlenmiştir. Hazırlanan kompleksin karakterizasyonu (partikül büyüklüğü, zeta potansiyeli, enkapsülasyon etkinliği), *in vitro* salım profili ve salım kinetiği ve pankreatik hücreler üzerindeki geçiş özellikleri incelenmiştir.

Bulgular: Yeni geliştirilen insülin yüklü LCS-NP kompleks, $2.85\pm 0.035 \mu\text{m}$ partikül büyüklüğüne ve $8.11\pm 1.025 \text{ mV}$ zeta potansiyele sahiptir. Enkapsülasyon verimi, 48 ± 1.1 olarak bulunmuştur. Komplekslerden *in vitro* insülin salımı 80.9 ± 2.71 bulunmuştur. β Tc hücre hattından insülin geçişi 30.50 olarak elde edilmiştir. Permeabilite katsayıları ($\log k$) insülin çözeltisi için -1.280 ± 0.070 , insülin yüklü kompleksler için -1.020 ± 0.062 olarak hesaplanmıştır.

Sonuç: Sonuç olarak bu çalışma ile yeni geliştirilen LCS-NP kompleksine insülinin başarılı bir şekilde yüklenebildiği, bu kompleks yapının uzun süreli salım ile diyabet tedavisinde kullanılabilecek etkili formülasyon potansiyeli taşıdığı düşünülmektedir.

Anahtar kelimeler: İnsülin, diyabet, kitozan nanopartikülü, lipozom-kitozan-nanopartikül kompleksi

*Correspondence: E-mail: cigdemyucel85@gmail.com, Phone: +90 505 534 17 40 ORCID-ID: orcid.org/0000-0002-0622-5150

Received: 08.06.2017, Accepted: 27.07.2017

©Turk J Pharm Sci, Published by Galenos Publishing House.

INTRODUCTION

Diabetes mellitus is a metabolic disorder that results in hyperglycemia associated with abnormalities in carbohydrate, fat, and protein metabolism, and insulin deficiency due to beta cell loss.^{1,2} Insulin, a peptide hormone produced by pancreatic β -cells, is used for the treatment of diabetes by regulating glucose concentration in blood. Although insulin therapy is the oldest and most effective in diabetes, some limitations have occurred. Insulin is commonly used via the parenteral route, which provides immediate action. However, there are many disadvantages of the parenteral route including pain, discomfort, and hypoglycemic episodes associated with multi-dose injections, which cause poor patient compliance.³ Administration of therapeutic peptide drugs such as insulin via the oral route, especially the gastrointestinal tract, represents one of the greatest challenges. Colloidal drug carriers have been developed for controlled drug release and represent an exciting approach to increase the uptake and transport of orally-administered peptide drugs such as insulin.⁴ In addition, these systems have many advantages including a decrease in multi-dose injections, improved patient compliance, decrease in drug plasma level fluctuations in the blood and total drug use, increased bioavailability of some drugs, and minimize drug toxicity.⁵ Liposomes and polymeric nanoparticles (NP) are suitable colloidal carriers for insulin delivery and many investigations have been performed for administration routes e.g., parenteral, ocular, nasal, pulmonary, transdermal, oral and buccal. Liposomes are spherical vesicles consisting of cholesterol (CHOL) and nontoxic phospholipids that are biodegradable, biocompatible, and non-immunogenic colloidal carriers. They increase peptide stability with protecting bioactive agents from digestion in the stomach and show significant levels of absorption in the gastrointestinal tract.⁶ Polymeric NPs are solid colloidal nanocarriers that provide controlled release of peptides depending on surface modifications by biodegradable polymers. Chitosan (CS), a hydrophilic natural polymer, has been used in protein and peptide encapsulated NP formulation for its unique characteristics including biocompatibility, biodegradability and mucoadhesivity.^{7,8}

Cell culture is a laboratory process based on the survival of cells under controlled conditions while preserving their viability and shows *in vivo-in vitro* characteristics. The major advantages of using cell culture are the consistency and reproducibility of results that can be obtained from using a batch of cells and high *in vivo* correlation.⁹ (Yücel Ç. Development and investigation of efficiency of embryonic stem cell and insulin-loaded liposome, NP and cochleate formulations. Ph.D. Thesis, Gazi University, Institute of Health Sciences, Ankara, 2015:2-3).

In the present study, insulin was encapsulated in a liposome-CS-NP (LCS-NP) complex and *in vitro* characterization studies were performed on complexes including particle size, zeta potential, surface morphology, release and transport studies through pancreatic beta Tc (β Tc). Furthermore, *in vitro* cytotoxicities of insulin solution with different concentrations and formulation components on β Tc cells were evaluated.

EXPERIMENTAL

Materials

Insulin (Humulin R), (Humulin® R 100 IU/mL), CS hydrochloride (Protasan CL 110) and pentasodium tripolyphosphate, (TPP) were purchased from Lilly (USA), FMC Biopolymers (Norway) and Kimetsan (Turkey), respectively. Distearoylphosphatidylcholine, (DSPC) and CHOL were supplied by Sigma (St. Louis, USA). All other chemicals used were analytical grade. β Tc cell lines were obtained from the American Type Culture Collection (CRL-11506). Cell culture flasks surface area 25 cm² and 75 cm² and 6-well cell culture plates were purchased from Corning®. Fetal Bovine Serum, Trypsin-ethylenediaminetetraacetic acid solution, dimethyl sulfoxide for cell culture, penicillin-streptomycin solution and MTT [3-(4,5-dimethylthiazol-2-yl)-2,5 diphenyl tetrazolium bromide] were purchased from Sigma (St. Louis, USA). Cedex Smart Slides and Trypan Blue solution were purchased from Roche (Switzerland). The insulin mouse enzyme-linked immunosorbent assay (ELISA) kit was obtained from Sunredbio. Dulbecco's modified Eagle's medium (DMEM) was purchased from Capricorn Scientific, Germany.

Analytical method and calibration

Drug content in formulations was measured using ultraviolet-spectrophotometry (Shimadzu-UV 1800). Initially, the absorbance of insulin was determined at respective wavelength. Stock solution of insulin (100 μ g/mL) was diluted from an insulin market preparation with distilled water. Working standard solutions were prepared by diluting the stock solution in the concentration range of 0.5-100 μ g/mL for calibration curves. Spectrophotometric determination was carried out at 756 nm. The method was found to be linear ($r^2=0.9992$) and reproducible.

Preparation of chitosan nanoparticles (CS-NPs)

Blank and insulin-loaded CS NPs were prepared according to the ionotropic gelation process as described by Aktaş et al.¹⁰ The ratio of CS/TPP was established as 1:1 according to the preliminary studies. Blank nanoparticles were obtained upon the addition of a TPP aqueous solution (0.4 mg/mL) to a CS solution (1.75 mg/mL) stirred at room temperature on a magnetic stirrer for an hour. The same protocol was applied to obtain insulin-loaded LCS-NPs. The initial insulin amount was determined according to the preliminary drug loading studies.

Preparation of liposomes (LPs)

Blank liposomes were prepared using dry film hydration according to Bangham et al.¹¹ DSPC and CHOL were added to the round-bottomed flask in a 6:4 molar ratio and dissolved in chloroform. The organic solvent was then evaporated on a rotary evaporator (Heidolph) at -45°C . The resulting thin film was then hydrated with 10 mL water for 30 min and vortexed.

Preparation of the complexes

Blank and insulin-loaded LCS-NP complexes were formed by the combination of liposomes/nanoparticles at a 2:1 ratio (w/w) followed by lyophilization (Labconco) in the presence of 5.0% mannitol for 24 h.^{12,13} Finally, the lyophilized

powders were reconstituted with distilled water for their physicochemical characterization and encapsulation efficiency (EE) determination.

Characterization of the LCS-NP complexes

The surface morphologies of the blank and insulin-loaded complexes were determined using an inverted microscope (Zeiss Primo Star, Germany). Particle size and zeta potential were determined using a Malvern Zeta Sizer. The EE of insulin was determined after centrifugation at 14,000 rpm, for 25 min of the LCS-NP complex dispersions. The amount of free insulin in the supernatant was measured using the Lowry method at 756 nm.

$$EE (\%) = \frac{\text{theoretical total amount of insulin-free insulin}}{\text{theoretical total amount of insulin}} \times 100$$

In vitro release studies

LCS-NP complex were placed in a tube and 2 mL of pH 7.4 phosphate buffer was added as release medium. The tubes were immersed in a water bath ($37 \pm 0.5^\circ\text{C}$) with a horizontal shaker. At various time intervals, samples of 1.5 mL were withdrawn and replaced with equal volumes of fresh medium. The samples were centrifuged at 14,000 rpm, for 25 min. Insulin in the supernatant was measured using the Lowry method as described above.¹⁴

Cell culture studies

β Tc cells were grown in a medium composed of DMEM containing 25 mM glucose, 5 mM glutamine supplemented with 15% fetal bovine serum and 1% penicilin-streptomycin in an incubator at 37°C under 5% CO_2 atmosphere. The medium was replaced with fresh DMEM every 48 h. The presence of a confluent monolayer was checked using a microscope.

Cytotoxicity assay

The effect of the insulin solution and formulation components on cell viability was investigated using the MTT [3-(4,5-dimethylthiazol-2-yl)-2,5 diphenyl tetrazolium bromide] test.¹⁵ β Tc cells were seeded (20,000 cells/well) in 96-well culture plates and kept at 37°C for 24 h for cell adherence.¹⁶ Then, the cells were treated with various insulin concentrations (100-6.25 $\mu\text{g}/\text{mL}$) for 24 hours. The color intensity corresponding to cellular activity was measured at 570 nm using a multi-well ELISA reader.

Transport experiments

β Tc cells were seeded at 4×10^4 cells/well on polycarbonate membranes (Corning® 6 Well Transwell® Inserts) with a pore size of 0.4 μm .¹⁷ Insulin, blank, and insulin-loaded complexes were dissolved in medium for the donor compartment. 95% O_2 and 5% CO_2 were delivered to the system at 37°C to maintain cell

viability. Samples were collected from the receptor compartment after 30, 60, 120, 180, 240, 360, 480, 720, and 1440 min. The insulin content of the samples was analyzed using the Lowry method and an ELISA kit and the apparent permeability (P_{app}) value was calculated using the following equation:¹⁸

$$P_{app} = (dQ / dt) \times (1 / A \times C_0)$$

dQ/dt refers to the permeability rate, A (cm^2) is the membrane diffusion area, and C_0 (mg/mL) is the initial concentration of insulin in the donor compartment.

RESULTS

In vitro studies

The surface morphologies of the LCS-NP complexes are shown in Figure 1. The mean particle size and zeta potential of the LCS-NP complexes are shown in Table 1.

The extent of the *in vitro* insulin release from LCS-NP complexes for 24 h was found as 80.9%. Insulin release was found to be compatible RRSBW kinetics and the correlation coefficient was found as 0.8995, as shown in Figure 2.

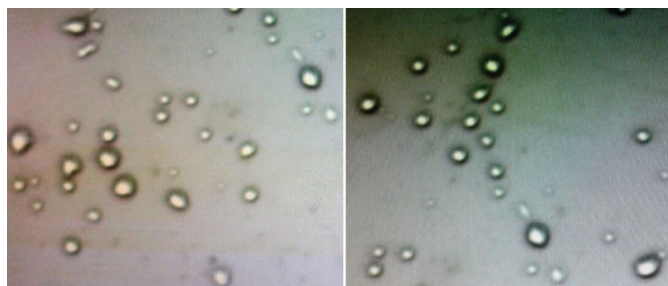


Figure 1. The surface morphologies of the LCS-NP complexes: Blank LCS-NP complex X40 (a), Insulin loaded LCS-NP complex X40 (b)

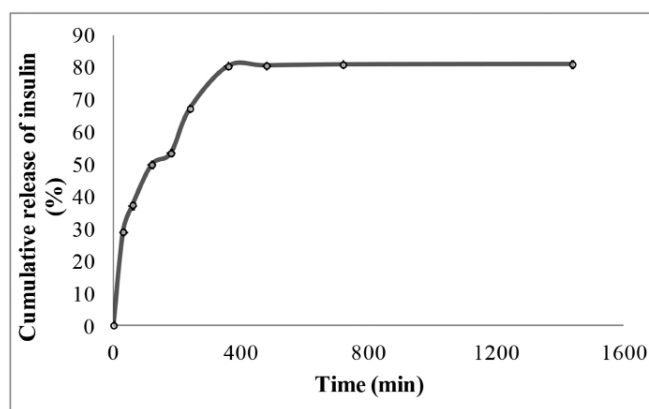


Figure 2. *In vitro* release profiles of insulin from LCS-NP complexes at pH 7.4 phosphate buffer (error bars represent standard deviations, n=3)

Table 1. Characterization parameters of the LCS-NP complexes (n=3)

Formulations	Particle size \pm SD (μm)	Zeta potential \pm SD (mV)	Encapsulation efficiency \pm SD (%)
Blank complex	3.25 \pm 0.083	10.40 \pm 2.411	-
Insulin loaded complex	2.85 \pm 0.035	8.11 \pm 1.025	48 \pm 11

LCS-NP: Liposome-chitosan-nanoparticle complex, SD: Standard deviation

Cell culture studies

The MTT assay was used to determine the toxic effects on β Tc cells. The effect of insulin solution, blank and insulin-loaded LCS-NP complexes on cell viability were investigated for 24 h. The wells containing only the medium were accepted as a positive control with a cell viability of 100%. The viability of cells as percentages is given on Figure 3.

Transport experiments of insulin from the solution and LCS-NP complex through β Tc cells were evaluated. The cumulative amounts of transported insulin from solution and LCS-NP complex at the end of the 24 hours were found as 37.46% and 30.50%, respectively. The results are presented in Figure 4. Papp (log k) values were calculated for insulin solution and LCS-NP complex (Table 2).

Table 2. Papp (log k) values was calculated from β Tc cell transport study results (n=3)

Samples	Log k values
Insulin solution	-1.280 \pm 0.070
Insulin LCS-NP complex	-1.020 \pm 0.062

LCS-NP: Liposome-chitosan nanoparticle complex

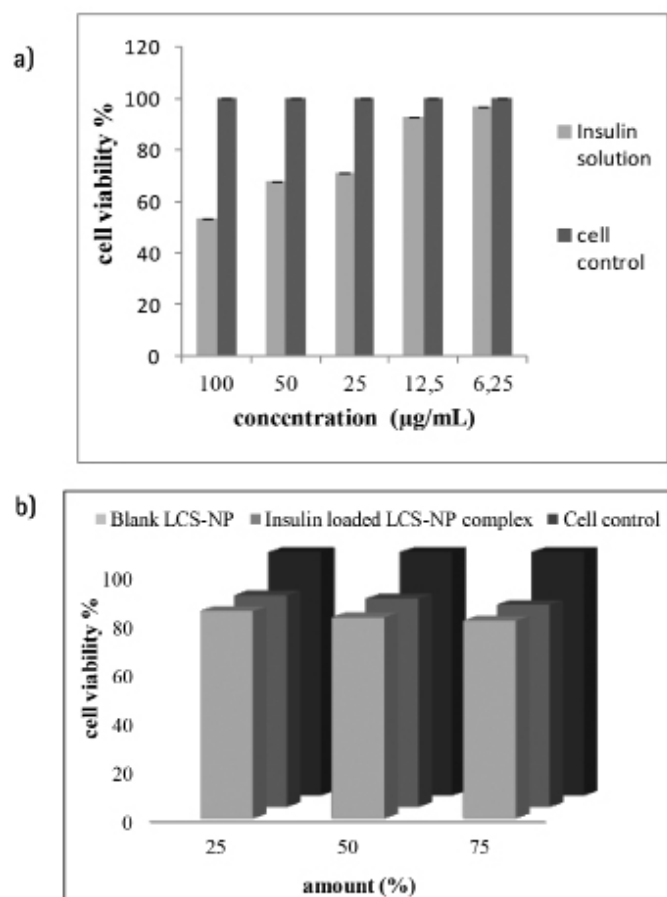


Figure 3. Cytotoxicity of various concentrations of insulin solutions (a) blank and insulin loaded LCS-NP complexes (b)

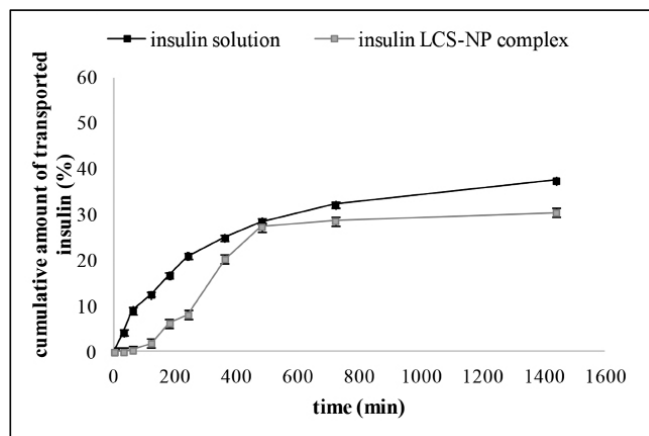


Figure 4. Cumulative amount of insulin from solution and LCS-NP complex transported through β Tc cells (error bars represent standard deviations, n=3)

LCS-NP: Liposome-chitosan-nanoparticle complex

DISCUSSION

Diabetes is a disease with an increasing prevalence in the world, which occurs as hyperglycemia due to a relative deficiency of the production of insulin by the pancreatic beta-cells.¹⁹ Insulin is a hydrophilic molecule, used in the treatment of diabetes mellitus that is commonly administered as multiple daily subcutaneous injections. Alternative routes for administration to improve patient compliance for insulin therapy have been investigated by designing drug delivery systems. Furthermore, various studies have been made on insulin-loaded drug delivery systems such as liposomes and polymeric micro/nanoparticles to improve bioavailability and provide long-term stability.^{20,21}

The aim of the present study was to combine the CS-NPs with the similarity of the liposomes to the biologic membranes to obtain a good alternative to insulin treatment. We developed and characterized insulin-encapsulated LCS-NP complexes to improve drug entrapment efficiency and evaluate their sustained efficiencies on pancreatic β Tc cell line.

In this study, blank liposomes and insulin-loaded CS-NPs were prepared using dry film hydration¹¹ and an ionotropic gelation process as described by Aktaş et al.,¹⁰ respectively. For the preparation of the LCS-NP complex, liposomes/nanoparticles at a 2:1 ratio (w/w) were used according to the method described by Carvalho et al.²¹ In the characterization studies, the mean particle size and zeta potential of blank and insulin-loaded LCS-NP complexes were found as 3.25 \pm 0.083 μm , 10.395 \pm 2.411 mV, 2.85 \pm 0.035 μm , and 8.115 \pm 1.025 mV, respectively. The encapsulating efficiency of the insulin-loaded LCS-NP complex was found as 48 \pm 0.1%, which is reported to be quite high.²² In the literature, Diebold et al.²³ developed and studied LCS-NPs, a class of colloidal system that combines liposomes and CS-NPs as a potential ocular drug delivery system, which had a mean size of from 407.8 \pm 9.6 to 755.3 \pm 30.0 nm and zeta potential of from +14.7 \pm 0.4 to +5.8 \pm 1.3 mV.

In another study, microspheres containing lipid/CS nanoparticle complexes were prepared for pulmonary delivery of therapeutic

proteins. Lipid and CS-NPs complexes had a particle size of approximately 2 μm and zeta potential of 2 mV.²⁴ Cui et al.⁴ prepared nanoparticles with biodegradable polymers such as poly(lactic acid), and poly(D,L-lactide-co-glycolide acid), loaded with an insulin-phospholipid complex for oral delivery. Spherical particles with a 200-nm mean diameter and a narrow size distribution were obtained.⁴ In another study, bioadhesive polysaccharide CS nanoparticles containing insulin were prepared by ionotropic gelation and particle size distributions and zeta potentials were determined. The ability of CS-NPs to enhance intestinal absorption of insulin and increase the relative pharmacologic bioavailability of insulin was investigated. The authors concluded that CS-NPs had shown an excellent capacity for the association of insulin. CS-NPs loading insulin showed a positive charge and rapid release kinetics *in vitro*. Also, obtaining a positive zeta potential is important for interaction with the negatively charged cell membrane. Therefore, our characterization findings appeared to be sufficient.^{8,25}

The *in vitro* release experiment was performed in pH 7.4 phosphate buffer. The medium for LCS-NP complex was selected as pH 7.4 phosphate buffer because the pH of DMEM (cell culture medium) was measured as 7.37 pH. The kinetic releases of insulin were found to be with RRSBW ($r^2=0.8995$) for insulin solution and LCS-NP complex. In this RRSBW kinetic, a steeper initial slope followed by a flattened tail in the final part was obtained.²⁶

For cytotoxicity studies, we used the MTT test, which is the most commonly used. The effects of insulin solution and formulation components on β Tc cell viability were investigated for 24 h. According to the MTT test results, insulin caused no cellular toxicity with the used dose of 33 $\mu\text{g}/\text{mL}$, which was decided as the encapsulated concentration in preparing CS-NPs. Additionally, blank and insulin-loaded LCS-NP complexes were also not found to be toxic to cells even at the highest concentrations (75%). In the literature, nanosystems have been designed consisting of CS nanoparticles and liposomes for ocular delivery. Diebold et al.²³ hypothesized that a combination of CS nanoparticles and liposomes would protect the peptide fluorescein isothiocyanate (FITC)-conjugated bovine serum albumin (BSA) from harsh environmental conditions while providing its sustained release. The authors showed that these complexes interacted with the mucus layer and transported the conjunctival cells. Furthermore, toxicity of the LCS-NP complexes in conjunctival cells was found very low.²³ Carvalho et al.²¹ developed nanosystems using the same method. They encapsulated insulin and (FITC)-conjugated BSA in LCS-NP complexes then evaluated these activities in conjunctival cells in *in vitro* cell culture studies. They also investigated activities of these complexes via the oral route and found that the complexes were well suited for controlled release with great stability in biologic fluids and provided a significant reduction in plasma glucose levels. They also found that the toxicity of LCS-NP complexes in conjunctival cells was found very low.²¹

The transport studies were performed for insulin solution and insulin-loaded LCS-NP complexes through pancreatic β Tc cells and permeability coefficients were calculated (Table 2).

Permeability coefficients (log k) were also calculated from solution and the LCS-NP complex and the lower value was -1.280 cm/h for insulin solution, the penetration value found for the insulin--loaded LCS-NP complex was -1.020 cm/h.

CONCLUSION

Although further experiments are warranted, these data indicate that LCS-NPs are potentially useful candidates for insulin delivery. Due to the similarities of liposomes in the cell membrane structures, LCS-NP complexes are able to penetrate more into the cells and are endocytosed more easily by the cells.

Conflict of interest: The authors declare that there are no conflicts of interest.

REFERENCES

1. Alberti KG, Zimmet PZ. Definition, diagnosis and classification of diabetes mellitus and its complications. Part 1: diagnosis and classification of diabetes mellitus provisional report of a WHO consultation. *Diabet Med.* 1998;15:539-553.
2. Swenne I. Pancreatic Beta-cell growth and diabetes mellitus. *Diabetologia.* 1992;35:193-201.
3. Elsayed AM. Oral Delivery of Insulin. In: Sezer AD, ed. *Recent Advances in Novel Drug Carrier Systems* 1th ed. Croatia; InTech; 2012:281-314.
4. Cui F, Shi K, Zhang L, Tao A, Kawashima Y. Biodegradable nanoparticles loaded with insulin-phospholipid complex for oral delivery: Preparation, *in vitro* characterization and *in vivo* evaluation. *J Control Release.* 2006;114:242-250.
5. Mukhopadhyay P, Mishra R, Rana D, Kundu PP. Strategies for effective oral insulin delivery with modified chitosan nanoparticles: A review. *Prog Polym Sci.* 2012;37:1457-1475.
6. Barenholz Y. Liposome application: problems and prospects. *Curr Opin. Colloid Interface Sci.* 2001;6:66-77.
7. Ding X, Alani AWG, Robinson JR. Extended release and Targeted Drug Delivery Systems. In: Troy DB, Beringer P, eds. *Remington: The Science and Practice of Pharmacy* 21st ed. USA; Lippincott Williams & Wilkins; 2006:939-964.
8. Pan Y, Li YJ, Zhao HY, Zheng JM, Xu H, Wei G, Hao JS, Cui FD. Bioadhesive polysaccharide in protein delivery system: chitosan nanoparticles improve the intestinal absorption of insulin *in vivo*. *Int J Pharm.* 2002;249:139-147.
9. Skelin M, Rupnik M, Cencic A. Pancreatic Beta Cell Lines and their Applications in Diabetes Mellitus Research. *ALTEX.* 2010;27:105-113.
10. Aktaş Y, Andrieux K, Alonso MJ, Calvo P, Gürsoy RN, Couvreur P, Capan Y. Preparation and *in vitro* evaluation of chitosan nanoparticles containing a caspase inhibitor. *Int J Pharm.* 2005;298:378-383.
11. Bangham AD, Standish MM, Watkins JC. Diffusion of univalent ions across the lamellae of swollen phospholipids. *J Mol Bio.* 1965;13:238-252.
12. Soppimath KS, Aminabhavi TM, Kulkarni AR, Rudzinski WE. Biodegradable polymeric nanoparticles as drug delivery devices. *J Control Release.* 2001;70:1-20.

13. Diop M, Auberval N, Viciglio A, Langlois A, Bietiger W, Mura C, Peronet C, Bekel A, Julien David D, Zhao M, Pinget M, Jeandidier N, Vauthier C, Marchioni E, Frere Y, Sigrist S. Design, characterisation, and bioefficiency of insulin-chitosan nanoparticles after stabilisation by freeze-drying or cross-linking. *Int J Pharm.* 2015;491:402-408.
14. Sajeesh S, Sharma CP. Cyclodextrin-insulin complex encapsulated polymethacrylic acid based nanoparticles for oral insulin delivery. *Int J Pharm.* 2006;325:147-154.
15. Fotakis G, Timbrell JA. *In vitro* cytotoxicity assays: comparison of LDH, neutral red, MTT and protein assay in hepatoma cell lines following exposure to cadmium chloride. *Toxicol Lett.* 2006;160:171-177.
16. Lapidot T, Walker MD, Kanner J. Antioxidant and prooxidant effects of phenolics on pancreatic beta-cells *in vitro*. *J Agric. Food Chem.* 2002;50:7220-7225.
17. Suzuki R, Okada N, Miyamoto H, Yoshioka T, Sakamoto K, Oka H, Tsutsumi Y, Nakagawa S, Miyazaki J, Mayumi T. Cyotomedical therapy for insulinopenic diabetes using microencapsulated pancreatic β cell lines. *Life Sci.* 2002;71:1717-1729.
18. Yücel C, Değim Z, Yılmaz Ş. Nanoparticle and liposome formulations of doxycycline: Transport properties through Caco-2 cell line and effects on matrix metalloproteinase secretion. *Biomed Pharmacother.* 2013;67:459-467.
19. Xu G, Stoffers DA, Habener JF, Bonner-Weir S. Exendin-4 stimulates both beta-cell replication and neogenesis, resulting in increased beta-cell mass and improved glucose tolerance in diabetic rats. *Diabetes.* 1999;48:2270-2276.
20. Vila A, Sanchez A, Tabio M, Calvo P, Alonso MJ. Design of biodegradable particles for protein delivery. *J Control Release.* 2002;78:15-24.
21. Carvalho EL, Grenha A, Remuñán-López C, Alonso MJ, Seijo B. Mucosal delivery of liposome-chitosan nanoparticle complexes. In: Düzgüneş N, ed. *Methods in Enzymology.* USA; Burlington: Academic Press; 2009:289-312.
22. Lasic DD. Novel applications of liposomes. *Trends Biotechnol.* 1998;16:307-321.
23. Diebold Y, Jarrín M, Sáez V, Carvalho EL, Orea M, Calonge M, Seijo B, Alonso MJ. Ocular drug delivery by liposome-chitosan nanoparticle complexes (LCS-NP). *Biomaterials.* 2007;28:1553-1564.
24. Grenha A, Remunan-Lopez C, Carvalho EL, Seijo B. Microspheres containing lipid/chitosan nanoparticles complexes for pulmonary delivery of therapeutic proteins. *Eur J Pharm Biopharm.* 2008;69:83-93.
25. Takeuchi H, Yamamoto H, Niwa T, Hino T, Kawashima Y. Enteral absorption of insulin in rats from mocoadhesive chitosan-coated liposomes. *Pharm Res.* 1996;13:896-901.
26. Özkan Y, Savaşer A, Özalp Y, İşimer A. Dissolution properties of different designed and formulated salbutamol tablet dosage forms. *Acta Pol Pharm.* 2000;57:271-276.



Screening Effects of Methanol Extracts of *Diplotaxis tenuifolia* and *Reseda lutea* on Enzymatic Antioxidant Defense Systems and Aldose Reductase Activity

Diplotaxis tenuifolia ve *Reseda lutea* Metanol Özütünün Antioksidan Savunma Sistemi Enzimleri ve Aldoz Redüktaz Aktivitesi Üzerinde Olan Etkisinin İncelenmesi

© Khalid Sharro ABDALRAHMAN¹, © Merve Gülşah GÜNEŞ¹, © Naznoosh SHOMALI^{1*}, © Belgin Sultan İŞGÖR², © Özlem YILDIRIM¹

¹Ankara University, Faculty of Science, Department of Biology, Ankara, Turkey

²Atılım University, Faculty of Engineering, Department of Chemical Engineering and Applied Chemistry, Ankara, Turkey

ABSTRACT

Objectives: The aim of the study was to investigate the effects of methanol extracts from the flowers and leaves of *Diplotaxis tenuifolia* and *Reseda lutea* on the activity of AR, CAT, GST, and GPx.

Materials and Methods: Total phenolic and flavonoid contents of the plant samples were evaluated using Folin-Ciocalteu reagent and aluminum chloride colorimetric methods. Also, the effects of extracts on CAT, GST, GPx, and AR enzyme activities were investigated using kinetic assays.

Results: The highest phenolic and flavonoid contents were detected in the methanol extract of *D. tenuifolia* leaves with 144.49±0.29 mg gallic acid equivalent/L and 250.485±0.002 quercetin equivalent/L, respectively. The best activity profile for GST and GPx were observed in the extract of leaves belonging to *D. tenuifolia* with IC₅₀ values of 121±0.05 and 140±0.001 ng/mL, respectively. According to the results, methanol extracts from leaves of *R. lutea* and *D. tenuifolia* showed no significant activity potential on AR. Moreover, none of the studied extracts demonstrated any reasonable CAT activation potential.

Conclusion: The results indicated that leaves of *D. tenuifolia* had good effect on the antioxidant enzymatic defense system, which it makes it a good constituent of the daily diet.

Key words: *Diplotaxis tenuifolia*, *Reseda lutea*, antioxidant enzymes, aldose reductase

ÖZ

Amaç: Bu çalışmada *Diplotaxis tenuifolia* ve *Reseda lutea*'nın çiçek ve yapraklarından elde edilmiş olan metanol özütlerinin AR, CAT, GST ve GPx enzimlerinin aktiviteleri üzerinde olan etkilerinin araştırılması amaçlanmıştır.

Gereç ve Yöntemler: Bu çalışmada, bitki örneklerinin toplam fenolik ve flavonoid içeriği; Folin-Ciocalteu ve alüminyum klorür reaktiflerinin yardımıyla kolorimetrik yöntemlerle değerlendirilmiştir. Ayrıca özütlerin CAT, GST, GPx ve AR enzimlerinin aktiviteleri üzerindeki etkileri kinetik analizler ile araştırılmıştır.

Bulgular: En yüksek miktarda fenolik ve flavonoid içeriği sırasıyla 144.49±0.29 mg galik asit eş değeri/L ve 250.485±0.002 quercetin eş değeri/L tespit edilmiştir. GST ve GPx için en iyi aktivite profilleri sırasıyla 121±0.05 ve 140±0.001 ng/mL IC₅₀ değerleri ile *D. tenuifolia* yaprak özütünde gözlemlenmiştir. Elde edilen sonuçlara göre, *R. lutea* ve *D. tenuifolia*'nın yapraklarından elde edilen metanol özütleri, AR enzimi üzerinde önemli ölçüde bir aktivite potansiyeli göstermemiştir. Bununla beraber, çalışılmış olan çiçek ve yaprak özütlerinin hiçbirisi yeterli düzeyde CAT aktivasyonu gösterememiştir.

Sonuç: Çalışma sonucunda, *D. tenuifolia*'nın yapraklarının antioksidan enzimatik savunma sistemi üzerinde iyi bir etkiye sahip olduğu gösterilmiştir. Bu sebeple günlük diyet için iyi bir besin kaynağı olarak kabul edilebilir.

Anahtar kelimeler: *Diplotaxis tenuifolia*, *Reseda lutea*, antioksidan enzimler, aldoz redüktaz

*Correspondence: E-mail: naznoosh_shomali@yahoo.com, Phone: +90 554 281 63 36 ORCID-ID: orcid.org/0000-0002-7366-1569

Received: 18.01.2017, Accepted: 16.03.2017

©Turk J Pharm Sci, Published by Galenos Publishing House.

INTRODUCTION

Reactive oxygen species (ROS) is a term used to describe a number of reactive molecules and free radicals derived from molecular oxygen, which are generated by all aerobic species. These molecules are generated as by-products during the mitochondrial electron transport of aerobic respiration or by oxidoreductase enzymes and metal catalyzed oxidation. In normal physiologic conditions, a number of defense mechanisms have evolved to provide a balance between the production and removal of ROS, but alterations of the balance between ROS production and the capacity to detoxify reactive intermediates lead to oxidative stress. It has been caused to a wide variety of states, processes and metabolic diseases such as heart disease, severe neural disorders such as Alzheimer's and Parkinson's, and some cancers.^{1,2} Under oxidative stress, an organism has a variety of defense mechanisms to prevent or neutralize negative ROS effects. These are mainly based on enzymes such as catalase (CAT), superoxide dismutase (SOD), glutathione peroxidase (GPx), glutathione reductase (GR), and glutathione-S-transferase (GST) or non-enzymatic components such as vitamin E, vitamin C, glutathione, and flavonoids.³ GST is one of the phase II enzymes and plays a critical role in the detoxification and metabolism of many xenobiotic compounds.⁴ GPx has an important role as a catalyst in the reduction of hydro peroxides, including hydrogen peroxides (H_2O_2), by using GSH. GPx also functions to protect the cell from oxidative damage. Several studies related dysfunctional GPx with cancer.⁵ CAT is a very important enzyme of living organisms, which catalyzes the decomposition of H_2O_2 to water and oxygen. Aldose reductase (AR) is a nicotinamide adenine dinucleotide phosphate (NADPH)-dependent enzyme and it has been implicated in the formation of cancer and diabetic complications such as retinopathy, neuropathy, nephropathy, and cardiovascular disorders.⁶

Plants synthesize a vast range of organic compounds that are traditionally classified as primary and secondary metabolites. Primary metabolites are compounds that have essential roles associated with photosynthesis, respiration, growth, and development. Other phytochemicals that accumulate in high concentrations in some species are known as secondary metabolites, which possess antioxidant activity. Antioxidant compounds found in different parts of plants involve phenolics, flavonoids, alkaloids, glycosides, tocopherols, carotenoids, and ascorbic acid. These are structurally diverse and many are distributed among a very limited number of species within the plant kingdom.⁷ Secondary metabolite compounds have played an important role in treating and preventing human diseases. They are important sources for new drugs and are also suitable lead compounds for further modification during drug development.⁴

Diplotaxis tenuifolia (L.) DC., commonly known as 'wild rocket', belongs to the *Brassicaceae* family. It was originally found as a crop in Mediterranean and Middle Eastern countries and became popular largely due its pungent aromas and tastes.⁸ In Turkish folk medicine, *D. tenuifolia* is known as "Yabani Roka" and widely distributed in North and West parts of Turkey.

Phytochemical studies show that the aerial parts of *D. tenuifolia* contain significantly high concentration of flavonoids, tannins, glucosinolates, sterols, and vitamin C.⁹

The genus *Reseda* is one of the herbs in the *Resedaceae* family. In Turkey, this genus is represented by 15 species including *Reseda lutea* L. and *Reseda luteola* L. It is known as yellow mignonette or wild mignonette and has economic importance. It is widely used in the carpet and rug industry as a source of natural dye due to its high luteolin content. In addition to its staining properties, luteolin has attracted great scientific interest because of its pharmacologic activities. Luteolin displays numerous anti-inflammatory effects at micromolar concentrations, which cannot be completely explained by its antioxidant capacities. In addition, phytochemical analysis of aerial parts of *R. lutea* has shown the presence of flavonoid, anthocyanin, and glucosides.¹⁰

The aim of the present study was to evaluate the total amount of the phenolic and flavonoid contents of methanol extract obtained from the flowers and leaves of *D. tenuifolia* and *R. lutea* and to determine their effects on the activity of AR, CAT, GST, and GPx. These enzymes play critical roles in the antioxidant defense system.

EXPERIMENTAL

Chemicals materials

In this study, 4-aminoantipyrine, H_2O_2 and sodium azide (NaN_3) were provided by Acros, USA. Ethylenediaminetetraacetic acid (EDTA), Folin-Ciocalteu reagent, reduced glutathione (GSH), GR, horseradish peroxidase, CAT, gallic acid (GA), and quercetin hydrate were supplied by Sigma Aldrich, Germany. Lithium sulphate (Li_2SO_4) and NADPH were purchased from Gerbu, Germany. All other chemicals used were analytical grade and provided by Sigma Aldrich, Germany.

Plant materials

Plant samples of *D. tenuifolia* and *R. lutea* were harvested in July 2010 from Ankara, Turkey, and were authenticated by Prof. Dr. Fatmagül Geven, in the Department of Biology, Ankara University. The plant specimens with their localities and the necessary field records were recorded and numerated as voucher specimen numbers. The voucher numbers of *D. tenuifolia* and *R. lutea* were FG-2010-10 and FG-2010-13, respectively. They were deposited in the herbarium department at Ankara University.

Extraction of plant

Different parts of fresh plant samples (flowers and leaves) were washed with tap water and dried at room temperature before analysis. For methanol extraction, 2 g of dried samples were weighed and ground into a fine powder with liquid nitrogen, then mixed with 20 mL methyl alcohol at room temperature in 160 rpm for 24 h. The obtained extract was filtered over Whatman No. 1 paper and the filtrate was collected. Methanol was then removed using a rotary evaporator at 40°C to obtain a dry extract. The obtained product was dissolved in DMSO and kept in the dark (4°C) to be prevent oxidative damage until analysis.¹¹

Total phenolics determination

The total phenolic content of the plant extracts was determined using the method of Slinkard and Singleton.¹² Each plant extract solution (0.1 mL) was mixed with 2 mL of a 2% (w/v) sodium carbonate solution and vortexed strongly. After 5 min, 0.1 mL of 50% Folin-Ciocalteu's reagent (w/v) was added and vortexed, then incubated for 1 hr at room temperature. Afterwards, the absorbance of each mixture was measured at 750 nm using an ultraviolet (UV) spectrophotometer (HP 8453 A, USA). Results were evaluated using 50, 100, 200 and 400 mg/L of GA as a standard curve and recorded as milligrams (mg) GA equivalent/L of extract.

Total flavonoid determination

The total concentration of flavonoids in the extracts was determined using aluminum chloride colorimetry, which was previously described¹³; 0.1 mL of each plant extract was separately mixed with 0.15 mL of 95% ethanol, 0.01 mL of 10% aluminum chloride, 0.01 mL of 1 M sodium acetate, and 0.25 mL of DMSO. The mixture was incubated at room temperature for 30 min and the absorbance of the reaction was measured at 415 nm with the UV spectrophotometer (HP 8453 A, USA). A standard curve was calculated by preparing quercetin solutions at different concentrations for 25, 50, 100, 150, and 200 mg/L. The total flavonoid content of the extract was expressed as milligrams (mg) quercetin equivalent/L of extract.

Isolation of cytosol from bovine liver

Bovine liver was obtained from a slaughterhouse in Kazan, Ankara, Turkey. The liver samples were homogenized in 10 mM potassium phosphate buffer (pH 7.0), containing 0.15 M KCl, 1.0 mM EDTA, and 1.0 mM of DTT, using a glass Teflon homogenizer and then centrifuged at 10,000 *g* for 20 min. The supernatant was filtered through cheesecloth and the filtrate was centrifuged at 30,000 *g* for 60 min. The collected supernatants were filtered again and the resultant filtrate was considered as cytosol.¹⁴ The prepared homogenates, containing 46.41 mg protein/mL, were kept in ultra-low freezer (-80°C) for future use. The total protein content was determined using the Lowry method.¹⁵

Isolation of aldose reductase from bovine liver

Bovine liver was obtained from a slaughterhouse in Kazan, Ankara, Turkey. The liver samples were cut into small pieces and washed with 1.0 mM EDTA. It was then weighed and homogenized with threefold 1.0 mM EDTA 50 μ M PMSF and centrifuged at +4°C, 10,000 rpm for 30 min. To obtain a 40% saturation, 22.6 g ammonium sulfate was added to every 100 mL supernatant solution and mixed for 5 min on a magnetic stirrer and then centrifuged at +4°C, 10,000 rpm for 25 min. To obtain 50% and 75% saturations, the previous method was repeated adding 5.8 g and 15.9 g of ammonium sulfate to the 100 mL supernatant solution, respectively. The obtained pellets were dissolved with 50 mM sodium chloride and kept in a deepfreeze at -80°C.¹⁶

Assay of glutathione-S-transferase

GSTs activity was determined against the substrate 1-chloro-2,

4-dinitrobenzene (CDNB), by monitoring thioether formation at 340 nm.¹⁷ Briefly described, the assay mixture containing plant extracts solution (final concentration in the range of 7-476 ng/mL), 200 mM potassium phosphate buffer (pH 6.5) with 50 mM CDNB and 3.2 mM GSH, and bovine liver cytosolic fractions (0.782 mg protein/mL) was prepared and used as the enzyme source to measure GST activity. GSH-CDNB conjugate formation was followed in a 250- μ L total volume assay using a multimode microplate reader (Specra Max M2e, USA) at 340 nm for 240 seconds. The initial rates of enzymatic reactions were determined as nanomoles of the conjugation product of GSH and reported as nmol/min/mg protein.

Assay of aldose reductase

AR activity was determined against the substrate, DL-Glyceraldehyde, by monitoring the oxidation of NADPH to NADP⁺ at 340 nm.¹⁸ In brief, the assay mixture consisting of plant extract (5 μ L) solution (final concentration in the range of 7-476 ng/mL), AR (4.54 mg/mL Li₂SO₄ (320 mM-400 mM), NADPH (9 \times 10⁻⁵ M) KP buffer (50 mM, pH 6.2), DL-GA (6 \times 10⁻⁴ M) was prepared and used as the enzyme source to measure AR activity. NADP⁺ oxidation was followed in 0.25 mL total volume assay using a multimode microplate reader at 340 nm for 4 min. The initial rates of enzymatic reactions were determined and reported as nmol/min/mg protein.

Assay of glutathione peroxidase

GPx activity was measured using a previously reported method.^{19,20} Also, GPx activity was measured against the substrate, tertiary butyl hydro-peroxide (t-BuOOH), and the decrease in NADPH was monitored at 340 nm. GPx activity changes were measured using purified GPx (37.5 \times 10⁻³ U/mL) and plant extracts (7-476 ng/mL) or control (DMSO alone), with 2.0 mM GSH, 0.25 mM NADPH, GSH-reductase (GR, 0.5 unit/mL) and 0.3 mM t-BuOOH, in 50 mM Tris-HCl (pH=8.0). The reaction was initiated by adding GPx and the change in absorbance was recorded at 340 nm for 5 min using a multimode microplate reader.

Assay of catalase

CAT inhibition was determined by monitoring a red quinoneimine dye remaining H₂O₂.^{21,22} The assay was miniaturized for microplate application and contained plant extraction solutions with a final concentration in the range of 7-476 ng/mL, 50 mM phosphate buffer (pH 7.0), 20 U/mL purified bovine liver CAT, and 0.0961 mM H₂O₂. The reaction was stopped using NaN₃ and incubated at room temperature for 5 min, followed by incubation with chromogen at room temperature for 40 min and then the absorbance was read at 520 nm. The enzyme activity was calculated with respect to the H₂O₂ remnant, which was determined using a calibration curve constructed in the range of 9.61-307.6 μ M H₂O₂.

Data analysis

The data analysis was performed using the Graphpad Prism 6.0 software. The activity of extracts against enzyme targets was calculated as 50% inhibitory concentration (IC₅₀) values obtained from dose-response curves. The enzyme calibration

and the dose-response curve construction were accomplished using 2-3 independent experiments, each in duplicate or triplicate using a multimode microplate reader, in 96-well microplates.

RESULTS

Each extract was prepared by dissolving 2 g of dry samples in 20 mL of methanol. The extraction yields for *D. tenuifolia* leaf samples was 13.02%, and 10.15% and 6.02% for *R. lutea* flower and leaf samples, respectively (Table 1).

The total phenolic contents of extracts were determined by using Folin-Ciocalteu's method. Additionally, the total amount of flavonoids in extracts were determined using aluminum chloride colorimetry. According to the results, the methanol extract of *D. tenuifolia* leaves has a high amount of total phenolic and flavonoid contents. The results of total phenolic and flavonoid contents of the methanol extracts of the plant samples are listed in Table 1.

The activation percent profile of GST, GPx, CAT, and AR enzymes and IC₅₀ values of the methanol extracts of plant samples are presented in Table 2. GST activity was determined against the substrate, CDNB, by monitoring the thioether formation at 340 nm. In order to calculate the percentage of GST activity and IC₅₀ values, the utilized final concentration of plant extracts in the assay was taken between 7-476 ng/mL. According to the results, which are presented in Table 2, the best activity effect was exhibited in the crude methanol extract of *D. tenuifolia* leaves with IC₅₀ value of 121±0.05 ng/mL.

The activity of GPx was determined as the amount of enzyme that converted 1 μM of NADPH per min in 1 mL which is expressed as U/mg of total protein. The final concentration of plant extracts within concentration range of 7-476 ng/mL were used in the assay to calculate the percentage of GPx activity and IC₅₀ values. The best activity profile for GPx was observed in the extract of leaves belonging to *D. tenuifolia* with an IC₅₀ value of 140±0.001 ng/mL.

AR activity was determined using the substrate DL-Glyceraldehyde, by monitoring the oxidation of NADPH to NADP⁺ at 340 nm. The methanol extracts from leaves of *R. lutea* and *D. tenuifolia* showed no significant activity with AR (Table 2). In addition, none of the studied extracts showed reasonable CAT activity potential.

DISCUSSION

The aim of the present study was to evaluate the total amount of the phenolic and flavonoid contents of methanol extract obtained from the flowers and leaves of *D. tenuifolia* and *R. lutea*. Furthermore, it was aimed to determine the effects of the extract on the activity of AR, CAT, GST and GPx. Phenolic compounds have at least one or more aromatic rings with one or more hydroxyl groups attached.²³ Many phenolic compounds and flavonoids have been reported to have potential for antioxidant, anticancer, anti-atherosclerotic, antibacterial, antiviral, and anti-inflammatory activities.²⁴ Flavonoids are phenolic compounds found throughout the plant kingdom. They have been shown to possess a variety of biologic activities in organisms. Many flavonoids possess antitumor, anti-proliferation, cell cycle arrest, induction of apoptosis and differentiation, inhibition of angiogenesis, antioxidant and reversal of multidrug resistance activities.²⁵⁻²⁷ Different studies have shown that plant extracts with high polyphenol contents are known as a good source of antioxidant activity.²⁸⁻³⁰

In this study, for the first time, it was shown that the methanol extract from leaves of *D. tenuifolia* contains a high amount of total phenolic and flavonoid compounds. The results indicated that the methanol extract from the leaves of *D. tenuifolia* had a significant effect on GST and GPx activities. Therefore, it can be said that the leaves of *D. tenuifolia* have a good effect on the antioxidant enzymatic defense system. However, it is found that the leaf extracts of *D. tenuifolia* had no effect on AR and CAT activities. It was also demonstrated that the methanol extract from leaves of *R. lutea* contained more phenolic and flavonoid

Table 1. The percentage yield of dry products obtained from methanol extraction procedure with total polyphenol and flavonoid contents of each plant sample

Family	Species	Parts of plants	% yield	TPC mg GAE/L	Flavonoid mgQE/L
Brassicaceae	<i>Diplotoxis tenuifolia</i>	Leaves	13.02	144.49±0.29	250.485±0.002
Resedaceae	<i>Reseda lutea</i>	Flowers	10.15	109.01±0.03	78.72±0.03
		Leaves	6.02	133.52±0.02	196.80±0.01

Table 2. Glutathione-S-transferase, glutathione peroxidase, catalase, and aldose reductase percentage activities

Family	Species	Parts of plants	GST		GPx		CAT		AR	
			%	IC ₅₀ ng/mL	%	IC ₅₀ ng/mL	%	IC ₅₀ ng/mL	%	IC ₅₀ ng/mL
Brassicaceae	<i>Diplotoxis tenuifolia</i>	Leaves	72	121±0.05	84	140±0.001	ND	ND	5	231±0.0
Resedaceae	<i>Reseda lutea</i>	Flowers	36	149±0.004	84	490±0.05	ND	ND	ND	ND
		Leaves	70	403±0.015	ND*	ND	ND	ND	20	601±0.002

ND: Not determined, GST: Glutathione-S-transferase, GPx: Glutathione peroxidase, CAT: Catalase, AR: Aldose reductase

contents than its flower samples. However, the flower extract of *R. lutea* showed good effects on GPx activity than the leaf extract and the opposite of this situation was seen in the GST results.

In a previous study, *D. tenuifolia* was analyzed for active compounds and antitumor actions on colorectal cancer cells. The results showed that *D. tenuifolia* was a good source of carotenoids, phenolics, and glucosinolate compounds. It also has antitumor activities on colorectal cancer.³¹ Marrelli et al.³² evaluated thirteen hydro alcoholic extracts of edible plants from Southern Italy for their *in vitro* antioxidant and antiproliferative activity on breast cancer MCF-7, hepatic cancer HepG2, and colorectal cancer LoVo. They showed that the lowest antioxidant activity was exhibited by *D. tenuifolia* (DT) extract. In addition, the authors reported that *D. tenuifolia* extract was able to induce an inhibitory activity of cell proliferation of more than 40%.

In another study, the polyphenol content and biologic activities of the main component of *D. simplex* extract was investigated. The analyzed extracts showed that flower extracts exhibited a potent *in vitro* antioxidant capacity using oxygen radical absorbance capacity and displayed a strong anti-inflammatory activity and inhibited nitric oxide release. The findings suggested that the *Diplotaxis* flower was a valuable source of antioxidants and anti-inflammatory agents.³³ Durazzo et al.³⁴ studied the nutritional and antioxidant properties of wild rocket [*D. tenuifolia* (L.) DC.]. The authors determined the bioactive molecular content (vitamin C, quercetin, lutein) and showed bioactivity of polyphenolic extracts from the edible part of rocket in Caco-2 cells. Atta et al.³⁵ isolated five main flavonoid glycosides from the ethanol extract of *D. harra* and identified them as quercetin, isorhamnetin 3-rhamnoside, isorhamnetin 3-*o*-rutinoside, isorhamnetin 3-glucosyl-4-rhamnoside and isorhamnetin 3-*o*- β -glucoside. They also evaluated the alcoholic extract of plants against some bacterial strains that showed moderate antibacterial activity. Martínez-Sánchez et al.⁹ studied antioxidant compounds, flavonoids, and vitamin C, and also the antioxidant activity of four species from *Brassicaceae* vegetables used for salads such as watercress (*Nasturtium officinale*), mizuna (*Brassica rapa*), wild rocket (*D. tenuifolia*), and salad rocket (*Eruca sativa*). They analyzed the characterization of phenolic compounds and they showed that the leaves of watercress, mizuna, wild rocket, and salad rocket, presented high contents of antioxidant compounds such as flavonoids and vitamin C. Therefore, they are good dietary sources of antioxidants with an important variability of bioactive compounds.

However, no pharmacologic studies have been performed with *R. lutea* extracts to date, but *Reseda* species have been reported to possess various pharmacologic properties such as anti-inflammatory, antioxidant, antibacterial, and antimicrobial effects. For the first time, Benmerache et al.³⁶ isolated six flavonoids from the aerial parts of *R. phyteuma*. They also found that the butanolic extract exhibited good antioxidant and antimicrobial activities. *R. luteola* L. has been used as a dye due to its high luteolin content since ancient times. Woelfl et al.³⁷

determined anti-proliferative and apoptosis-inducing effects of the *R. luteola* extract RF-40. They found that it contained 40% flavonoids, primarily luteolin, luteolin-7-*O*-glucoside, and apigenin. Further, it was observed that the isolated flavonoids dose-dependently inhibited cell proliferation and induced apoptotic oligonucleosomes in PHA-stimulated peripheral blood mononuclear cells. Moreover, they showed that *Reseda* extract was an interesting raw material dyeing purposes and for further pharmacologic investigation. In another study, Berrehal et al.³⁸ investigated the methanolic and n-butanolic extracts of *R. duriaeana* and *R. villosa* for their antioxidant activity. The authors indicated that the methanolic and n-butanolic extracts of *R. duriaeana* exhibited better antioxidant activity than the respective extracts of *R. villosa*. This may be explained by the presence of more quercetin derivatives in *R. duriaeana*.

From a consideration of ethnobotanical information, seeds of 45 Scottish plant species were obtained from authentic seed suppliers. The n-hexane, dichloromethane (DCM), and methanol (MeOH) extracts were assessed for free radical scavenging activity in a DPPH assay. The results showed that the methanol extract of *R. lutea* seeds exhibited moderate levels of free radical scavenging activity. Also, the n-hexane extract was much less active than the MeOH and DCM extracts.³⁹ Tawaha et al.⁴⁰ determined the relative levels of antioxidant activity and the total phenolic content of aqueous and methanolic extracts of a total of 51 Jordanian plant species. They indicated that the aqueous and methanolic extracts of *R. lutea* had remarkably high total phenolic contents and showed good levels of antioxidant activity.

CONCLUSION

In conclusion, the biologic potential of *D. tenuifolia* and *R. lutea* on the antioxidant defense system such as GST, GPx, CAT, and AR were considered in this research. It was shown that the methanol extract of *D. tenuifolia* leaves had a high amount of phenolic and flavonoid compounds. Also, it is indicated that it has good activity potential on GPx and GST. These results might be related to the high content of phenolics and flavonoids found in the species. This work highlights the importance of *D. tenuifolia* as a part of the daily diet.

ACKNOWLEDGEMENTS

This study was supported by the grant from The Coordination of Scientific Research Projects of Ankara University awarded to Prof. Dr. Özlem Yıldırım (Grant No:13L4240008).

Conflict of Interest: No conflict of interest was declared by the authors.

REFERENCES

1. Hancock JT, Desikan R, Neill SJ. Role of Reactive Oxygen Species in Cell Signaling Pathways. *Biochem Soc Trans.* 2001;29:345-350.
2. Ye ZW, Zhang J, Townsend DM, Tew KD. Oxidative stress, redox regulation and diseases of cellular differentiation. *Biochim Biophys Acta.* 2015;1850:1607-1621.

3. Lushchak VI. Free radicals, reactive oxygen species, oxidative stress and its classification. *Chem Biol Interact.* 2014;224:164-175.
4. Ata A, Van den Bosch SA, Harwanik DJ, Pidwinski GE. Glutathione S-transferase- and acetylcholinesterase-inhibiting natural products from medicinally important plants. *Pure and Appl Chem.* 2007;79:2269-2276.
5. Hu YJ, Diamond AM. Role of glutathione peroxidase 1 in breast cancer: loss of heterozygosity and allelic differences in the response to selenium. *Cancer Res.* 2003;63:3347-3351.
6. Lee EH, Song DG, Lee JY, Pan CH, Um BH, Jung SH. Inhibitory Effect of the Compounds Isolated from *Rhus verniciflua* on Aldose Reductase and Advanced Glycation Endproducts. *Biol Pharm Bull.* 2008;31:1626-1630.
7. Croteau R, Kutchan TM, Lewis NG. Natural products (secondary metabolites). *Biochemistry and Molecular Biology of Plant.* 2000;24:1250-1318.
8. Bell L, Wagstaff C. Glucosinolates, Myrosinase Hydrolysis Products, and Flavonols Found in Rocket (*Eruca sativa* and *Diplotaxis tenuifolia*). *J Agric Food Chem.* 2014;62:4481-4492.
9. Martínez-Sánchez A, Gil-Izquierdo A, Gil MI, Ferreres F. A Comparative Study of Flavonoid Compounds, Vitamin C, and Antioxidant Properties of Baby Leaf *Brassicaceae* Species. *J Agric Food Chem.* 2008;56:2330-2340.
10. Radulovic NS, Zlatkovic DB, Ilic-Tomic T, Senerovic L, Nikodinovic-Runic J. Cytotoxic effect of *Reseda lutea* L.: A case of forgotten remedy. *J Ethnopharmacol.* 2014;153:125-132.
11. Moghaddam NS, Isgor BS, Isgor YG, Geven F, Yildirim O. The Evaluation of Inhibitory Effects of Selected Plant Extracts on Antioxidant Enzymes. *Fresenius Environmental Bulletin.* 2015;24:63-70.
12. Slinkard K, Singleton VL. Total phenol analyses: Automation and comparison with manual methods. *Am J Enol Vitic.* 1977;28:49-55.
13. Chang CC, Yang MH, Wen HM, Chern JC. Estimation of total flavonoid content in propolis by two complementary colorimetric methods. *J Food Drug Anal.* 2002;10:178-182.
14. Çoruh N, Sagdicoglu Celep AG, Ozgokce F, Iscan M. Antioxidant capacities of *Gundelia tournefortii* L. extracts and inhibition on glutathione-S-transferase activity. *J Food Chem.* 2007;100:1249-1253.
15. Lowry OH, Rosebrough NJ, Farr AL, Randall RJ. Protein measurement with the Folin phenol reagent. *J Biol Chem.* 1951;193:265-275.
16. Onay M. Investigation for Natural Extract Inhibitors of Bovine Lens Aldose Reductase Responsible for the Formation of Diabetes Dependent Cataract. Middle East Technical University; Ankara, Turkey; 2008.
17. Habig WH, Pabst MJ, Jakoby WB. Glutathione-S-transferases the first enzymatic step in mercapturic acid formation. *J Biol Chem.* 1974;249:7130-7139.
18. Hayman S, Kinoshita JH. Isolation and Properties of Lens Aldose Reductase. *J Biol Chem.* 1965;240:877-882.
19. Geller BL, Winge DR. Subcellular distribution of superoxide dismutases in rat liver. *Methods Enzymol.* 1984;105:105-114.
20. Weydert CJ, Cullen JJ. Measurement of superoxide dismutase, catalase and glutathione peroxidase in cultured cells and tissue. *Nat Protoc.* 2009;5:51-66.
21. Bai JZ, Saafi EL, Zhang S, Cooper GJ. Role of Ca²⁺ in apoptosis evoked by human amylin in pancreatic islet beta-cells. *Biochem J.* 1999;343:53-61.
22. Yıldırım Ö, Aras S, Ergül A. Response of antioxidant systems to short-term NaCl stress in grapevine rootstock-1616c and *Vitis vinifera* L. cv. Razaki. *Acta Biol Cracoviensia Series Bot.* 2004;46:151-158.
23. Fresco P, Borges F, Diniz C, Marques MP. New insights on the anticancer properties of dietary polyphenols. *Med Res Rev.* 2006;26:747-766.
24. Udenigwe CC, Ata A, Samarasekera R. Glutathione-S-transferase inhibiting chemical constituents of *Caesalpinia bonduc*. *Chem Pharm Bull (Tokyo).* 2007;55:442-445.
25. Ren W, Qia Z, Wang H, Zhu L, Zhang L. Flavonoids: promising anticancer agents. *Med Res Rev.* 2003;23:519-534.
26. Valko M, Leibfritz D, Moncol J, Cronin MT, Mazur M, Telse J. Free radicals and antioxidants in normal physiological functions and human disease. *Int J Biochem Cell Biol.* 2007;39:44-84.
27. Zeng S, Liu W, Nie FF, Zhao Q, Rong JJ, Wang J, Tao L, Qi Q, Lu N, Li ZY, Guo QL. LYG-202, a new flavonoid with a piperazine substitution, shows antitumor effects *in vivo* and *in vitro*. *Biochem Biophys Res Commun.* 2009;385:551-556.
28. Aruoma OI, Bahorun T, Jen LS. Neuroprotection by bioactive components in medicinal and food plant extracts. *Mutat Res.* 2003;544:203-215.
29. Cai YZ, Luo Q, Sun M, Corke H. Antioxidant activity and phenolic compounds of 112 traditional Chinese medicinal plants associated with anticancer. *Life Sci.* 2004;74:2157-2184.
30. Cai YZ, Mei Sun, Jie Xing, Luo Q, Corke H. Structure-radical scavenging activity relationships of phenolic compounds from traditional Chinese medicinal plants. *Life Sci.* 2006;78:2872-2888.
31. Ramos-Bueno RP, Rincón-Cervera MA, González-Fernández MJ, Guil-Guerrero JL. Phytochemical Composition and Antitumor Activities of New Salad Greens: Rucola (*Diplotaxis tenuifolia*) and Corn Salad (*Valerianella locusta*). *Plant Foods Hum Nutr.* 2016;27:197-203.
32. Marrelli M, Cristaldi B, Menichini F, Conforti F. Inhibitory effects of wild dietary plants on lipid peroxidation and on the proliferation of human cancer cells. *Food Chem Toxicol.* 2015;86:16-24.
33. Oueslatib S, Ellilic A, Legaultb J, Pichetteb A, Ksouria R, Lachalc M, Karray-Bouraoui N. Phenolic content, antioxidant and anti-inflammatory activities of Tunisian *Diplotaxis simplex* (*Brassicaceae*). *Nat Prod Res.* 2015;29:1189-1191.
34. Durazzo A, Azzini E, Lazzè MC, Raguzzini A, Pizzala E, Maiani M. Italian Wild Rocket [*Diplotaxis tenuifolia* (L.) DC.]: Influence of Agricultural Practices on Antioxidant Molecules and on Cytotoxicity and Antiproliferative Effects. *Agriculture.* 2013;3:285-298.
35. Atta EM, Hashem AI, Ahmed AM, Elqosy MS, Jaspars M, El-Sharkaw ER. Phytochemical studies on *Diplotaxis isharra* growing in Sinai. *Euro J of Chem.* 2011;2:535-538.
36. Benmerache A, Berrehal D, Khalfallah A, Kabouche A, Semra Z, Kabouche Z. Antioxidant, antibacterial activities and flavonoids of *Reseda phyteuma* L. *Der Pharma Lettre.* 2012;4:1863-1867.
37. Woelfl U, Simon-Haarhaus B, Merfort I, Schempp CM. *Reseda luteola* L. Extract Displays Antiproliferative and Pro-Apoptotic Activities that are Related to its Major Flavonoids. *Phytother Res.* 2010;24:1033-1036.
38. Berrehal D, Khalfallah A, Betina SB, Kabouche Z, Kacem N, Kabouche A, Calliste CA, Duroux JL. Comparative antioxidant activity of two Algerian *Reseda* species. *Chem Nat Compds.* 2010;4:456-458.
39. Kumarasamy Y, Cox PJ, Jaspars M, Nahar L, Sarker SD. Screening seeds of Scottish plants for antibacterial activity. *J Ethnophar.* 2002;83:73-77.
40. Tawaha K, Alali FQ, Gharaibeh M, Mohammad M, El-Elimat T. Antioxidant activity and total phenolic content of selected Jordanian plant species. *Food Chem.* 2007;104:1372-1378.



Chemical Constituents of *Cymbocarpum erythraeum* (DC.) Boiss., and Evaluation of Its Anti-*Helicobacter pylori* Activity

Cymbocarpum erythraeum (DC.) Boiss.'in Kimyasal Bileşikleri ve *Helicobacter pylori*'ye Karşı Etkisi

© Samaneh HEIDARI¹, © Azadeh MANAYI², © Soodabeh SAEIDNIA², © Hossein MIGHANI¹, © Hamid Reza MONSEF ESFAHANI³, © Ahmad Reza GOHARI^{2*}, © William N SETZER⁴

¹Golestan University, Faculty of Science, Department of Chemistry, Golestan, Iran

²Tehran University of Medical Sciences, Faculty of Pharmacy, Medicinal Plants Research Center, Tehran, Iran

³Tehran University of Medical Sciences, Faculty of Pharmacy, Department of Pharmacognosy, Tehran, Iran

⁴University of Alabama in Huntsville, Faculty of College of Science, Departments of Chemistry, Huntsville, USA

ABSTRACT

Objective: *Cymbocarpum erythraeum* (Apiaceae) is an endemic species in Iran. Up to now, there have been no phytochemical and biological investigations on this species. Therefore, isolation of the main secondary metabolites of the plant along with its anti-*H. pylori* activity have been considered in this paper.

Materials and Methods: The dried parts of the plant were extracted with different solvents using solvent percolation and the antibacterial activity of the extracts evaluated by the disk diffusion method. Four compounds were isolated using different column chromatography methods.

Results: The compounds were identified by proton nuclear magnetic resonance and carbon-13 nuclear magnetic resonance as isoquercetin (1), rutin (2), β -sitosterol (3) and 2-decenol (4).

Conclusion: Anti-*H. pylori* evaluation of the extracts and isolated compounds against three clinical isolates of *H. pylori* revealed that hexane extract of the plant inhibited all *H. pylori* strains.

Key words: Apiaceae, *C. erythraeum*, chromatography, disk diffusion, *H. pylori*

ÖZ

Amaç: *Cymbocarpum erythraeum* (Apiaceae) İran'a endemik bir türdür. Bu zamana kadar, bu tür üzerinde herhangi bir fitokimyasal ve biyolojik aktivite çalışmasına rastlanmamıştır. Bu nedenle, bu çalışmada, bitkinin ana sekonder metabolitlerinin ve *Helicobacter pylori*'ye karşı etkisinin araştırılması amaçlanmıştır.

Gereç ve Yöntemler: Kurutulmuş bitki kısımları perkolasyon yöntemi ile farklı çözücüler kullanılarak ekstre edilmiş ve ekstrelerin antibakteriyel etkisi disk difüzyon yöntemiyle değerlendirilmiştir. Farklı kolon kromatografisi yöntemleri kullanılarak dört bileşik izole edilmiştir.

Bulgular: Bileşiklerin yapıları, proton nükleer manyetik rezonans ve karbon-13 nükleer manyetik rezonans tekniği ile izokersetin (1), rutin (2), β -sitosterol (3) ve 2-dekenol (4) olarak belirlenmiştir.

Sonuç: Ekstrelerin ve izole edilen bileşiklerin üç *H. pylori* klinik izolatına karşı etkilerinin değerlendirildiği bu çalışmada, bitkinin hekzan ekstresinin tüm *H. pylori* suşlarını ihibe ettiği tespit edilmiştir.

Anahtar kelimeler: Apiaceae, *C. erythraeum*, kromatografi, disk difüzyon, *H. pylori*

*Correspondence: E-mail: a_goharii@tums.ac.ir, Phone: +9821-64121202 ORCID-ID: orcid.org/0000-0001-9071-1663

Received: 16.04.2017, Accepted: 27.07.2017

©Turk J Pharm Sci, Published by Galenos Publishing House.

INTRODUCTION

Cymbocarpum is represented in Iran by three species that occur naturally in the wild, including *Cymbocarpum marginatum*, *Cymbocarpum erythraeum*, and *Cymbocarpum anethoides*.^{1,2} The essential oils had been obtained from these three species of *Cymbocarpum* from Iran and analyzed indicating that the oils of all three plants were rich in aliphatic aldehydes. Furthermore, the oil of *C. erythraeum*, with main constituent (*E*)-2-decenal (52.22%), showed larvicidal activity.³ The main components of the essential oils of the fruits and herbal parts of *Cymbocarpum wiedemannii* were found to be aliphatic aldehydes and aliphatic acids.⁴

A major cause of bacterial gastrointestinal infections is *Helicobacter pylori*. In fact, *H. pylori* has been designated as a class I carcinogen by World Health Organization and its eradication has been reported to be beneficial in preventing gastric disorders specially ulcer and cancer.⁵ Given the extensive treatment with antibiotics for decades, the failure rates due to antimicrobial resistance range from 20% to 40% and the eradication failure rate remains as high as 5-20%.⁶⁻⁸ Regarding the previous study which indicated that methanol extract of the plant showed antibacterial activity⁹ and anti-*H. pylori* activity of some flavonoids¹⁰ the present study was designed to evaluate anti-*H. pylori* property of the plant extracts and its flavonoids.

MATERIALS AND METHODS

Plant material

The flowering aerial parts of *C. erythraeum* were collected from the East Azerbaijan province (June 2010) with voucher No. 214 at the Herbarium of Institute of Medicinal Plants, Iranian Academic Centre for Education, Culture and Research, Karaj, Iran.

General

Silica gel (70-230 mesh, F254 pre-coated plates) (Merck, Germany), reverse phase silica gel 90 (RP-18C; Fluka, Switzerland) and Sephadex LH-20 (Fluka, Switzerland) were used for isolation of compounds. Semi-preparative high-performance liquid chromatography [HPLC (RP-18C; Knauer, Germany)] and medium-pressure liquid chromatography [MPLC (Silica gel, 230-400 mesh; Butchi, Switzerland)] were used for more purification. Nuclear magnetic resonance (NMR) experiments were performed on Bruker (Billerica, USA) DRX 500 instrument [500 MHz for proton NMR (¹H-NMR), 125 MHz for carbon-13 (¹³C-NMR)] with tetramethylsilane as an internal standard. Ultraviolet (UV) spectra were measured on Optizen (Daejeon, Korea) model 2021 UV plus. All solvents were distilled before use.

Isolation procedure

Dried aerial parts of *C. erythraeum* (500 g) were extracted with hexane, methanol and water-methanol (1:1) using the solvent percolation method at room temperature. Extracts were concentrated to obtain 11, 80, 34 g of hexane, methanol and methanol-water (1:1) extracts, respectively. The methanol extract was further partitioned by petroleum ether, butanol and

water. The butanol fraction (8 g) was subjected to Sephadex LH₂₀ column to afford B_A-B_E fractions and those suspected to contain flavonoids under UV light were loaded on another column for more purification. A sub-fractions (B_A: 3980 mg, B_B: 84 mg) were loaded on Sephadex LH₂₀ column with methanol as eluent to obtain compounds 1 (8.4 mg) and 3 (12 mg). The other sub-fraction (B_C: 106.6 mg) was injected to HPLC (RP-18C) eluted with different percentage of methanol-water (2:3, 1:1, and 3:2) to yield compound 2 (27 mg). In addition, the hexane extract was injected to MPLC (normal phase silica gel column) eluted with hexane-chloroform (4:1 and 0:1) to give 12 primary fractions (H_A-H_L). One fraction (H_J: 239 mg) was subjected to Sephadex LH₂₀ column with chloroform-ethyl acetate-methanol (1:1:1) as eluent to provide pure compound 4 (4.1 mg).

Anti-*H. pylori* assay

Clinical *H. pylori* (HP₁, HP₂, and HP₃) strains were used to determine antimicrobial susceptibility following previously published protocols using the disk diffusion method.^{11,12} Serial dilutions of the test samples were made in dimethyl sulfoxide (DMSO). Suspensions of bacteria in normal saline were prepared with the turbidity of McFarland standard No. 2 (6×10⁸ cell/mL). Plates of non-selective blood agar were inoculated with 100 μL of each bacterial suspension and allowed to dry at room temperature. Ten μL of test samples was introduced into a sterile blank disks and deposited on the surface of the inoculated plates. Negative and positive control included blank disks impregnated with 10 μL of DMSO and amoxicillin (1 μg/mL), respectively. Plates were incubated at 37°C under microaerobic conditions and examined after 3-5 days. The mean inhibition zone diameters (IZD) ± standard deviation were recorded.

RESULTS AND DISCUSSION

The isolated compounds from aerial parts of *C. erythraeum* were identified as isoquercetin (1), rutin (2),^{13,14} along with β-sitosterol (3),¹⁵⁻¹⁷ and 2-decenol (4) based on the spectroscopic data (¹H-NMR, ¹³C-NMR) and compared to the pertinent spectroscopic data in previously published literature (Figure 1).⁹

To the best of our knowledge, this is the first report on the isolation and elucidation of secondary metabolites of *C.*

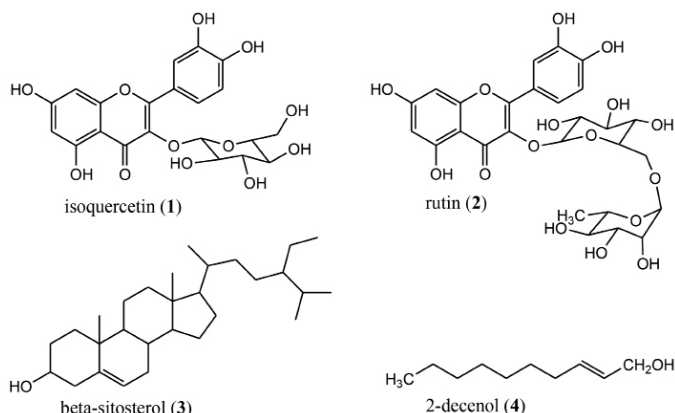


Figure 1. Chemical structures of the isolated compounds from *C. erythraeum*

Table 1. Inhibition zone diameters \pm standard deviation of some active extracts of *C. erythraeum* against clinical isolates of *H. pylori*

Samples	IZD \pm SD (mm)											
	1 Conc.			½ Conc.			¼ Conc.			1/8 Conc.		
	HP1	HP2	HP3	HP1	HP2	HP3	HP1	HP2	HP3	HP1	HP2	HP3
Hexane ¹	15 \pm 0.03	17 \pm 0.04	20 \pm 0.03	14 \pm 0.05	15 \pm 0.03	18 \pm 0.01	10 \pm 0.03	14 \pm 0.05	16 \pm 0.04	9 \pm 0.01	10 \pm 0.02	12 \pm 0.05
Methanol ²	-	-	14 \pm 0.04	-	-	13 \pm 0.04	-	-	10 \pm 0.02	-	-	-
PE ³	-	-	15 \pm 0.02	-	-	12 \pm 0.03	-	-	10 \pm 0.03	-	-	-

Conc.: Concentration, ¹: 440 mg/mL, ²: 464 mg/mL, ³: 226 mg/mL, HP: Strains of *H. pylori*, PE: Petroleum ether, -: Not sensitive, IZD for amoxicillin (1 μ g/mL): 30 \pm 0.04 mm, SD: Standard deviation

erythraeum and its anti-*H. pylori* activity. The susceptibility of the tested bacteria were different related to the extracts and HP₃ was the most susceptible strain. The IZD of the effective test samples against *H. pylori* are summarized in (Table 1). The growth of all bacterial strains were suppressed by amoxicillin (1 μ g/mL) with IZD of 30 \pm 0.04 mm, while DMSO showed no inhibitory activity toward the tested organisms. Methanol (464 mg/mL) and petroleum ether (226 mg/mL) extracts had inhibited one of the clinical isolates of *H. pylori* (HP₃) with IZD of 14 \pm 0.04 and 15 \pm 0.02 mm, respectively, while compounds 1 (16 mg/mL), 2 (14 mg/mL) and the flavonoid fraction (138 mg/mL), along with other extracts were not effective against the isolated strains.

In a previous study, rutin isolated from *Gardenia jasminoides* exhibited antibacterial activity toward *H. pylori*, however this present study showed the compound not to be active against the isolated strains.¹⁸ Additionally, some flavonoids are known to be antibacterial agents.¹⁹ For example, the flavonoid-rich extract of *Glycyrrhiza glabra* inhibited *H. pylori* growth by inhibition of protein synthesis, DNA gyrase and dihydrofolate reductase¹⁰, while the flavonoid fraction of *C. erythraeum* was not active against examined strains, which may be presumably due to the difference in the flavonoid constituents of the plants and/or the susceptibility of bacteria. Whereas in this study, the hexane extract of the plant mainly inhibited the *H. pylori* strains attributed to the presence of non-polar compounds. It was reported that essential oil of *C. erythraeum*, which was rich in (*E*)-2-decenal (52.22%), was biologically active and exhibited larvicidal activity.³ In the present study, the alcoholic compound 2-decenol (**4**), which was isolated from hexane fraction, is likely to be one of the active constituents of this fraction as well as other constituents in this fraction. The medium-chain-length alcohol decanol, from *Coriandrum sativum* oil, showed antibacterial activity especially against Gram-positive strains.^{20,21} As a matter of fact, the relatively polar substances such as flavonoids and other polar fractions are not generally able to effectively prevent the bacterium growth, suggesting that the anti-*H. pylori* activity of this plant can be largely attributed to other non-polar secondary metabolites.

Conflict of Interest: No conflict of interest was declared by the authors.

REFERENCES

- Ajani Y, Mojab F, Tabatabaai S, Ramazan-Pour B. Analysis of the essential oils from 3 species of *Cymbocarpum* (Apiaceae) from Iran. *Res Pharm Sci.* 2012;7:s708.
- Ajany Y. Studied taxonomic genus, *Cymbocarpum*, *Diplotaenia*, *Johrenia*, *Dorema haussknechtia*, *Azilia*, *Opopanax*, *Smyrniopsis* of *Umbelliferus* Iran; Tehran University; 2004.
- Aksakal Ö, Uysal H, Çolak DA, Mete E. Inhibition effects of essential oil of *Cymbocarpum erythraeum* (DC.) Boiss., on percentage of survival from larvae to adult in *Drosophila melanogaster* and its chemical composition. *MAKÜ FEBED.* 2012;3:32-36.
- Baser KHC, Özek T, Vural M. Essential Oil of *Cymbocarpum wiedemannii* Boiss. *J Essent Oil Res.* 1999;11:679-680.
- Zaidi SF, Muhammad JS, Shahryar S, Usmanghani K, Gilani AH, Jafri W, Sugiyama T. Anti-inflammatory and cytoprotective effects of selected Pakistani medicinal plants in *Helicobacter pylori*-infected gastric epithelial cells. *J Ethnopharmacol.* 2012;141:403-410.
- Li Y, Xu C, Zhang Q, Liu JY, Tan RX. *In vitro* anti-*Helicobacter pylori* action of 30 Chinese herbal medicines used to treat ulcer diseases. *J Ethnopharmacol.* 2005;98:329-333.
- Lien HM, Wang CY, Chang HY, Huang CL, Peng MT, Sing YT, Chen CC, Lai CH. Bioevaluation of *Anisomeles indica* extracts and their inhibitory effects on *Helicobacter pylori*-mediated inflammation. *J Ethnopharmacol.* 2013;145:397-401.
- Zhang XQ, Gu HM, Li XZ, Xu ZN, Chen YS, Li Y. Anti-*Helicobacter pylori* compounds from the ethanol extracts of *Geranium wilfordii*. *J Ethnopharmacol.* 2013;147:204-207.
- Ajani Y, Mojab F, Hajiaghahi R, Taghizadeh F, Jamalifar H. Assaying of volatile oil components and antimicrobial effects of methanolic extract of it in *Cymbocarpum erythraeum* (DC.) Boiss and *C anethoides* DC; 2012.
- Asha MK, Debraj D, Prashanth D, Edwin JR, Srikanth HS, Muruganantham N, Deth SM, Anirban B, Jaya B, Deepak M, Agarwal A. *In vitro* anti-*Helicobacter pylori* activity of a flavonoid rich extract of *Glycyrrhiza glabra* and its probable mechanisms of action. *J Ethnopharmacol.* 2013;145:581-586.
- Manayi A, Khanavi M, Saeidnia S, Azizi E, Mahmoodpour MR, Vafi F, Malmir M, Siavashi F, Hadjiakhoondi A. Biological activity and microscopic characterization of *Lythrum salicaria* L. *Daru.* 2013;21:61.
- Siavoshi F, Saniee P, Latifi-Navid S, Massarrat S, Sheykholeslami A. Increase in resistance rates of *H. pylori* isolates to metronidazole and tetracycline--comparison of three 3-year studies. *Arch Iran Med.* 2010;13:177-187.
- Gohari A, Saeidnia S, Shahverdi A, Yassa N, Malmir M, Mollazade K, Naghinejad AR. Phytochemistry and antimicrobial compounds of *Hymenocrater calycinus*. *Eur Asia J BioSci.* 2009;3:64-68.

14. Jafari S, Saeidnia S, Hajimehdipoor H, Ardekani MR, Faramarzi MA, Hadjiakhoondi A, Khanavi M. Cytotoxic evaluation of *Melia azedarach* in comparison with *Azadirachta indica* and its phytochemical investigation. *Daru*. 2013;21:37.
15. Saeidnia S, Ghamarinia M, Gohari AR, Shakeri A. Terpenes from the root of *Salvia hypoleuca* Benth. *Daru*. 2012;20:66.
16. Saeidnia S, Nourbakhsh MS, Gohari AR, Davood A. Isolation and identification of the main compounds of *Satureja sahendica* Bornm. *Aust J Basic Appl Sci*. 2011;5:1450-1453.
17. Saeidnia S, Gohari AR, Malmir M, Moradi-Afrapoli F, Ajani Y. Tryptophan and sterols from *Salvia limbata*. *J Med Plants*. 2011;10:41-44.
18. Lee JH, Kang KJ, Lee YM, Kim PN, Jeong CS. Effects of *Gardenia jasminoides* Ellis ethanol extract and its constituents on anti-gastritis and anti-gastric cancer cells. *Planta Med*. 2008;74:289.
19. Sahreen S, Khan MR, Khan RA, Shah NA. Estimation of flavonoids, antimicrobial, antitumor and anticancer activity of *Carissa opaca* fruits. *BMC Complement Altern Med*. 2013;13:372.
20. Huhtanen CN. Inhibition of *Clostridium botulinum* by Spice Extracts and Aliphatic Alcohols. *J Food Prot*. 1980;43:195-196.
21. Kubo I, Muroi H, Kubo A. Antibacterial activity of long-chain alcohols against *Streptococcus mutans*. *J Agric Food Chem*. 1993;41:2447-2450.



Anti-inflammatory Effects of *Pelargonium endlicherianum* Fenzl. Extracts in Lipopolysaccharide-stimulated Macrophages

Pelargonium endlicherianum Fenzl. Ekstrelerinin Lipopolisakkarit ile Uyarılan Makrofajlarda Anti-enflamatuvar Etkileri

© Ahmet CUMAĞLU^{1*}, © Gökçe Şeker KARATOPRAK², © Mükerrerem Betül YERER³, © Müberra KOŞAR²

¹Erciyes University, Faculty of Pharmacy, Department of Biochemistry, Kayseri, Turkey

²Erciyes University, Faculty of Pharmacy, Department of Pharmacognosy, Kayseri, Turkey

³Erciyes University, Faculty of Pharmacy, Department of Pharmacology, Kayseri, Turkey

ABSTRACT

Objectives: This study was designed to investigate the anti-inflammatory effects of *Pelargonium endlicherianum* Fenzl. and *Pelargonium quercetorum* Agnew. root extracts compared with the effects of commercial *Pelargonium sidoides* root extract by production of pro-inflammatory substances and inflammatory signal transduction on LPS-stimulated macrophages.

Materials and Methods: To measure the effects of root extracts on pro-inflammatory mediators, we used the following methods: 3-(4,5-dimethylthiazol-2-yl)-2,5-diphenyltetrazolium bromide assay (cell viability or cytotoxicity), enzyme-linked immunosorbent assay (cytokine production, prostoglandin E2 production), reverse transcriptase-polymerase chain reaction (COX-2, iNOS mRNA), Western blotting analysis [MAPK activation and NF-κB (p65) translocation] and the Griess reaction (NO production).

Results: Stimulation of the RAW 264.7 cells with LPS (0.5 µg/mL, 6 hrs treatment) caused an elevated production of pro-inflammatory cytokines (TNF-α and IL-6), increased mRNA expression of COX-2 and inducible NO synthase with release of PGE2 and NO, activated MAPK (phosphorylation of c-Jun N-terminal kinase, extracellular signal-regulated kinase, P38) signalling pathway, and nuclear translocation of NF-κB (p65), which were markedly inhibited by the pre-treatment with 11% ethanol and 70% methanol root extracts of *P. endlicherianum* without causing any cytotoxic effects. *P. quercetorum* root extract only decreased TNF-α production and *P. sidoides* root extract alleviated P38/MAPK activation and COX-2 mRNA expression with PGE2 production.

Conclusion: Our data indicate that especially 11% ethanol root extract of *P. endlicherianum* targets the inflammatory response of macrophages via inhibition of COX-2, IL-6, and TNF-α through inactivation of the NF-κB signalling pathway, supporting the pharmacologic basis of *P. endlicherianum* as a traditional herbal medicine for the treatment of inflammation and its associated disorders.

Key words: Pelargonium species, inflammation, cytokines, cyclooxygenase-2, macrophages

ÖZ

Amaç: Bu çalışma *Pelargonium endlicherianum* Fenzl. ve *Pelargonium quercetorum* Agnew. kök ekstrelerinin anti-enflamatuvar etkilerini, ticari *Pelargonium sidoides* kök ekstresinin etkileri ile kıyaslayarak LPS ile uyarılmış makrofaj hücrelerinde pro-enflamatuvar bileşiklerin üretimi ve enflamatuvar sinyal iletimi yoluyla incelemek üzere dizayn edildi.

Gereç ve Yöntemler: Kök ekstrelerinin pro-enflamatuvar araçlar üzerine etkisini ölçmek için takip eden yöntemler kullanıldı: 3-(4,5-dimethylthiazol-2-yl)-2,5-diphenyl tetrazolium bromid deneyi (hücre canlılığı veya sitotoksosite deneyi), enzime bağlı immünosorbent deneyi (sitokin üretimi, prostoglandin E2 üretimi), ters transkriptaz-polimeraz zincir reaksiyonu (COX-2, iNOS mRNA düzeyleri), Western Blot analizi [MAPK aktivasyonu ve NF-κB (p65) translokasyonu] ve Griess reaksiyonu (NO üretimi).

Bulgular: RAW 264.7 hücrelerinde LPS ile uyarım pro-enflamatuvar sitokinlerin üretimini, COX-2 ve iNOS mRNA düzeylerini, PGE2 ve NO üretimini, MAPK sinyali (c-Jun N-terminal kinaz, hücre dışı sinyalle düzenlenen kinaz, P38 fosforilasyonu) yolunda aktivasyonu ve NF-κB (p65) translokasyonunu artırırken tüm bu değerler *P. endlicherianum* %11 etanol ve %70 metanol ekstrelerinin ön-uygulaması ile herhangi bir sitotoksositeye

*Correspondence: E-mail: ahmetcumaoglu@yahoo.com, Phone: +90 533 340 51 04 ORCID-ID: orcid.org/0000-0002-3997-7746

Received: 18.04.2017, Accepted: 01.06.2017

©Turk J Pharm Sci, Published by Galenos Publishing House.

neden olmadan baskılanmıştır. *P. quercetorum* TNF- α düzeylerini azaltırken *P. sidoides* ile ön-uygulama P38/MAPK aktivasyonunu, COX-2 mRNA düzeylerini PGE2 üretimi ile birlikte azaltmıştır.

Sonuç: Sonuçlarımız göstermektedir ki, özellikle *P. endlicherianum* %11 etanol ekstresi COX-2, IL-6, and TNF- α inhibisyonu, NF- κ B ve MAPK sinyal yollarının inaktivasyonu ile enflamatuvar cevabı hedef almıştır, bu durum da enflamasyon ve enflamasyonla ilişkili hastalıkların tedavisinde bitkisel ilaç açısından *P. endlicherianum* ekstresinin farmakolojik esasını destekler.

Anahtar kelimeler: Pelargonium türleri, enflamasyon, sitokinler, siklooksijenaz-2, makrofajlar

INTRODUCTION

Inflammation is a host response to harmful stimuli. This biologic response is a protective mechanism of organisms for the defence against injurious stimuli.¹ Acute inflammation occurs with several typical processes including increased blood flow, increased permeability, and migration of neutrophils and eosinophils. These migrated immune cells are able to neutralize and eliminate potentially injurious stimuli.² If acute inflammation is not resolved, the inflammation may pass to a longer term chronic phase. In chronic inflammation, accumulation of white blood cells also continues, but the composition of the cells changes. The primary cells of chronic inflammation are lymphocytes and macrophages.³ Macrophages play an important role in the initiation and propagation of inflammatory responses by managing inflammation-related signalling pathways such as mitogen-activated protein kinases (MAPKs) signalling cascade and nuclear factor (NF)- κ B signalling⁴ with over-production of pro-inflammatory cytokines and other inflammatory mediators [prostaglandins and nitric oxide (NO)], generated by activated cyclooxygenase-2 (COX-2) and inducible NO synthase (iNOS).⁵⁻⁷ A number of inflammatory stimuli such as pro-inflammatory cytokines⁸ and bacterial lipopolysaccharides (LPS)⁹ activate macrophages to up-regulate such inflammatory states. The involvement of macrophages in chronic inflammatory conditions has been the subject of considerable experimental investigation in recent years for developing new anti-inflammatory agents and exploring the molecular anti-inflammatory mechanisms of potential drugs.¹⁰ Over-expression of inflammation-producing enzymes and their inflammatory mediators in macrophages is involved in many inflammation-related diseases such as atherosclerosis,¹¹ rheumatoid arthritis,¹² and cancers.¹³ Additionally, RAW 264.7 murine mouse macrophage cells, which can be stimulated to an inflammatory state by LPS treatment, have been used as an *in vitro* inflammatory cellular model to investigate the effects of anti-inflammatory drugs, herb-derived compounds, and plant extracts.

The *Pelargonium* species, members of the Geraniaceae family, comprise about 750 species and approximately 80% of the genus is indigenous to South Africa. A native South African medicinal plant called *Pelargonium sidoides* DC. has been traditionally used to treat cough, sore throat, congestion, and other respiratory ailments.¹⁴ Pharmacologic studies have demonstrated antibacterial, antituberculosis, antiviral, and immune-modulatory activities of *P. sidoides*.¹⁵⁻¹⁷ Following a number of clinical studies, a medicine with the international name of Umkaloabo, which comes from the plant's local name, has been manufactured using the roots of *P. sidoides*.^{18,19} In Turkey, *Pelargoniums* are represented by two species: *Pelargonium endlicherianum* Fenzl. and *Pelargonium quercetorum* Agnew. *P.*

endlicherianum is known by the common name "solucanotu" (Tansy) and *P. quercetorum* "tolik" in Turkey. The extracts prepared from these species roots and the fresh flowers are used for the treatment of intestinal parasites.²⁰

According to the literature, no scientific study has been reported on the anti-inflammatory activities of *P. endlicherianum* and *P. quercetorum*. Therefore, the aim of this study was to investigate the anti-inflammatory effects of *Pelargonium* species growing in Turkey by measuring MAPK activation, NF- κ B nuclear translocation, pro-inflammatory cytokines, and other inflammatory mediators (prostaglandins and NO), generated by activated COX-2 and iNOS on LPS-stimulated RAW 264.7 macrophages.

MATERIALS AND METHODS

Chemicals

Chromatographic standards, LPS, and all remaining reagents were of the highest purity available and obtained from the Sigma Chemical Company (St. Louis, MO, USA). Cell culture medium and medium supplements were purchased from GIBCO (Invitrogen, USA).

Plant materials and preparation of the extracts

P. endlicherianum was collected from Eskişehir, Dağköprü village in August 2013 and *P. quercetorum* was collected from Hakkari in May 2014. A voucher specimen of *P. endlicherianum* was deposited at the herbarium of the Anadolu University Faculty of Pharmacy, Eskişehir, Turkey (ESSE 14453) and a voucher specimen of *P. quercetorum* was deposited at the herbarium of the Hacettepe University Ankara, Turkey (HUB 30648). The dried *P. endlicherianum* and *P. quercetorum* roots were powdered and extracted with a sufficient amount of 70% methanol and 11% ethanol for 24 h at 40°C in a water bath with shaking. This procedure was repeated three times using the same batch of starting material and the resultant filtrates were combined and the solvent was removed under vacuum (40°C). All extracts were lyophilized and stored at -20°C until required for analysis.

Determination of the total flavonoid and phenolic contents

The total flavonoid content was estimated as catechin equivalents using an aluminium chloride colorimetric assay.²¹ The total phenolic content of the extract was determined using the Folin-Ciocalteu method²² and estimated as gallic acid equivalents (GAE), per gram of extract.

High-performance liquid chromatography determination

Liquid chromatographic equipment (Agilent Technologies 1200 Series) with a photodiode array detector were used. Separations were performed on a 250 x 4.6 mm i.d., 5- μ m

particle size, reverse-phase Mediterranean-C18 analytical column operating at room temperature (22°C) at a flow rate of 1 mL min⁻¹. Detection was performed between the wavelengths of 200 and 550 nm. Elution was conducted using a ternary non-linear gradient of the solvent mixture MeOH/H₂O/CH₃COOH (10:88:2, v/v/v) (solvent A), MeOH/H₂O/CH₃COOH (90:8:2, v/v/v) (solvent B) and MeOH (solvent C). Components were identified by comparison of their retention times to those of standards.

Cell culture

RAW 267.4 murine macrophage cells (a kind gift from Prof. Asuman Sunguroğlu, Department of Medical Biology, University of Ankara, Ankara, Turkey) were grown in DMEM medium containing 2 mM L-glutamine supplemented with 10% heat-inactivated fetal bovine serum (FBS), 100 IU/mL penicillin, and 100 µg/mL streptomycin.

Cell viability assay

RAW 267.4 cell viability was evaluated using the 3-(4,5-dimethylthiazol-2-yl)-2,5-diphenyltetrazolium bromide (MTT) colorimetric assay as described by Janjic and Wollheim.²³ A cell monolayer with cell density of 3×10^4 cells/well was seeded in 96-well plates. After cell attachment, 100 µL of serially diluted extract (concentrations ranging from 400 to 25 µg/mL) in DMEM with 1% FBS was added to the wells. After incubation, 10 µL of MTT solution (5 mg/mL in dH₂O) was pipetted into each well followed by a 3-hour incubation. Violet-coloured formazan crystals were dissolved with 100 µL DMSO and absorbance was determined at 570 nm using a microplate reader (Bio-Tek ELX800, BioTek Instruments Inc., Winooski, VT).

Enzyme-linked immunosorbent assay (ELISA)

Mediums collected after pre-treatment with extracts (20 µg/mL) for 24 h followed by LPS (0.5 µg/mL) treatment (in non-phenol red, serum-free medium) for 6 h and assayed for cytokines [tumor necrosis factor- α (TNF- α) and interleukin-6 (IL-6)] and prostaglandin E₂ (PGE₂) production using eBiosciences ELISA kits (San Diego, CA, USA) following the manufacturer's protocol.

Western blotting

RAW 267.4 cells were cultured in 6-well plates pre-treatment with extracts (20 µg/mL) for 24 h, followed by LPS (0.5 µg/mL) treatment (in non-phenol red, serum-free medium) for 6 h. Cells were lysed in 250 µL of RIPA lysis buffer [25 mM Tris (pH 7.4), 150 mM NaCl, 0.5% sodium deoxycholate, 1% NP-40] supplemented with a protease inhibitor cocktail (Complete Mini™, Roche, Mannheim, Germany) and 1 mM Na₃VO₄. Protein concentrations were determined using the BCA protein assay (Pierce). Thirty micrograms of protein lysates were heated for 5 min at 94°C in Laemmli sample buffer containing 4% β -mercaptoethanol and loaded on 4–12% Tris-glycine sodium dodecyl sulphate-polyacrylamide gel electrophoresis gels, then transferred electrophoretically to polyvinylidene difluoride membranes. The membranes were incubated overnight at 4°C with anti-SAPK/JNK, phospho-SAPK/JNK (Thr183/Tyr185), anti-extracellular signal-regulated kinase (ERK), phospho-ERK (Thr202/Tyr204), anti-P38, phospho-P38 (Thr180/Tyr182), and anti-NF- κ B p65

antibodies (Cell Signalling Technology). Protein bands were detected using horseradish peroxidase-conjugated secondary antibodies (Cell Signalling Technology) and visualized using West-Pico enhanced chemiluminescent reagents (Pierce).

Quantitative Real-time polymerase chain reaction (PCR)

RAW 267.4 cells were cultured in 6-well plates pre-treatment with extracts (20 µg/mL) for 24 h followed by LPS (0.5 µg/mL) treatment (in non-phenol red, serum-free medium) for 6 h. Total RNA was isolated using RNAzol isolation reagent (Sigma-Aldrich, St. Louis, MO), in accordance with the manufacturer's instructions. Total RNA (1 µg) was reverse-transcribed to cDNA using a Transcriptor High Fidelity cDNA Synthesis Kit (Roche Diagnostics GmbH, Mannheim, Germany). Real-time PCR was performed using a Light Cycler Nano System (Roche Diagnostics GmbH, Mannheim, Germany). To quantify cDNA, qPCR was performed using a *FastStart Essential DNA probe master mix* (Roche Diagnostics GmbH, Mannheim, Germany) and a catalogue assay kit (kits consist mix of primers and probes for determination of iNOS, COX-2, β -actin). For each sample, the level of target gene transcripts was normalized to β -actin.

Nitric oxide [total nitrite-nitrate (NO_x)] measurement

The mediums were collected after pre-treatment with extracts (20 µg/mL) for 24 h followed by LPS (0.5 µg/mL) treatment (in non-phenol red, serum-free medium) for 6 h and production of NO was assayed using the Griess method with a nitrate-nitrite colorimetric assay kit (Cayman Chemical).

Statistical analysis

Possible associations between groups were analyzed using the SigmaPlot 12. statistical software with Student's t-test. P values <0.05 were considered statistically significant. Fold increase or decrease of mRNA levels was also calculated using the Relative Expression Software Tool software developed for groupwise comparison and statistical analysis of relative expression results.

RESULTS

The total phenol and flavonoid contents of the extracts are shown in Table 1. The total phenolic contents in the obtained extracts ranged from 162.9 to 242.9 mg GAE/g DW. The highest concentration of phenols was measured in the methanol extract of *P. quercetorum*. The total phenolic content was found to be higher in the ethanol extract of *P. endlicherianum* than the ethanol extract of *P. quercetorum*. The total flavonoid contents in the obtained extracts ranged from 36.0 to 64.9 mg RE/g DW. The concentration of flavonoids in the ethanol extract of *P. endlicherianum* was found to be less than the ethanol extract of *P. quercetorum*. The total phenolic and flavonoid compounds were found to be higher in methanol extracts than in the ethanol extracts. The high solubility of phenols and flavonoids in polar solvents provides high concentrations of these compounds in the extracts depending on the polarity of the solvents used in extraction.

The chemical compositions of the extracts were determined using high performance liquid chromatography (HPLC) analyses (Table 2). Apocynin [1-(4-hydroxy-3-methoxyphenyl) ethanone] was identified as the main compound in the *P. endlicherianum* extracts. Based on the results of quantitative HPLC analysis, the highest content of apocynin (3.51 ± 0.016 %_{extract}) had 70% methanol extract of *P. endlicherianum*. The *P. endlicherianum* 11% ethanol extract had lower (2.48 ± 0.002 %_{extract}) apocynin levels than the 70% methanol extract of *P. endlicherianum*. The apocynin content of 11% ethanol and 70% methanol extracts of *P. quercetorum* was found as 0.51 ± 0.01 and 0.049 ± 0.01 %_{extract}, respectively. Gallic acid was also identified both in *P. endlicherianum* and *P. quercetorum*. The highest gallic acid content was found in the 11% ethanol extract of *P. endlicherianum* (1.070 ± 0.004 %_{extract}). The gallic acid content of *P. quercetorum* was found as 0.012 ± 0.001 and 0.098 ± 0.001 %_{extract}, respectively, for 11% ethanol and 70% methanol extracts.

RAW 264.7 macrophage cells were pre-treated with increasing

concentration (10, 20, 25, 50, 100, and 200 $\mu\text{g}/\text{mL}$) of *P. sidoides* (EPs® 7630) and each of the other extracts for 24 h. According to these findings (Figure 1), *P. sidoides* (EPs® 7630) was found to be the most cytotoxic towards RAW 264.7 macrophage cells and non-toxic (20 $\mu\text{g}/\text{mL}$) concentrations of extracts were selected and used in the subsequent experiments for testing their protective effect on LPS-induced inflammatory response.

The response to LPS (0.5 $\mu\text{g}/\text{mL}$, 6 h) treatment, release of pro-inflammatory cytokines TNF- α (Figure 2A) and IL-6 (Figure 2B) were increased approximately 2.0-fold and 38.2-fold, respectively. Pre-treatment with *P. endlicherianum* 11% ethanol extract and *P. quercetorum* 11% ethanol extract caused a reduction in the release of TNF- α and IL-6, but the reduction of IL-6 release after treatment with *P. quercetorum* 11% ethanol extract did not reach statistically significance.

Treatment with LPS resulted in significant upregulation of COX-2 (Figure 3A) and iNOS (Figure 3B) mRNA levels 5.8-fold and 2.9-fold, respectively. However, pre-treatment with *P. sidoides*, *P. endlicherianum* 11% ethanol and *P. endlicherianum* 70% methanol extract displayed a marked decrease in the induction of COX-

Table 1. Total phenol and flavonoid content of ethanolic and methanolic extracts of *P. endlicherianum* and *P. quercetorum* root extracts. Each value is the average of three analysis \pm standard deviation

	Total phenols ^c	Total flavonoids ^d
(<i>P. endlicherianum</i> ^a)	173.93 \pm 7.72	36.03 \pm 0.76
(<i>P. endlicherianum</i> ^b)	201.85 \pm 6.44	41.70 \pm 0.46
(<i>P. quercetorum</i> ^a)	162.90 \pm 6.95	46.63 \pm 1.93
(<i>P. quercetorum</i> ^b)	242.97 \pm 5.52	64.95 \pm 2.95
^a 11% ethanol extract		
^b 70% methanol extract		
^c mg gallic acid equivalent/g dry weight		
^d mg rutin equivalent/g dry weight		

Table 2. Phenolic compound apocynin and gallic acid content of extracts. Each value is average of three analysis \pm standard deviation

	Apocynin ^c	Gallic acid ^c
(<i>P. endlicherianum</i> ^a)	2.486 \pm 0.002	1.070 \pm 0.004
(<i>P. endlicherianum</i> ^b)	3.509 \pm 0.016	0.458 \pm 0.008
(<i>P. quercetorum</i> ^a)	0.510 \pm 0.015	0.012 \pm 0.001
(<i>P. quercetorum</i> ^b)	0.490 \pm 0.012	0.098 \pm 0.001
^a 11% ethanol extract		
^b 70% methanol extract		
^c % extract		

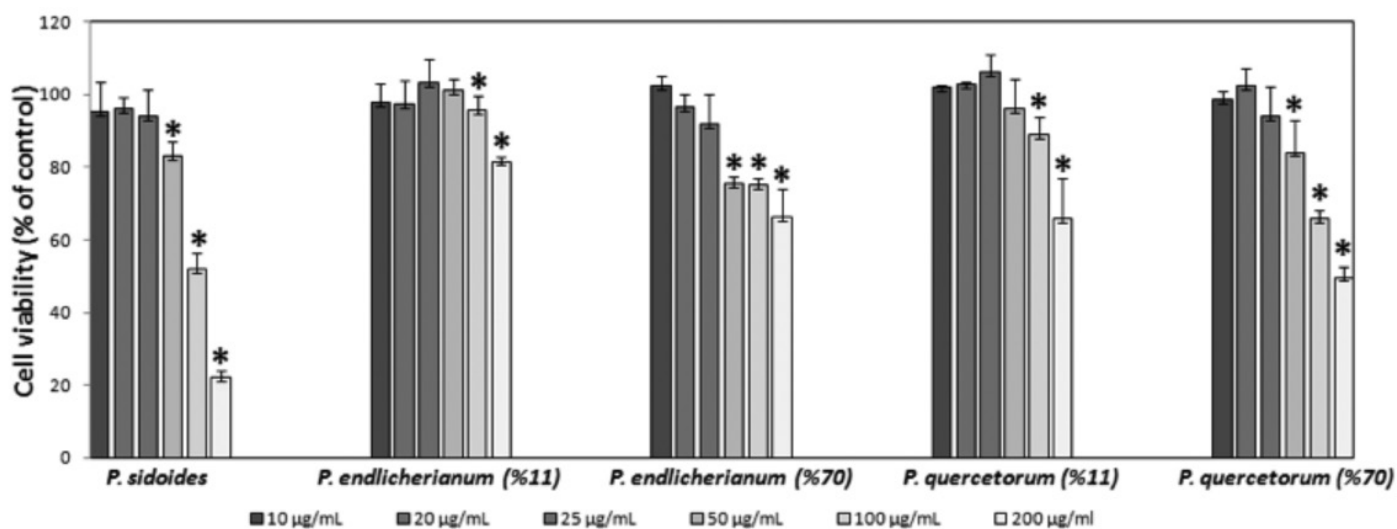


Figure 1. Effects of *Pelargonium* extracts on cell viability
n=4, *p<0.05 vs control

2 mRNA levels. Only pre-treatment with *P. endlicherianum* 11% ethanol extract inhibited the mRNA expression levels of iNOS in LPS-activated RAW 264.7 cells. The increase of COX-2 and iNOS expression in LPS-activated murine macrophage RAW 264.7 was accompanied by the release of large amounts of their products, PGE₂ (Figure 4A) and NO (Figure 4B), respectively. *P. sidoides*, *P. endlicherianum* 11% ethanol and *P. endlicherianum* 70% methanol extract produced also a considerable decrease in the levels of the COX-2 product, PGE₂, which confirms the inhibitory effect of *Pelargonium* extracts toward the COX-2 enzyme. *P. endlicherianum* 11% ethanol extract and *P. quercetorum* 11% ethanol extract completely suppressed the NO production induced by LPS.

In the current study, an increased expression of NF- κ B (p65) protein in the cytoplasm and enhanced p65 nuclear translocation were observed upon LPS activation. All studied extracts excluding *P. sidoides* caused a significant reduction on

cytoplasmic p65 protein expression (Figure 5A). Moreover, *P. endlicherianum* 11% ethanol and 70% methanol extracts had an inhibitory effect on p65 nuclear translocation (Figure 5B).

Finally, we investigated the inhibition of MAPKs activation by *Pelargonium* extracts. Western Blot analysis of RAW 264.7 cells exposed to LPS revealed expression levels of MAPKs, which were partly or markedly downregulated by *Pelargonium* extracts (Figure 6). LPS exposure to RAW 264.7 cells resulted in significant activation in MAPKs including phosphorylated-ERK (p-ERK) (Figure 7A), p-P38 MAPK (p-P38) (Figure 7B), and p-c-Jun N-terminal kinases (p-JNK) (Figure 7C). The LPS-induced activation of ERK was prominently blocked by both *P. endlicherianum* 11% ethanol and 70% methanol extracts. The overactivation of P38 by LPS was suppressed in the presence of *P. sidoides* and *P. endlicherianum* 11% ethanol extract. Activated JNK by LPS exposure was blocked by *P. endlicherianum* 11% ethanol, 70% methanol and *P. quercetorum* 70% methanol extracts.

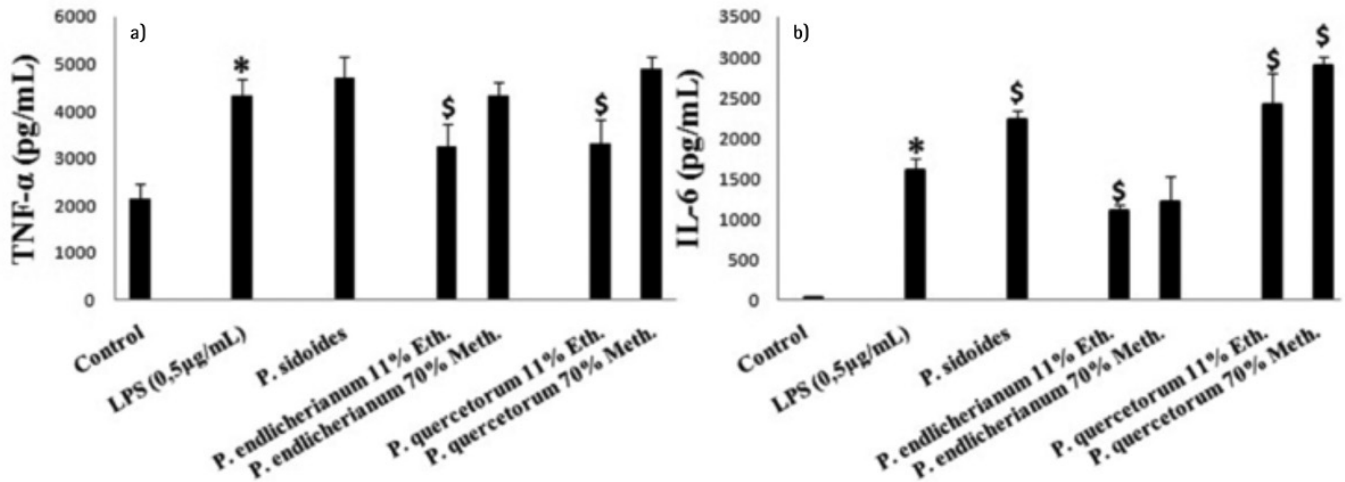


Figure 2. Pre-treatment with extracts modulate cytokine production in LPS treated macrophages

n=4, *p<0.05 vs. control, \S p<0.05 vs. lipopolysaccharide, LPS: Lipopolysaccharide, TNF- α : Tumor necrosis factor- α , IL-6: Interleukin-6

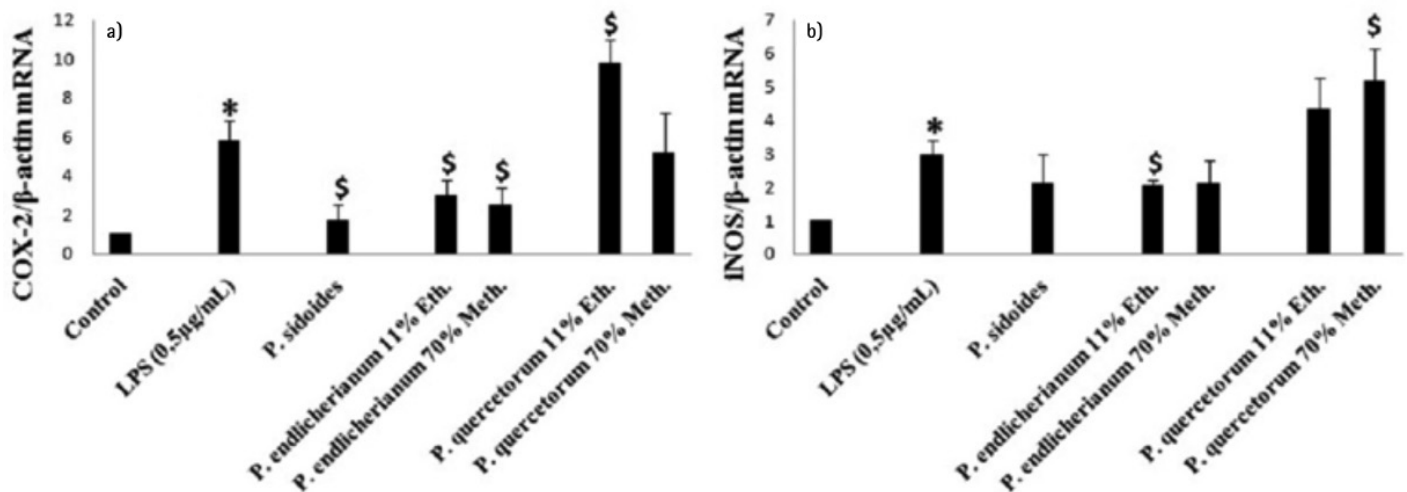


Figure 3. Effect of extracts on inflammation-producing enzymes mRNA levels in LPS treated macrophages

n=3, *p<0.05 vs control, \S p<0.05 vs lipopolysaccharide, LPS: Lipopolysaccharide, COX-2: Cyclooxygenase-2, iNOS: Inducible nitric oxide synthase

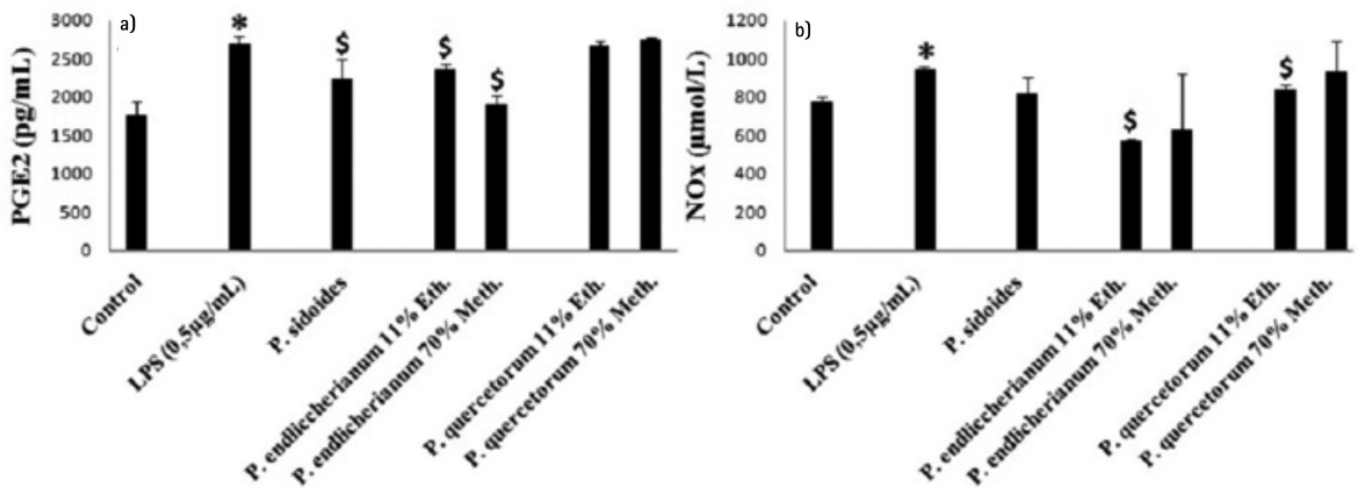


Figure 4. Effect of extracts on the levels of pro-inflammatory mediators; PGE2 and iNOS in LPS treated macrophages n=3, *p<0.05 vs control, \$p<0.05 vs lipopolysaccharide, PGE2: Prostaglandin E2, LPS: Lipopolysaccharide, NO: Nitric oxide

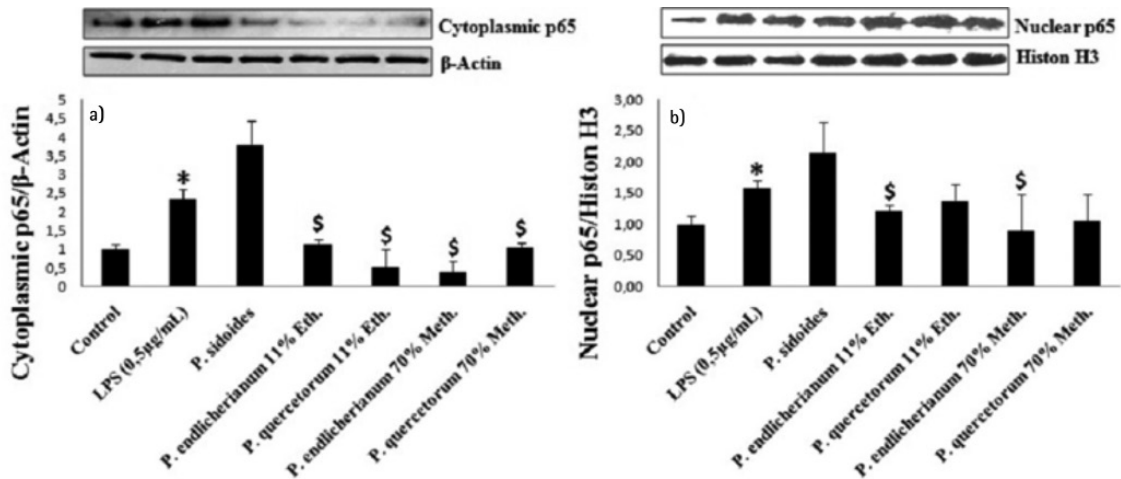


Figure 5. Activation of NF-κB by LPS treatment in macrophage cells and the effects of extracts on cytoplasmic p65 levels and p65 nuclear translocation n=3, *p<0.05 vs control, \$p<0.05 vs lipopolysaccharide, LPS: Lipopolysaccharide

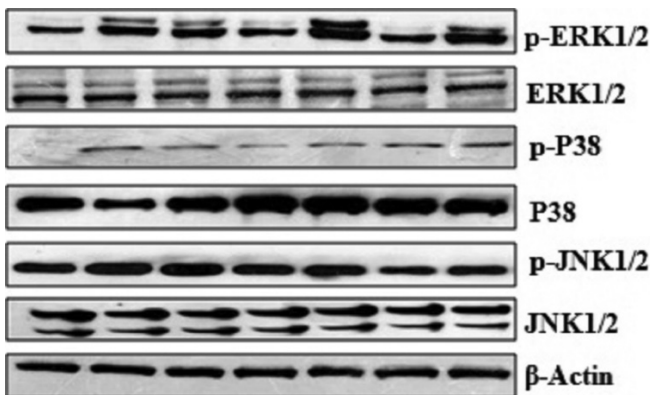


Figure 6. Activation of MAPK pathway by LPS treatment and the inhibitory effects of extracts were shown with Western Blot analysis. Line 1: Control, Line 2: LPS, Line 3: *P. sidoides*+LPS, Line 4: *P. endlicherianum* 11% eth.+LPS, Line 5: *P. endlicherianum* 70% meth.+LPS, Line 6: *P. quercetorum* 11% eth.+LPS, Line 7: *P. quercetorum* 70% meth.+LPS

LPS: Lipopolysaccharide, MAPK: Mitogen-activated protein kinase

DISCUSSION

Medicinal plants continue to be an important source of new chemical substances with potential therapeutic effects. Numerous natural products have been tested in various *in vitro* and *in vivo* models for the development of new anti-inflammatory agents. This study was designed to investigate the anti-inflammatory activities of the root extract (11% ethanol and 70% methanol) of *P. endlicherianum* and *P. quercetorum*, and especially, compare the effects of *P. sidoides* (EPs® 7630) on the induction of inflammatory signalling and production of pro/anti-inflammatory substances in LPS-stimulated RAW 264.7 macrophages.

In South Africa, polyphenol-rich herbal preparations made from roots of *P. sidoides* and *Pelargonium reniforme* are traditionally used to treat respiratory and gastrointestinal infections, dysmenorrhea, and hepatic disorders.¹⁴⁻¹⁶ Inspired by the healing of his tuberculosis, Charles Henry Stevens introduced this phytomedical drug to England in 1897.²⁴ More

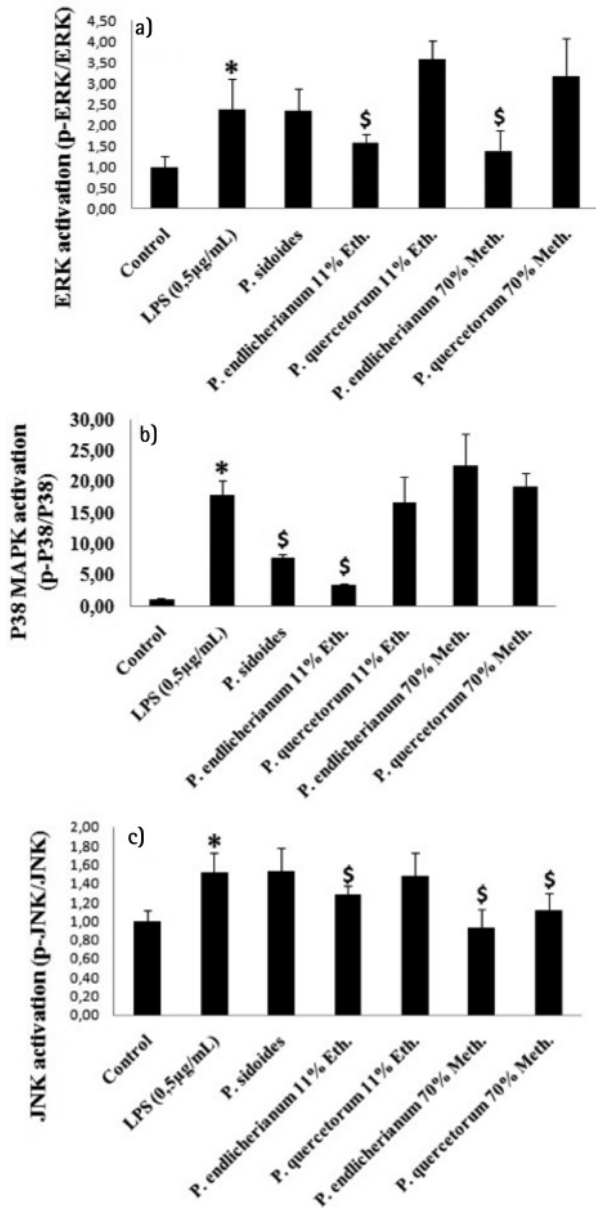


Figure 7. MAPK activation by LPS treatment and the inhibitory effects of extract

A: ERK activation, B: P38 MAPK activation, C: JNK activation. n=3, *p<0.05 vs. control, \$p<0.05 vs. LPS. LPS: Lipopolysaccharide, MAPK: Mitogen-activated protein kinase

than seven decades later, a special ethanol extract of *P. sidoides* roots, was finally developed (EPs® 7630; ISO Arzneimittel, Ettlingen, Germany). In Germany, EPs 7630 is approved today for therapeutic use in patients with acute bronchitis. In addition, EPs 7630 was shown to be effective in clinical trials on patients with tonsillopharyngitis, rhinosinusitis, common cold or chronic obstructive pulmonary disease.²⁵⁻³⁰

According to a meta-analysis about *P. sidoides*, there are several studies exploring the effects of *P. sidoides* in treating acute upper respiratory tract infections; 2,871 patients participated in these studies, an average of 261 in each and the clinical trials were performed in adults, adolescents, and children.²⁶

In Turkey, *Pelargoniums* are represented by two species: *P. endlicherianum* Fenzl. and *P. quercetorum* Agnew. The molecular mechanisms of *P. sidoides* have been partly identified but there are no relevant data revealing the similar effects of *P. endlicherianum* and *P. quercetorum*. Understanding the molecular effects of *P. endlicherianum* and *P. quercetorum* is key to taking advantage of their medical potential such as with *P. sidoides*. To date, data regarding its target cells and effects thereof within the human immune system are lacking. To address this issue, we first investigated how *P. endlicherianum* and *P. quercetorum* influenced the anti/pro-inflammatory responses of LPS-induced RAW 264.7 cells and compared the results with those of *P. sidoides*.

When investigating the signalling cascades induced by *P. endlicherianum* and *P. quercetorum*, we first activated the RAW 264.7 cells with LPS. LPS exposure to RAW 264.7 cells resulted in significant activation in MAPKs including p-ERK, p-P38, and p-JNK, whereas the LPS-induced activation of ERK was prominently blocked by both *P. endlicherianum* 11% ethanol and 70% methanol extracts. The overactivation of P38 by LPS was suppressed in the presence of *P. sidoides* and *P. endlicherianum* 11% ethanol extract. Activated JNK by LPS exposure was blocked by *P. endlicherianum* 11% ethanol, 70% methanol and *P. quercetorum* 70% methanol extracts.

Witte et al.²⁵ treated human peripheral blood mononuclear cells that were isolated from the blood of healthy donors to compare the bacterial and viral stimulation of the immune system and EP7630. The authors found a strong MAPK kinase pathway activation, which included phosphorylation of JNK, ERK1/2, and P38. Furthermore, EPs 7630 slightly provoked NF- κ B and phosphoinositide 3-kinase pathway activation. However, pharmacologic blockage of only P38 resulted in a strongly decreased monocyte TNF- α production. The observation that this signalling pattern differed from that induced by TLR3 and TLR4 ligand, inflammatory cytokines, and CD3/CD28 engagement suggests that *Pelargonium* extract affects monocytes via receptors different from those used by the mentioned stimuli.

Differing from the Witte et al.²⁵ study, in our experimental design the cells were stimulated by LPS and the effects of *P. sidoides*, *P. endlicherianum*, *P. quercetorum* were compared in terms of the inflammatory response. Pre-treatment with the extracts decreased the effects of inflammation. Furthermore, stimulation of the RAW 264.7 cells with LPS (0.5 μ g/mL, 6 hrs treatment) caused an elevated production of pro-inflammatory cytokines (TNF- α and IL-6), increased mRNA expression of COX-2 and iNOS, with release of prostaglandin E2 and NO, activated MAPK (phosphorylation of JNK, ERK, P38) signalling pathway, and nuclear translocation of NF- κ B (p65), which were markedly inhibited by the pre-treatment with 11% ethanol and 70% methanol root extracts of *P. endlicherianum* without causing any cytotoxic effects. *P. quercetorum* root extract only decreased TNF- α production and *P. sidoides* root extract alleviated P38/MAPK activation and COX-2 mRNA expression with PGE2 production.

A study designed to investigate the effects of *P. sidoides* on inflammatory responses was conducted on Leishmania major-infected murine macrophages. In that study, EPs 7630 increased cellular NO production and mRNA levels of iNOS and several cytokines (IL-1 β , IL-10, IL-12, IL-18, TNF- α , IFN- α , IFN- γ).³¹ However, our knowledge regarding the influence of *Pelargonium* extract on human immune cells, in particular on their cytokine production, is still highly restricted. To gain insight into this matter we comprehensively studied the immune-regulatory effects of *P. endlicherianum* and *P. quercetorum* and compared them with the effects of *P. sidoides* on murine macrophage cells. According to our study, TNF- α , IL-6, COX-2, PGE2, iNOS expressions were inhibited by *P. endlicherianum*.

Witte et al.²⁵ revealed that *P. sidoides* (EPs 7630) strongly and dose-dependently induced the production of the pro-inflammatory cytokines TNF- α and IL-6 in human blood immune cells. Moreover, a less prominent induction of the anti-inflammatory acting IL-10 was observed. In line with this study, *P. sidoides* root extract alleviated P38/MAPK activation and COX-2 mRNA expression with PGE2 production. Our data indicate that the 11% ethanol root extract of *P. endlicherianum* in particular targets the inflammatory response of macrophages via inhibition of COX-2, IL-6, and TNF- α through inactivation of the NF- κ B signalling pathway, supporting the pharmacologic basis of *P. endlicherianum* as a traditional herbal medicine for treatment of inflammation and its associated disorders. However, *P. endlicherianum* and *P. quercetorum* pre-treatment inhibited the activation of this pathway revealing that *P. sidoides* has pro-inflammatory effects and can be used more for its protective effect but *P. endlicherianum* can be used as a potential herbal medicine for treatment.

Furthermore, according to our results, apocynin was the major component of the *P. endlicherianum* root extract, which has also been identified by this study for the first time. Apocynin has shown to have strong anti-inflammatory effects in several studies.³²⁻³⁴ In one of the recent studies³⁴ conducted on the RAW 264.7 cells with apocynin, the effects of apocynin on the extracellular release of NO and PGE2 were examined in LPS-stimulated RAW 264.7 macrophages. Cells were incubated with apocynin for 1 h prior to LPS treatment (200 ng/mL). While LPS increased the extracellular release of NO and PGE2 production, approximately 10- and 30-fold, respectively, in RAW 264.7 cells, apocynin (100-500 mM) attenuated the release in a concentration-dependent manner. According to the same study, apocynin inhibited the expression of iNOS and COX-2, reduced NF- α , and inhibited the phosphorylation of MAP kinases JNK, ERK and P38. According to our results, *P. endlicherianum* root extracts, but not the *P. quercetorum* root extracts, were rich in apocynin and the similar strong anti-inflammatory effects that we observed by *P. endlicherianum* might be dependent on the rich apocynin ingredient because *P. quercetorum* did not show such a strong anti-inflammatory effect as *P. endlicherianum*.

CONCLUSION

The present study demonstrated that *P. endlicherianum* suppressed LPS-induced inflammatory responses via the suppression of MAP kinase signalling pathways in LPS-challenged RAW 264.7 macrophages, whereas *P. sidoides* seems to be pro-inflammatory rather than anti-inflammatory. Furthermore, it clearly showed that *P. endlicherianum* is rich in apocynin and probably exerts its anti-inflammatory effects via the suppression of LPS-induced activation MAP kinase signalling pathways over apocynin. In conclusion, all these results suggest that *P. endlicherianum* might be a useful herbal medicine for dissecting inflammation-related pathologies.

ACKNOWLEDGEMENTS

This study was supported by the Scientific and Technical Research Council of Turkey (TUBITAK) (project no. 103S803). *Pelargonium sidoides* (EPs[®] 7630) crude extract was obtained from Dr. Willmar Schwabe GmbH & Co. KG as a gift.

Conflict of interest: The authors declare that there are no conflicts of interest.

REFERENCES

1. Medzhitov R. Inflammation 2010: new adventures of an old flame. *Cell*. 2010;140:771-776.
2. Nathan C, Ding A. Nonresolving inflammation. *Cell*. 2010;140:871-882.
3. Allison AC, Ferluga J, Prydz H, Schorlemmer HU. The role of macrophage activation in chronic inflammation. *Agents Actions*. 1978;8:27-35.
4. Ivashkiv LB. Inflammatory signaling in macrophages: transitions from acute tolerant and alternative activation states. *Eur J Immunol*. 2011;41:2477-2481.
5. Kim JB, Han AR, Park EY, Kim JY, Cho W, Lee J, Seo EK, Lee KT. Inhibition of LPS-induced iNOS, COX-2 and cytokines expression by poncirin through the NF-kappa B inactivation in RAW 264.7 macrophage cells. *Biol Pharm Bull*. 2007;30:2345-2351.
6. Sharif O, Bolshakov VN, Raines S, Newham P, Perkins ND. Transcriptional profiling of the LPS induced NF-kappa B response in macrophages. *BMC Immunol*. 2007;8:1.
7. Lee S, Shin S, Kim H, Han S, Kim K, Kwon J, Kwak JH, Lee CK, Ha NJ, Yim D, Kim K. Anti-inflammatory function of arctiin by inhibiting COX-2 expression via NF- κ B pathways. *J Inflamm (Lond)*. 2011;8:16.
8. Fernando MR, Reyes JL, Iannuzzi J, Leung G, McKay DM. The pro-inflammatory cytokine, interleukin-6, enhances the polarization of alternatively activated macrophages. *PLoS One*. 2014;9:e94188.
9. Meng F, Lowell CA. Lipopolysaccharide (LPS)-induced macrophage activation and signal transduction in the absence of Src-family kinases Hck, Fgr, and Lyn. *J Exp Med*. 1997;185:1661-1670.
10. Dax CI, Lottspeich F, Müllner S. *In vitro* model system for the identification and characterization of proteins involved in inflammatory processes. *Electrophoresis*. 1998;19:1841-1847.
11. Hansson GK, Robertson AK, Söderberg-Nauclér C. Inflammation and atherosclerosis. *Annu Rev Pathol*. 2006;1:297-329.
12. Dey P, Panga V, Raghunathan S. A Cytokine Signalling Network for the Regulation of Inducible Nitric Oxide Synthase Expression in Rheumatoid Arthritis. *PLoS One*. 2016;11:e0161306.

13. Berraondo P, Minute L, Ajona D, Corrales L, Melero I, Pio R. Innate immune mediators in cancer: between defense and resistance. *Immunol Rev.* 2016;274:290-306.
14. Kolodziej, H. Fascinating metabolic pools of *Pelargonium sidoides* and *Pelargonium reniforme*, traditional and phytomedicinal sources of the herbal medicine Umckaloabo. *Phytomedicine.* 2007;14:9-17.
15. Kolodziej H, Kiderlen AF. *In vitro* Evaluation of Anti bacterial and Immunomodulatory Activities of *Pelargonium reniforme*, *Pelargonium sidoides* and the related herbal drug preparation EPs® 7630. *Phytomedicine.* 2007;14(Suppl 6):18-26.
16. Mativandlela SPN, Lall N, Meyer JJM. Antibacterial, antifungal and antitubercular activity of (the roots of) *Pelargonium reniforme* (CURT) and *Pelargonium sidoides* (DC) (*Geraniaceae*) root extracts. *S Afr J Bot.* 2006;72:232-237.
17. Schnitzler P, Schneider S, Stintzing FC, Carle R, Reichling J. Efficacy of an aqueous *Pelargonium sidoides* extract against herpesvirus. *Phytomedicine.* 2008;15:1108-1116.
18. Kolodziej H, Kayser O, Radtke OA, Kiderlen AF, Koch E. Pharmacological profile of extracts of *Pelargonium sidoides* and their constituents. *Phytomedicine.* 2003;10(Suppl 4):18-24.
19. Brendler T, van Wyk BE. A historical, scientific and commercial perspective on the medicinal use of *Pelargonium sidoides*. *J Ethnopharmacol.* 2008;119:420-433.
20. Baytop T. *Therapy with medicinal plants in Turkey past and present*, 2nd ed. Nobel Tip Kitabevi; Istanbul; 1999.
21. Zhishen J, Mengcheng T, Jianming W. The determination of flavonoid contents in mulberry and their scavenging effects on superoxide radicals. *Food Chem.* 1999;64:555-559.
22. Kaur C, Kapoor HC. Anti-oxidant activity and total phenolic content of some Asian vegetables. *Int J Food Sci Technol.* 2002;32:153-161.
23. Janjic D, Wollheim CB. Islet cell metabolism is reflected by the MTT (tetrazolium) colorimetric assay. *Diabetologia.* 1992;35:482-485.
24. Brendler T, vanWyk BE. A historical, scientific and commercial perspective on the medicinal use of *Pelargonium sidoides* (*Geraniaceae*). *J Ethnopharmacol.* 2008;119:420-433.
25. Witte K, Koch E, Volk HD, Wolk K, Sabat R. The *Pelargonium sidoides* Extract EPs 7630 Drives the Innate Immune Defense by Activating Selected MAP Kinase Pathways in Human Monocytes. *PLoS One.* 2015;10:e0138075.
26. Agbabiaka TB, Guo R, Ernst E. *Pelargonium sidoides* for acute bronchitis: a systematic review and meta-analysis. *Phytomedicine.* 2008;15:378-385.
27. Bachert C, Schapowal A, Funk P, Kieser M. Treatment of acute rhinosinusitis with the preparation from *Pelargonium sidoides* EPs 7630: a randomized, double-blind, placebo-controlled trial. *Rhinology.* 2009;47:51-58.
28. Bereznoy VV, Riley DS, Wassmer G, Heger M. Efficacy of extract of *Pelargonium sidoides* in children with acute non-group A beta-hemolytic streptococcus tonsillopharyngitis: a randomized, double-blind, placebo-controlled trial. *Altern Ther Health Med.* 2003;9:68-79.
29. Lizogub VG, Riley DS, Heger M. Efficacy of a *Pelargonium sidoides* preparation in patients with the common cold: a randomized, double blind, placebo-controlled clinical trial. *Explore (NY).* 2007;3:573-584.
30. Matthys H, Pliskevich DA, Bondarchuk OM, Malek FA, Tribanek M, Kieser M. Randomised, double blind, placebo-controlled trial of EPs 7630 in adults with COPD. *Respir Med.* 2013;107:691-701.
31. Trun W, Kiderlen AF, Kolodziej H. Nitric oxide synthase and cytokines gene expression analyses in Leishmania-infected RAW 264.7 cells treated with an extract of *Pelargonium sidoides* (Eps 7630). *Phytomedicine.* 2006;13:570-575.
32. Abdelmageed ME, El-Awady MS, Suddek GM. Apocynin ameliorates endotoxin-induced acute lung injury in rats. *Int Immunopharmacol.* 2016;30:163-170.
33. Kucera J, Binó L, Stefková K, Jaros J, Vasíček O, Vecera J, Kubala L, Pacherník J. Apocynin and Diphenyleiiodonium Induce Oxidative Stress and Modulate PI3K/Akt and MAPK/ERK Activity in Mouse Embryonic Stem Cells. *Oxid Med Cell Longev.* 2016;2016:7409196.
34. Kim SY, Moon KA, Jo HY, Jeong S, Seon SH, Jung E, Cho YS, Chun E, Lee KY. Anti-inflammatory effects of apocynin, an inhibitor of NADPH oxidase, in airway inflammation. *Immunol Cell Biol.* 2012;90:441-448.

ERRATUM

Turk J Pharm Sci 2018;15(1):116

DOI: 10.4274/tjps.e0001

Jalpa U. P, Usmangani K. C. A Synchronous Fluorescence Spectrofluorometric Method for the Simultaneous Determination of Clonazepam and Paroxetine Hydrochloride in Combined Pharmaceutical Dose Form. Turk J Pharm Sci 2017;14(3):251-256.

DOI: 10.4274/tjps.84856

Upon request of the corresponding author, Purvi A. Shah has been added as author:

Jalpa U. P, Usmangani K. C., Purvi A. S. A Synchronous Fluorescence Spectrofluorometric Method for the Simultaneous Determination of Clonazepam and Paroxetine Hydrochloride in Combined Pharmaceutical Dose Form. Turk J Pharm Sci 2017;14:251-256.